Contributions to the Design of Sampled-Data Controllers for Takagi-Sugeno Models

Adriano N.D. Lopes

UNIVERSITÉ DE REIMS CHAMPAGNE-ARDENNE
ÉCOLE DOCTORALE SCIENCES DU NUMÉRIQUE ET DE L'INGÉNIEUR (n°620)

THÈSE

Pour obtenir le grade de

DOCTEUR DE L'UNIVERSITÉ DE REIMS CHAMPAGNE-ARDENNE

Discipline: AUTOMATIQUE ET TRAITEMENT DE SIGNAL

Spécialité: AUTOMATIQUE

Présentée et soutenue publiquement par

Adriano NOGUEIRA DRUMOND LOPES

Le 10 Février 2022

Contributions on the design of sampled-data controllers for Takagi-Sugeno models

---

Thèse dirigée par **Kevin GUELTON et Laurent ARCESE**

JURY

M. Alexandre SEURET	Directeur de Recherche,	LAAS-CNRS, Toulouse	**Président**
M^{me} Zsófia LENDEK	Professeur des Universités,	Technical University of Cluj-Napoca (RO),	**Rapporteur**
M. Dalil ICHALAL	Professeur des Universités,	Université d'Evry Val d'Essonne,	**Rapporteur**
M. Benoît MARX	Maître de Conférences HDR,	Université de Lorraine,	**Examinateur**
M. Valter J. S. LEITE	Professeur des Universités,	CEFET-MG, Divinópolis (BR),	**Examinateur**
M. Laurent ARCESE	Maître de Conférences,	Université de Reims Champagne Ardenne,	**Co-encadrant de thèse**
M. Kevin GUELTON	Professeur des Universités,	Université de Reims Champagne Ardenne,	**Directeur de thèse**

Acknowledgements

A wise man once told me that the most important part of a work is this one, that I'm humbling writing now, with the hope of not forgetting someone who contributed to the development of this manuscript.

First, I would like to thank Ms. Zsófia Lendek and Mr. Dalil Ichalal, for accepting being the reviewers of this work. I would like to also thank Mr. Benoît Marx and Mr. Valter J.S. Leite, who closely followed the construction of the contributions here presented, giving their valuable remarks, and for being members of the evaluation committee. I would like to especially thank Mr. Alexandre SEURET for being President of the evaluation committee and for his remarks which allowed the improvement of this work.

Then, since no work can be properly done without a helpful administrative structure, in this part I wish to thank all these players. First, I would like to thank the Region Grand Est and the University of Reims Champagne-Ardenne for funding this research project. I would like to acknowledge the support received from Ms. Lolita Lebrun, from the International Office of the University of Reims Champagne-Ardenne, for helping me dealing with the state bureaucracy. I would like to also thank Mr. Bernard Riera, director of the CReSTIC for welcoming me into the laboratory to conduct my research. I need also to thank Mr. Rezak Ayad and Ms. Ségolène Buffet, who are respectively director, and secretary of the Doctoral School for dealing with the formation processes. I wish to extend my thanks to Ms. Ida Lenclume and Ms. Marielle TUR who helped me with all the administrative procedures through the conclusion of this work. Also, I would like to show my appreciation to CEFET-MG for conceding a leaving period for working on this Ph.D. Thesis.

For sure, this work would not be possible without the support of my advisors. I will never forget the arrival at Reims' train station at 16h14 on the last Friday of September 2018. After two flights, one transfer and a train trip, which took almost twenty hours of travel, my wife and I were there, with four 23 kg luggage, two of them, broken during the flight, without internet connection and without any clue about the next step. This was the context of my first in-person meeting with Mr. Laurent Arcese, my co-advisor. Since then, I knew that I could count on him all along this work. Thank you, Laurent, for being so supportive. Now, I need to dedicate some lines to Mr. Kevin Guelton, my advisor, who I took the liberty to consider as a friend. Our first meeting was on WCCI 2018, from then, he has been playing the hard task of pushing me, from challenging me in formulating questions during congress presentations to delivering a final version of this work. Thank you for all the wise advice, for sharing priceless ideas, and for being so available and supportive. I will be in debt for life with you for preparing all the housing details for us. Also, thank you, Kevin and Nathalie, for welcoming us to Reims, you introduced us to the real French cuisine and some good stuff.

The time spent in France would not be so memorable without speaking the French language, and therefore I need to thank the Centre International d'Etudes Françaises of the University of Reims Champagne-Ardenne. I would like to especially thank Ms. Laurence Oudin-Arnoult, Ms. Emilie GREAULT and Mr. Rémy VIAU for their support to my wife and me. If speaking French

is a must, living in France, making friends it is essential, especially when you are far from your family. So, I would like to thank Jéssica, Jerônymo, Mariana e Anderson for your friendship and for sharing your lives with us, you were extremely important in our adaptation to this new life. Getting through my manuscript required more than academic support, so, I would like to thank my COACH's Team mates, especially Mr. Nadhir Messai, Alan, and Khalil, thank you for all the fruitful discussions and for your patience with my systematic manner. I would like to also thank the colleagues from CReSTIC who I had the pleasure of exchanging some words, especially Alexandre, Gwendoline, Noémie, Paul, Rafiq, Soizic, Stéphane and Tom, who I spent most of my lunch times, talking about the French culture, agriculture, countryside expressions and giving some free Babyfoot lessons. Thank you for making my day life on the lab lighter and for sharing with us some especial moments such as your marriage Alex and Gwen. I would like to extend my thanks to the old friends who made themselves close even being thousands of kilometers far away.

Most importantly, none of this could have happened without my family support. I must express my very profound gratitude to my wife Viviane who boarded the idea of living this adventure with me. Thank you darling for being present through all the difficult moments and for sharing especial memories with me. I wish to extend the thank to her parents and her sister who gave us daily doses of strength. I would like to thank my parents Simone and Edison, and my brother Juliano for providing me with unfailing support and continuous encouragement throughout my years of study. Thank you for being always present, you are my stronghold and my biggest source of motivation.

Finally, I want to record my gratitude to one and all, who directly or indirectly helped on this work.

Notations

Acronyms

T-S	Takagi-Sugeno
LPV	Linear Parameter Varying
FMB	Fuzzy Model-Based
MF	Membership Function
LMI	Linear Matrix Inequality
DOF	Degree of Freedom
PDC	Parallel Distributed Compensation
QLF	Quadratic Lyapunov Function
NQLF	Non-Quadratic Lyapunov Function
NQLKF	Non-Quadratic Lyapunov-Krasovskii Functional
NCS	Networked Controller Systems
LKF	Lyapunov-Krasovskii Functional
PLC	Programmable Logic Computer
PI	Proportional-Integral
PD	Proportional-Derivative
PID	Proportional-Integral-Derivative
LQR	Linear-Quadratic Regulator

Sets, matrices and vectors

$\mathbb{R}$	Set of real numbers
$\mathcal{I}_r$	Denotes the set of integers $\{1, \ldots, r\}$
$\mathbb{N}$	Set of all positive integers
$\mathbb{R}^n$	The n-dimensional real space
$\mathbb{R}^{n\times m}$	The set of real matrices of dimensions $n \times m$
M^T	The transpose of a matrix M
$M_{(\ell)}$	The ℓth row of a matrix M
e_0	Represents a matrix of zeros, defined as $e_0 = \begin{bmatrix} 0_{n\times pn} \end{bmatrix} \in \mathbb{R}^{n\times pn}$, $\forall p \in \mathbb{Z}^+$
e_j	Represents the matrix $\begin{bmatrix} 0_{n\times(j-1)n} & I_{n\times n} & 0_{n\times(p-j)n} \end{bmatrix} \in \mathbb{R}^{n\times pn}$, $\forall j \in \mathcal{I}_p$
$\mathtt{diag}\{M_1, \ldots, M_n\}$	Denotes a block diagonal matrix.
$\mathtt{sign}(x)$	The sign function of $x \in \mathbb{R}$
$\mathtt{rank}(M)$	The rank of a matrix M
$\mathcal{H}(M)$	Stands for $M + M^T$
$col\{a_1, \ldots, a_n\}$	Denotes a column vector with scalar entries
$\star$	Stands for symmetric blocks in the expression of a matrix

Contents

List of Figures

General Introduction

In our everyday life as well as in industry, the place that takes autonomous systems is continuously growing. Such devices are intended to autonomously perform simple daily or even complex tasks (e.g. in manufacturing, services, entertainment...), making accessible some applications, in terms of reduced costs or even viability, that were not previously possible. For instance, in the past few decades, due to the globalization of industrial production, the manufacturing world witnessed growing research toward more efficient processes with increasing requirements in quality associated with the need for cost cuts to maintain the competitiveness, testifying to the increasing employment of robots and specialized machines in production plants (Brecher et al., 2021). In this context, Industry 4.0 emerged as a step further in integrating automated systems. Using programmable machines, process data analysis, and network interconnected systems makes viable to manufacture complex products that previously demanded numerous unskilled workers with only few skilled ones. These brought back competitiveness in manufacturing technological products in developed countries, where the salaries wages are higher than in underdeveloped countries, previously chosen because of their weak labors' protection, which consequently implied in a reduced outlay (Naghavi, 2007). This paradigm change reduced the overall costs and the transportation losses between the production site and the consumers market, which partially addresses the demand for environment-friendly production. Also, in our daily life, technological devices become more and more essential or unavoidable since they are now spreading into many common areas. For instance, we are facing an invasion of Internet of Things (IoT) systems, such like, in home automation, where autonomous vacuum cleaners or many other connected devices are intending to simplify our lives. Another example is the ongoing revolution of transportation with autonomous electric cars, or the use of Unmanned Aerial Vehicles (UAV) for making deliveries or even for entertainment, and so on.

This contextualization is intended to give an overview of the field where this thesis research is inserted. In this regard, it is important to highlight that most of the above mentioned technological devices involve continuous-time dynamics, usually mathematically modeled through a set of differential equations. Moreover, to perform the task they are designed for, they usually need to be controlled. Hence, with the advance of actual technologies, their controllers are often implemented on digital devices that process sampled data during scan cycles to compute the adequate control signals, see e.g. (Ogata, 2010; Åström and Hägglund, 2011). Additionally, the

dynamics of these plants are often nonlinear and their sensors and actuators can be connected to the controllers through communication channels. In this context, there are two main points to be addressed. The control of nonlinear systems and the hybrid characteristics of the closed-loop dynamics of such systems where continuous and discrete-time signals are involved (Liu et al., 2020; Hetel et al., 2017).

Among the nonlinear control theory researchers, Takagi and Sugeno have provided, in the mid 80's, an interesting way to represent nonlinear systems (Takagi and Sugeno, 1985). Initially based on the fuzzy IF-THEN rules formalism, Takagi-Sugeno (T-S) models provide polytopic approximations of nonlinear systems as weighted sums of linear subsystems. Then, with the introduction of the sector nonlinearity decomposition (Kawamoto et al., 1992; Morère, 2001; Tanaka and Wang, 2001), when analytic nonlinear models are available, T-S models can exactly match nonlinear ones on a compact set of their state space. Such a feature filled the gap with other well-known polytopic approaches that were developed at the same time in the control community, namely the quasi-LPV models, introduced in (Shamma, 1988; Shamma and Cloutier, 1993), which are now well-known as equivalent to T-S models.

A vast literature is available for various T-S model-based control problems, for instance dealing with continuous-time controller design, see e.g. (Guerra et al., 2012; Cherifi et al., 2018, 2019), discrete-time ones, see e.g. (Xie et al., 2017a; Lopes et al., 2020b), T-S systems with time-delays, see e.g. (Peng et al., 2008; Li and Liu, 2009; Bourahala et al., 2017, 2019), or also sampled-data control, see e.g. (Yoneyama, 2010; Zhang and Han, 2011; Cheng et al., 2017). Indeed, thanks to their convex polytopic structures, stability conditions and controller design conditions for T-S systems are usually studied via Lyapunov approaches and solved in the Linear Matrix Inequality (LMI) framework (Boyd et al., 1994; Skelton et al., 1998). Nevertheless, these LMI-based results provide only sufficient conditions and so suffer from conservatism, which reduction is an important and common challenge in the quasi-LPV/T-S community, see e.g. (Sala, 2009; Guerra et al., 2015; Lam, 2018; Nguyen et al., 2019a) and references therein. Indeed, successive improvements are found in the literature to relax the LMI conditions, from the use of basic quadratic Lyapunov functions (Wang et al., 1996) to non-quadratic ones (Jadbabaie, 1999; Blanco et al., 2001; Tanaka et al., 2003; Mozelli et al., 2009; Guerra et al., 2012), by relaxing the parameterized double fuzzy summation structure of LMI conditions (Kim and Lee, 2000; Tuan et al., 2001; Xiaodong and Qing-ling, 2003), or even considering T-S descriptors (Taniguchi et al., 2001; Tanaka et al., 2003; Marx and Ragot, 2008; Guelton et al., 2008), or introducing descriptor redundancy (Tanaka et al., 2007; Guelton et al., 2009; Bouarar et al., 2013). Similarly to these previous related works, this thesis aims at providing relaxed LMI-based controller design procedures for stabilizing T-S models, especially when continuous-time nonlinear systems are controlled by digital devices.

As mentioned above, the control algorithms are nowadays often implemented on digital devices, (i.e. evolving in a discrete-time basis), rather than continuous-time analog ones. However, many physical systems evolve in continuous-time while the action of digital controllers are updated only at specific sampling time instants, e.g. mechatronic systems, embedded systems,

networked control systems, and so on. In this context, Figure 1 illustrates an usual control topology of a basic sampled-data system driven by a discrete-time state-feedback controller, which can be implemented into a platform based on an Arithmetic Logic Unit (ALU), such as an industrial Programmable Logic Controller (PLC), a computer, or a microcontroller board, which can be embedded, installed on a control panel with dedicated communication wires, or connected via a data network. Then, based on the sampled measurements $x(t_k)$ of the system's state $x(t)$, provided by an Analog to Digital Converter (ADC), the input control signal $u(t_k)$ is fed-back to the continuous-time nonlinear plant through a Digital to Analog Converter (DAC) and a Zero-Order Hold (ZOH).

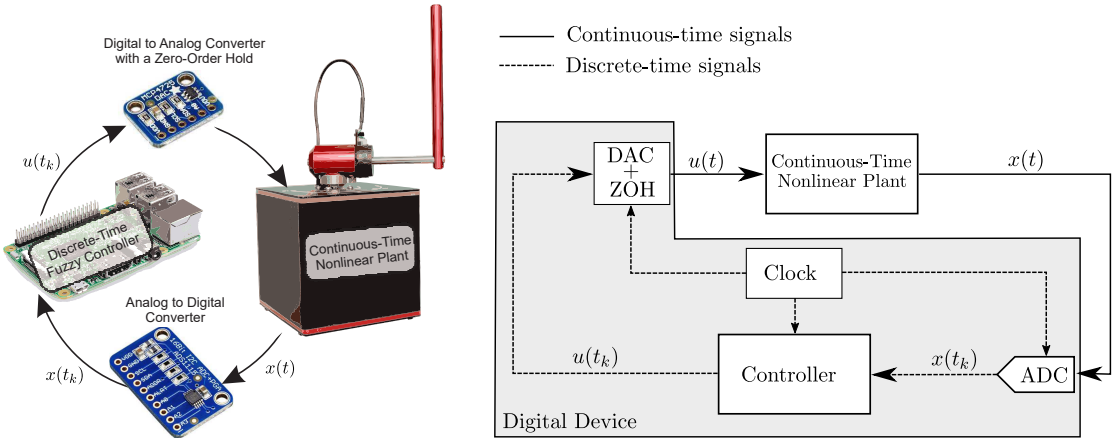

Figure 1: Illustration and block diagram of a continuous-time plant controlled by a discrete-time state-feedback controller processed on a digital device.

From the literature, it is possible to gather the main approaches employed to meet such requirements in which practical continuous-time applications are driven by digital controllers into three groups according to the characterization of the sampling interval, the strategy adopted for the project of digital controllers and the associated stability guarantees (Fridman, 2010):

- *Emulation*: It consists on the discretization of continuous-time controllers designed ignoring samplings. This is often a common choice in practical applications. However, from the theoretical point-of-view and for a rigorous research perspective, it is worth to highlight that, estimating the maximal allowable sampling period would be very conservative or even analytically tricky (Di Ferdinando and Pepe, 2019).

- *Direct Design*: From a discretized realization of the plant model, a discrete-time controller is designed, disregarding the continuous-time behavior between consecutive samples (Lopes et al., 2020b; Ogata, 1995). It is to be noticed that discretization procedures lead to approximations. Indeed, standard discretization procedure usually consider the well-known Euler transforms (Ogata, 1995) and recent works in this topic aim at improving the discretization procedure to improve discrete-time models' accuracy, e.g. by considering Taylor series expansions (Braga et al., 2019), Tustin bilinear transforms (Ogata, 1995; Åström and Hägglund, 2011) or using the Cayley-Hamilton Theorem (Heemels et al., 2010). How-

ever, it is worth to point-out that such discrete-time approach may fail to capture the inter-sampling behavior of the continuous-time plant and so stabilize it, especially when large or aperiodic sampling intervals are required (Hetel et al., 2017).

- *Sampled-data Design*: To circumvent the aforementioned drawback of the Direct Design approach, the goal is to take into account the inter-sampling behavior of the continuous-time system for the design of the discrete-time controller with some closed-loop stability guarantees. Among the sampled-data analysis methodologies (Hetel et al., 2017), the most celebrated approaches are the input-delay one (Fridman, 2001) and the study of the problem in the Hybrid framework (Naghshtabrizi et al., 2008; Hetel et al., 2013; Goebel et al., 2009).

Recognizing the attractiveness of both the *Direct Design* and *Sampled-Data design* techniques, a brief survey about these approaches is presented in the sequel. This work investigates these techniques to address the sampled-data controller's design problem for nonlinear systems described by T-S models. In this context, the *Direct Design* has the appeal of having a consolidated framework that allows us to focus the investigation on the input constraints issues and set-point tracking problem. In contrast, the input-delay approach for *Sampled-Data design* appears as an interesting and recent alternative to improve stability guarantees under large and/or aperiodic sampling intervals.

Because of their easy implementation on industrial controllers like PLCs, the direct discrete-time design for sampled-data systems is the most commonly used technique in industry. In the T-S model-based framework, it is the subject of many studies, see e.g. (Guerra and Vermeiren, 2004; Gonzalez and Guerra, 2014; Ichalal et al., 2016; Lendek et al., 2018). Also, most industrial applications involve practical constraints such like input saturation, set-point tracking, and so on. Classical linear Proportional-Integral-Derivative (PID) controllers have been widely recognized both in academic and industrial environments, because of their easy implementation aligned with their nice performance properties. Indeed, the proportional action allows to tune the transient speed, the integral action provides the closed-loop system with robustness against model or static errors, and the derivative part helps to improve settling time and stability of the closed-loop system. A number of tuning rules for conventional PID controllers can be found in the literature, see e.g. (O'Dwyer, 2009). The simplicity, robustness and the success of this classical linear controller has influenced other control research fields, including fuzzy control systems. For instance, in (Qiao and Mizumoto, 1996), a PID-type fuzzy controller has been introduced, that has attracted lots of attention in scientific community. Moreover, several fuzzy PI control applications can be found in different fields such as, among others, in power electronics (Nouri et al., 2017; Tamilarasi and Sivakumaran, 2018), wind energy generation (Ounnas et al., 2016), level control (Gao et al., 2015; Kmetóvá et al., 2013), power train (Dragos et al., 2011), robotics (Fateh, 2010), electrical motors (Precup et al., 2009; Chen et al., 2016), magnetic levitation (Sun et al., 2019; Yu et al., 2010; Yu and Huang, 2009) and spacecraft applications (Sari et al., 2019). Despite an abundant literature in the T-S model-based framework, we observe that a

reduced number of works are concerned with the discrete-time counterpart of fuzzy PI controllers implementation (Precup et al., 2009; Preitl and Precup, 2006; Preitl et al., 2005). Note that the discrete-time counterpart of PI controllers can be convenient to be implemented in cheap digital processors, for instance in embedded or industrial dedicated applications. In this context, discrete-time PI-type controllers, can be implemented in a Parallel Distributed Compensator (PDC) control scheme or in a non-PDC structure for conservatism reduction (Gonzalez and Guerra, 2014). Usually, the PDC structure requires less computational effort allowing to use less expensive processors (Laurain et al., 2018). Moreover, the above mentioned works do not handle actuators' saturation, which can lead to small regions of attraction and poor performances in real world applications (Tarbouriech et al., 2011; Kong and Yuan, 2019). In this case, a local stability analysis is required (Nguyen et al., 2017; Klug et al., 2015; Du and Zhang, 2009), which motivated recent works on T-S model-based control to handle input or state constraints (Nguyen et al., 2017; Fan et al., 2017; Li et al., 2016a; Kong and Yuan, 2019), domain of validity fuzzy models (Lendek et al., 2018; Klug et al., 2015) or even sensors' saturation (Zhang et al., 2017). A consequence of actuators' saturation is the region of attraction in which one must carefully analyze the effects of exogenous inputs in the closed-loop system. Indeed, exogenous signals, such as set-point changes, may drive the trajectories of the system outside of the region of attraction. In this case, both the performance and the stability can be impaired. This effect has been investigated in (Lopes et al., 2018) where non-PDC PI-like controller has been proposed, but with quite small achieved region of attraction. Moreover, in (Lopes et al., 2018), a slow enough time-variation of the state vector of the system is required. However, these bad effects on stability and performance may be mitigated by using an anti-windup action (Zaccarian and Teel, 2011; Mehdi et al., 2014). It is worth to say that to the best of the author's knowledge, no works in the previous literature handle these issues for the design of discrete-time fuzzy PI-like controllers. This point will be the subject of the first contribution of this thesis, developed in **Chapter 2**.

Nevertheless, as mentioned above, one of the main drawbacks of the *Direct Design* approach remains on the fact that discretization procedures bring approximations, leading to loss of information regarding the continuous-time systems' dynamics. Indeed, it is worth to highlight that the so designed discrete-time controller does not strictly guarantee the convergence of the continuous system but rather for the discrete-time model, which is particularly true even when the sampling period cannot be small enough to represent the continuous-time plant correctly. Moreover, note that the digital controller part must synchronize the sampling instants, receives the sampled measures from the ADC, computes the control action and sends it to the DAC (see Figure 1). These tasks are often assumed to be done on a constant sampling interval τ_s basis, which has allowed the development of the discrete-time model-based approach for sampled-data systems. However, this assumption is not always accurate since the intervals between two successive sampling instants may vary due to practical constraints. Indeed, even in a point-to-point digital control topology, clock inaccuracy and system architecture characteristics, such like real-time scheduling, can induce jitters, imperfect synchronization and/or computation delays (Witten-

mark et al., 1995; Hetel et al., 2017). When dealing with Networked Controlled Systems (NCS), in which sampled-data systems are controlled through communication networks (Hetel et al., 2017; Fridman, 2014a), aperiodic sampling intervals are almost inevitable. This is why, several approaches consider triggering the sampling intervals to reduce the network usage (de Souza et al., 2021). To circumvent these problems, the *Sampled-Data Design* approach is investigated in **Chapter 3** and **Chapter 4**. Emerging as a promising research topic in control theory, it consists on the investigation of the overall closed-loop stability of continuous-time plants driven by sampled-data controllers, see, *e.g.* (Fridman et al., 2004). In this approach, the control signals are kept constant during the sampling period, and evolve according to discrete samples of the continuous plant, taking into consideration the inter-sampling behavior of the system. An elegant and powerful way to do so is to rewrite the closed-loop dynamics as a continuous-time system with input-time varying delay, also known as a time-delay approach for stabilization of sampled-data systems (Fridman et al., 2004). Furthermore, it is widely known from the literature that most real applications exhibit nonlinear dynamics, and if many efforts have been made by prior authors to stabilize linear dynamical systems from sampled-data measurements, this is not the case for nonlinear systems. Thus, this problem emerges as an exciting subject for our research, which was first explored in the T-S model-based framework in (Nishikawa et al., 2000). Further, in the specific context of T-S sampled-data controllers, due to the time hybridization of the closed-loop dynamics, asynchronous membership functions arise. This aspect kept the attention of many authors, who have proposed continuous relaxation improvements for the design of sampled-data controllers for T-S systems. For instance, in (Yoneyama, 2010), Lyapunov-Krasovskii Functionals (LKF) and relaxation techniques based on the Leibniz-Newton formula and free-weighting matrix were considered. Moreover, note that the delayed membership functions involved in the fuzzy controller are mismatching the ones existing in the T-S representation of the continuous-time plant. Hence, to handle this issue, several attempts have been proposed: the upper bounds of the asynchronous errors of the membership functions have been assumed to be known and introduced in the design conditions (Zhang and Han, 2011; Lam, 2012; Jia et al., 2014; Zhang et al., 2015); enlargement scheme has been introduced in the stabilization criteria in (Zhu et al., 2012, 2013); the ratio bounds (assumed to be known) of asynchronous membership functions have been considered in (Marouf et al., 2016; Pan and Yang, 2017; Peng et al., 2017) or the upper bounds of the time-derivatives of the membership functions (Wang et al., 2017, 2018; Kim et al., 2018); (Cheng et al., 2017) have implemented a structured vertex separator to reduce the number of LMIs constraints. From these studies, it is clearly shown how important is to take into account the membership functions information into the closed-loop sampled-data stability conditions to reduce their conservatism. However, in the sequel of this thesis, we will show that this brings local results, which have not been considered yet, and so require further meticulous investigation of the closed-loop domain of attraction. Another significant way to reduce the conservatism consists on the convenient choice of a Lyapunov-Krasowskii Functional (LKF), then introducing free weighting matrices, and employing some bounding techniques based on integral terms and modified inequalities (Han and Ma, 2019). A looped LKF

was first proposed for the sampled-data stabilization of linear systems in (Seuret, 2012), then extended to the T-S model-based framework (Lee and Park, 2018; Zeng et al., 2019; Hua et al., 2020). Indeed, looped LKF appears to be relevant for sampled-data systems as it allows to cope at once with the discrete-time and continuous-time nature of the involved quantities. Following these ideas, in **Chapter 3**, from the choice of a convenient looped LKF and the application of the Finsler's Lemma, new LMI conditions are obtained for the design of sampled-data PDC controllers, together with the proposition of a dedicated relaxation scheme for asynchronous double summation structures. Then, these results are extended in **Chapter 4**. From a looped Non-Quadratic Lyapunov-Krasovskii Functional (NQLKF), relaxed controller design conditions for a class of regular nonlinear descriptors subject to actuators' saturation are proposed. Also, throughout this last chapter, it is highlighted that sampled-data control methodology is only valid locally in the T-S model based-framework. Indeed, there are three main sources of locality: the domain of validity of the T-S model, the assumption of the bounds for the time-derivatives of the membership functions to cope with the asynchronous membership functions (and also when considering a NQLKF), and the input constraints due to the actuators' saturation. In any of these cases, the characterization of an estimate of the closed-loop domain of attraction, where the closed-loop stability is guaranteed, is to be done with scrutiny. Particularly, to the best of the author's knowledge, this point of interest has been disregarded by previous authors in the context of stability analysis and controller design for sampled-data nonlinear systems expressed by T-S models, and is an important contribution brought by this work.

Summarizing, the remaining of this manuscript is organized as follows. In **Chapter 1**, the preliminaries on T-S model-based control are provided to better apprehend the contribution of this PhD thesis. **Chapter 2** presents the first contribution, which consists on the anti-windup T-S model-based PI-like set-point tracking control for nonlinear systems with saturated actuators, with enlargement procedure of the guaranteed closed-loop domain of attraction. Then, the input delay approach for the sampled-data stabilization of T-S models is proposed in **Chapter 3**, where conservatism reduction is proposed from the selection of a convenient looped LKF and the proposition of a new relaxation scheme for asynchronous double fuzzy summation structures. These results are extended in **Chapter 4** to the class of T-S descriptors subject to actuators' saturation, together with a meticulous investigation of the resulting sampled-data closed-loop domain of attraction. Finally, this manuscript ends with a general conclusion, where perspective of these works are discussed.

Author's Publications Related to this Work

Journal papers:

- Lopes, A. N. D., Leite, V. J. S., Silva, L. F. P. and Guelton, K. (2020). Anti-windup TS Fuzzy PI-like Control for Discrete-time Nonlinear Systems with Saturated Actuators, *International Journal of Fuzzy Systems* **22**: 46–61.

- Lopes, A. N. D., Guelton, K., Arcese, L. and Leite, V. J. S. (2021). Local Sampled-data Controller Design for T-S Fuzzy Systems with Saturated Actuators, *IEEE Control Systems Letters* **5**(4): 1169–1174.

Papers published in conferences proceedings:

- Lopes, A. N. D., Guelton, K., Arcese, L. and Leite, V. J. (2021a). Sampled-data Controller Design for Mechatronic Systems Described by Takagi-Sugeno Descriptors, *2021 IEEE/ASME International Conference on Advanced Intelligent Mechatronics (AIM)*, pp. 653–660.

- Lopes, A. N. D., Arcese, L. and Guelton, K. (2021). Synthèse non-quadratique de contrôleurs échantillonnés pour les modèles flous de type T-S décrits en temps continu, *Rencontres Francophones sur la Logique Floue et ses Applications (LFA2021)*, Paris, France, pp. 117–124.

- Rouamel, M., Bourahala, F., Lopes, A. N. D., Nafir, N. and Guelton, K. (2021). Mixed Actual and Memory Data-based Event-Triggered H_∞ Control Design for Networked Control Systems, *4th IFAC Conference on Embedded Systems, Computational Intelligence and Telematics in Control*, pp. 1–6.

- Lopes, A. N. D., Arcese, L., Guelton, K. and Cherifi, A. (2020b). Sampled-data Controller Design with Application to the Quanser Aero 2-DOF Helicopter, *2020 IEEE International Conference on Automation, Quality and Testing, Robotics (AQTR)*, pp. 1–6.

- Lopes, A. N. D., Guelton, K., Arcese, L., Leite, V. J. S. and Bourahala, F. (2020a). Finsler-based Sampled-data Controller Design for Takagi-Sugeno systems, *21th IFAC World Congress*, pp. 1–6.

- Bourahala, F., Guelton, K. and Lopes, A. N. D. (2019). Relaxed Non-Quadratic Stability Conditions for Takagi-Sugeno Systems with Time-varying Delays: A Wirtinger's Inequalities Approach, *2019 IEEE International Conference on Fuzzy Systems (FUZZ-IEEE)*, pp. 1–6.

Traduction en Français de l'Introduction Générale:

Dans notre vie quotidienne comme dans l'industrie, la place que prennent les systèmes autonomes ne cesse de croître. Ces dispositifs sont destinés à effectuer de manière autonome des tâches aussi simples que complexes (e.g. dans la fabrication, les services, le divertissement...), rendant accessibles certaines applications, en termes de réduction des coûts ou même de faisabilité, qui n'étaient pas envisageables auparavant. À titre d'illustration, au cours des dernières décennies, en raison de la mondialisation de la production industrielle, le monde manufacturier a été témoin de nombreuses avancées vers des procédés plus efficaces avec des exigences croissantes en matière de qualité, associées à la nécessité de réduire les coûts pour maintenir la compétitivité, avec l'utilisation croissante de robots et/ou de machines spécialisées dans les usines de production (Brecher et al., 2021). Dans ce contexte, l'Industrie 4.0 est apparue comme une étape supplémentaire dans l'intégration des systèmes automatisés. L'utilisation de machines programmables, d'analyses de données de processus et de systèmes interconnectés en réseau permet la fabrication de produits complexes qui exigeaient auparavant de nombreux travailleurs non qualifiés pour seulement quelques autres qualifiés. L'Industrie 4.0 a pour objectif de ramener de la compétitivité pour la fabrication de produits technologiques. Notamment, dans les pays développés, l'automatisation permet de réduire les coût de fabrication alors que les salaires sont plus élevés que dans d'autres pays moins développés, parfois plébiscités en raison des bas salaires, de la faible protection sociale des travailleurs, et de l'allègement des contraintes environnementales (Naghavi, 2007). Ce changement de paradigme doit permettre de réduire les coûts globaux, de réduire les pertes liées au transport entre le site de production et les consommateurs, répondant en partie à la demande de production respectueuse de l'environnement. Par ailleurs, dans notre vie quotidienne, les dispositifs technologiques deviennent de plus en plus essentiels ou inévitables. Par exemple, l'Internet des objets (IoT, appareils connectés) envahit notre quotidien par la domotique (aspirateurs autonomes, ampoules connectées...), dans l'intention de simplifier nos vies. Un autre exemple est la révolution en cours dans les transports, avec l'arrivée probable de véhicules électriques autonomes, ou l'utilisation de véhicules aériens sans pilote (UAV) afin d'effectuer des livraisons, voire pour du divertissement, etc.

Cette contextualisation vise à donner un aperçu du large domaine dans lequel cette thèse s'inscrit. À cet égard, il est important de souligner que la plupart des dispositifs technologiques mentionnés ci-dessus possèdent une dynamique d'évolution en temps continu, habituellement modélisée mathématiquement par un ensemble d'équations différentielles. Aussi, afin d'accomplir les tâches pour lesquelles ils sont conçus, ils doivent habituellement être contrôlés. Par conséquent, avec le développement des nouvelles technologies, de tels contrôleurs sont souvent mis en œuvre à l'aide de dispositifs numériques qui traitent les données de manière discrète, sur la base de l'échantillonnage de signaux mesurés, pour fournir la commande adéquate, e.g. (Ogata, 2010; Åström and Hägglund, 2011). En outre, la dynamique de ces systèmes est souvent non linéaire et leurs capteurs ou actionneurs peuvent être connectés à la partie commande par des canaux de communication numérique. Dans ce contexte, deux points principaux sont à aborder : Le contrôle des systèmes non linéaires, et les caractéristiques hybrides de la dynamique en boucle fermée de ces systèmes où des signaux continus et discrets sont impliqués (Liu et al., 2020; Hetel et al., 2017).

Parmi les nombreuse approches de la théorie du contrôle non linéaire, Tomohiro Takagi et Michio Sugeno ont fourni, au milieu des années 80, une approche intéressante pour représenter les systèmes non linéaires (Takagi and Sugeno, 1985). Initialement basés sur le formalisme flou de règles SI-ALORS, les modèles Takagi-Sugeno (T-S) fournissent des

approximations sous forme polytopique des systèmes non linéaires, i.e. sous forme de sommes pondérées de modèles linéaires locaux. Puis, avec l'introduction de la décomposition en secteurs non linéaires (Kawamoto et al., 1992; Morère, 2001; Tanaka and Wang, 2001), lorsque des modèles non linéaires analytiques sont disponibles, les modèles T-S peuvent représenter exactement des modèles non linéaires sur un compact de leurs espaces d'état. Une telle caractéristique a comblé le fossé qui les séparait d'autres approches polytopiques bien connues et qui étaient développées en parallèle au sein de la communauté automaticienne, à savoir les modèles quasi-LPV, introduits dans (Shamma, 1988; Shamma and Cloutier, 1993), qui sont aujourd'hui communément connus comme équivalents aux modèles T-S.

Une vaste littérature est disponible pour divers problèmes de contrôle basés sur le modèle T-S; par exemple la conception de contrôleurs à temps continu, e.g. (Guerra et al., 2012; Cherifi et al., 2018, 2019); les systèmes à temps discrets, e.g. (Xie et al., 2017a; Lopes et al., 2020b); les systèmes T-S avec retards, e.g. (Peng et al., 2008; Li and Liu, 2009; Bourahala et al., 2017, 2019); ou la synthèse de contrôleur à base de signaux échantillonnées, e.g. (Yoneyama, 2010; Zhang and Han, 2011; Cheng et al., 2017). En effet, grâce à leurs structures polytopiques convexes, les conditions de stabilité et les conditions de synthèse pour les systèmes T-S sont généralement étudiées via la seconde méthode de Lyapunov et résolues sur la base d'inégalités linéaires matricielles (LMIs) (Boyd et al., 1994; Skelton et al., 1998). Néanmoins, ces résultats fondés sur des contraintes LMIs ne fournissent que des conditions suffisantes et souffrent donc de conservatisme, dont la réduction est un défi important et commun au sein de la communauté traitant les approches quasi-LPV/T-S, e.g. (Sala, 2009; Guerra et al., 2015; Lam, 2018; Nguyen et al., 2019a). De ce fait, des améliorations successives ont été proposées afin de relâcher les conditions LMIs; depuis l'utilisation de fonctions quadratiques de Lyapunov (Wang et al., 1996) jusqu'aux fonctions non quadratiques (Jadbabaie, 1999; Blanco et al., 2001; Tanaka et al., 2003; Mozelli et al., 2009; Guerra et al., 2012); en relâchant la structure en double somme paramétrée des conditions LMIs (Kim and Lee, 2000; Tuan et al., 2001; Xiaodong and Qing-ling, 2003); en considérant la classe des modèles descripteurs T-S (Taniguchi et al., 2001; Tanaka et al., 2003; Marx and Ragot, 2008; Guelton et al., 2008); ou encore en tirant parti de la redondance des descripteurs (Tanaka et al., 2007; Guelton et al., 2009; Bouarar et al., 2013). À l'instar de ces travaux antérieurs, cette thèse vise à fournir des procédures de conception relâchées sous la forme de LMIs pour la stabilisation des modèles T-S, en particulier lorsque les systèmes non linéaires en temps continu sont contrôlés par des dispositifs numériques.

Comme mentionné ci-dessus, les algorithmes de contrôle sont aujourd'hui souvent mis en œuvre sur des dispositifs numériques (i.e. évoluant dans une base de temps discret), plutôt que sur des dispositifs analogiques. Cependant, de nombreux systèmes physiques évoluent en temps continu, tandis que l'action des contrôleurs numériques n'est mise à jour qu'à des instants précis et échantillonnés. C'est le cas, par exemple, des systèmes mécatroniques, des systèmes embarqués, des systèmes contrôlés en réseaux, etc. Dans ce contexte, la Figure 1 illustre une topologie de contrôle usuelle d'un système continu, piloté par un contrôleur par retour d'état échantillonné. Celui-ci peut être implémenté dans un Automate Programmable Industriel (API), un ordinateur ou encore une carte microcontrôleur, et éventuellement déporté via un réseau de communication. De plus, sur la base des mesures échantillonnées $x(t_k)$ de l'état du système $x(t)$, fournies par un convertisseur analogique-numérique (ADC), le signal de contrôle d'entrée $u(t_k)$ est transmis au système continu non linéaire à commander via un convertisseur numérique-analogique (DAC) et maintenu par un bloqueur d'ordre zéro (ZOH).

À partir de la littérature, on constate que les principales approches employées pour

répondre à ces exigences, dans lesquelles les applications évoluant en temps continu sont pilotées par des contrôleurs numériques, peuvent être classifiées en trois approches décrites ci-dessous, selon la façon dont est caractérisé l'intervalle d'échantillonnage, la stratégie adoptée pour la synthèse du contrôleur numérique, ou encore les garanties de stabilité associées (Fridman, 2010) :

- *Émulation* : Cette approche consiste en la discrétisation de contrôleurs continus, synthétisés sur la base d'un modèle continu ignorant les contraintes d'échantillonnage. Il s'agit ici d'un choix courant dans les applications pratiques. Toutefois, du point de vue théorique et dans une perspective de recherche rigoureuse, il convient de souligner que l'estimation de la période maximale d'échantillonnage admissible serait très conservative, voire difficile à obtenir (Di Ferdinando and Pepe, 2019).

- *Synthèse Directe* : A partir d'une réalisation discrète du modèle du système à contrôler, une loi de commande en temps discret est synthétisée, sans tenir compte du comportement continu du système entre deux instants d'échantillonnage consécutifs (Lopes et al., 2020b; Ogata, 1995). Notons que les procédures de discrétisation conduisent à des approximations. En effet, la procédure de discrétisation standard considère généralement la célèbre transformation d'Euler (Ogata, 1995). Aussi, des travaux récents sur ce sujet considèrent d'autres procédures de discrétisation pour améliorer la précision des modèles à temps discret, e.g. en considérant les décompositions en série de Taylor (Braga et al., 2019), la transformation bilinéaire de Tustin (Ogata, 1995; Åström and Hägglund, 2011), ou en utilisant le Théorème de Caley-Hamilton (Heemels et al., 2010). Cependant, il convient de souligner qu'une telle approche à temps discret peut ne pas capturer fidèlement le comportement du système continu entre les instants d'échantillonnage successifs, et donc le contrôleur ainsi synthétisé peut échouer à stabiliser le système continu, en particulier lorsque de grands intervalles d'échantillonnage ou des intervalles apériodiques sont nécessaires (Hetel et al., 2017).

- *Synthèse continue-échantillonnée* : Pour contourner l'inconvénient susmentionné de l'approche de *Synthèse Directe*, l'objectif est de prendre en compte le comportement inter-échantillonnage du système à temps continu pour la conception du contrôleur à temps discret avec certaines garanties de stabilité en boucle fermée. Parmi les méthodologies d'analyse des données échantillonnées (Hetel et al., 2017), les approches les plus répandues considère la réécriture de la boucle fermée sous la forme d'un système à retard sur l'entrée (Fridman, 2001) ou l'étude du problème selon le formalisme des systèmes hybrides (Naghshtabrizi et al., 2008; Hetel et al., 2013; Goebel et al., 2009).

Reconnaissant l'attrait des techniques de *Synthèse Directe* et de *Synthèse continue-échantillonnée*, un bref état de l'art sur ces approches est présenté dans la suite. Ce travail étudie ces techniques pour résoudre le problème de synthèse du contrôleur basé sur des données échantillonnées pour les systèmes non linéaires décrits par les modèles T-S. Dans ce contexte, la *Synthèse Directe* dispose d'un cadre consolidé qui nous permet de nous concentrer sur les problèmes de contraintes sur l'entrée et le problème de suivi des points de consigne. En revanche, l'approche de *Synthèse continue-échantillonnée* apparaît comme une alternative intéressante et récente à l'élaboration de conditions garantissant la stabilité en boucle fermée pour des intervalles d'échantillonnage importants et/ou apériodiques.

En raison de leur mise en œuvre facile sur des contrôleurs industriels tels que les APIs, la *Synthèse Directe* à temps discret est la technique la plus couramment utilisée dans l'industrie. Dans le cadre des modèle T-S, cette approche fait l'objet de nombreuses études, e.g. (Guerra and Vermeiren, 2004; Gonzalez and Guerra, 2014; Ichalal et al., 2016; Lendek et al., 2018). En outre, la plupart des applications industrielles possèdent des contraintes pratiques telles que la saturation sur les entrées, le suivi des points de consigne, etc. Les contrôleurs Proportionnel-Intégrale-Dérivée (PID) linéaires classiques sont largement employés en raison de leur facilité de mise en œuvre. En effet, l'action proportionnelle permet de régler le temps de réponse, l'action intégrale fournit au système en boucle fermée une robustesse contre les erreurs statiques, et la partie dérivée contribue à réduire les oscillations du système en boucle fermée. Un certain nombre de règles de réglage pour les contrôleurs PID conventionnels peuvent être trouvées dans la littérature, e.g. (O'Dwyer, 2009).

La simplicité, la robustesse et le succès de ces contrôleurs linéaires classiques ont influencé d'autres domaines de recherche en automatique, y compris les systèmes de contrôle flou. Par exemple, dans (Qiao and Mizumoto, 1996), un contrôleur flou de type PID a été introduit, qui a attiré beaucoup d'attention dans la communauté scientifique. De plus, plusieurs applications de contrôleurs flous PI existent dans différents domaines tels que, entre autres, l'électronique de puissance (Nouri et al., 2017; Tamilarasi and Sivakumaran, 2018), la production d'énergie éolienne (Ounnas et al., 2016), le contrôle de niveau (Gao et al., 2015; Kmetóvá et al., 2013), la robotique (Fateh, 2010), les moteurs électriques (Precup et al., 2009; Chen et al., 2016), la lévitation magnétique (Sun et al., 2019; Yu et al., 2010; Yu and Huang, 2009) et des applications spatiales (Sari et al., 2019). Malgré une littérature abondante dans le cadre des modèles T-S, nous observons qu'un nombre réduit d'études sont concernées par la contrepartie discrète des contrôleurs PI flous et de leur implémentation (Precup et al., 2009; Preitl and Precup, 2006; Preitl et al., 2005). Notons que, la contrepartie de temps discret du contrôleur PI peut être intéressante pour être mis en œuvre sur des processeurs numériques bon marché, ou pour des applications intégrées ou industrielles dédiées. Dans ce contexte, des contrôleurs flous PI à temps discret peuvent être implémentés dans un schéma de Compensation Parallèle Distribuée (PDC) ou dans une structure non-PDC pour la réduction du conservatisme (Gonzalez and Guerra, 2014). Habituellement, la structure PDC nécessite moins d'effort de calcul permettant d'utiliser des processeurs moins coûteux (Laurain et al., 2018). En outre, les travaux mentionnés ci-dessus ne prennent pas en compte la saturation des actionneurs, ce qui peut conduire à de petites régions d'attraction et de mauvaises performances dans les applications réelles (Tarbouriech et al., 2011; Kong and Yuan, 2019). Dans ce cas, une analyse minutieuse de la stabilité locale est requise (Nguyen et al., 2017; Klug et al., 2015; Du and Zhang, 2009), qui a motivé des travaux récents sur le contrôle des modèles T-S soumis à des contraintes d'entrée ou d'état (Nguyen et al., 2017; Fan et al., 2017; Li et al., 2016a; Kong and Yuan, 2019; Lendek et al., 2018; Klug et al., 2015; Zhang et al., 2017). Une conséquence de la saturation des actionneurs est la région d'attraction dans laquelle il faut analyser soigneusement les effets des entrées exogènes dans le système en boucle fermée. En effet, les signaux exogènes, tels que les changements de points de consigne, peuvent entraîner les trajectoires du système en dehors de la région d'attraction. Dans ce cas, la performance et la stabilité peuvent être altérées. Cet effet a été étudié dans (Lopes et al., 2018) où un contrôleur de type PI non-PDC a été proposé, mais conduisant à une région d'attraction relativement restreinte. En outre, dans (Lopes et al., 2018), l'hypothèse d'une variation suffisamment lente du vecteur d'état du système est rendue nécessaire. Cependant, ces effets néfastes sur la stabilité et les performances peuvent être atténués en utilisant une action anti-windup (Zaccarian and Teel, 2011; Mehdi et al.,

2014). Il est intéressant de dire que, à la connaissance de l'auteur, aucune étude antérieure ne considère ces questions pour la synthèse de contrôleurs PI flous à temps discret. Ce point fera l'objet de la première contribution de cette thèse, développée dans le **Chapitre 2**.

Néanmoins, comme cela a été mentionné ci-dessus, l'un des principaux inconvénients de l'approche de *Syntèse Directe* repose sur le fait que les procédures de discrétisation apportent des approximations, conduisant à la perte d'informations concernant la dynamique des systèmes en temps continu. En effet, il convient de souligner que, dans ce cas, le contrôleur à temps discret ainsi conçu ne garantit pas strictement la convergence du système continu, mais seulement celle du système discret, ce qui est particulièrement vrai lorsque la période d'échantillonnage ne peut pas être assez petite pour représenter correctement la dynamique en temps continu.

De plus, notons que la partie commande numérique (voir Figure 1) doit synchroniser les instants d'échantillonnage, recevoir les mesures échantillonnées de l'ADC, calculer l'action de commande et l'envoyer au DAC. Ces tâches sont souvent réalisées sous l'hypothèse d'un intervalle d'échantillonnage τ_s constant, ce qui a permis le développement de l'approche de *Syntèse Directe*. Toutefois, cette hypothèse n'est pas toujours exacte puisque les intervalles successifs entre deux instants d'échantillonnage peuvent varier en raison de contraintes pratiques. En effet, même dans une topologie de contrôle numérique point-à-point, l'imprécision de l'horloge et les caractéristiques de l'architecture du système, comme la programmation en temps réel, peuvent induire une synchronisation imparfaite et/ou des retards de calcul (Wittenmark et al., 1995; Hetel et al., 2017). De plus, lorsqu'il s'agit de systèmes contrôlés en réseau (NCS), les intervalles d'échantillonnage apériodiques sont presque inévitables (Hetel et al., 2017; Fridman, 2014a). Par ailleurs, plusieurs approches envisagent le déclenchement d'intervalles d'échantillonnage variables pour réduire l'utilisation du réseau (de Souza et al., 2021). Pour contourner ces problèmes, l'approche de *Synthèse continue-échantillonnée* est étudiée dans le **Chapitre 3** et le **Chapitre 4**. Émergeant comme un sujet de recherche prometteur dans la théorie du contrôle, cette approche consiste à étudier la stabilité globale en boucle fermée des systèmes en temps continu pilotés par des contrôleurs basés sur des données échantillonnées (Fridman et al., 2004). Dans cette approche, les signaux de contrôle sont maintenus constants pendant la période d'échantillonnage et évoluent selon des échantillons discrets, en tenant compte du comportement inter-échantillons du système continu. Une façon élégante et puissante de le faire est de réécrire la dynamique en boucle fermée en tant que système à temps continu avec des retards variables sur l'entrée (Fridman et al., 2004). En outre, puisque la plupart des applications réelles présentent une dynamique non linéaire, si de nombreux travaux existent pour la stabilisation des systèmes dynamiques linéaires à partir de données échantillonnées, ce n'est pas le cas pour les systèmes non linéaires. Ainsi, ce problème apparaît comme un sujet passionnant, qui a initialement été exploré dans le cadre des modèles T-S dans (Nishikawa et al., 2000). En outre, dans le contexte spécifique des contrôleurs basés sur des données échantillonnées, dans le cadre des modèles T-S, cela conduit à l'hybridation temporelle de la dynamique en boucle fermée, i.e. à l'apparition de fonctions d'appartenance asynchrones. Cet aspect a retenu l'attention de nombreux auteurs qui ont proposés des réductions du conservatisme. Par exemple, dans (Yoneyama, 2010), une fonctionnelle de Lyapunov-Krasovskii (LKF) associée à des techniques de relaxation basées sur la formule de Leibniz-Newton et l'introduction de matrices de décision libres, ont été considérées. Ensuite, considérant que les fonctions d'appartenance retardées impliquées dans le contrôleur flou ne correspondent pas à celles existant dans la représentation T-S du système non linéaire continu, les limites supérieures des erreurs asynchrones sont supposées connues et introduites dans les conditions de synthèse (Zhang

and Han, 2011; Lam, 2012; Jia et al., 2014; Zhang et al., 2015; Zhu et al., 2012, 2013); les limites du ratio (supposées connues) des fonctions d'appartenance asynchrones ont été considérées dans (Marouf et al., 2016; Pan and Yang, 2017; Peng et al., 2017) ou encore les limites supérieures des dérivées temporelles des fonctions d'appartenance dans (Wang et al., 2017, 2018; Kim et al., 2018); un séparateur de sommets structurés pour réduire le nombre de contraintes LMI a été proposé dans (Cheng et al., 2017). À partir de ces études, il est clairement démontré à quel point il est important de tenir compte des fonctions d'appartenance dans les conditions de stabilité des données échantillonnées en boucle fermée pour réduire leur conservatisme. Cependant, dans la suite de cette thèse, nous montrerons que cela conduit à des résultats locaux, qui n'ont pas encore été considérés, et donc nécessitent une étude plus méticuleuse du domaine d'attraction en boucle fermée. Une autre façon significative de réduire le conservatisme consiste à choisir une LKF plus adéquate, puis à introduire des matrices de décision libres, et à employer quelques techniques de majoration des termes sous la forme d'intégrale (Han and Ma, 2019). Une LKF "bouclée" a été proposée pour la stabilisation des données échantillonnées des systèmes linéaires dans (Seuret, 2012), puis étendu au cadre des modèle T-S (Lee and Park, 2018; Zeng et al., 2019; Hua et al., 2020). En effet, l'utilisation d'une LKF "bouclée" s'avère pertinente pour les systèmes de commande à base de données échantillonnées car il permet de faire face à la fois à la nature discrète et continue des quantités concernées. Sur la base de ces idées, dans le **Chapitre 3**, à partir du choix d'une LKF "bouclée" adéquate et de l'application du Lemme de Finsler, de nouvelles conditions de synthèse LMIs sont obtenues, ainsi que la proposition d'un schéma de relaxation dédié pour les structures à double somme asynchrones. Ces résultats sont ensuite étendus dans le **Chapitre 4**. À partir d'une fonctionnelle de Lyapunov-Krasovskii non quadratique (NQLKF) "bouclée", des conditions de synthèse relâchées pour une classe de systèmes descripteurs non linéaires réguliers soumis à la saturation des actionneurs sont proposées. De plus, tout au long de ce dernier chapitre, il est souligné que la méthodologie de commande à base de données échantillonnées n'est valide que localement dans le cadre des modèles T-S. En effet, il existe trois sources principales de contraintes locales : le domaine de validité du modèle T-S, l'hypothèse effectuée sur les dérivées temporelles des fonctions d'appartenance, et les contraintes sur l'entrée dues à la saturation des actionneurs. Dans chacun de ces cas, la caractérisation d'une estimation du domaine d'attraction en boucle fermée, où la stabilité en boucle fermée peut être garantie, doit être effectuée avec un examen minutieux. Notons que, à la connaissance de l'auteur, ce point d'intérêt a été ignoré par la plupart des auteurs dans les études précédentes, ce qui constitue une contribution importante de ce travail de thèse.

En résumé, le reste de ce manuscrit est organisé comme suit. Dans le **Chapitre 1**, les préliminaires sur la commande des modèle T-S sont fournis pour mieux appréhender la contribution de cette thèse de doctorat. Le **Chapitre 2** présente la première contribution de ce travail de thèse, qui consiste en la proposition de nouvelles conditions LMI pour la synthèse de lois de commande PI en suivi de consigne, avec action anti-windup, pour les modèles T-S en temps discret soumis à des saturations sur l'entrée. Ensuite, l'approche de *Synthèse continu-échantillonnée*, pour la stabilisation des modèles T-S continus par des contrôleurs discrets est considérée dans **Chapitre 3**, où des réductions du conservatisme sont proposées à partir de la sélection d'une LKF "bouclée" adéquate et de la proposition d'un nouveau schéma de relaxation pour les structures à double somme asynchrones. Ces résultats sont étendus dans le **Chapitre 4** à la classe de systèmes T-S descripteurs soumis à des saturations des actionneurs, ainsi qu'à une étude minutieuse du domaine d'attraction en boucle fermée qui en résulte. Enfin, dans la conclusion générale, les perspectives de ces travaux sont discutées.

Chapter 1

Preliminaries on T-S model-based approaches and sampled-data control

Résumé en Français : Préliminaires sur les approches à base de modèles T-S et la commande échantillonnée.

Ce chapitre donne une vue d'ensemble des méthodes et des techniques employées dans cette thèse. Il présente également quelques investigations préliminaires dans le but de mieux cerner le problème étudié et les verrous scientifiques associés pour établir clairement les objectifs de ce travail de thèse. Ainsi, le principal objectif de cette thèse est de proposer de nouvelles conditions relâchées sous la forme d'inégalités matricielles linéaires (LMI) pour la synthèse de contrôleurs basés sur des données échantillonnées, dans le but de garantir la stabilité asymptotique des systèmes non linéaires à temps continu, commandés par des contrôleurs numériques.

Parmi les approches dévolues au contrôle des systèmes non linéaires, nous nous focaliserons sur celles relevant des modèles de type quasi-LPV/T-S (Takagi and Sugeno, 1985; Shamma and Cloutier, 1993). En effet, ceux-ci permettent de représenter fidèlement les systèmes non linéaires par des modèles polytopiques convexes sur un compact de leurs espaces d'états. Ainsi dans ce chapitre, après avoir présenté la classe des modèles de type quasi-LPV/T-S à temps continu et les différentes méthodes pour les obtenir, nous présentons comment définir les modèles à temps discret qui leur sont associés avec une période d'échantillonnage constante. Ensuite, à partir de la seconde méthode de Lyapunov, les conditions élémentaires de stabilité et de synthèses de contrôleurs sont présentées sous forme de LMIs, dans le cas continu et le cas discret (Tanaka et al., 2001). Puisque de telles conditions ne sont que suffisantes, des méthodes classiquement employées pour réduire le conservatisme sont présentées (Sala, 2009).

Sur la base de ces travaux pionniers pour les systèmes quasi-LPV/T-S, les limitations de la synthèse de contrôleurs pour les modèles à temps discret sont discutées ainsi que certaines contraintes pratiques telles que la saturation des actionneurs. En effet, une approche basée sur les modèles à temps discret ne donne des résultats satisfaisant que pour des périodes d'échantillonnage relativement petites au regard de la dynamique du système considéré. Aussi, une alternative intéressante est présentée. Celle-ci consiste à représenter la dynamique en boucle fermée par un système à retard variable sur l'entrée (Fridman et al., 2004), lorsqu'un système continu est contrôlé sur la base de données échantillonnées. Notons que cette approche convient également lorsque de larges intervalles apériodiques d'échantillonnage sont nécessaires (Hetel et al., 2017).

Sur la base de l'ensemble des considérations mises en lumière dans ce chapitre, en soulignant certaines limites et défis dans le cadre de la stabilisation des systèmes T-S à temps continu à partir de contrôleurs numériques, ce chapitre se termine par une conclusion où les principales contributions de cette thèse, présentées dans les chapitres suivants sont introduites. À savoir : la synthèse de contrôleurs Proportionnel-Intégral (PI) locaux pour le suivi de consignes continues par morceaux des modèles T-S à temps discret dans le ***Chapitre 2****; la réduction de conservatisme pour la synthèse de contrôleur échantillonné pour les systèmes T-S à temps continu par l'approche à retard variable sur l'entrée dans le* ***Chapitre 3****; L'extension de cette approche pour le cas des systèmes T-S descripteurs soumis à des saturations sur l'entrée, conjointement à l'estimation du domaine d'attraction en boucle fermée, dans le* ***Chapitre 4****.*

1.1 Introduction

This chapter gives an overview of the methods and techniques employed in this thesis. It also presents some preliminary investigations, done to fill gaps in the comprehension of the studied problem, which helped to define the methodology and establishing the goals. At the end of this chapter, it should be clear that our main target in this thesis is to propose relaxed Linear Matrix Inequalities (LMI) based conditions for the design of sampled-data controllers, in order to guarantee the asymptotic stability of continuous-time nonlinear systems driven by digital devices.

Among the nonlinear control theory, we focus on quasi-LPV/T-S approaches because of their faculty to accurately represent nonlinear systems as convex polytopic systems. Hence, in this chapter, after presenting the class of continuous-time quasi-LPV/T-S models and the different ways to obtain them, we present how to get their discrete-time realization from constant sampling periods. Then, based on the second Lyapunov method, the basic stability and controller design conditions are presented in terms of LMIs. Also, because such conditions are only sufficient, the most common ways to reduce their conservatism are presented. From these basic approaches, the limitations of discrete-time model-based controller design will be discussed, together with some practical constraints like actuators' saturation. Finally, an elegant alternative to discrete-time model based approaches, suitable when large aperiodic sampling intervals are required, namely the input time-varying delay approach for sampled-data systems, is presented, with highlights on the fact that it is only locally suitable in the T-S model based framework.

Based on the proposed materials and consideration, pointing-out some limitations and challenges involved in the context of stabilizing continuous-time T-S systems from sampled-data controllers, this chapter ends with a conclusion where the main contributions of this thesis, brought in the next chapters, are introduced.

1.2 Presentation of Quasi-LPV / Takagi-Sugeno models

In this thesis, we consider the class of affine-in-control nonlinear dynamical systems represented by their nonlinear state space models given by:

$$\begin{cases} \dot{x}(t) = f_x(x(t), u(t)) \\ y(t) = g_y(x(t), u(t)) \end{cases} \tag{1.1}$$

where $x(t) \in \mathbb{R}^n$, $u(t) \in \mathbb{R}^m$ and $y(t) \in \mathbb{R}^q$ are respectively the system's state, input and output time-varying vectors; $f_x : \mathbb{R}^{n+m} \to \mathbb{R}^n$ and $g_y : \mathbb{R}^{n+m} \to \mathbb{R}^q$ are nonlinear functions of the state and input vectors'.

Note that (1.1) describes the nonlinear input-output relationships of a nonlinear system where the first equation, called the state space equation, consists in a finite number of coupled first-order ordinary differential equations, while the second equation, called the output equation, represents the direct static transfer from the state and input to the outputs. Moreover, in the sequel of this thesis, rather than output feedback control approach, which is the subject of many specific studies from the literature (see e.g. (Zerar et al., 2008; Guelton et al., 2009; Chadli and Guerra, 2012; Bouarar et al., 2013; Estrada-Manzo et al., 2019) and reference therein), we will stay in the context of state feedback control, with the following assumption, where the characterization of the output equation is not required.

Assumption 1.1. *In the sequel of this thesis, we assume that the nonlinear system* (1.1) *is affine-in-control without direct transfer from the input to the output, such that* (1.1) *can be reduced to:*

$$\begin{cases} \dot{x}(t) = f(x(t)) + B(x(t))u(t) \\ y(t) = g(x(t)) \end{cases} \tag{1.2}$$

where $f : \mathbb{R}^n \to \mathbb{R}^n$, $B : \mathbb{R}^n \to \mathbb{R}^{n\times m}$ *and* $g : \mathbb{R}^n \to \mathbb{R}^q$ *are nonlinear functions depending only on the state entries.*

Among the nonlinear control approaches, Takagi-Sugeno (T-S) fuzzy models (Takagi and Sugeno, 1985) have been widely considered in the past few decades because of their ability to represent a large class of nonlinear systems as convex polytopic systems. A vast literature is available for various T-S model-based control problems, for instance dealing with continuous-time controller design (see e.g. (Guerra et al., 2012; Cherifi et al., 2014, 2018)), discrete-time ones (see e.g. (Guerra et al., 2009; Xie et al., 2017b)), or also the control of T-S systems with time-delays (see e.g. (Peng et al., 2008; Li and Liu, 2009; Bourahala et al., 2017)). Historically, T-S fuzzy models (Takagi and Sugeno, 1985) propose to represent affine-in-control nonlinear models (1.2) by the inference of r fuzzy rules with, as conclusion part, local analytic linear state space models. Thereby, the i-th rules ($i \in \mathcal{I}_r$) of a T-S fuzzy model can be described in the following form:

$$\begin{aligned} \textit{Rule } i\textit{:}\quad & \textbf{IF } z_1(t) \text{ is } M_{i1} \text{ and } \cdots \text{ and } z_p(t) \text{ is } M_{ip}, \\ & \textbf{THEN } \begin{cases} \dot{x}(t) = A_i x(t) + B_i u(t) \\ y(t) = C_i x(t) \end{cases} \end{aligned} \tag{1.3}$$

where, for $i = 1, \ldots, r$ and $j = 1, \ldots, p$, $z_j(t)$ are premise variables depending only (for control purpose) on the states and/or on the output of the system and M_{ij} are fuzzy sets; the matrices $A_i \in \mathbb{R}^{n\times n}$, $B_i \in \mathbb{R}^{n\times m}$ and $C_i \in \mathbb{R}^{q\times n}$ are known constant matrices describing the dynamics of each local linear models.

For the antecedent part of each i-th fuzzy rule, a weighting function $w_i(t)$ is assigned. It characterizes the instantaneous contribution of each sub-model of the T-S model, and this function depends on the grade of membership of the premise variables z_p regarding a fuzzy subset M_{ij} such as:

$$w_i(z(t)) = \prod_{j=1}^{p} M_{ij}(z_j(t)) \geq 0, \quad i \in \mathcal{I}_r, \tag{1.4}$$

where $z(t) = \begin{bmatrix} z_1(t) & z_2(t) & \cdots & z_p(t) \end{bmatrix}^T$ is the vector of premises.

Hence, we can define the normalized membership function as:

$$\alpha_i(z(t)) = \frac{w_i(z(t))}{\sum_{j=1}^{r} w_j(z(t))} \tag{1.5}$$

which holds, $\forall t$, the convex sum properties $\alpha_i(z(t)) \geq 0$ and $\sum_{i=1}^{r} \alpha_i(z(t)) = 1$.

Then, considering such fuzzy inferences, yields the T-S model in its compact defuzzified form given by:

$$\begin{cases} \dot{x}(t) = \sum_{i=1}^{r} \alpha_i(z(t)) \left(A_i x(t) + B_i u(t)\right) \\ y(t) = \sum_{i=1}^{r} \alpha_i(z(t)) C_i x(t) \end{cases} \tag{1.6}$$

Remark 1.1. *Note that T-S models (1.6) belong to the class of polytopic systems (i.e., a collection of linear systems blended together by time-varying functions). In the control literature, other class of polytopic systems are often considered to deal with nonlinear or quasi-linear control. For instance, Linear Parameter Varying (LPV) systems, introduced in (Shamma, 1988), also belong to the class of polytopic systems. Their main difference with the above described T-S models relies on the fact that LPV models are weighted by time-varying parameters that does not necessary or analytically depend on the states or input variables of the systems. Another interesting class of polytopic systems, namely quasi-LPV systems, has been introduced in (Shamma and Cloutier, 1993) to provide an exact representation of an affine-in-control nonlinear system on a compact set of its state space. It is worth to point-out that the scheduling parameters of quasi-LPV systems depend on the state (or eventually the input) variables, similarly to T-S models. Indeed, as it will be shown in the next section, with the development of the sector nonlinearity approach for obtaining T-S models that exactly match nonlinear ones (Kawamoto et al., 1992; Tanaka and Wang, 2001; Morère, 2001), the gap has been filled so that they are nowadays known as strictly equivalent to quasi-LPV models.*

1.2.1 Construction of a T-S fuzzy Model

The construction of the T-S fuzzy model is an essential step for the analysis and synthesis of a Fuzzy Model-Based (FMB) control system. In a practical fashion, the fuzzy T-S models can be obtained through an identification or linearization procedure or from a convex polytopic transformation usually based on the sector nonlinearity. In the sequence, these three approaches are summarized.

Identification: Initially proposed in the pioneer works of Takagi and Sugeno (Takagi and Sugeno, 1985), basically consists on the identification from input/output data of the structure and parameters of the system around a set of predefined operation points. Then, these local models are blended together with chosen membership functions (gaussian, triangular, trapezoidal, etc.), which parameters can be further adjusted, as proposed in (Gasso et al., 2000). If these approaches are very appealing when an analytic nonlinear model of the plant is unavailable, let us recall that such obtained T-S models are only approximately representing the nonlinear systems, so those results (stability analysis, controller and observer design...) should be considered with caution.

Linearization: This method is based on the linearization of a nonlinear model around a finite number of operating points (Ma et al., 1998; Tanaka and Wang, 2001). Then a T-S representation is obtained by the interconnection of the local linear polytopes by some well chosen membership functions (gaussian, triangular, trapezoidal, etc.). We must highlight that this approach also results in an approximation of the nonlinear system and usually the number of models depends on the complexity of the system, the specified modeling precision and the choice of the membership functions.

Sector Nonlinearity Approach: The idea of using the sector nonlinearity for the construction of the fuzzy T-S representation is based on the idea that, for any continuous scalar nonlinear functions $f : \mathbb{R} \to \mathbb{R}$, with $f(0) = 0$, there exists $\mathcal{D}_x \subseteq \mathbb{R}$ such that, $\forall x \in \mathcal{D}_x$ we have $f(x) \in \begin{bmatrix} a_1 & a_2 \end{bmatrix} x$ where a_1 and a_2 are finite scalars. Then, when $\mathcal{D}_x = \mathbb{R}$, the nonlinear sector is said to be global, otherwise, when $\mathcal{D}_x \subset \mathbb{R}$ (e.g. $\mathcal{D}_x = \{x \in [-d, d]\}$, with $d > 0$) it is local, as illustrated in Figure 1.1 (Tanaka and Wang, 2001).

For a large majority of systems it is reasonable to have a well defined operation region and consequently to have bounded state variables. So, it is wise to use this information for the fuzzy T-S model construction, which will be exactly matching the nonlinear model in a compact subset of its state space, to generalize the above definition of nonlinear sectors for $x(t) \in \mathbb{R}^n$, given by:

$$\mathcal{D}_x = \{x(t) \in \mathbb{R}^n \mid \mathfrak{L}x(t) \leq d\} \tag{1.7}$$

where κ is the number of bounds of the state variables, which constitutes the entries of the vector $d \in \mathbb{R}^\kappa$ and $\mathfrak{L} \in \mathbb{R}^{\kappa \times n}$ is a state component selection matrix.

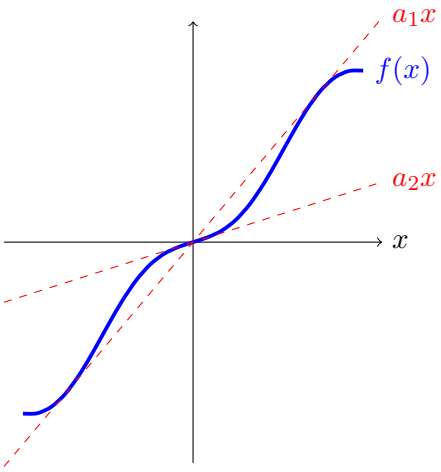

Figure 1.1: Global sector nonlinearity.

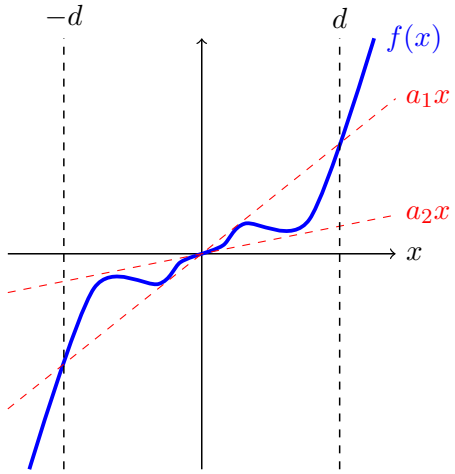

Figure 1.2: Local sector nonlinearity.

The set $\mathcal{D}_x$ defines the domain of validity of the fuzzy T-S model. Therefore, a systematic procedure to obtain the vertices and membership functions of the fuzzy T-S model can be applied, for instance based on the following Lemma 1.1 inspired from (Morère, 2001).

Lemma 1.1. *Let $f_s : \mathcal{D}_x \to [\underline{f}_s, \bar{f}_s]$ a bounded function. There always exists a pair of scalar functions $w_1 : \mathcal{D}_x \to [0,1]$ and $w_2 : \mathcal{D}_x \to [0,1]$ and two scalars a and b such that:*

$$f_s(x) = w_1(x)a + w_2(x)b,$$

where $w_1(x) + w_2(x) = 1$.

For instance, let us assume that the nonlinear affine-in-control systems (1.2) can be rewritten as:

$$\begin{cases} \dot{x}(t) = A(x(t))x(t) + B(x(t))u(t) \\ y(t) = C(x(t))x(t) \end{cases} \tag{1.8}$$

where the matrices $A(x(t)) \in \mathbb{R}^{n\times n}$, $B(x(t)) \in \mathbb{R}^{n\times m}$ and $C(x(t)) \in \mathbb{R}^{q\times n}$ contain p nonlinear entries of the state variables, denoted $f_j : \mathcal{D}_x \to [\underline{f}_j, \bar{f}_j]\,(j \in \mathcal{I}_p)$.
Then, $\forall x(t) \in \mathcal{D}_x$, with $a, b \geq 0$ we can write:

$$f_j(x(t)) = \underbrace{\frac{f_j(x(t)) - \underline{f}_j}{\bar{f}_j - \underline{f}_j}}_{w_j^1(x(t))} \bar{f}_j + \underbrace{\frac{\bar{f}_j - f_j(x(t))}{\bar{f}_j - \underline{f}_j}}_{w_j^2(x(t))} \underline{f}_j, \tag{1.9}$$

with $w_j^1(x(t)) + w_j^2(x(t)) = 1$, $w_j^1(x(t)) \geq 0$ and $w_j^2(x(t)) \geq 0$.

So, we may readily get a T-S model in the compact form (1.6) that exactly matches (1.8) on $\mathcal{D}_x$ with the following $r = 2^p$ normalized membership functions $\alpha_i(x(t))(i \in \mathcal{I}_r)$ and matrices

defining the vertices:

$$\begin{cases} \alpha_1(x(t)) = w_1^1(x(t))w_2^1(x(t))\dots w_{p-1}^1(x(t))w_p^1(x(t)),\ M_1 = M(\bar{f}_1, \bar{f}_2, \dots, \bar{f}_{p-1}, \bar{f}_p), \\ \alpha_2(x(t)) = w_1^1(x(t))w_2^1(x(t))\dots w_{p-1}^1(x(t))w_p^2(x(t)),\ M_2 = M(\bar{f}_1, \bar{f}_2, \dots, \bar{f}_{p-1}, \underline{f}_p), \\ \alpha_3(x(t)) = w_1^1(x(t))w_2^1(x(t))\dots w_{p-1}^2(x(t))w_p^1(x(t)),\ M_3 = M(\bar{f}_1, \bar{f}_2, \dots, \underline{f}_{p-1}, \bar{f}_p), \\ \alpha_4(x(t)) = w_1^1(x(t))w_2^1(x(t))\dots w_{p-1}^2(x(t))w_p^2(x(t)),\ M_4 = M(\bar{f}_1, \bar{f}_2, \dots, \underline{f}_{p-1}, \underline{f}_p), \\ \quad \vdots \\ \alpha_{r-2}(x(t)) = w_1^1(x(t))w_2^2(x(t))\dots w_{p-1}^1(x(t))w_p^2(x(t)),\ M_{r-2} = M(\bar{f}_1, \underline{f}_2, \dots, \bar{f}_{r-1}, \underline{f}_p), \\ \alpha_{r-1}(x(t)) = w_1^2(x(t))w_2^1(x(t))\dots w_{p-1}^2(x(t))w_p^1(x(t)),\ M_{r-1} = M(\underline{f}_1, \bar{f}_2, \dots, \underline{f}_{p-1}, \bar{f}_p), \\ \alpha_p(x(t)) = w_1^2(x(t))w_2^2(x(t))\dots w_{p-1}^2(x(t))w_p^2(x(t)),\ M_r = M(\underline{f}_1, \underline{f}_2, \dots, \underline{f}_{-1}, \underline{f}_p), \end{cases} \tag{1.10}$$

where $M \in \{A, B, C\}$.

Remark 1.2. *It is worth to emphasize that only the sector nonlinearity approach provides a methodology to get a T-S model which exactly matches a nonlinear one on a compact subset of its state space $\mathcal{D}_x$. As a consequence, analysis of nonlinear systems based on such obtained T-S models are often only locally valid inside $\mathcal{D}_x$ (especially when $\mathcal{D}_x \subset \mathbb{R}^n$ is obtained from local sectors). Therefore, when dealing with stability analysis, control or observer design, the characterization of the domain of attraction should be investigated. Moreover, when T-S models are obtained from identification or linearization, since they are only approximating the considered nonlinear systems, no formal guarantee can be provided, especially when critical constraints are introduced. This last point will be illustrated through simulation examples along the thesis.*

In the sequence, two examples give an overview on the procedure to obtain a fuzzy T-S representation for a nonlinear system from the sector nonlinearity approach.

Example 1.1. *Let us consider the following academic example of a nonlinear system:*

$$\begin{cases} \dot{x}_1(t) = 2x_1(t) + x_1(t)x_2(t) + (2 - \cos x_2(t))u(t) \\ \dot{x}_2(t) = -2x_1(t)\cos x_2(t) + x_2(t) \end{cases} \tag{1.11}$$

Defining $x(t) = \begin{bmatrix} x_1(t) & x_2(t) \end{bmatrix}^T$, *it can be rewritten as:*

$$\dot{x}(t) = A(x(t))x(t) + B(x(t))u(t) \tag{1.12}$$

with:

$$A(x(t)) = \begin{bmatrix} 2 & x_1(t) \\ -2\cos x_2(t) & 1 \end{bmatrix} \text{ and } B(x(t)) = \begin{bmatrix} 2 - \cos x_2(t) \\ 0 \end{bmatrix}$$

which includes two nonlinear functions $f_1(x(t)) = x_1(t)$ and $f_2(x(t)) = \cos x_2(t)$, that are dependent on the state variables. From (1.9), to obtain a T-S representation, $\forall (x_1(t), x_2(t)) \in [-b,\, a] \times \mathbb{R} = \mathcal{D}_x$, we can write:

$$f_1(x(t)) = \underbrace{\frac{x_1(t)+b}{a+b}}_{w_1^1(z(t))} a + \underbrace{\frac{a-x_1(t)}{a+b}}_{w_1^2(z(t))}(-b) \text{ and } f_2(x(t)) = \underbrace{\frac{\cos x_2(t)+1}{2}}_{w_2^1(z(t))} 1 + \underbrace{\frac{1-\cos x_2(t)}{2}}_{w_2^2(z(t))}(-1)$$

So, from (1.10), we readily get the following normalized membership functions and vertices:

$$\begin{cases} \alpha_1(x(t)) = w_1^1(x(t))w_2^1(x(t)),\ A_1 = \begin{bmatrix} 2 & a \\ -2 & 1 \end{bmatrix},\ B_1 = \begin{bmatrix} 1 \\ 0 \end{bmatrix}, \\ \alpha_2(x(t)) = w_1^1(x(t))w_2^2(x(t)),\ A_2 = \begin{bmatrix} 2 & a \\ 2 & 1 \end{bmatrix},\ B_2 = \begin{bmatrix} 3 \\ 0 \end{bmatrix}, \\ \alpha_3(x(t)) = w_1^2(x(t))w_2^1(x(t)),\ A_3 = \begin{bmatrix} 2 & -b \\ -2 & 1 \end{bmatrix},\ B_3 = B_1, \\ \alpha_4(x(t)) = w_1^2(x(t))w_2^2(x(t)),\ A_4 = \begin{bmatrix} 2 & -b \\ 2 & 1 \end{bmatrix},\ B_4 = B_2, \end{cases}$$

which define the following T-S models with $r = 4$:

$$\dot{x}(t) = \sum_{i=1}^{4} \alpha_i(z(t))(A_i x(t) + B_i u(t)) \tag{1.13}$$

where, $\forall i \in \mathcal{I}_r$, $\alpha_i(z(t)) \geq 0$ and $\sum_{i=1}^{4} \alpha_i(z(t)) = 1$.

Example 1.2 (1 Degree of Freedom (DOF) Inverted Pendulum)**.** *The first step when projecting model based controllers is to obtain a good representation of the original system. Let us consider the problem of stabilizing the inverted pendulum depicted in Figure 1.3. The dynamical behavior of this system can be described by the following differential equation:*

$$mgL\sin\theta(t) - kL\dot{\theta}(t) + u(t) = mL^2\ddot{\theta}(t)$$

where $\theta(t)$ denotes the angular position regarding the vertical axis, $u(t)$ is the control input torque, $g = 9.8\ m/s^2$ is the gravitational acceleration, $m = 0.5\ kg$ refers to the pendulum mass, $L = 0.8\ m$ is associated with the length of the Pendulum and last, $k = 0.2\ SI$ is the coefficient of friction at the pivot point.

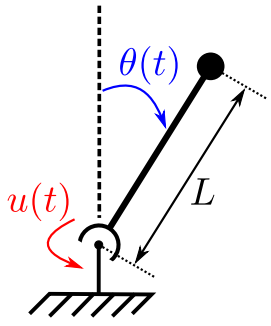

Figure 1.3: 1-DOF Inverted Pendulum.

Defining the state vector $x^T(t) = \begin{bmatrix} \theta(t) & \dot{\theta}(t) \end{bmatrix}$, a state-space representation of (1.3) can be given as:

$$\dot{x}(t) = \begin{bmatrix} 0 & 1 \\ \frac{g}{L}\frac{\sin x_1(t)}{x_1(t)} & -\frac{k}{mL} \end{bmatrix} x(t) + \begin{bmatrix} 0 \\ \frac{1}{mL^2} \end{bmatrix} u(t) \tag{1.14}$$

Taking benefit from the fact $z(x_1(t)) = (\sin x_1(t))/x_1(t) \in [\rho, 1]$ *is always bounded (e.g., for* $x_1(t) \in \mathbb{R}$, $\rho \approx -0.217234$*), we get:*

$$z(x(t)) = \underbrace{\frac{z(x(t)) - \rho}{1 - \rho}}_{\alpha_1(x(t))} 1 + \underbrace{\frac{1 - z(x(t))}{1 - \rho}}_{\alpha_2(x(t))} \rho \tag{1.15}$$

which readily gives the following globally matching T-S model with $r = 2$*:*

$$\dot{x}(t) = \sum_{i=1}^{2} \alpha_i(x(t)) \left(A_i x(t) + B_i u(t)\right) \tag{1.16}$$

with:

$$A_1 = \begin{bmatrix} 0 & 1 \\ \frac{g}{L} & -\frac{k}{mL} \end{bmatrix}, A_2 = \begin{bmatrix} 0 & 1 \\ \frac{g}{L}\rho & -\frac{k}{mL} \end{bmatrix} \text{ and } B_1 = B_2 = \begin{bmatrix} 0 \\ \frac{1}{mL^2} \end{bmatrix}.$$

1.2.2 Discrete-time T-S fuzzy models

Until now, we presented T-S models in the continuous-time framework. However, some dynamical systems may also evolve in the discrete-time. This is the case of digital systems, where the dynamics is characterized by discrete sequences of $k \in \mathbb{N}$. Also, recall that most of continuous-time systems are nowadays driven by digital devices. In this case, design procedures are often based on a discretized representation of their continuous-time dynamics. This being said, a discrete-time version of T-S models is given by the following recurrence equation:

$$\begin{cases} x_{k+1} = \sum_{i=1}^{r} \alpha_i(z_k) \left(\mathcal{A}_i x_k + \mathcal{B}_i u_k\right) \\ y_k = \sum_{i=1}^{r} \alpha_i(z_k) \mathcal{C}_i x_k \end{cases} \tag{1.17}$$

where $x_k \in \mathbb{R}^n$, $u_k \in \mathbb{R}^m$ and $y_k \in \mathbb{R}^q$ denote respectively the state, the input and the output vectors taken at the discrete instant k; $\forall i \in \mathcal{I}_r$, $\mathcal{A}_i \in \mathbb{R}^{n \times n}$, $\mathcal{B}_i \in \mathbb{R}^{n \times m}$ and $\mathcal{C}_i \in \mathbb{R}^{q \times n}$ are real constant matrices describing the local discrete-time dynamics of the system.

In this thesis, we are mainly focused on the control of continuous-time systems by digital controllers. Therefore, let us now discuss the way to get a discrete-time T-S model (1.17) from the continuous-time ones (1.6). One of the most considered approach consists in the forward Euler discretization of the continuous-time system (Chen, 1999; Tanaka and Wang, 2001). Hence, let:

$$\dot{x}(t) = \lim_{\tau_s \to 0} \frac{x(t + \tau_s) - x(t)}{\tau_s}, \tag{1.18}$$

Then, when $\tau_s \to 0$, from the continuous-time T-S model (1.6), we can write:

$$\begin{cases} x(t + \tau_s) = \sum_{i=1}^{r} \alpha_i(z(t)) \left((I + \tau_s A_i)x(t) + \tau_s B_i u(t)\right) \\ y(t) = \sum_{i=1}^{r} \alpha_i(z(t)) C_i x(t) \end{cases} \tag{1.19}$$

Therefore, assuming a sampling period τ_s, at sampling instant $t_k = k\tau_s$ ($k \in \mathbb{N}$), the discrete-time T-S model (1.17) approximates the continuous-time one (1.6) with:

$$\mathcal{A}_i = (I + \tau_s A_i),\ \mathcal{B}_i = \tau_s B_i \text{ and } \mathcal{C}_i = C_i. \tag{1.20}$$

As a matter of fact, it is often assumed that the error introduced by discretization is negligible when a sufficiently small enough sampling period is selected regarding the highest-frequency component of a system time response. In this context, the Shannon sampling Theorem brings some rules for choosing an appropriated sampling period.

Theorem 1.1 (Shannon sampling Theorem)**.** *(Åström and Hägglund, 2011) For a uniformly sampled digital signal processing system, an analog signal can be perfectly recovered as long as the sampling rate is at least twice as large as the highest-frequency component of the analog signal to be sampled.*

However, identifying the highest-frequency component of a system time-response can be complex, and usually, a more empirical rule is adopted. From this approach, the constant sampling period τ_s is often taken in order to produce a ratio of 4 to 10 times between the rise time τ_r and the fixed sampling interval τ_s, i.e., to have the sampling rate 4 to 10 times faster than the system dominant time constant τ_c in the case of first-order systems (Åström and Hägglund, 2011).

Moreover, it is important to highlight that the choice of the sampling period τ_s has a great influence on the discrete-time realization, and, sometimes due to the control project limitations such as cost reduction or energy consumption, it is necessary to find a suitable trade-off between catching all of the dynamics of the plant or alleviating the hardware requirements for the control device. Some other approaches exist to obtain a discrete-time approximation of a continuous-time system with better accuracy than the forward Euler approach, e.g. using Tustin bilinear transforms (Ogata, 1995; Åström and Hägglund, 2011), using Taylor series expansions or the Cayley-Hamilton theorem (Heemels et al., 2010), or more recently using a descriptor system-based approach in the T-S framework (Braga et al., 2019). Even if appealing, these will be left-out from this thesis since it is not our purpose to compare every discretization approaches.

Remark 1.3. *The choice of the sampling period τ_s may affect the accuracy of the discrete-time representation of a continuous-time system. Therefore, when considering discrete-time realization for the stability analysis, control or observer design, conclusions regarding to the continuous-time system must be taken with care, especially when τ_s cannot be chosen small enough. Indeed, in this case, it is well-known that discrete-time models fail to capture the inter-sampling behavior of dynamical continuous-time systems (Hetel et al., 2017). This absence of guarantee for large sampling period can be seen as a drawback of such approaches, especially when the controller is implemented on a low-cost device or when considering networked control systems to drive plants, and especially when they involve fast dynamics.*

The usual way to obtain a T-S discrete-time model from a continuous one being presented, the following example is proposed to illustrate the effect of the choice of the sampling period τ_s on the accuracy of the discrete-time realization.

Example 1.3. *Consider the continuous-time T-S model of the 1-DOF inverted pendulum presented in (1.16). Assuming a sampling period τ_s allows us to obtain a discrete-time T-S model*

(1.17) *with* $r = 2$ *and the following matrices:*

$$\mathcal{A}_1 = \begin{bmatrix} 1 & \tau_s \\ \frac{g}{L}\tau_s & 1 - \frac{k}{mL}\tau_s \end{bmatrix}, \mathcal{A}_2 = \begin{bmatrix} 1 & \tau_s \\ \frac{g}{L}\tau_s\rho & 1 - \frac{k}{mL}\tau_s \end{bmatrix} \text{ and } \mathcal{B}_1 = \mathcal{B}_2 = \begin{bmatrix} 0 \\ \frac{\tau_s}{mL^2} \end{bmatrix} \tag{1.21}$$

If obtaining the matrices (1.21) *via Euler discretization for the discrete-time T-S fuzzy model* (1.16) *happens to be an easy task, the choice of the constant sampling instant is not so evident since we are dealing with an unstable nonlinear systems. Indeed, from the best of author's knowledge, there is no generic approach in the literature to find the minimal sampling interval required to precisely describe this class of systems. Thus, two approaches are explored to give some thoughts on how to choose a reasonable value for the fixed sampling period* τ_s*.*

First, the open-loop time response of the continuous system (1.14) *is compared with the one for the discrete-time T-S fuzzy model* (1.17) *with* (1.21) *and different values of* τ_s *picked as* $1ms$*,* $5ms$*,* $20ms$ *and* $50ms$*. The open-loop responses are depicted in Figure 1.4 to illustrate the compromise between accuracy and sampling effort. For that simulation, the system initial condition* $x(0) = \begin{bmatrix} \pi/6 & 0 \end{bmatrix}^T$*. To compare these first results, Figure 1.4 also plots the normalized error between the state variable* $\theta(t)$ *of the continuous-time response and its discrete counterpart* $\theta(t_k)$ *for each discrete-time model. It shows that the discrete-time fuzzy model with a sampling period of* $\tau_s = 50ms$ *does not represent the inverted-pendulum dynamics around the equilibrium point* $\theta = \pi$*, meanwhile, the choice of* $\tau_s = 20ms$ *produced a closely-related behavior. However, seeing the zoom box, we can notice a kind of induced delay, probably related to the Zero-Order Hold* (ZOH)*, and an error of about* 10%*. Then, our choice is confined to* $1ms$ *or* $5ms$*, if the first option delivery an accuracy of at about* 1%*, it also requires* 5 *times faster samplings than the second, while the error from it raise to less than* 3%*. So, thinking in terms of compromise, it seems that* $\tau_s = 5ms$ *is a reasonable choice for the constant sampling period.*

In other hand, let us highlight that, because the introduction of a controller makes the closed-loop dynamics having different characteristics (constant of time, highest frequency components...) than the open-loop, the above chosen sampling period may be irrelevant for closed-loop systems. To illustrate this fact, let us consider here a continuous-time linear state feedback controller $u(t) = Kx(t)$*, with* $K = \begin{bmatrix} 4.24 & 0.16 \end{bmatrix}$*, to stabilize this 1 DOF inverted pendulum around its unstable equilibrium point (*$\theta = 0$*) with closed-loop eigenvalues* $\lambda_{1,2} = -0.5 \pm i\sqrt{(3)}/2$*. Then, the continuous-time dynamics is discredited using the forward Euler approach with different values of* τ_s *picked as* $20ms$*,* $50ms$*,* $100ms$*,* $200ms$ *and* $300ms$*. For all these cases, the closed-loop time-responses are depicted in Figure 1.5 with there respective normalized discretization errors. From these results, we now notice that choosing* $\tau_s = 20ms$ *brings a normalized error which is less than* 3%*, which is almost the same than in the open-loop test but with a four times larger sampling period. This illustrate the difficulty to choose the most suitable sampling period in this discrete-time controller design framework.*

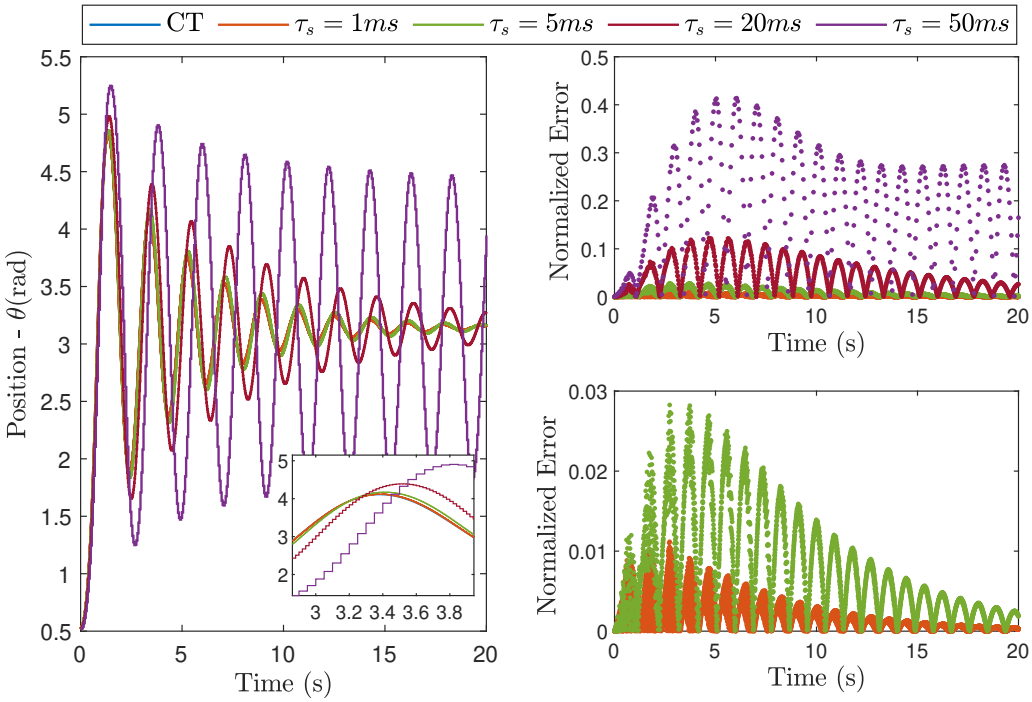

Figure 1.4: Open-loop response for discrete-time fuzzy T-S models taken from different sampling periods τ_s compared with the continuous-time version.

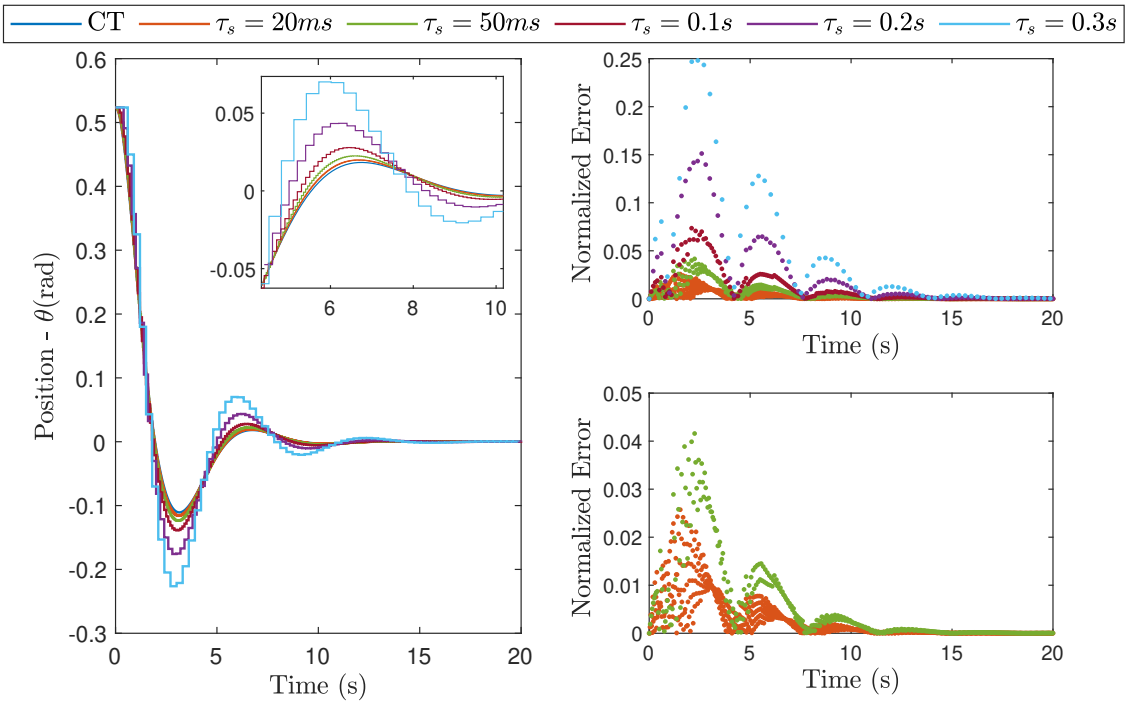

Figure 1.5: Comparison between the time response of the closed-loop system regarding its discrete-time fuzzy T-S model considering different sampling periods τ_s together with the normalized error.

1.3 Basic Stability Analysis and Stabilization of T-S models

In this section, the goal is to present the basic stability conditions for T-S models, then to present their extension to controller design. Because T-S models belong to the class of nonlinear systems, we will first recall some basics of the Lyapunov theory, which is commonly considered in this framework.

1.3.1 Second Lyapunov method for the stability analysis of dynamical systems

One of the most important results in the analysis of dynamical system was the theory proposed by Aleksandr Lyapunov, at the end of the 19th century in its original thesis "The general problem of the stability of motion", translated from Russian in (Lyapunov, 1992). The main idea relies in the fact that if a dynamical system loses energy over time and the energy is never restored, then the system must grind to a stop and reach some final resting state.

Let us consider an autonomous nonlinear system given in the continuous-time framework by:

$$\dot{x}(t) = f(x(t)) \tag{1.22}$$

or in the discrete-time framework by:

$$x_{k+1} = f(x_k) \tag{1.23}$$

where the origin $\mathcal{O}$ is, without loss of generality by a change of origin, assumed to be an equilibrium point.

The concept of stability is strictly related to the Lyapunov stability theory. This theory establishes that systems whose trajectories asymptotically converge to an equilibrium point progressively lose energy in a monotonic way. Lyapunov generalizes the notion of energy using a $V : \mathbb{R}^n \to \mathbb{R}_+$ function called "Lyapunov candidate function" which depends on the system's states. This function is usually a norm or a distance. The main theorems, adapted from (Khalil, 2001) for the continuous and discrete-time framework, are given in the sequence.

Theorem 1.2. *Let $x = \mathcal{O}$ be an equilibrium point for (1.22) in the continuous-time framework (or (1.23) in the discrete-time framework). Let $V : \mathbb{R}^n \to \mathbb{R}$ be a continuously differentiable function. It is said to be a candidate Lyapunov function if:*

$$V(0) = 0 \text{ and } V(x) > 0, \forall x \neq \mathcal{O} \tag{1.24}$$

Then, the continuous-time system (1.22) (or the discrete-time system (1.23)) is asymptotically stable (at least locally at the origin $\mathcal{O}$) and V is said to be a Lyapunov function if, $\forall x(t) \neq \mathcal{O}$:

$$\dot{V}(x) < 0, \text{ in the continuous-time framework,} \tag{1.25}$$

or:

$$V(x_{k+1}) - V(x_k) < 0, \text{ in the discrete-time framework,} \tag{1.26}$$

Moreover, if V is radially unbounded, then the continuous-time system (1.22) (or the discrete-time system (1.23)) is globally asymptotically stable if:

$$||x|| \to \infty \Rightarrow V(x) \to \infty \tag{1.27}$$

Next, another definition of the Lyapunov stability conditions is presented which uses comparison functions, known as class $\mathcal{K}$ functions and defined as follows.

Definition 1.1 (Class $\mathcal{K}$ comparison functions (Khalil, 2001))**.** *A continuous function $\beta : [0, a) \to [0, \infty)$ is said to belong to class $\mathcal{K}$ if it is strictly increasing and $\beta(0) = 0$. It is said to belong to class $\mathcal{K}_\infty$ if $a = \infty$ and $\beta(r) \to \infty$ as $r \to \infty$.*

Theorem 1.3. *Let $x = \mathcal{O}$ be an equilibrium point of (1.22) in the continuous-time framework (or (1.23) in the discrete-time framework) and Ω a neighborhood of the origin $\mathcal{O}$. Let $V : \mathbb{R}^n \to \mathbb{R}$ be a candidate Lyapunov function. If there exists three class $\mathcal{K}$ functions β_1, β_2 and β_3 such that, $\forall x \in \Omega$:*

$$\beta_1(||x||) \leq V(x) \leq \beta_2(||x||), \tag{1.28}$$

and:

$$\dot{V}(x) \leq -\beta_3(||x||), \text{ in the continuous-time framework,} \tag{1.29}$$

or:

$$V(x_{k+1}) - V(x_k) \leq -\beta_3(||x||), \text{ in the discrete-time framework,} \tag{1.30}$$

then the system is asymptotically stable (at least locally at the origin $\mathcal{O}$) and V is a Lyapunov function.
Moreover, if $\Omega = \mathbb{R}^n$ and β_1, β_2 and β_3 are $\mathcal{K}_\infty$ functions, V is radially unbounded and the system is globally asymptotically stable.

From Theorem 1.2, a continuously differentiable function $V(x)$ satisfying (1.24) and (1.25) (or (1.26)) is called a Lyapunov function and, for some $c > 0$, $V(x) = c$ is called an equipotential level set of Lyapunov. Therefore, the condition $\dot{V} \leq 0$ implies that when a trajectory crosses an equipotential of Lyapunov, the system's trajectories necessary move towards a lower equipotential and so, the set $\mathcal{L}(c) = \{x \in \mathbb{R}^n | V(x) \leq c\}$ is said to be contractive and the trajectories can never come out again. That property is often used when only local stability can be guaranteed, i.e. when (1.27) cannot be satisfied, to characterize an estimate of the stability domain of attraction.

The main definition of the Lyaponov stability conditions which will be considered in this thesis being presented, the next subsection provides the pioneer results on the stability analysis of T-S models.

1.3.2 Stability Analysis and Stabilization of T-S Models

In the context of polytopic models, Linear Matrix Inequalities (LMIs) are a fundamental tool for the stability analysis and synthesis of controllers for nonlinear systems and can be

easily implemented through convex optimization techniques (*e.g.,* see (Skelton et al., 1998; Boyd et al., 1994; Scherer et al., 1997)). Since the introduction of semidefinite programming (SDP), several problems from control theory have been formulated as a convex optimization problem and numerically solved. They seldom include a linear objective function subject to a constraint written as an affine combination of symmetric matrices (Boyd et al., 1994).

Together, the Lyapunov functions were extensively employed for the stability study of polytopic systems (Boyd et al., 1994; Tanaka and Wang, 2001; Scherer et al., 1997). The main advantage of this combination is the possibility of expressing the stability criteriums in terms of LMIs. This last has been efficiently numerically solved using interior-point methods, and from this approach, an optimal solution is guaranteed. Today, several software toolboxes are available to write LMIs problems like the Control Robust Toolbox for MATLAB®(Gahinet et al., 1995) and YALMIP (Löfberg, 2004) and solve them via interior-point algorithms, such as SeDuMi (Sturm, 1999) and Mosek (ApS, 2019).

In the next subsections, we will provide the basic LMI-based quadratic stability conditions for autonomous T-S models, then the pioneer LMI-based results for T-S model-based quadratic design of dedicated controllers.

Quadratic stability analysis:

Let us focus on the stability analysis of the following autonomous T-S models:

$$\dot{x}(t) = \sum_{i=1}^{r} \alpha_i(z(t)) A_i x(t) \tag{1.31}$$

or in their discrete-time version:

$$x_{t+k} = \sum_{i=1}^{r} \alpha_i(z_k) \mathcal{A}_i x_k \tag{1.32}$$

Then, to apply Theorem 1.2, consider the following Quadratic Lyapunov Function (QLF) candidate:

$$V(x) = x^T P x, \text{ with } x \equiv x(t) \text{ or } x \equiv x_k, \tag{1.33}$$

which satisfies (1.24) if $P \in \mathbb{R}^{n \times n}$ is a symmetric and positive definite Lyapunov candidate matrix.

The continuous-time T-S model (1.31) or the discrete-time T-S model (1.32)) are asymptotically stable (at least locally) if, $\forall x \neq \mathcal{O}$:

- *In continuous-time framework:*

$$\dot{V}(x(t)) = \dot{x}^T(t) P x(t) + x^T(t) P \dot{x}(t) = x^T(t) \sum_{i=1}^{r} \alpha_i(z(t)) \left(A_i^T P + P A_i \right) x(t) < 0 \tag{1.34}$$

- *In discrete-time framework:*

$$V(x_{k-1}) - V(x_k) = x_{k+1}^T P x_{k+1} - x_k^T P x_k = x_k^T \sum_{i=1}^{r} \alpha_i(z_k) \left(\mathcal{A}_i^T P \mathcal{A}_i + P \right) x_k < 0 \tag{1.35}$$

The T-S models (1.31) and (1.32) being convex polytopic models, we always have $\alpha_i(x) \geq 0$ ($\forall i \in \mathcal{I}_r$), yielding to the first quadratic stability conditions given as a convex optimization procedure to be solved as LMIs and summarized by the following theorem.

Theorem 1.4. *(Tanaka and Sugeno, 1992) The autonomous continuous-time T-S model (1.31) (or the discrete-time T-S model (1.32)) is asymptotically stable (at least locally) if there exists $0 < P = P^T \in \mathbb{R}^{n\times n}$ such that the following LMI's are satisfied for all $i \in \mathcal{I}_r$:*

$$A_i^T P + P A_i < 0, \text{ in the continuous-time framework,} \tag{1.36}$$

$$A_i^T P A_i - P < 0, \text{ in the discrete-time framework.} \tag{1.37}$$

The basic quadratic stability conditions having been established, the following subsection presents their extension to controller design.

Quadratic design of stabilizing PDC controllers:

T-S models belonging to the class of convex polytopic systems, assuming that the state are available from measurement, and assuming that the premise variables depend only on the state, a convenient way to drive them is to employ a gain-scheduled polytopic controller based on the same interconnection structure (membership functions), namely the Parallel-Distributed-Compensation (PDC) state feedback controllers given by, for continuous-time T-S models (1.6):

$$u(t) = \sum_{j=1}^{r} \alpha_j(z(t)) K_j x(t) \tag{1.38}$$

and for discrete-time T-S models (1.17):

$$u_k = \sum_{j=1}^{r} \alpha_j(z_k) K_j x_k \tag{1.39}$$

Substituting the PDC control laws (1.38) and (1.39) into (1.6) and (1.17), respectively expresses the continuous-time and discrete-time closed-loop dynamics as:

$$\dot{x}(t) = \sum_{i=1}^{r}\sum_{j=1}^{r} \alpha_i(z(t))\alpha_j(z(t)) \left(A_i + B_i K_j\right) x(t) \tag{1.40}$$

and:

$$x_{k+1} = \sum_{i=1}^{r}\sum_{j=1}^{r} \alpha_i(z_k)\alpha_j(z_k) \left(\mathcal{A}_i + \mathcal{B}_i K_j\right) x_k \tag{1.41}$$

Therefore, assuming a candidate quadratic Lyapunov function (1.33) and applying Theorem 1.2, we can readily get that the closed-loop dynamics (1.40) and (1.41) are respectively asymptotically stable (at least locally) if:

$$\sum_{i=1}^{r}\sum_{j=1}^{r} \alpha_i(z(t))\alpha_j(z(t)) \Big((A_i + B_i K_j)^T P + P(A_i + B_i K_j) \Big) < 0 \tag{1.42}$$

and:

$$\sum_{i=1}^{r}\sum_{j=1}^{r} \alpha_i(z_k)\alpha_j(z_k) \Big((\mathcal{A}_i + \mathcal{B}_i K_j)^T P (\mathcal{A}_i + \mathcal{B}_i K_j) - P \Big) < 0 \tag{1.43}$$

From the Schur complement, (1.43) is equivalent to:

$$\sum_{i=1}^{r}\sum_{j=1}^{r}\alpha_i(z_k)\alpha_j(z_k)\begin{bmatrix} -P & \star \\ \mathcal{A}_i+\mathcal{B}_iK_j & -P^{-1}\end{bmatrix}<0 \tag{1.44}$$

Then, let $M_j = K_jP^{-1}$, by congruence of (1.42) with $X = P^{-1}$ and (1.43) with $\texttt{diag}\{X, I\}$, and from the fact that:

$$\sum_{i=1}^{r}\sum_{j=1}^{r}\alpha_i(.)\alpha_j(.)\Gamma_{ij} = \sum_{i=1}^{r}\alpha_i^2(.)\Gamma_{ij} + \frac{1}{2}\sum_{i=1}^{r}\sum_{j=1}^{r}\alpha_i(.)\alpha_j(.)(\Gamma_{ij}+\Gamma_{ji}),$$

we get the conditions expressed in the following theorem.

Theorem 1.5. *(Tanaka et al., 1998) The continuous-time T-S model (1.6) (or the discrete-time T-S model (1.17)) is asymptotically stabilized (at least locally) by the PDC control law (1.38) (or (1.39)) if there exists $0 < X = X^T \in \mathbb{R}^{n\times n}$ such that the following LMI's are satisfied for all $(i, j) \in \mathcal{I}_r^2$:*

$$\Gamma_{ii} < 0 \tag{1.45}$$

$$\Gamma_{ij}+\Gamma_{ji} < 0,\ \forall i < j \tag{1.46}$$

with:

$$\Gamma_{ij} = A_iX + XA_i^T + B_iM_j + M_j^TB_i^T, \text{ in the continuous-time framework,} \tag{1.47}$$

and:

$$\Gamma_{ij} = \begin{bmatrix} -X & \star \\ \mathcal{A}_iX+\mathcal{B}_iM_j & -X\end{bmatrix}, \text{ in the discrete-time framework.} \tag{1.48}$$

In that case, the PDC controller gains and Lyapunov matrices can be recovered by the change of variables $K_j = M_jX^{-1}$ and $P = X^{-1}$.

Remark 1.4. *It is worth to highlight that, when T-S models are obtained from global sectors from nonlinear systems, we get $\mathcal{D}_x = \mathbb{R}^n$ and the satisfaction of the conditions in Theorem 1.4 or Theorem 1.5 guarantee global asymptotical stability since the quadratic Lyapunov function (1.33) satisfies (1.27). However, when T-S models are obtained from local sectors from nonlinear systems, it implies $\mathcal{D}_x \subset \mathbb{R}^n$, so the result turns local and an estimate of the domain of attraction can be characterized by searching the outermost level set $c > 0$ such that $\mathcal{L}(c) = \{x \in \mathbb{R}^n \,|\, V(x) \leq c\} \subseteq \mathcal{D}_x$.*

The conditions of Theorem 1.4 and Theorem 1.5 do not require any information about the membership functions, which holds the convex sum properties. This implies that these conditions are only sufficient ones and so suffer from conservatism (Sala and Ariño, 2007). In other words, not finding a solution for a convex optimization problem from these conditions does not mean that the considered T-S model is unstable or cannot be stabilized. Different ways to reduce the conservatism of LMI-based conditions will be discussed in the next subsection.

Before going to the next subsection, let us highlight some limitations from the use of discrete-time T-S model based approach to control a continuous-time system. Indeed, because the discretization of a continuous-time system involves approximations, it is well-known that such

designed discrete-time controller ensures the stability of the discrete-time model, but not necessarily of the original continuous-time system it is dedicated to, especially when large sampling period are considered. This happens because the inter-sampling behavior of a continuous-time system is lost in the above detailed discrete-time framework (Hetel et al., 2017). To circumvent such drawback, appealing approaches appeared during the last few decades, especially the input-delay approach for sampled-data systems (Fridman et al., 2004; Hetel et al., 2017), which will be further presented and the focus of our contributions in Chapters 3 and 4.

Some usual ways to relax LMI-based conditions for T-S models:

As mentioned above, the basic conditions expressed for the stability analysis and controller design suffer from conservatism. Among the sources of conservatism investigated, we recall in the following the currently investigated ones in the T-S model-based framework, which will be considered to get the new results proposed in this thesis.

First, note that the closed-loop dynamics (1.40) and (1.41) involve a convex double sum structure and so, also the Lyapunov conditions (1.42) and (1.44). Hence, checking the negativity of all their vertices make the results very pessimistic. A first relaxation of such double sum constraint is presented in Theorem 1.5. However, further relaxation improvements have been proposed in the literature, see e.g. (Kim and Lee, 2000; Tuan et al., 2001; Xiaodong and Qingling, 2003). In this thesis, we will consider Tuan's relaxation lemma given below, since it is commonly considered as a good compromise between complexity and conservatism reduction (Sala, 2009; Lam, 2018).

Lemma 1.2. *(Tuan et al., 2001): For $(i,j) \in \mathcal{I}_r^2$, let Γ_{ij} be matrices of appropriate dimensions. The inequality $\sum_{i=1}^{r}\sum_{j=1}^{r} \alpha_i(.)\alpha_j(.)\Gamma_{ij} < 0$ is satisfied if the following conditions hold:*

$$\forall i \in \mathcal{I}_r : \Gamma_{ii} < 0 \tag{1.49}$$

$$\forall (i,j) \in \mathcal{I}_r^2, i \neq j : \frac{2}{r-1}\Gamma_{ii} + \Gamma_{ij} + \Gamma_{ji} < 0 \tag{1.50}$$

Another widely investigated source of conservatism is the choice of a candidate Lyapunov function. Indeed, with the QLF (1.33), solving the conditions of Theorem 1.4 or 1.5 means that we need to find a common decision variable P, solution to a set of several LMI constraints, which is indeed restrictive. To relax such conditions, one of the most considered approach is to employ a Non-Quadratic Lyapunov Function (NQLF) candidate introduced by (Jadbabaie, 1999), for instance for controller design in the continuous-time case:

$$V(x(t)) = x^T(t)\left(\sum_{i=1}^{r}\alpha_i(z(t))P_i\right)^{-1}x(t) \tag{1.51}$$

with the non-PDC control law:

$$u(t) = \sum_{i=1}^{r}\alpha_i(z(t))K_i\left(\sum_{j=1}^{r}\alpha_j(z(t))P_j\right)^{-1}x(t) \tag{1.52}$$

The application of Theorem 1.2 leads to the non-quadratic closed-loop stability condition given by:

$$\sum_{i=1}^{r}\sum_{j=1}^{r}\alpha_i(z(t))\alpha_j(z(t))\left(A_iP_j+P_jA_i^T+B_iK_j+K_j^TB_i^T\right)-\sum_{k=1}^{r}\dot{\alpha}_k(z(t))P_k<0 \tag{1.53}$$

Note that (1.53) involves the derivatives of the membership functions (this vanishes in the discrete-time framework as shown in (Guerra and Vermeiren, 2004)). To cope with this, assuming that $|\dot{\alpha}_k(z(t)|\leq\phi_k$, we can bound (1.53), as firstly proposed in (Jadbabaie, 1999; Blanco et al., 2001), by:

$$\sum_{i=1}^{r}\sum_{j=1}^{r}\alpha_i(z(t))\alpha_j(z(t))\left(A_iP_j+P_jA_i^T+B_iK_j+K_j^TB_i^T\right)+\sum_{k=1}^{r}\phi_kP_k<0 \tag{1.54}$$

Then, refinements have been proposed to further reduce the conservatism of (1.54), see e.g. (Tanaka et al., 2003, 2007; Mozelli et al., 2009; Guerra et al., 2012). Among them, we provide below the conditions proposed in (Mozelli et al., 2009) since they also constitute a good compromise between complexity and conservatism reduction.

Lemma 1.3. *(Mozelli et al., 2009) Assume that $|\dot{h}_k|\leq\phi_k,\ \forall k\in\mathcal{I}_r$. The T-S fuzzy system (1.6) is stable if the following LMIs are satisfied:*

$$\begin{aligned}&P_i=P_i^T>0,\quad i\in\mathcal{I}_r,\\&P_i+X\geq 0,\quad i\in\mathcal{I}_{r-1}\},\\&\bar{P}_\phi+\frac{1}{2}(A_i^TP_j+P_jA_i+A_j^TP_i+P_iA_j)<0,\quad i\leq j,\end{aligned} \tag{1.55}$$

where $(i,j)\in\mathcal{I}_r^2$, $\bar{P}_\phi=\sum_{k=1}^{r-1}\phi_k(P_k+X)$, and ϕ_k are scalars.

Furthermore, it is important to highlight that, assuming the bounds of the time-derivatives make the results valid only locally in the regard of the compact subset:

$$\mathcal{D}_\phi=\bigcap_{k=1}^{r}\{x(t)\in\mathbb{R}^n:\ |\dot{\alpha}_k(z)|\leqslant\phi_k\} \tag{1.56}$$

which, combined with the domain of validity of the T-S model $\mathcal{D}_x$, allows to provide an estimate of the domain of attraction by searching the outermost level set $c>0$ such that $\mathcal{L}(c)=\{x\in\mathbb{R}^n|V(x)\leq c\}\subseteq\mathcal{D}_x\cap D_\phi$.

Remark 1.5. *In the above non-quadratic context, we need to estimate the bounds of the time-derivatives which are parameters to solve the LMI conditions. This task is in general difficult or even impossible if global stability results are required. Otherwise, in (Guerra et al., 2012), a systematic approach has been proposed to avoid setting these parameters while providing an estimate of the closed-loop domain of attraction. Some other approaches consider the use of Line-Integral Lyapunov functions (Rhee and Won, 2006), but restricted to second order systems (Guelton et al., 2010, 2014), or consider Lyapunov functions involving the mean values of the membership functions (Marquéz et al., 2017; Cherifi et al., 2019), appealing when membership*

functions are piecewise continuous, which is not the purpose of this thesis. This being said, in some special cases, the bounds of the time-derivatives of the membership functions can be analytically computed (see e.g. Chapter 3, Subsection 3.5.2) or, when considering local results and input limitations, an estimate of the bounds can be numerically computed as it will be shown in Chapter 4.

Finally, another way of interest for this thesis to reduce the conservatism is the introduction of slack decision variables into the stability conditions. This can be done, for instance, by considering descriptor redundancy approaches (Tanaka et al., 2007; Guelton et al., 2009; Bouarar et al., 2010, 2013), by applying Peaucelle's transforms (Peaucelle et al., 2000; Cherifi et al., 2019) or the Finsler's Lemma (Skelton et al., 1998; Oliveira et al., 2011; Jaadari et al., 2012; Bourahala and Guelton, 2017), or S-procedure (Tarbouriech et al., 2011; Boyd et al., 1994) presented below.

Lemma 1.4. *Finsler's Lemma (Skelton et al., 1998). Let $\xi \in \mathbb{R}^n$, $G \in \mathbb{R}^{m\times n}$ and $Q = Q^T \in \mathbb{R}^{n\times n}$ such that $rank(G) < n$. The following statements are equivalent:*

$$\xi^T Q \xi < 0, \quad \forall \xi \in \{\xi \in \mathbb{R}^n : \xi \neq 0, G\xi = 0\} \tag{1.57}$$

$$\exists R \in \mathbb{R}^{n\times m} : Q + RG + G^T R^T < 0 \tag{1.58}$$

Lemma 1.5. *S-procedure (Boyd et al., 1994). Let $T_0, \ldots, T_p \in \mathbb{R}^{n\times n}$ be symmetric matrices. If there exists $\lambda_1 \geq 0, \ldots, \lambda_p \geq 0$, such that*

$$T_0 - \sum_{i=1}^{p} \lambda_i T_i > 0 \tag{1.59}$$

then

$$x^T T_0 x > 0, \forall x \neq 0 \text{ such that } x^T T_i x \geq 0,\ i = 1, \ldots, p$$

When $p = 1$, the converse holds if there exists x_0 such that $x_0^T T_1 x_0 > 0$.

1.4 Preliminaries on specific control problems investigated in the sequel of the thesis

The basics on T-S models and their stability analysis and controller design being now recalled, let us now introduce the preliminaries related to the more specific control problems investigated in the sequel of this thesis. First, because most physical systems are subject to actuators' limitation, the preliminary concepts which will be used in this thesis to deal with such issues will be presented (Tarbouriech et al., 2011). Then, because it has been shown that some issues may occur when applying discrete-time model-based controller design for continuous-time systems, we present some preliminaries on input-delay approaches for sampled-data controller design (Fridman et al., 2004; Hetel et al., 2017).

1.4.1 Preliminaries on controller design with actuators' limitations

Among the practical characteristics sometimes miscarried in controller design procedures, the saturation of actuators is one of the most critical aspects (Tarbouriech et al., 2011; Hu and Lin, 2003). When not correctly considered, actuators saturation can lead to limit-cycles, the emergence of new equilibrium points, degeneration in performance, or the induction of unstable behavior even on stable systems. Indeed, since it is present in nearly all systems and processes, actuator saturation remains an essential investigation subject. In this context, let us consider the following nonlinear affine-in-control system (1.2), where the input signal is constrained such that:

$$\dot{x}(t) = A(x(t))x(t) + B(x(t))\mathtt{sat}u(t) \tag{1.60}$$

where $A(x(t)) \in \mathbb{R}^{n\times n}$ and $B(x(t)) \in \mathbb{R}^{n\times m}$ are matrices that may nonlinearly depend only on the state entries, and $\mathtt{sat}(u_{(\ell)}(t))$ is a generic saturation function, where $-\underline{u}_{(\ell)}$ and $\bar{u}_{(\ell)}$ are the minimum and maximal value allowed for the ℓ-th control signal, which define the compact set of input values denoted by:

$$\mathcal{D}_u = \{u(t) \in \mathbb{R}^m : -\underline{u} \leq \mathtt{sat}(u(t)) \leq \bar{u}\} \tag{1.61}$$

where the inequalities are to be understood component-wise.

To illustrate the saturation function, let us consider the state-feedback control law (1.38), rewritten as $u(t) = K(x(t))x(t)$ to alleviate the mathematical expressions, constrained by the saturation function:

$$\mathtt{sat}(K(x(t))x(t))_{(\ell)} = \begin{cases} \bar{u}_{(\ell)} & \text{if} \quad (K(x(t))x(t))_{(\ell)} > \bar{u}_{(\ell)} \\ (K(x(t))x(t))_{(\ell)} & \text{if} \quad -\underline{u}_{(\ell)} \leq (K(x(t))x(t))_{(\ell)} \geq \bar{u}_{(\ell)} \\ -\underline{u}_{(\ell)} & \text{if} \quad (K(x(t))x(t))_{(\ell)} < -\underline{u}_{(\ell)} \end{cases} \tag{1.62}$$

According to the saturation function, when actuators reach their saturation level, a nonlinearity is introduced into the closed-loop dynamics, leading to degradation of the closed-loop performance (which may be even unstable), even when the open-loop system is stable. To deal with such issue, three main approaches are often considered. The first one considers that the saturation is written in terms of polytopic models (Hu and Lin, 2003), in the second, saturation regions are defined (Molchanov and Pyatnitskiy, 1989) and in the third, the actuator saturation is treated as a sector nonlinearity (Khalil, 2001). In the sequel of this work, the developments are limited to the third approach since it has been found less conservative than polytopic approaches, especially when the characterization of the closed-loop domain of attraction is needed (Tarbouriech et al., 2011).

Generally speaking, the stabilization of nonlinear systems under saturated actuators can be considered as a Lur'e problem (Tarbouriech et al., 2011), with the dead-zone sector-nonlinearity defined as follows.

Definition 1.2. *The dead-zone is a saturated signal defined as* $\psi(u(t)) = \mathtt{sat}(u(t)) - u(t)$*, with*

$\psi(u(t)) \in \mathbb{R}^q$ *such that,* $\forall \ell = 1, \ldots, q$*:*

$$\psi(u_{(\ell)}(t)) = \begin{cases} \bar{u}_{(\ell)} - u_{(\ell)}(t) & \text{if} \quad u_{(\ell)}(t) > \bar{u}_{(\ell)} \\ 0 & \text{if} \quad -\underline{u}_{(\ell)} \leq u(t) \leq \bar{u}_{(\ell)} \\ -u_{(\ell)}(t) - \underline{u}_{(\ell)} & \text{if} \quad u_{(\ell)}(t) < -\underline{u}_{(\ell)} \end{cases},$$

The closed-loop dynamics can be expressed as:

$$\dot{x}(t) = (A(x(t)) + B(x(t))K(x(t)))x(t) + B(x(t))\psi(u(t)), \tag{1.63}$$

Hence, the design of the controller's gain $K(x(t))$ will only ensure the local closed-loop stability of (1.63) and the goal is to provide relaxed margins regarding the input saturation, as illustrated in Figure 1.6, given by:

$$-\underline{u}^{\lambda}_{(\ell)} = \frac{-\underline{u}_{(\ell)}}{1-\lambda_{(\ell)}} \leq u_{(\ell)}(t) \leq \frac{\bar{u}_{(\ell)}}{1-\lambda_{(\ell)}} = \bar{u}^{\lambda}_{(\ell)}$$

where $\lambda_{(\ell)} \in [0, 1)$.

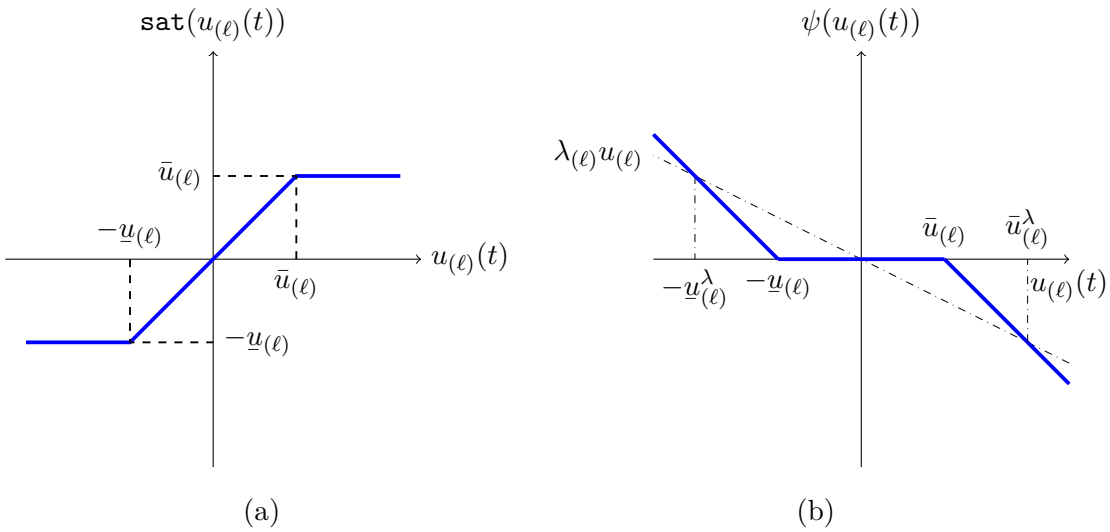

(a) (b)

Figure 1.6: Functions: (a) saturation, and (b) Dead-zone non-linearity in a local sector.

Therefore, the design of a controller which locally stabilizes the closed-loop dynamics (1.63) can be done with the second Lyapunov method (see e.g. Theorem 1.2), while considering the following Lemma to cope with the dead-zone nonlinearity $\psi(u(t))$ (see Chapter 2 and 4 for more developments in the context of this thesis).

Lemma 1.6. *Generalized Sector Condition, Lemma 1.6 in (Tarbouriech et al., 2011). Consider the vector* $\bar{u} \in \mathbb{R}^m$ *and signals* $u \in \mathbb{R}^m$ *and* $\omega \in \mathbb{R}^m$ *belonging to the set* $\mathcal{S}$ *given by:*

$$\mathcal{S}(\bar{u}) = \{u \in \mathbb{R}^m, \omega \in \mathbb{R}^m : |u_{(\ell)} - \omega_{(\ell)}| \leq \bar{u}_{(\ell)}, \ell \in \mathcal{I}_m\} \tag{1.64}$$

Then the dead-zone function satisfies $\psi(u)^T D(\psi(u) + \omega) \leq 0$ *for any* $m \times m$ *diagonal matrix* $D > 0$.

Moreover, when dealing with local results, it is fair to provide an estimate of the closed-loop domain of attraction based on the knowledge of the bounds of the input signals, i.e. the domain of admissible input values $\mathcal{D}_u$, defined in (1.61). In the context of T-S fuzzy models, this has to be taken into consideration together with the other constraints brought by modeling considerations, i.e. the domain of validity $\mathcal{D}_x$ of the considered T-S model defined in (1.7), or brought by the choice of the Lyapunov function, e.g. the subset $\mathcal{D}_\phi$ defined in (1.56). Combining these constraints allows to provide an estimate of the domain of attraction, e.g. by searching the outermost level set $c > 0$ such that $\mathcal{L}(c) = \{x \in \mathbb{R}^n | V(x) \leq c\} \subseteq \mathcal{D}_x \cap D_\phi \cap \mathcal{D}_u$. This motivated several recent works on T-S model-based control to handle such constraints. For instance, (Lendek et al., 2018; Klug et al., 2015) focus on handling the domain of validity of T-S models. Input or state constraints have been considered in (Nguyen et al., 2017; Fan et al., 2017; Li et al., 2016a; Kong and Yuan, 2019). Our works in the 2$^{\text{nd}}$ and 4$^{\text{th}}$ chapters will follow the same guidelines.

1.4.2 Preliminaries on the input delay approach for sampled-data control

To circumvent the above mentioned drawbacks and limitations of T-S model-based discrete-time controllers applied to continuous-time systems, an appealing approach considers on rewriting the overall continuous-time closed-loop dynamics as a dynamical system with input-time varying delays (Fridman et al., 2004; Hetel et al., 2017). This subsection aims at presenting the preliminaries about this approach, projected in the T-S model framework, to better apprehend our contributions in Chapter 3 and 4.

Let us consider a continuous-time T-S model (1.6) driven by a discrete-time state feedback PDC controller (1.39), maintained between two successive sampling instants t_k and t_{k+1} by a ZOH. $\forall t \in [t_k, t_{k+1})$, the closed-loop dynamics is expressed as:

$$\dot{x}(t) = \sum_{i=1}^{r} \sum_{j=1}^{r} \alpha_i(z(t))\alpha_j(z(t_k)) \left(A_i x(t) + B_i K_j x(t_k)\right) \tag{1.65}$$

It is important to highlight that, with the sequence of hold sampling instants:

$$0 = t_0 < t_1 < \ldots < t_k < t_{k+1} < \ldots, \lim_{k\to\infty} t_k = \infty, \tag{1.66}$$

the sampling interval can be either constant $t_{k+1} - t_k \equiv \tau_s$ or variable, with k-dependent $\eta_k = t_{k+1} - t_k$. Hence, the following assumption is done.

Assumption 1.2. *We assume that the aperiodic sampling intervals η_k are bounded such that they admit a maximal allowable value $\bar{\eta}$, i.e.:*

$$\eta_k = t_{k+1} - t_k \leq \bar{\eta}, \forall k \in \mathbb{N}. \tag{1.67}$$

Remark 1.6. *In many real applications, the assumption (1.2) is accurate since the intervals between two successive sampling instants may be varying due to practical constraints. Even in a point-to-point digital control topology, clock inaccuracy and system architecture characteristics such as real-time scheduling can induce jitters, imperfect synchronization, and computation*

delays (Wittenmark et al., 1995; Hetel et al., 2017). Over the past decades, there has been an expansion in the study of Networked Controlled Systems (NCS), in which sampled-data systems are controlled through communication networks (Hetel et al., 2017; Fridman, 2014a). In these circumstances, aperiodic sampling intervals are almost inevitable due to constraints induced by the network, e.g. event-triggering (de Souza et al., 2021; Rouamel et al., 2021), network-induced time-varying delays and packet dropouts (Nafir et al., 2021), and so on.

The main idea of the input-delay approach consist in rewriting sampled signals maintained by a ZOH as continuous-time signal involving a time-varying delay. To do so, let us consider the sawtooth functions, illustrated in Figure (1.7), defined by:

$$\tau(t) = t - t_k, \, \forall t \in [t_k, t_{k+1}), \, \forall k \in \mathbb{N} \tag{1.68}$$

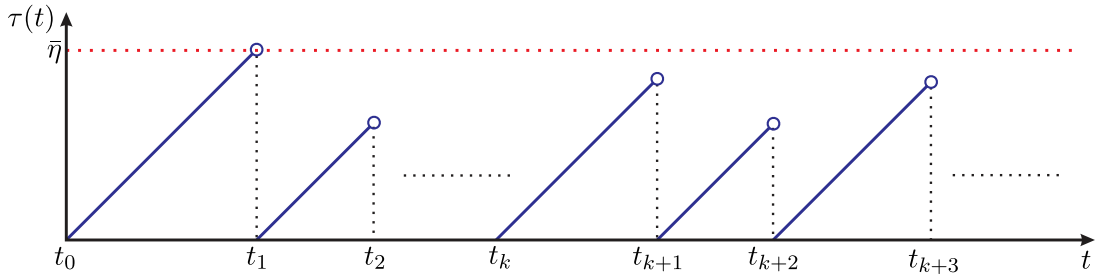

Figure 1.7: Representation of the time-varying delay ($\tau(t) = t - t_k$) with a sawtooth function (o marks the left-limits of right-continuous piecewise functions).

Note that, from Assumption 1.2, the sawtooth function (1.68) has the following properties:

$$\tau(t) \in [0, \eta_k) \subseteq [0, \bar{\eta}), \, \forall t \in [t_k, t_{k+1}), \, \forall k \in \mathbb{N} \tag{1.69}$$

and:

$$\dot{\tau}(t) = 1, \, \forall t \in [t_k, t_{k+1}), \, \forall k \in \mathbb{N} \tag{1.70}$$

Therefore, from (1.68), any sampled signals $s(t_k)$ maintained by a ZOH can be rewritten as $s(t-\tau(t))$, which allows us to rewrite the closed-loop dynamics (1.65) as the following continuous-time system with time-varying delays:

$$\dot{x}(t) = \sum_{i=1}^{r} \sum_{j=1}^{r} \alpha_i(z(t))\alpha_j(z(t-\tau(t))) \left(A_i x(t) + B_i K_j x(t-\tau(t))\right) \tag{1.71}$$

Rewriting the closed-loop dynamics is such a fashion make usual tools dedicated to the stability analysis and controller design for systems involving time-varying delays suitable for the design of sampled-data controllers. Two main approaches are often considered to deal with time-varying delays from the use of Lyapunov-Razumikhin Functionals (LRF) or Lyapunov-Krasovskii Functionals (LFK). In the linear system control framework, LKF were first proposed to cope with slow varying time-delays, i.e. $\dot{\tau}(t) < 1$ (Niculescu et al., 1998). Unfortunately, such approach were not suitable for fast time-varying delays, i.e. when $\dot{\tau}(t) = 1$, so the stability issue was first investigated via LRF (see e.g. (Hale and Lunel, 1993)), because no restrictions on the

derivative of the delay in this case, but it usually leads to conservative results. More recently, robust stability conditions for systems involving fast input time-varying delay (i.e. $\dot{\tau}(t) = 1$ almost everywhere, as illustrated in Figure 1.7) were provided via LKF in (Fridman and Shaked, 2002, 2003; Fridman et al., 2004). From these pioneer works, the time-delay approach became popular to cope with sampled-data systems and NCSs (Fridman, 2014a), especially bringing several conservatism improvements in the linear system framework, see e.g. (Fridman et al., 2004; Fridman, 2014a,b; Hetel et al., 2017; Bourahala et al., 2021; Nafir et al., 2021; Rouamel et al., 2021).

Among the several improvements made with the choice of a convenient LKF in sampled-data controller design, looped LKF inspired by (Seuret, 2009; Fridman, 2010) retains our attention because it allows to take into account the characteristic of the sawtooth function $\tau(t)$, especially when $\dot{\tau}(t) = 1$ ($\forall t \neq t_k$), to provide derivative-dependent stability conditions. Such a looped LKF is of the form (Hetel et al., 2017):

$$V(x(t)) = x^T(t)Px(t) + (\eta_k - \tau(t)) \int_{t-\tau(t)}^{t} \dot{x}^T(s)R\dot{x}(s)ds \tag{1.72}$$

which presents the advantage of being left and right continuous at each sampling instants t_k, i.e.:

$$V(x(t_k^-)) = V(x(t_k^+)) = V(x(t_k)) = x^T(t_k)Px(t_k) \tag{1.73}$$

Therefore, as illustrated on Figure 1.8, assuming $P = P^T > 0$, (1.72), $\forall t \in [t_k, t_{k+1})$, if $\dot{V}(x(t)) < 0$, then, $\forall t \in \mathbb{R}^+$, $V(x(t))$ is monotonously decreasing and the considered system with input time-varying delay is asymptotically stable.

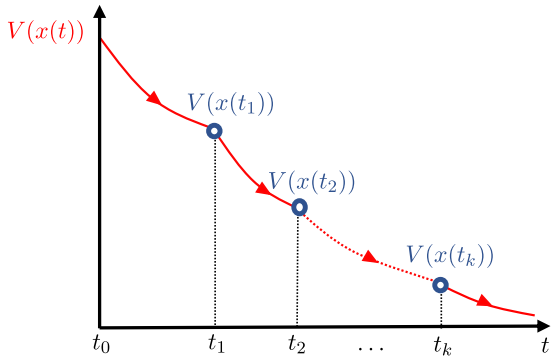

Figure 1.8: Illustration of a decreasing looped LKF.

In the context of T-S model-based sampled-data control, several attempts to reduce the conservatism have been done from different choices of an LKF, see e.g. (Yoneyama, 2010; Zhu and Wang, 2011; Zhang and Han, 2011; Zhu et al., 2012; Gunasekaran and Joo, 2019; Zhu et al., 2013; Cheng et al., 2017). Among them, only few authors have considered looped LKF (Zhu et al., 2012, 2013; Cheng et al., 2017), but with significant conservatism reduction. To further relax the conditions, refinements on the choice of a convenient looped LKF are proposed in Chapter 3 and 4 where LMI-based conditions will be proposed with the help of the following lemmas.

Lemma 1.7. *(Fridman, 2014b) For any matrix $P = P^T > 0$ with appropriate dimensions, $\tau(t) \in [0, \eta_k)$ and $\dot{\tau}(t) = 1$, the following inequality holds:*

$$\int_{t-\tau(t)}^{t} x^T(s)Px(s)ds \geq \eta_k^{-1} \int_{t-\tau(t)}^{t} x^T(s)ds P \int_{t-\tau(t)}^{t} x(s)ds \tag{1.74}$$

Lemma 1.8. *(Zhang and Han, 2013) For any constant matrix $R \in \mathbb{R}^{n\times n}$, $R = R^T > 0$, a scalar function $\tau(t)$ with $0 < \tau(t) \leq \bar{\eta}$ and a vector function $\dot{x} : [-\bar{\eta}, 0] \to \mathbb{R}^n$ such that the integration concerned is well defined, let*

$$\int_{t-\tau(t)}^{t} \dot{x}(s)ds = E\psi(t) \tag{1.75}$$

where $E \in \mathbb{R}^{n\times k}$ and $\psi(t) \in \mathbb{R}^k$. Then the following inequality holds for any matrix $M \in \mathbb{R}^{n\times k}$

$$-\int_{t-\tau(t)}^{t} \dot{x}^T(s)R\dot{x}(s)ds \leq \psi^T(t)\Upsilon_1\psi(t) \tag{1.76}$$

where $\Upsilon_1 = -E^TM - M^TE + \tau(t)M^TR^{-1}M$.

Lemma 1.9. *(Kim, 2016). Let us consider a quadratic function $f(\eta(t)) = a_2\eta(t)^2 + a_1\eta(t) + a_0$, where a_2, a_1 and $a_0 \in \mathbb{R}$. If:*

$$(i)\, f(0) < 0, \quad (ii)\, f(\bar{\eta}) < 0 \quad (iii)\, f(0) - \bar{\eta}^2 a_2 < 0, \tag{1.77}$$

then $f(\eta(t)) < 0$, $\forall \eta(t) \in [0, \bar{\eta}]$.

Moreover, note that the sampled-data closed-loop dynamics (1.71) involves a mismatching double sum interconnection structure and so, applying the second Lyapunov method will lead to closed-loop stability conditions given in terms of parameterized LMIs involving summation structure such like:

$$\sum_{i=1}^{r}\sum_{j=1}^{r} \alpha_i(x(t))\alpha_j(x(t-\tau(t)))\Gamma_{ij} < 0 \tag{1.78}$$

Figure 1.9 illustrates the mismatch between the continuous-time membership function $\alpha_i(x(t))$ of plant and the sampled ones, maintained by a ZOH such that $\alpha_i(x(t_k)) = \alpha_i(x(t-\tau(t)))$.

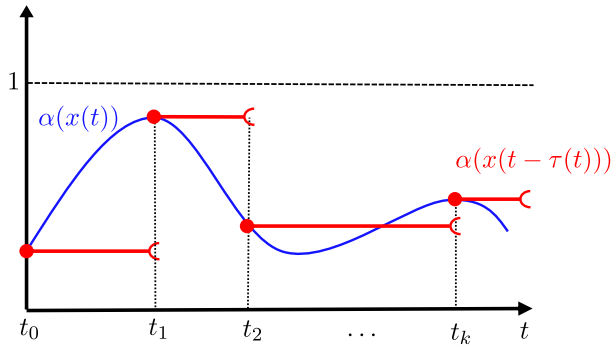

Figure 1.9: Mismatch between controller's and T-S model's membership function.

Hence, to provide relaxed parameter independent LMI-based conditions from (1.78), Lemma 1.2 or other usual double sum relaxation schemes cannot be employed directly. To circumvent

this drawback, most of the authors assume that, $\forall \rho \in \mathcal{I}_r$, there exists σ_ρ such that $|\alpha_\rho(x(t-\tau(t))) - \alpha_\rho(x(t))| \leq \sigma_\rho$, in order to provide mismatching double sum relaxation scheme, such like the one given by the following recent lemma.

Lemma 1.10. *(Koo et al., 2017): For any real matrix $\Gamma_{ij} = \Gamma_{ij}^T$ for $(i,j) \in \mathcal{I}_r^2$ and the continuous-time functions $a_i(t)$, $b_i(t)$ for $i \in \mathcal{I}_r$ with $(a_i(t), b_i(t)) \in [0,1]^2$, $\sum\limits_{i=1}^{r} a_i(t) = \sum\limits_{i=1}^{r} b_i(t) = 1$ and considering $|a_i(t) - b_i(t)| \leq \sigma_i$, the inequality:*

$$\sum_{i=1}^{r}\sum_{j=1}^{r} a_i(t)b_j(t)\Gamma_{ij} < 0,$$

holds, if there exists some matrices Y_i and Z_i, such that

$$\begin{aligned}
&\Gamma_{ii} + Z_i < 0, \quad \forall i \in \mathcal{I}_r,\\
&\Gamma_{ij} + \Gamma_{ji} + Z_i + Z_j < 0, \quad \forall (i,j) \in \mathcal{I}_r^2,\ i < j,\\
&\Gamma_{ij} + Y_i > 0, \quad \forall (i,j) \in \mathcal{I}_r^2,\\
&\sum_{j=1}^{r} \sigma_j(F_{ij} + Y_i) - Z_i < 0, \quad \forall i \in \mathcal{I}_r.
\end{aligned} \tag{1.79}$$

Note that Lemma (1.10) consists in an extension to the case of mismatched membership functions of the first proposed double sum relaxation scheme in (Tanaka et al., 1998), which were found more conservative than the further proposed double sum relaxation scheme in Lemma (1.2) (Tuan et al., 2001). Hence, we believe that there is still space for conservatism improvements. Moreover, let us highlight an important fact. Assuming that there exists σ_ρ such that $|\alpha_\rho(x(t-\tau(t))) - \alpha_\rho(x(t))| \leq \sigma_\rho$ to get LMI-based conditions for sampled-data controller means that such assumption need to be at least post-verified from extensive numerical closed-loop simulation, which is not an easy task to do. Hence, because many authors assume these parameters without post-verification, they may loose asymptotic stability guarantee if it occurs that $|\alpha_\rho(x(t-\tau(t))) - \alpha_\rho(x(t))|$ is not bounded by $\sigma_\rho \forall t$. Therefore, we believe that more investigations are required to cope with that issue. As a matter of fact, it is easy to show that these parameters are related to the bounds of the time-derivatives of the membership functions. Indeed, we can write, $\forall \rho \in \mathcal{I}_r$:

$$\alpha_\rho(x(t)) - \alpha_\rho(x(t-\tau(t))) = \int_{t-\tau(t)}^{t} \dot{\alpha}_\rho(x(s))ds \tag{1.80}$$

Therefore, assuming that, $\forall \rho \in \mathcal{I}_r$, there exists ϕ_ρ such that $|\dot{\alpha}_\rho(x(t))| \leq \phi_\rho$, yields:

$$-\phi_\rho\bar{\eta} \leq -\phi_\rho\tau(t) \leq \int_{t-\tau(t)}^{t} \dot{\alpha}_\rho(x(s))ds \leq \phi_\rho\tau(t) \leq \phi_\rho\bar{\eta} \tag{1.81}$$

Moreover, since, $\forall t$, $\alpha_\rho(x(t)) \in [0,1]$, we have:

$$-1 \leq \alpha_\rho(x(t)) - \alpha_\rho(x(t-\tau(t))) \leq 1 \tag{1.82}$$

Consequently, from (1.80)-(1.82), we always have $|\alpha_\rho(x(t-\tau(t))) - \alpha_\rho(x(t))| \leq \sigma_\rho$ with $\sigma_\rho = \min\{1, \phi_\rho\bar{\eta}\}$.

Based on such considerations, in Chapter 3, an improved double sum relaxation Lemma, extending Tuan's lemma 1.2 to the case of mismatching sampled-data membership functions will be provided and compared with Lemma 1.10. Let us point-out that if a solution can be found with $\sigma_\rho = 1$, then the assumption of a known ϕ_ρ is no more required (unless non-quadratic Lyapunov Functions are employed). However, $\sigma_\rho = 1$ being the more conservative case, we will often have to provide ϕ_ρ, e.g. as explained in Remark 1.5, such that $\bar{\eta}\phi_\rho \leq 1$, leading to local results constrained by $\mathcal{D}_\phi$ given in (1.56). Nevertheless, it is worth to say that, to the best of the authors' knowledge, there exists no previous results dealing with the estimation of the closed-loop domain of attraction in the context of sampled-data controller design for T-S models. This being understood as a major issue, this point will be the subject of one of the contributions proposed in Chapter 4, from the convenient choice of a looped non-quadratic LKF.

1.5 Conclusion

In this chapter, some preliminaries on T-S model-based control have been presented. First, from a continuous-time nonlinear systems, the usual ways to get a T-S representation have been surveyed. Also, because the main goal of this thesis is to investigate the control of continuous-time systems driven by digital devices, basics on the discretization of continuous-time T-S models have been presented, together with the basic stability and LMI-based controller design conditions in both the continuous and discrete-time frameworks. The limitations of standard discrete-time controllers, designed from discrete-time T-S model, have been pointed-out since it fails to accurately cope with the inter-sampling behavior of continuous-time systems, especially when large sampling periods are employed, or when aperiodic sampling occurs. Then, it has been shown that an elegant way to cope with such issues is to reconsider the closed-loop sampled-data dynamics as a continuous-time system with input time-varying delays but, once again, with some limitation in the T-S model framework, such as the locality of the results or the overall conservatism of the design conditions. In addition, because most real applications involve input limitations, some usual ways to cope with actuators saturation have been presented. All of these concerns motivate the contributions presented in the sequel of this thesis, which can be classified into two balanced research lines presented as follows.

First, acknowledging that discrete-time model-based approach are mainly considered in industrial applications because of their easy implementation on industrial controller like Programmable Logic Computers (PLCs), some improvements of actual discrete-time T-S model-based approach are proposed in Chapter 2, especially to cope with practical goals and constraints like set-point tracking under saturating actuators. Under these constraints, the designed controller only locally guarantees the stabilization of the considered discrete-time T-S model, so the investigation and maximization of the closed-loop domain of attraction will be proposed. These results will be experimentally validated on an industrial benchmark, namely an interactive tank system, having slow dynamics, making relevant the use of discrete-time approaches.

Then, as an alternative to discrete-time model-based control design, the input time-varying

delay approach for continuous-time sampled-data systems is investigated in the remaining of the thesis. In Chapter 3, based on the choice of a convenient looped quadratic LKF, LMI-based relaxed conditions are proposed for the design of sampled-data PDC controllers, together with the proposition of a new relaxation scheme for double summation structures involving mismatching membership functions. Then, in Chapter 4, some extensions are proposed to the class of T-S descriptors, known as efficient to cope with mechanical systems, involving actuators saturation, in the looped non-quadratic LKF framework, together with the proposition of strategies to estimate and maximize the closed-loop domain of attraction. These theoretical contributions are validated and compared to previous related results, in simulation with the nonlinear benchmark of an inverted pendulum on a cart.

Chapter 2

Anti-windup PI-like Controllers Design for Discrete-time T-S Models

Résumé en Français : Synthèse de contrôleurs PI avec action Anti-windup pour les modèles T-S à temps discret.

Ce chapitre présente la synthèse de contrôleurs pour les systèmes à temps discret, dont les bases ont été exposées dans le chapitre précédent. Dans ce cas, lorsque de tels contrôleurs discrets sont appliqués. à un système continu, les signaux de commande sont maintenus par un bloqueur d'ordre zéro entre deux instants d'échantillonage. Nécessitant une période d'échantillonnage fixe, cette approche a fait l'objet de nombreuses études depuis les années 1950, conduisant à une théorie bien établie pour les systèmes à temps invariant (LTI). Cette approche est donc encore largement répandue pour contrôler des systèmes industriels puisqu'elle permet une mise en œuvre rapide sur des automates programmables, avec des performances acceptables et une bonne précision lorsque les pé-riodes d'échantillonnage constantes sont suffisamment petites par rapport à la dynamique du système à contrôler.

Plus précisément, dans ce chapitre, nous nous intéressons au suivi de trajectoire à partir de points de consigne pour les modèles de type T-S à temps discret sujet à la saturation des actionneurs. Cette dernière contrainte menant à l'obtention d'un résultat local, nous proposons une analyse de l'estimation de la région d'attraction en boucle fermée, en prenant en compte les entrées exogènes induites par le changement des points de consigne, menant à des changements d'origine de la dynamique en boucle fermée. En effet, en négligeant une telle analyse, les évolutions des points de consigne peuvent amener le système à suivre des trajectoires en dehors de la région d'attraction, de sorte que tant les performances que la stabilité de la boucle fermée peuvent être compromises. Cet aspect a été étudié dans (Lopes et al., 2018) où un contrôleur non-PDC de type PI a été proposé, mais possédant une région d'attraction modeste. De plus, dans (Lopes et al., 2018), une condition requise est que la variation temporelle du vecteur d'état du système soit lente. Cependant, comme le montrent (Zaccarian and Teel, 2011; Mehdi et al., 2014), de tels inconvénients peuvent être limités en considérant une action anti-windup. Néanmoins, à la connaissance de l'auteur, aucun travail antérieur ne semble avoir abordé ce point pour la synthèse de contrôleurs de type PI à temps discret dans le cadre des modèles de type T-S.

Par conséquent, la principale contribution de ce chapitre est de proposer une méthode d'optimisation convexe pour la synthèse de contrôleurs flous de type PI à temps discret avec une action anti-windup pour une stabilisation locale et un suivi de points de con-

signe pour les systèmes non linéaires représentés par des modèles T-S. En particulier, la synthèse du contrôleur flou de type PI consiste en une boucle interne avec retour d'état associée à une boucle avec retour de sortie. Ce schéma de contrôle permet de garantir à terme une erreur nulle entre la sortie et les points de consigne. De plus, la saturation du signal de commande est abordée à partir des conditions données dans (Tarbouriech et al., 2011) et une optimisation de la région d'attraction est proposée. Un ensemble de résultats de simulation et d'expérimentation est présenté et discuté. Les résultats expérimentaux ont été obtenus sur un banc d'essai (système de réservoirs connectés), inspiré de (Johansson, 2000), et disponible au CEFET-MG (Divinópolis, Brésil). Les résultats obtenus montrent l'intérêt de l'approche présentée dans ce chapitre par rapport aux travaux antérieurs présentés dans (Lopes et al., 2018; Wang et al., 2019).

2.1 Introduction

This chapter investigates the design of discrete-time controllers for continuous-time systems based on the direct discrete-time model-based approach, whose basics have been presented in Chapter 1, Sections 1.2.2 and 1.3.2. Following this method, discrete-time fuzzy T-S models are employed to represent nonlinear systems for the design of discrete-time controllers, which are then implemented using a ZOH. Despite imposing a fixed sampling period, this procedure has been studied since the 1950s, leading to a mature discrete-time control theory for Linear Time-Invariant (LTI) systems. This is why it is still widely employed to control many industrial or practical applications, allowing easy implementation on digital devices like PLCs, with reasonable performances and good accuracy when small enough fixed sampling periods can be set with regard to the system's dynamics to be controlled (see Remark 1.3 and Example 1.3).

More specifically, in this chapter, we are concerned with the set-point tracking of discrete-time T-S models subject to actuators' saturation. The latter constraints bringing locality, therefore we propose a careful analysis of the estimation of the closed-loop region of attraction by taking into account the effects of exogenous inputs induced by the change of the set-points in the closed-loop dynamics. Indeed, neglecting such analysis, set-point changes may drive the trajectories of the system outside of the region of attraction, so that both the performances and the closed-loop stability can be impaired. This effect has been investigated in (Lopes et al., 2018) where non-PDC PI-like controller has been proposed, but with quite small region of attraction. Moreover, in (Lopes et al., 2018) it is required a slow enough time-variation of the state vector of the system. However, as shown in (Zaccarian and Teel, 2011; Mehdi et al., 2014), such drawbacks can be mitigated by considering an anti-windup action.

In fuzzy model-based control, PID controllers have been studied with various goals including: *(a)* to compare the performance (Ounnas et al., 2016; Kmetóvá et al., 2013; Blažič et al., 2002) with fuzzy PID controllers; *(b)* to control systems modeled through T-S approach (Estrada-Manzo et al., 2019; Gao et al., 2015; Yu et al., 2010; Yu and Huang, 2009; Wang et al., 2019; Yi and Guo, 2009); *(c)* for output feedback with T-S fuzzy observers (Lin et al., 2008); *(d)* to blend local gains through T-S rules (Yi et al., 2008) to improve the performance of a PI structure with both state and output feedback; *(e)* to develop self-tuning techniques by *i)*

blending conventional PI controllers adjusted for local operational points or for different control objectives, such as disturbance rejection and reference tracking (Sun et al., 2019; Nouri et al., 2017; Mishra et al., 2015; Fattah and Abdel-Qader, 2015; Dragos et al., 2011; Fateh, 2010), *ii)* particle swarm approach (Bouallegue et al., 2012) *iii)* Cuckoo search parameter fuzzy PID optimization (Hamzaa et al., 2017), etc. Nevertheless, to the best of the author's knowledge, no works in the previous literature handle the use of anti-windup action to improve the estimation of the region of attraction for the design of discrete-time PI-like set-point tracking controllers under actuators' saturation in the Takagi-Sugeno framework.

Therefore, the main contribution of this chapter is to propose a convex optimization method for the design of discrete-time fuzzy PI-like controllers with a fuzzy anti-windup gain, for the local stabilization and set-point tracking of nonlinear systems represented by discrete-time T-S models. In particular, the proposed fuzzy PI control scheme consists of an internal state-feedback loop combined with an output feedback one. The proposed topology is dedicated to ensure null output tracking errors for piecewise constant set-point references. Additionally, the saturation of the control signal is handled by the generalized sector condition (Tarbouriech et al., 2011), and a maximization procedure is proposed to enlarge the provided estimates of the closed-loop domain of attraction.

A set of simulation and experimental results is presented and discussed, obtained from the application of the proposed methodology to an industrial benchmark, namely the interactive tank system available at the CEFET-MG (Divinópolis, Brazil), inspired by (Johansson, 2000), illustrating the improvements achieved with the approach presented in this chapter with regard to previous works (Lopes et al., 2018; Wang et al., 2019).

2.2 Problem statement

In this chapter, we consider the class of nonlinear dynamic systems with input saturations represented by:

$$\begin{cases} \dot{x}(t) = f(x(t)) + g(x(t))\mathtt{sat}u(t) \\ y(t) = Cx(t) \end{cases} \tag{2.1}$$

where $u(t) \in \mathbb{R}^m$ is the control vector, $\mathtt{sat} : \mathbb{R}^m \to \mathbb{R}^m$ is the centered vector valued function, defined as:

$$\mathtt{sat}u_{(\ell)}(t) = \mathtt{sgn}(u_{(\ell)}(t)) \min\{\bar{u}_{(\ell)}, \mid u_{(\ell)}(t) \mid\}, \forall \ell \in \mathcal{I}_m$$

with symmetric bounds $\bar{u}_{(\ell)}$ that restricts the ℓ^{th} control input, the state vector $x(t) \in \mathbb{R}^n$ and the output signals vector $y(t) \in \mathbb{R}^q$. The functions $f : \mathbb{R}^n \to \mathbb{R}^n$ and $g : \mathbb{R}^m \to \mathbb{R}^n$ belong to the subset $\mathcal{D}_x \subseteq \mathbb{R}^n$. We assume that the output matrix $C \in \mathbb{R}^{q \times n}$ is known and system (2.1) is controlled through a discrete-time control law with a sample-time of τ_s seconds.

In this chapter, we will consider the discrete-time control of (2.1). Hence, from Euler discretization with an appropriate (fixed) sampling period τ_s and applying the sector nonlinearity approach (Tanaka and Wang, 2001), the following discrete-time T-S model (with r rules) can

be obtained to represent (2.1) on $\mathcal{D}_x$ in the discrete-time framework:

$$\begin{cases} x_{k+1} = \sum_{i=1}^{r} \alpha_i(z_k)(A_i x_k + B_i \mathtt{sat} u_k) \\ y_k = C x_k \end{cases} \tag{2.2}$$

where z_k is the vector of premise variables, which is assumed to depend only on the state variables, for $i \in \mathcal{I}_r$, $A_i \in \mathbb{R}^{n\times n}$ and $B_i \in \mathbb{R}^{n\times m}$ are known real matrices, and $\alpha_i \geq 0$ are the membership functions satisfying the convex sum property $\sum_{i=1}^{r} \alpha_i = 1$

In the sequel, for all the matrices with fuzzy summation structures, we will adopt the following notations:

$$M_\alpha = \sum_{i=1}^{r} \alpha_i(z_k) M_i,\ M_{\alpha\alpha} = \sum_{i=1}^{r}\sum_{j=1}^{r} \alpha_i(z_k)\alpha_j(z_k) M_{ij} \tag{2.3}$$

Remark 2.1. *In this work, the time-sampling period τ_s is chosen as large as possible, but small enough to ensure that the discretized model provides a good approximation of the continuous-time dynamics in (2.1), e.g., see Chapter 1, Section 1.2.2 for highlights regarding such consideration.*

The goal of this chapter is to provide an LMI-based methodology for the design of a discrete-time controller such that the output y_k tracks piecewise constant reference signals y_{r_k} with null error. To this end, we use the topology shown in Figure 2.1, where a (discrete-time) integral action over the set-points tracking error is included.

From the proposed topology, a PDC fuzzy PI-like control law can be readily derived as:

$$u_k = K_\alpha^I v_k - K_\alpha^P x_k \tag{2.4}$$

where $K_\alpha^P \in \mathbb{R}^{m\times n}$ and $K_\alpha^I \in \mathbb{R}^{m\times q}$ are fuzzy control gains to be designed, which keep the fuzzy sum structure (2.3), and v_k corresponds to an additional state induced by the integral action in the whole closed-loop system (see the blue dashed box in Figure 2.1);

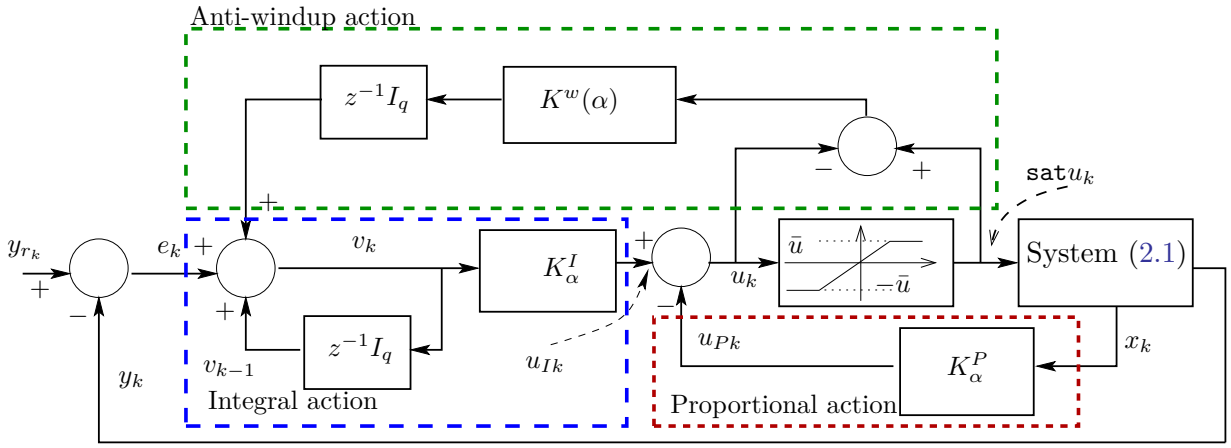

Figure 2.1: Control topology with discretized integral and anti-windup actions.

Moreover, the windup effect can appear in the integral action due to the saturating actuators. To mitigate such an impact, we proposed a non-PDC anti-windup action (see the green dashed box in Figure 2.1) delivered by the signal $a_{w,k}$, which is computed as:

$$a_{w,k} = K^w(\alpha)(\mathtt{sat} u_k - u_k) \tag{2.5}$$

with $K^w(\alpha) = E^c_\alpha S^{-1}_\alpha$ and where $E^c_\alpha \in \mathbb{R}^{m\times q}$ and $S_\alpha \in \mathbb{R}^{q\times q}$ are the anti-windup gains, which keep the fuzzy sum structure (2.3).

In what follows, we assume that the output of the system can be driven in certain region such that, for some piecewise constant bounded reference signals y_{r_k} belonging to:

$$\mathcal{W} = \{y_{r_k} \in \mathbb{R}^q \ : \ \|y_{r_k}\| \leq \beta\}, \quad \beta \in \mathbb{R}_+, \tag{2.6}$$

the output error $e_k = y_{r_k} - y_k \to 0$ when $k \to +\infty$, while the state belongs to a bounded region of attraction (y_{r_k} is attractive) during transients, i.e. $x_k \in \mathcal{D}_a \subseteq \mathcal{D}_x$, centered on the origin $\mathcal{O}$ of the considered plant.

The goal of this chapter is to develop a convex optimization based methodology to design the fuzzy gains K^I_α, K^P_α, and $K^w(\alpha)$ such that the overall closed-loop set-points tracking control plant represented in Figure 2.1, i.e. the system (2.1) under the control signal $\texttt{sat}u_k$, with u_k given in (2.4) and $y_{r_k} \in \mathcal{W}$, is locally stable. Indeed, due to the saturating actuators, the convergence of the set-point tracking error e_k, and so the stationary point achieved by the state, will be impacted by the initial state of the system. Therefore, the region of attraction centered on the origin $\mathcal{O}$, denoted by $\mathcal{D}_a$, can be defined by the set of initial conditions such that the tracking error trajectories goes to zero, i.e.:

$$\mathcal{D}_a = \{x(0) \in \mathbb{R}^n; \ e_k = y_{r_k} - Cx_k \to 0 \text{ as } k \to \infty\}. \tag{2.7}$$

As it is well-known in the literature, the complete characterization of the region of attraction $\mathcal{D}_a$ is a challenging task because it may be non-convex and even open (Tarbouriech et al., 2011). Usually an estimate of this region, $\mathcal{D}^*_a \subseteq \mathcal{D}_a$, is computed instead. Therefore, in this chapter, we are concerned with both the following problems:

$\mathcal{P}_1$**:** *(Closed-loop stabilization)* For $y_{r_k} = 0$, the objective is to compute the fuzzy gains K^I_α, K^P_α, and $K^w(\alpha)$, and to estimate the larger set of initial conditions $\mathcal{D}^*_a \subseteq \mathcal{D}_a$ such that, $\forall k \geq 0$, $x_k \in \mathcal{D}^*_a$ and the closed-loop system is stable, i.e. $k \to \infty \Rightarrow x_k \to \mathcal{O}$.

$\mathcal{P}_2$**:** *(Closed-loop set-points tracking)* $\forall y_{r_k} \in \mathcal{W}$, the objective is to compute the fuzzy gains K^I_α, K^P_α, and $K^w(\alpha)$ **that maximize** β, and to estimate **the larger related set** of initial conditions $\mathcal{D}^*_a \subseteq \mathcal{D}_a$ such that, $\forall k \geq 0$, $x_k \in \mathcal{D}^*_a$ and $k \to \infty \Rightarrow e_k \to 0$, when y_{r_k} is constant over a sufficiently large number of samples.

2.3 Preliminary results

In this preliminary results section, the goal is to introduce the overall closed-loop dynamics including the integral and anti-windup actions, then to propose a way to deal with the saturation and so, to provide an useful preliminary lemma for the estimation of the domain of attraction.

One way to implement the integral action in discrete-time systems is to follow the counterpart path of what is done in continuous-time domain (Kailath, 1980). This is shown in the block diagram presented in Figure 2.1, where the integral action can be written as $v_k = e_k + v_{k-1} +$

$a_{w,k-1}$, where v_k is the signal preceding the fuzzy integral gain K_α^I. Thus, in our approach we propose a fuzzy PI-like controller with an internal state proportional control loop, combined with an integral tracking error one and an anti-windup action. Hence, by considering (2.2) and (2.5), we can express v_{k+1} as:

$$v_{k+1} = y_{r_k} - CA_\alpha x_k - CB_\alpha \mathtt{sat} u_k + v_k + K^w(\alpha)(\mathtt{sat} u_k - u_k) \tag{2.8}$$

Let $\xi_k = \begin{bmatrix} x_k^T & v_k^T \end{bmatrix}^T$ be an extended state vector, we can combine (2.2)–(2.4) and (2.8) as:

$$\xi_{k+1} = \mathcal{A}_\alpha \xi_k + \mathcal{B}_\alpha \mathtt{sat} u_k + \mathcal{B}_\alpha^e(\mathtt{sat} u_k - u_k) + \mathcal{B}^w y_{r_k} \tag{2.9}$$

where:

$$\mathcal{A}_\alpha = \begin{bmatrix} A_\alpha & \mathbf{0} \\ -CA_\alpha & \mathbf{I} \end{bmatrix}, \mathcal{B}_\alpha = \begin{bmatrix} B_\alpha \\ -CB_\alpha \end{bmatrix},$$
$$\mathcal{B}^w = \begin{bmatrix} \mathbf{0} & \mathbf{I} \end{bmatrix}^T, \mathcal{B}_\alpha^e = \begin{bmatrix} \mathbf{0} & K_\alpha^{wT} \end{bmatrix}^T.$$

Then, the fuzzy PI control law can be rewritten as:

$$u_k = -K_\alpha \xi_k \tag{2.10}$$

with $K_\alpha = \begin{bmatrix} K_\alpha^P & -K_\alpha^I \end{bmatrix}$.

Moreover, by using the decentralized dead-zone function $\psi(u_k) = \mathtt{sat} u_k - u_k$ to deal with the saturation of the actuators, we can rewrite (2.9) as:

$$\xi_{k+1} = (\mathcal{A}_\alpha - \mathcal{B}_\alpha K_\alpha)\xi_k + (\mathcal{B}_\alpha + \mathcal{B}_\alpha^e)\psi(u_k) + \mathcal{B}^w y_{r_k} \tag{2.11}$$

Furthermore, to deal with the saturation problem and to cope with the above defined decentralized dead-zone function, an auxiliary set $\mathbb{S}$ is considered as:

$$\mathbb{S} = \{\xi_k \in \mathbb{R}^{n+q} : \forall \ell \in \mathcal{I}_r, |-(K_{\alpha(\ell)} + G_{\alpha(\ell)})\xi_k| \leq \bar{u}_{(\ell)}\} \tag{2.12}$$

where G_α is an appropriate fuzzy matrix (i.e. having the same structure as (2.3)).

Thus, $\mathbb{S}$ is a set where the modulus of the control signal component $-K_{\alpha(\ell)}\xi_k$ can be greater than $\bar{u}_{(\ell)}$, but not the auxiliary signal $-(K_{\alpha_{(\ell)}} + G_{\alpha_{(\ell)}})\xi_k$. This means that the proposed design allows the saturation of the actuator, yielding a more energetic control signal than those obtained by saturation avoidance approach, see e.g. (Tarbouriech et al., 2011). In this context, the following lemma is provided to deal with the nonlinearity $\psi(u_k)$.

Lemma 2.1. *: If $\xi \in \mathbb{S}$, then the relation*

$$\psi(u_k)^T T_\alpha [\psi(u_k) - G_\alpha \xi_k] \leq \mathbf{0} \tag{2.13}$$

is verified for all diagonal matrices $0 < T_\alpha \in \mathbb{R}^{m \times m}$.

Proof. : Straightforward from adapting Lemma 1.6 in (Tarbouriech et al., 2011) by considering the convex sum structure of the matrices T_α and G_α. □

In the sequel, the local stability of the overall closed-loop dynamics (2.11) will be investigated by means of the following fuzzy Lyapunov candidate function:

$$V(\xi_k) = \xi_k^T W_\alpha^{-1} \xi_k \tag{2.14}$$

where W_α is a fuzzy Lyapunov matrix (i.e. holding the fuzzy structure (2.3)).

If we can find the matrices $W_i = W_i^T > 0$, $\forall i \in \mathcal{I}_r$, such that (2.14) is a Lyapunov function, then it can be used to define the Lyapunov level set $\mathcal{L}_\mathcal{V}(\mu)$, with $0 < \mu < \infty$, such that:

$$\mathcal{L}_\mathcal{V}(\mu) = \{\xi_k \in \mathbb{R}^{(n+q)} : V(\xi_k) \leq \mu^{-1}\}. \tag{2.15}$$

The next lemma will be used to compute an estimate $\mathcal{D}_a^*$ of the region of attraction, composed of the intersection of all the level sets defined by a fuzzy Lyapunov function. The details are presented in Section 4.

Lemma 2.2. *(Jungers and Castelan, 2011): Suppose that (2.14) is a Lyapunov function. Then an estimate $\mathcal{D}_a^*$ of the region of attraction $\mathcal{D}_a$ is given by the level set $\mathcal{L}_\mathcal{V}(\mu)$ such that:*

$$\mathcal{D}_a^* = \mathcal{L}_\mathcal{V}(\mu) = \bigcap_{\xi_k \in \mathcal{D}_\xi} \mathcal{E}(W_\alpha^{-1}, \mu) = \bigcap_{i \in \mathcal{I}_r} \mathcal{E}(W_i^{-1}, \mu), \tag{2.16}$$

with $\mathcal{E}(W_i^{-1}, \mu) = \{\xi_k \in \mathbb{R}^{n+1} \ : \ \xi_k^T W_i^{-1} \xi_k \leq \mu^{-1}\}$.
Thus, it means that $\mathcal{D}_a^*$ can be computed by using only the vertices W_i^{-1}, $i \in \mathcal{I}_r$.

2.4 Main Results

Based on the materials presented in the previous sections, the goal is now to proposed LMI-based conditions for the design of the PI-like controller and anti-windup gains such that $\mathcal{P}_1$ and $\mathcal{P}_2$ are satisfied. The main result is summarized by the following theorem.

Theorem 2.1. *Consider the overall closed-loop dynamics (2.11) with the known upper bounds of the decentralized saturation vector $\bar{u} \in \mathbb{R}_+^m$, and that there exist positive scalar parameters η, τ_1 and τ_2, the matrices $\mathbf{0} < W_i^T = W_i \in \mathbb{R}^{(n+q)\times(n+q)}$, the diagonal matrices $\mathbf{0} < S_i \in \mathbb{R}^{m\times m}$, the matrices $U \in \mathbb{R}^{(n+q)\times(n+q)}$, $Y_i \in \mathbb{R}^{m\times(n+q)}$, $Z_i \in \mathbb{R}^{m\times(n+q)}$, and $E_i^c \in \mathbb{R}^{m\times q}$, for $i = 1, \ldots, r$, such that the following LMI-based conditions are verified for $p = 1, \ldots, r$, $j = p, \ldots, r$, and $\ell = 1, \ldots, m$:*

$$\begin{bmatrix} -W_i & \Gamma_{12}^{(p,j)} & \Gamma_{13}^{(p,j)} & \mathcal{B}^w \\ \star & \Gamma_{22}^{(p,j)} & (Z_p^T + Z_j^T)/2 & \mathbf{0} \\ \star & \star & -S_p - S_j & \mathbf{0} \\ \star & \star & \star & -\tau_2 \boldsymbol{I}_q \end{bmatrix} < \mathbf{0}, \tag{2.17}$$

$$\begin{bmatrix} W_p - U - U^T & Y_{p(\ell)}^T + Z_{p(\ell)}^T \\ \star & -\eta \bar{u}_{p(\ell)}^2 \end{bmatrix} \leq \mathbf{0}, \tag{2.18}$$

$$-(1-\tau_1)\delta + \eta\tau_2 < \mathbf{0}, \tag{2.19}$$

with

$$\Gamma_{12}^{(p,j)} = [(\mathcal{A}_p + \mathcal{A}_j)U + (\mathcal{B}_p Y_j + \mathcal{B}_j Y_p)]/2, \tag{2.20}$$

$$\Gamma_{22}^{(p,j)} = \tau_1[(W_p + W_j)/2 - U - U^T], \tag{2.21}$$

$$\Gamma_{13}^{(p,j)} = (\mathcal{B}_p S_j + \mathcal{B}_j S_p + \mathcal{B}_p^e + \mathcal{B}_j^e)/2, \tag{2.22}$$

$$\mathcal{B}_i^e = \begin{bmatrix} \boldsymbol{0} & E_i^{cT} \end{bmatrix}^T. \tag{2.23}$$

Then the fuzzy PI-like control law:

$$u_k = -\begin{bmatrix} K_\alpha^P & -K_\alpha^I \end{bmatrix} \begin{bmatrix} x_k \\ v_k \end{bmatrix}$$

and the anti-windup control action:

$$a_{w,k} = K^w(\alpha)(\mathtt{sat} u_k - u_k)$$

with the fuzzy gain matrices computed as:

$$\begin{bmatrix} K_\alpha^P & -K_\alpha^I \end{bmatrix} = -\sum_{i=1}^{r} \alpha_i(x_k) Y_i U^{-1} \tag{2.24}$$

and:

$$K^w(\alpha) = \sum_{i=1}^{r} \alpha_i(x_k) E_i^c \left(\sum_{i=1}^{r} \alpha_i(x_k) S_i \right)^{-1}, \tag{2.25}$$

ensure:

1. *for $y_{r_k} = 0$ the local asymptotic stability of the respective fuzzy closed-loop for all initial conditions belonging to $\mathcal{D}_a^* = \bigcap_{i \in \mathcal{I}_r} \mathcal{E}(W_i^{-1}, 1)$;*

2. *for any y_{r_k} verifying $\|y_{r_k}\| \leq \delta^{-1/2} = \beta$, the trajectories of the closed-loop system, for all initial conditions $x(0)$ taken in $\mathcal{D}_a^*$ do not leave such a set.*

Proof. Let the functions defined by $\kappa_i : [0,\ \infty) \to [0,\ \infty)$, $i \in \{0, 1, 2\}$, be $\mathcal{K}_\infty$ and strictly increasing functions with $\kappa_i(0) = 0$ and $\lim_{a \to \infty} \kappa_i(a) = \infty$. The inequality (2.17) ensures that $W_i > \mathbf{0}$ and:

$$0 < \kappa_1(\|\xi_k\|) \leq V(\xi_k, \alpha_k) = \xi_k^T P(\alpha_k) \xi_k < \kappa_2(\|\xi_k\|) \tag{2.26}$$

with $P(\alpha_k) = \sum_{i=1}^{N} \alpha_{ki} W_i^{-1}$. From the S-procedure, we can write:

$$\Delta V(\xi_k) = V(\xi_{k+1}) - V(\xi_k) < -\kappa_0(\|\xi_k\|) \tag{2.27}$$

for ξ_k belonging to the trajectory of (2.11).
Then, similarly to the approach proposed in (Tarbouriech et al., 2011), $\forall \xi_k$ such that $\xi_k^T P(\alpha_k) \xi_k \geq \eta^{-1}$, for any $y_{r_k} \in \mathcal{W}$ and for all $u_k \in \mathbb{S}$, the closed-loop tracking problem $\mathcal{P}_2$ of (2.11) is ensured if:

$$\begin{aligned} &\Delta V(\xi_k) + (1 - \tau_1)(\xi_k^T W_\alpha^{-1} \xi_k - \eta^{-1}) \\ &+ \tau_2(\delta^{-1} - {y_{r_k}}^T R y_{r_k}) - 2\psi(u_k)^T T_\alpha[\psi(u_k) - G_\alpha \xi_k] \leq 0 \end{aligned} \tag{2.28}$$

with $0 < \tau_1 < 1$, $\tau_2 > 0$, $\kappa_1(\|\xi_k\|) = \epsilon\|\xi_k\|^2$ with small enough $\epsilon > 0$, and $\kappa_2(\|\xi_k\|) = \sum_{i=1}^{s} \lambda_{\max}(P_i)\|\xi_k\|^2$.

Now, for the closed-loop stabilization problem $\mathcal{P}_1$, i.e. $y_{r_k} = 0$, the inequality (2.28) reduces to:

$$\begin{aligned} &\Delta V(\xi_k) + (1-\tau_1)(\xi_k^T W_\alpha^{-1}\xi_k - \eta^{-1}) \\ &\leq (1-\tau_1)(\kappa_2\|\xi_k\| - \eta^{-1}) = -\kappa_0(\|\xi_k\|) \leq 0. \end{aligned} \tag{2.29}$$

As it is demonstrated later, the inequality (2.18) implies that the set $\mathcal{E}(P,\eta)$ is inside the set $\mathbb{S}$ and thus, the generalized sector condition in Lemma 2.1 is ensured, i.e.:

$$\psi(u_k)^T T_\alpha[\psi(u_k) - G_\alpha\xi_k] \leq 0. \tag{2.30}$$

Thus, $\forall \xi_k \notin \text{int}(\mathcal{E}(P,\eta))$ and $\forall y_{r_k} \in \mathcal{W}$, the inequality (2.28) ensures:

$$\Delta V(\xi_k) \leq -\kappa_0(\|\xi_k\|) \tag{2.31}$$

Let us assume that, for $k = k_1$, $\xi_{k_1} \in \partial\mathcal{E}(P,\eta)$ and $y_{r_k} \in \mathcal{W}$, then $\Delta V(\xi_{k1}) < -\kappa_0\|\xi_k\|$. This implies that $\xi_{k1+1} \in \text{int}(\mathcal{E}(P,\eta))$ and allows us to conclude that the verification of (2.28) ensures that the trajectories starting in $\mathcal{E}(P,\eta)$ do not leave such a set for all $y_{r_k} \in \mathcal{W}$, and thus, $\mathcal{E}(P,\eta)$ is a robustly positively invariant set for (2.11).

Therefore, to verify (2.28), we perform the following sequence of operations:

i) multiply (2.17) by α_i, α_p, and α_j, then sum it up for $i = 1,\ldots,r$, $p = 1,\ldots,r$ and $j = p,\ldots,r$;

ii) replace Y_α, Z_α, and S_α by $-K_\alpha U$, $G_\alpha U$ and T_α^{-1}, respectively;

iii) using the fact $-U^T W_\alpha^{-1} U \leq W_\alpha - U - U^T$ and, with W_+ standing for $W_{\alpha_{k+1}}$, get:

$$\tilde{\Theta} = \begin{bmatrix} -W_+ & \theta_{12} & \mathcal{B}_\alpha T_\alpha^{-1} + B_{e\alpha} & \mathcal{B}_\alpha^\omega \\ \star & \theta_{22} & U_\alpha^T G_\alpha^T & \mathbf{0} \\ \star & \star & -2T_\alpha^{-1} & \mathbf{0} \\ \star & \star & \star & -\tau_2\mathbf{I}_q \end{bmatrix},$$

with:

$$\theta_{12} = \mathcal{A}_\alpha U - \mathcal{B}_\alpha K_\alpha U, \quad \text{and} \quad \theta_{22} = -\tau_1(U^T W_\alpha^{-1} U);$$

iv) thanks to the regularity of U we use the similarity transformation $\Theta = \mathcal{T}^T\tilde{\Theta}\mathcal{T}$, with:

$$\mathcal{T} = \texttt{diag}\{\mathbf{I}_n, U^{-1}, T_\alpha^T, \mathcal{I}_q\};$$

v) replace W_α by P_α^{-1}, $(\mathcal{A}_\alpha - \mathcal{B}_\alpha K_\alpha)$ by $\mathcal{A}_{cl_\alpha}$, and $E_{c_\alpha} T_\alpha = K^w(\alpha)$;

vi) apply the Schur's complement, then pre- and post-multiply respectively by:

$$\varsigma_k^T = \begin{bmatrix} \xi_k^T & \psi(u_k)^T & {y_{r_k}}^T \end{bmatrix}$$

and ς_k, then recover (2.11) to get:

$$\xi_{k+1}^T P(\alpha_{k+1})\xi_{k+1} - \tau_1\xi_k^T P(\alpha_k)\xi_k - \tau_2 {y_{r_k}}^T y_{r_k} - 2\psi(u_k)^T T_\alpha(\psi(u_k) - G_\alpha\xi_k) < 0$$

vii) then, from the fact that $\Delta V(\xi_k) = \xi_{k+1}^T P(\alpha_{k+1})\xi_{k+1} - \xi_k^T P(\alpha_k)\xi_k$, we get:

$$\Delta V(\xi_k) + (1-\tau_1)\xi_k^T P(\alpha_k)\xi_k - \tau_2 {y_{r_k}}^T y_{r_k} - 2\psi(u_k) T_\alpha(\psi(u_k) - G_\alpha\xi_k) \leq 0. \tag{2.32}$$

In this last inequality, the term $\psi(u_k)T_\alpha(\psi(u_k) - G_\alpha\xi_k)$ is ensured to be negative if u_k belongs to $\mathbb{S}$, which is ensured by (2.18). To verify this, follow the sequence:
viii) multiply (2.18) by $\alpha_{k(m)}$ and sum it up for $m = 1, \ldots, r$;
ix) replace $W(\alpha_k) - U - U^T$ by $-U^T W(\alpha_k)^{-1}U$, also Y_α by $-K_\alpha U$, and Z_α by $G_\alpha U$;
x) pre- and post-multiply the resulting condition by $\texttt{diag}\{U^{-T},\ 1\}$ and its transpose;
xi) apply the Schur complement then pre- and post multiply the result by ξ_k^T and ξ_k to get:

$$-\xi_k^T P(\alpha_k)\xi_k + \xi_k^T(-K_{\alpha(\ell)} - G_{\alpha(\ell)})^T(\eta\bar{u}^2_{(\ell)})^{-1} \times (-K_{\alpha(\ell)} - G_{\alpha(\ell)})\xi_k \leq 0, \tag{2.33}$$

which implies that $\mathcal{E}(P,\eta) \subseteq \mathbb{S}$. Therefore, (2.18) ensure that any trajectory starting in $\mathcal{E}(P,\eta)$ remains in this set;
xii) apply the *S*-Procedure (see Lemma 1.5) with (2.19) and (2.32) to obtain (2.28).
To conclude this proof, we observe that the region of attraction can be computed through the intersection of the ellipsoidal sets as $\mathcal{D}_a^* = \bigcap_{i\in\mathcal{I}_r} \mathcal{E}(W_i^{-1}, 1)$ by using Lemma 2.2. □

Therefore, Theorem 2.1 provides a solution to both problems $\mathcal{P}_1$ and $\mathcal{P}_2$. It is worth to say that we can choose $\eta = 1$ without loss of generality. Moreover, the parameter τ_1 relates the exponential stability: from (2.32) with the Lemma 2.1 and $y_{r_k} = 0$, we can conclude that $\Delta V(\xi_k) \leq -(1-\tau_1)V(\xi_k) \Rightarrow V(\xi_{k+1}) \leq \tau_1 V(\xi_k)$. Thus, the smaller τ_1, the faster the trajectory convergence. Consequently, a search on $\tau_1 \in (0, 1]$ is useful to improve the convergence rate of the closed-loop. Moreover, the design condition proposed in (Lopes et al., 2018) can be recovered from Theorem 2.1 by imposing $K^w(\alpha) = \mathbf{0}$. In this case, we get the following Corollary.

Corollary 2.1. *(Lopes et al., 2018) Consider the overall closed-loop dynamics (2.11) with $K^w(\alpha) = \mathbf{0}$, the known upper bounds of the decentralized saturation vector $\bar{u} \in \mathbb{R}^m_+$, and that there exist positive scalar parameters η, τ_1, the matrices $\mathbf{0} < W_i^T = W_i \in \mathbb{R}^{(n+q)\times(n+q)}$, the diagonal matrices $\mathbf{0} < S_i \in \mathbb{R}^{m\times m}$, the matrices $U \in \mathbb{R}^{(n+q)\times(n+q)}$, $Y_i \in \mathbb{R}^{m\times(n+q)}$, and $Z_i \in \mathbb{R}^{m\times(n+q)}$, $i = 1, \ldots, r$, such that (2.18)–(2.19) and the following LMI-based conditions are verified for $p = 1, \ldots, r$, $j = p, \ldots, r$, and $i = 1, \ldots, q$:*

$$\begin{bmatrix} -W_i & \Gamma_{12}^{(p,j)} & \hat{\Gamma}_{13} & \hat{\Gamma}_{14} \\ \star & \Gamma_{22}^{(p,j)} & 0.5(Z_p^T + Z_j^T) & \mathbf{0} \\ \star & \star & -S_p - S_j & \mathbf{0} \\ \star & \star & \star & -\tau_2 \boldsymbol{I}_q \end{bmatrix} < \mathbf{0} \tag{2.34}$$

with $\hat{\Gamma}_{13} = 0.5(\mathcal{B}_p S_j + \mathcal{B}_p S_j)$, $\hat{\Gamma}_{14} = 0.5(\mathcal{B}_p^\omega + \mathcal{B}_j^\omega)$, $\Gamma_{12}^{(p,j)}$ given by (2.20), and $\Gamma_{22}^{(p,j)}$ by (2.21). Then the fuzzy PI-like control law (2.10) with gains computed by:

$$K_i = -Y_i U^{-1} \tag{2.35}$$

ensures:

1. *for $y_{r_k} = 0$, the local asymptotic stability for the respective fuzzy closed-loop system, for all initial conditions belonging to $\mathcal{D}_a^* = \bigcap_{i\in\mathcal{I}_r} \mathcal{E}(W_i^{-1}, 1)$;*

2. *for any* y_{r_k} *verifying* $||y_{r_k}|| \leq \delta^{-1/2} = \beta$, *the trajectories of the mentioned closed-loop system, for all initial conditions* $x(0)$ *taken in* $\mathcal{D}_a^*$, *do not leave such a set.*

Remark 2.2. *Conditions of Corollary 2.1 also provide a solution for problems* $\mathcal{P}_1$ *and* $\mathcal{P}_2$, *but such a solution is usually more conservative than that achieved by Theorem 2.1 because no anti-windup action is considered. In this sense, whenever Corollary 2.1 has a solution, the feasibility of conditions (2.17)–(2.19) are ensured, but not the contrary.*

Remark 2.3. *The conditions proposed in Theorem 2.1 and Corollary 2.1 encompass the quadratic stability based approach, i.e., we can impose* $W_i = W$, *for* $i \in \mathcal{I}_r$ *in conditions (2.17), (2.18), (2.21), and (2.34). In this case, it is expected that the estimate of the region of attraction is more restricted than in the case with fuzzy Lyapunov functions.*

The solutions provided by Theorem 2.1 and Corollary 2.1 can be used to optimize objectives associated with problems $\mathcal{P}_1$ and $\mathcal{P}_2$. A particular interest consists in maximizing the estimate of the region of attraction, which can be achieved by the following convex optimization procedure for Theorem 2.1:

$$\mathcal{S}_\nu : \begin{cases} \min\limits_{\nu, W_i, S_i, Y_i, Z_i, U} \quad \nu \\ \quad i \in \mathcal{I}_r \\ \text{s.t. (2.17), (2.18), (2.19) and } \begin{bmatrix} \nu\mathbf{I} & \mathbf{I} \\ \mathbf{I} & W_i \end{bmatrix} \geq 0. \end{cases} \tag{2.36}$$

Another interesting objective can be to maximize the amplitude bound of the tracking reference signal y_{r_k}, i.e. to maximize the allowable amplitude changes in the reference signal, such that the trajectories starting in $\mathcal{D}_a^*$ do not leave it. In this case, the following convex optimization procedure can apply with Theorem 2.1:

$$\mathcal{S}_\delta : \begin{cases} \min\limits_{\delta, W_i, S_i, Y_i, Z_i, U, E_{ci}} \quad \delta \\ \text{s.t. (2.17), (2.18), and (2.19).} \end{cases} \tag{2.37}$$

Remark 2.4. *The optimization procedures* $\mathcal{S}_\nu$ *and* $\mathcal{S}_\delta$ *can be used without the anti-windup design. In this case, it is enough to replace (2.17) by (2.34), and thus, employing Corollary 2.1 in these procedures.*

2.5 Illustrative Examples

In what follows, before going to the experimental validation of the proposed approach on an industrial oriented process, a numerical example is presented to illustrate the relevance of the proposed design procedure, considering the bounds of the actuators saturation, and to compare the obtained results with recent relevant works from the literature (Lv et al., 2019) and (Wang et al., 2019).

2.5.1 Numerical example

Assume the T-S fuzzy model given by (2.2)-(2.3) and investigated in (Lv et al., 2019) with the matrices:

$$A_1 = \begin{bmatrix} 0 & 1 \\ 0.1 & -2 \end{bmatrix}, \; A_2 = \begin{bmatrix} 0 & 1 \\ 0 & -0.5 \end{bmatrix}, \; A_3 = \begin{bmatrix} 0.6 & -1 \\ 1 & 0 \end{bmatrix}, \; B_1 = \begin{bmatrix} 0 \\ 1.1 \end{bmatrix},$$
$$B_2 = \begin{bmatrix} 0.1 \\ 0.4 \end{bmatrix}, \; B_3 = \begin{bmatrix} 0.2 \\ 0.3 \end{bmatrix}, \; C_1 = \begin{bmatrix} -0.1 \\ 0.3 \end{bmatrix}^T, C_2 = \begin{bmatrix} 0.4 \\ -0.1 \end{bmatrix}^T, C_3 = \begin{bmatrix} 0.3 \\ 0.5 \end{bmatrix}^T,$$

and the normalized membership functions given by:

$$\begin{cases} \alpha_1(x_{1,k}) = 1, \; \alpha_2(x_{1,k}) = \alpha_3(x_{1,k}) = 0, \; \text{for } ||x_{1,k}|| > 5, \\ \alpha_1(x_{1,k}) = 0, \; \alpha_2(x_{1,k}) = (5 - ||x_{1,k}||)/5, \; \alpha_3(x_{1,k}) = 1 - \alpha_2, \; \text{otherwise.} \end{cases} \tag{2.38}$$

Although (Lv et al., 2019) considers time-delay, this part is left-out from this example as it is not the concern of our study.

Additionally, let us assume that the control signal is bounded by ± 10. Our objective is to design a controller solving the Problem $\mathcal{P}_1$ with $K^w(\alpha) = 0$, $\eta = 1$, $\tau_1 = 0.9999$, and $y_{r_k} = 0$, thus, maximizing the estimate of the region of attraction. Therefore, we use the convex optimization procedure $\mathcal{S}_\nu$ in (2.36) with the conditions proposed in Corollary 2.1 with C_m, $m = 1, \ldots, 3$. The achieved estimate of the region of attraction is shown in Figure 2.2, where the points belonging to the intersection of the ellipses (black dashed line) correspond to the optimized border of the estimated region of attraction. However, when the design procedure proposed in (Lv et al., 2019) is considered, the convergence of the trajectories cannot be ensured. Indeed, in this case, many initial conditions lead to unstable trajectories. Some of them are marked in blue $\times$ in Figure 2.2. A similar comparison is proposed with a recent fuzzy PID controller proposed in (Wang et al., 2019). Using the conditions proposed in (Wang et al., 2019, Th. 2) the convergence of the trajectories cannot be ensured for several initial conditions. Some examples of initial conditions yielding a divergent trajectory are marked with a red circle, $\circ$, in Figure 2.2. This clearly shows the relevance of our approach in terms of conservatism reduction and its potential, especially in real industrial applications, will be illustrated in the following section with the nonlinear control level of a two interactive tanks system.

To conclude this numerical example, let us consider the optimization procedure (2.37) to maximize the bound variation of y_{r_k} by using both Theorem 2.1 and Corollary 2.1. By employing $\eta = 1$ and $\tau_1 = 0.21$, the maximum achievable bounds were $\beta = 167.97$ with Corollary 2.1, and $\beta = 182.30$ with Theorem 2.1. Thus, thanks to the anti-windup control action, the maximal variation of the reference signal has augmented by 7.86%. This clearly demonstrates the advantage of considering such a control strategy. Moreover, let us point-out that the approaches proposed in (Lv et al., 2019) and (Wang et al., 2019) cannot be used, because they cannot handle amplitude bounded exogenous signals.

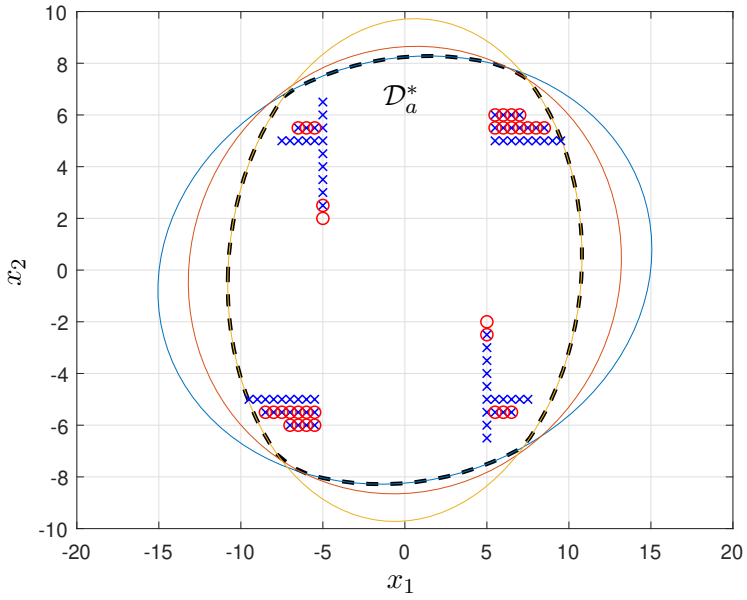

Figure 2.2: Region of attraction achieved with Corollary 2.1 and the optimization procedure $\mathcal{S}_\nu$ (dashed black) and unstable initial conditions obtained with previous works ($\times$ (Lv et al., 2019), $\circ$ (Wang et al., 2019)).

2.5.2 Experimental Validation

This section is devoted to illustrate and validate the proposed PI-like fuzzy controller design conditions on a real experimental setup, consisting of the level control problem of coupled tanks, with standard industrial equipment. First, we will present the experimental setup, then its physical modeling and finally the experimental results followed by a discussion.

Experimental setup:

The considered test-bench consists of an interactive tank system inspired by (Johansson, 2000), shown in Figure 2.3. This plant is composed of four 200 liters tanks, TQ-01 to TQ-04, actuated by two water pumps of $1cv$, BA-01 and BA-02, fed by two 400 liters reservoirs and controlled by two independent three-phase inverters. Each levels of the tanks are measured by pressure sensors, whose signals are collected by a Siemens PLC which ensures the interlock security and also sends the control signals to the pumfrag (actuators). The experiments were performed by running the control algorithms on a notebook running Linux (Ubuntu 16.04 distribution), connected to the PLC through an open-source Python-based interface (Sousa et al., 2018).

In what follows, a specific configuration of two tanks, as illustrated in Figure 2.4, has been used. In the following experiments, the manual valves FV-01 (connection between the tanks TQ-01 and TQ-02) and FV-02 (outflow) are kept with constant opening. Let $u^*(t)$ be the power delivered to the pump BA-01 given as a percentage of its maximal capability, the tank TQ-01 receives the controlled flow $q_{i,1}(\texttt{sat}u^*(t))$ and is connected through FV-01 to the tank TQ-02 that has an outlet flow $q_o(h_2(t))$. The continuous states of the system are $h_1(t)$ and

Figure 2.3: Interactive Tank System used in the experiments available at the CEFET-MG, Divinópolis, Brazil.

$h_2(t)$, respectively the levels of TQ-01 and TQ-02. The cross section area of TQ-02 is constant ($a_2 = 3.019 \times 10^{-5} cm^2$) while TQ-01 has a nonlinear variable cross section area due to solid body placed inside it as indicated in Figure 2.4. In this case, the area is given by:

$$a_1(h_1(t)) = \frac{8.1r^2}{5} - \frac{300r\cos(0.025\pi(h_1(t)-8)-0.4))}{2.75\sqrt{2\pi}} \times \exp\left(\frac{-((h_1(t)-8)10^{-2}-0.4)^2}{0.605}\right) \tag{2.39}$$

where $r = 31cm$ is the radius of the tank.

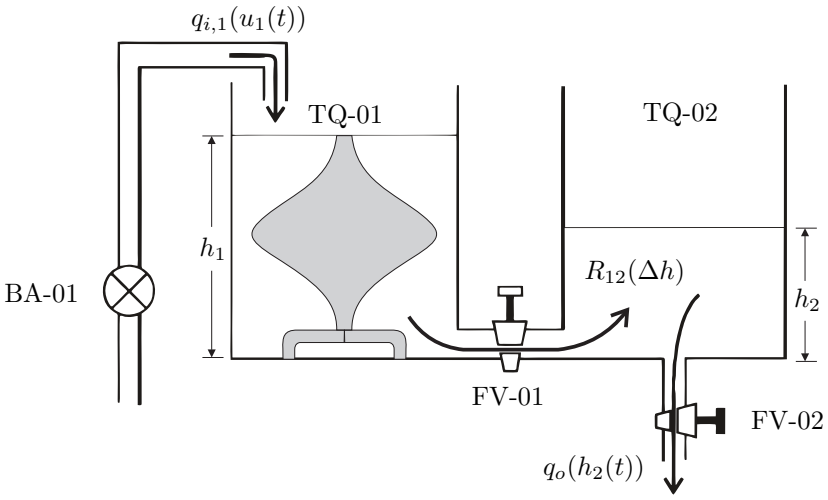

Figure 2.4: Coupled Tank System Schematic.

Hence, because of the nonlinearity (2.39), it is convenient to employ the T-S modeling of

the whole system, and so the application of the proposed approach for PI-like fuzzy controller design.

T-S fuzzy modeling of the considered two tanks system:

The dynamical model of the considered coupled tank system is obtained from the mass balance equations, which are resulting in:

$$\dot{h}_1(t) = \frac{K_b \mathtt{sat} u^*(t)}{a_1(h_1(t))} - \frac{h_1(t) - h_2(t)}{a_1(h_1(t)) R_{12}(h_1(t), h_2(t))} \tag{2.40}$$

$$\dot{h}_2(t) = \frac{h_1(t) - h_2(t)}{R_{12}(h_1(t), h_2(t)) a_2} - \frac{1}{a_2} q_o(h_2(t)) \tag{2.41}$$

where $K_b = 16.998$ is a gain for the pump BA-01 and $R_{12}(h_1, h_2) = (0.412(h_1(t) - h_2(t)) + 11.488)10^{-3}$ is the flow resistance between the two tanks, the outlet flow is modeled as $q_o(h_2(t)) = (12.241 h_2(t) + 868.674)\ cm^3/s$.

All the above-given values of parameters and scalars functions were identified from experimental data.

Let T be the sampling time period used in the digital control of the plant, $h_k = \begin{bmatrix} h_{1,k} & h_{2,k} \end{bmatrix}^T$ and u_k^* be respectively the discrete-time state vector and input signal. By using Euler discretization methods, a discrete-time model representing (2.40) is given by:

$$h_{k+1} = \begin{bmatrix} 1 - z_{1,k} z_{3,k} & z_{1,k} z_{3,k} \\ \frac{z_{1,k}}{a_2} & 1 - \frac{z_{1,k} + z_{2,k}}{a_2} \end{bmatrix} h_k + \begin{bmatrix} T K_b z_{3,k} \\ 0 \end{bmatrix} \mathtt{sat} u_k^* \tag{2.42}$$

with:

$$z_{1,k} = \frac{T}{R_{12}(h_{1,k}, h_{2,k})}, \tag{2.43}$$

$$z_{2,k} = \frac{T q_0(h_{2,k})}{h_{2,k}}, \tag{2.44}$$

$$z_{3,k} = (a_1(h_{1,k}))^{-1}, \tag{2.45}$$

and $a_1(h_1)$ computed by (2.39).

In what follows, to obtain a T-S fuzzy model of this discretized dynamic equation we choose the following operating range (in centimeters) for the state variables verifying $20 \leq h_1 \leq 74$ and $12 \leq h_2 \leq 50$. Taking into account that both tanks have a maximal level of $75cm$, the level of tank TQ-01 can vary from 26.7% up to 98.7%, and the level for tank TQ-02 from 16% up to 66.7% of the maximal allowed level ($75cm$). These choices have been made to avoid tank overflows as well as to avoid turbulent flows at low levels due to the resistance of valve FV-01.

Therefore, we assume $z_{1,k}$, $z_{2,k}$, and $z_{3,k}$ as the premise variables such that:

$$\begin{cases} z_{1,k} \in [\underline{z}_1, \bar{z}_1], \underline{z}_1 = 124.6572, \ \bar{z}_1 = 216.3098; \\ z_{2,k} \in [\underline{z}_2, \bar{z}_2], \underline{z}_2 = 118.4579, \ \bar{z}_2 = 338.5220; \\ z_{3,k} \in [\underline{z}_3, \bar{z}_3], \underline{z}_3 = 0.0004, \ \bar{z}_3 = 0.0048. \end{cases} \tag{2.46}$$

By applying the sector nonlinearity approach (Tanaka and Wang, 2001), for $j = 1, \ldots, 3$, we can rewrite (2.46) as:

$$z_{j,k} = w_{1,k}^j \underline{z}_j + w_{2,k}^j \bar{z}_j, \tag{2.47}$$

where $w_{j,k}^1 \geq 0$, $w_{j,k}^2 \geq 0$, $w_{j,k}^1 + w_{j,k}^2 = 1$ and:

$$w_{1,k}^j = \frac{\bar{z}_j - z_{j,k}}{\bar{z}_j - \underline{z}_j}, \text{ and } w_{2,k}^j = \frac{z_{j,k} - \underline{z}_j}{\bar{z}_j - \underline{z}_j}. \tag{2.48}$$

This allows to derive an exact T-S model (2.2) representing the dynamic equation of h_{k+1} having $N = 8$ vertices with the matrices:

$$A_1 = \begin{bmatrix} 1 - \frac{\underline{z}_1 \underline{z}_3}{a_2} & \frac{\underline{z}_1 \underline{z}_3}{a_2} \\ \frac{\underline{z}_1}{a_2} & 1 - \frac{\underline{z}_1 + \underline{z}_2}{a_2} \end{bmatrix}, A_2 = \begin{bmatrix} 1 - \frac{\underline{z}_1 \bar{z}_3}{a_2} & \frac{\underline{z}_1 \bar{z}_3}{a_2} \\ \frac{\underline{z}_1}{a_2} & 1 - \frac{\underline{z}_1 + \bar{z}_2}{a_2} \end{bmatrix}$$

$$A_3 = \begin{bmatrix} 1 - \frac{\underline{z}_1 \underline{z}_3}{a_2} & \frac{\underline{z}_1 \underline{z}_3}{a_2} \\ \frac{\underline{z}_1}{a_2} & 1 - \frac{\underline{z}_1 + \bar{z}_2}{a_2} \end{bmatrix}, A_4 = \begin{bmatrix} 1 - \frac{\underline{z}_1 \bar{z}_3}{a_2} & \frac{\underline{z}_1 \bar{z}_3}{a_2} \\ \frac{\underline{z}_1}{a_2} & 1 - \frac{\underline{z}_1 + \bar{z}_2}{a_2} \end{bmatrix}$$

$$A_5 = \begin{bmatrix} 1 - \frac{\bar{z}_1 \underline{z}_3}{a_2} & \frac{\bar{z}_1 \underline{z}_3}{a_2} \\ \frac{\bar{z}_1}{a_2} & 1 - \frac{\bar{z}_1 + \underline{z}_2}{a_2} \end{bmatrix}, A_6 = \begin{bmatrix} 1 - \frac{\bar{z}_1 \bar{z}_3}{a_2} & \frac{\bar{z}_1 \bar{z}_3}{a_2} \\ \frac{\bar{z}_1}{a_2} & 1 - \frac{\bar{z}_1 + \bar{z}_2}{a_2} \end{bmatrix}$$

$$A_7 = \begin{bmatrix} 1 - \frac{\bar{z}_1 \underline{z}_3}{a_2} & \frac{\bar{z}_1 \underline{z}_3}{a_2} \\ \frac{\bar{z}_1}{a_2} & 1 - \frac{\bar{z}_1 + \bar{z}_2}{a_2} \end{bmatrix}, A_8 = \begin{bmatrix} 1 - \frac{\bar{z}_1 \bar{z}_3}{a_2} & \frac{\bar{z}_1 \bar{z}_3}{a_2} \\ \frac{\bar{z}_1}{a_2} & 1 - \frac{\bar{z}_1 + \bar{z}_2}{a_2} \end{bmatrix}$$

$$B_1 = B_3 = B_5 = B_7 = \begin{bmatrix} TK_b \underline{z}_3 & 0 \end{bmatrix}^T,$$

$$B_2 = B_4 = B_6 = B_8 = \begin{bmatrix} TK_b \bar{z}_3 & 0 \end{bmatrix}^T,$$

with the following membership function vector

$$\alpha_k = \Big[\; w_{1,k}^1 w_{1,k}^2 w_{1,k}^3 \quad w_{1,k}^1 w_{1,k}^2 w_{2,k}^3 \quad w_{1,k}^1 w_{2,k}^2 w_{1,k}^3 \quad w_{1,k}^1 w_{2,k}^2 w_{2,k}^3 \quad \dots$$
$$w_{2,k}^1 w_{1,k}^2 w_{1,k}^3 \quad w_{2,k}^1 w_{1,k}^2 w_{2,k}^3 \quad w_{2,k}^1 w_{2,k}^2 w_{1,k}^3 \quad w_{2,k}^1 w_{2,k}^2 w_{2,k}^3 \; \Big]^T$$

where, $\forall i = 1, \dots, 8$, $\alpha_{k(i)} \geq 0$, $\sum_{i=1}^{8} \alpha_{k(i)} = 1$, and the functions $w_{i,k}^j$ computed as in (2.48) with $z_{j,k}$ given by (2.43)-(2.45).

Even that both levels h_1 and h_2 are measured from pressure sensors, only h_2 is controlled. Therefore, to design the PI-like PDC controller, the output matrix $C = \begin{bmatrix} 0 & 1 \end{bmatrix}$ will be considered to implement the design conditions expressed in Theorem 2.1 or Corollary 2.1. Moreover, there is no operational interest to drive the considered system to the points $(h_1, h_2) = (0, 0)$ since it represents the empty tanks situation. Hence, to drive our experiment and to test the proposed anti-windup scheme, we assume that the input signal is saturated such that $u_k^* \in [\underline{u}^*, \bar{u}^*]$, where $\underline{u}^* = 30\%$ and $\bar{u}^* = 70\%$ of the capability of the pump. This case illustrates that the actuator saturation bounds may arise not only by physical limitations, but also for operational security reasons. Thus, to apply our control strategy, a change of origin is required and given by:

$$x_k = \begin{bmatrix} x_{1,k} = h_{1,k} - h_1^{\mathcal{O}} \\ x_{2,k} = h_{2,k} - h_2^{\mathcal{O}} \end{bmatrix}, \text{ and } u_k = u_k^* - u^{\mathcal{O}} \tag{2.49}$$

where $h_1^{\mathcal{O}} = 0.537m$ and $h_2^{\mathcal{O}} = 0.271m$ correspond to the new origin $\mathcal{O}$, i.e. the stationary point achieved for a constant input $u^{\mathcal{O}} = 70.8722$ set at 50% of the variation range of the pump BA-01, leading to $u_k \in [-\bar{u}, \bar{u}]$ with $\bar{u} = 20\%$.

To conclude this modeling subsection, an experimental validation of the obtained discrete-time T-S fuzzy model (2.2) representing the equation h_{k+1} at the change of origin (2.49) is proposed from data measurements on the real system. To do so, a sample time period of $T = 4s$ has been chosen such that the maximum of the absolute error between the open-loop response of the real coupled tank system and the one of the obtained discrete-time T-S fuzzy model is less than 1% of the level ranges, see Figure 2.5. This sampled time period is used in the next subsection to conduct the closed-loop control experiments.

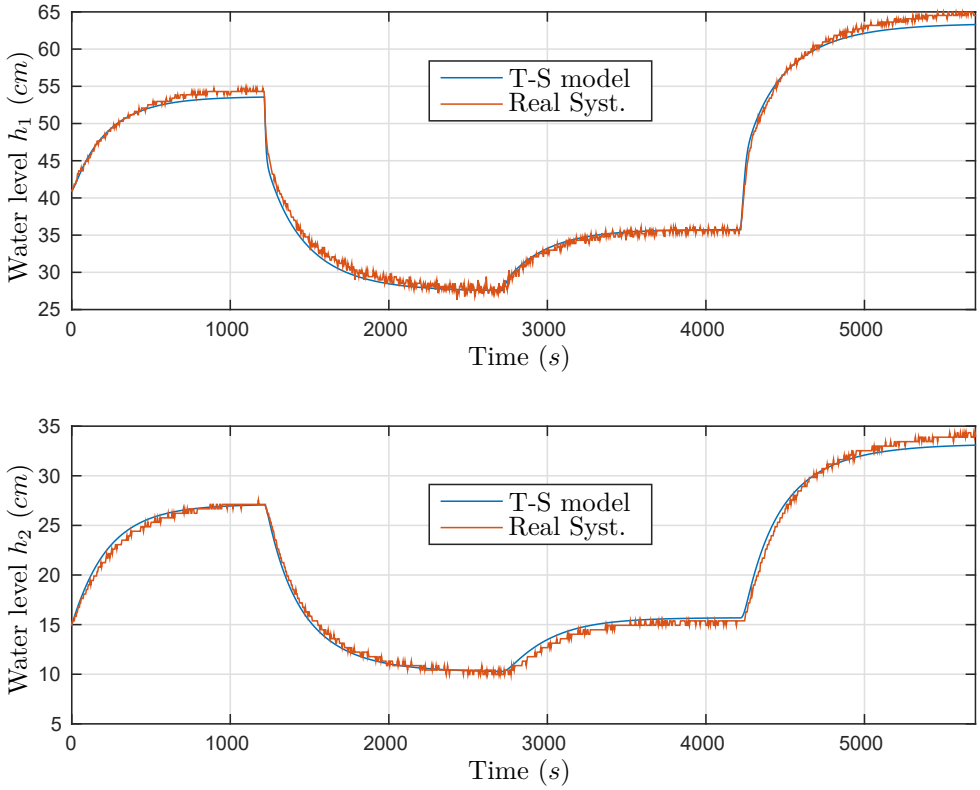

Figure 2.5: Open-loop validation of the discrete-time T-S model in simulation from data measurements on the real system.

Controller design and closed-loop experiments:

In this subsection, the proposed design methodology of the fuzzy controller is considered to solve both problems $\mathcal{P}_1$ and $\mathcal{P}_2$. Due to the change of origin (2.49), an offset of the reference signal to be tracked also occurs, i.e.:

$$y_{r_k} = y^*_{r_k} - h_2^{\mathcal{O}} \tag{2.50}$$

where $y^*_{r_k}$ denotes the absolute reference signal before the change of origin.

Let us first consider the **stabilization problem** $\mathcal{P}_1$, i.e. $y_{r_k} = 0$, and evaluate the proposed fuzzy PI-like controller design conditions with and without the anti-windup action. This can be achieved by solving the optimization procedure $\mathcal{S}_\nu$ given in (2.36) with the design conditions expressed in Theorem 2.1 and Corollary 2.1, accordingly to Remark 2.4. We show in Figure 2.6 the obtained estimates $\mathcal{R}_e$ of the regions of attraction from Theorem 2.1 and Corollary

2.1. Each plotted points correspond to initial conditions $\xi_0 = \begin{bmatrix} x_{1,0} & x_{2,0} & v_0 \end{bmatrix}^T$ taken in $\mathcal{R}_e$ with an equally spaced grid by 0.5. Let us highlight that the number of points in $\mathcal{R}_e$ with the anti-windup action (Theorem 2.1) raised 2.55×10^7, whereas without the anti-windup action (Corollary 2.1) it is only 6.97×10^5 points, i.e. about 2.7% of the region computed with anti-windup action. Thus, this illustrates the significant improvement when the anti-windup action is considered. Furthermore, the presented results have been obtained under the assumption of a fuzzy Lyapunov function (2.14). Obviously, if a quadratic approach is considered as quote in Remark 2.3, we may expect more conservative results. Indeed, in the quadratic framework with anti-windup action, we get a smaller estimate of the region of attraction, which is about 31.5% of the corresponding region with anti-windup action and the proposed fuzzy Lyapunov function (the plot of the quadratic region is left-out since it doesn't bring new information).

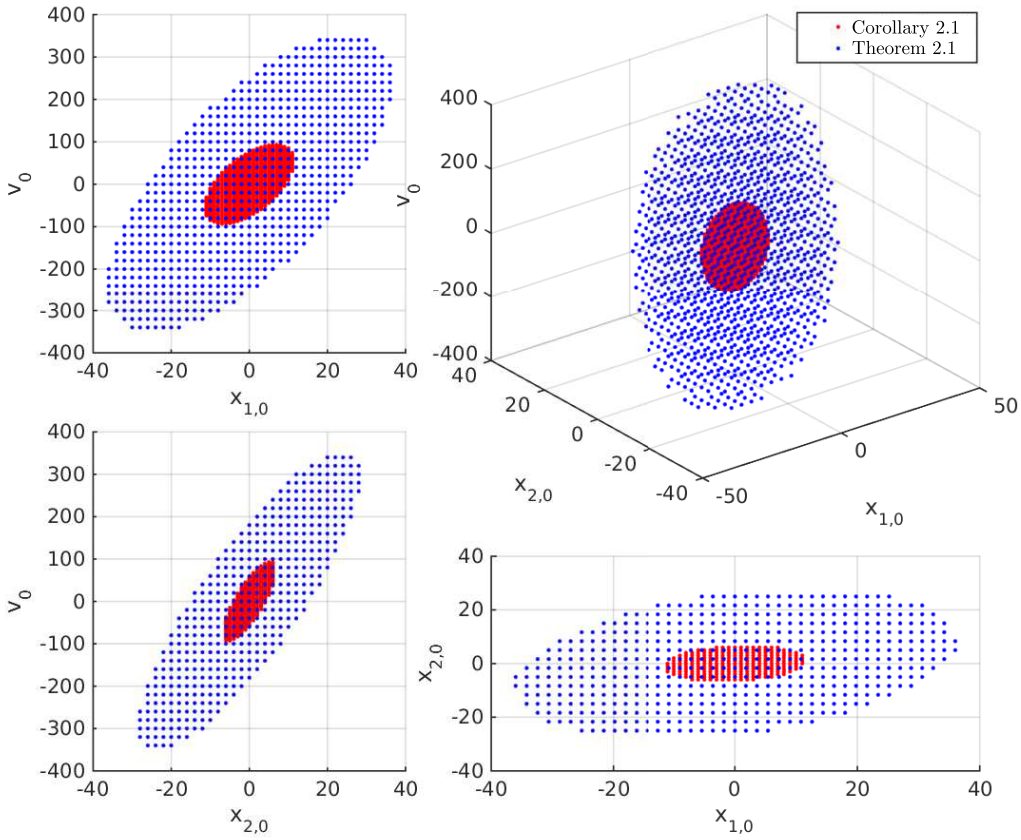

Figure 2.6: Estimate of the regions of attraction $\mathcal{D}_a^*$ for the stabilization problem $\mathcal{P}_1$ obtained from Theorem 2.1 (•) and Corollary 2.1 (•).

Now, let us consider the set-point tracking problem $\mathcal{P}_2$, where the reference signal y_{r_k} to be tracked is piecewise constant over a sufficient number of samples. By solving the proposed conditions with and without the anti-windup action, respectively Theorem 2.1 and Corollary 2.1, the goal is now to maximize the allowable amplitude range β of the set-point y_{r_k}, which means minimizing δ with the optimization procedure $\mathcal{S}_\delta$ given in(2.37) and Remark 2.4, around its considered origin (see (2.50)). The related regions of attraction, shown in Figure 2.7, have been computed similarly as in the previous case. Once again, it clearly appears that the estimated

region of attraction obtained from Theorem 2.1, i.e. including the integral and the anti-windup action, is much bigger than the one obtained from Corollary 2.1, i.e. without the anti-windup action. Indeed, with the same equally spaced grid by 0.5, the region of attraction contains 1.54×10^7 points with Theorem 2.1 and 2.36×10^5 points with Corollary 2.1, i.e. about 1.54% of the region computed with anti-windup. This illustrates, one more time, the benefit when the anti-windup scheme is considered. Moreover, as expected, the regions achieved by solving Theorem 2.1 for Problem $\mathcal{P}_2$ are about 60.3% smaller than the ones obtained for Problem $\mathcal{P}_1$. Indeed, let us recall that the set-point tracking problem is more constrained than the simple stabilization one. A particular set-point tracking trajectory is also plotted in Figure 2.7 (see black dots), this will be discussed latter.

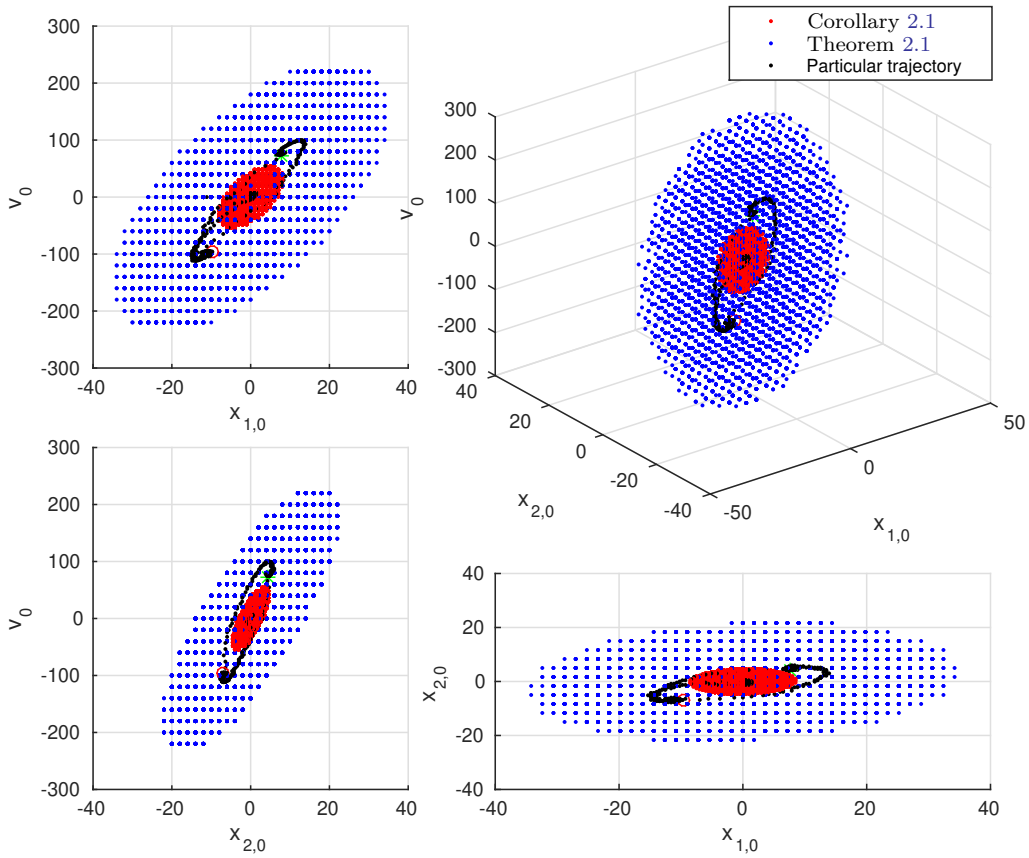

Figure 2.7: Estimate of the regions of attraction $\mathcal{D}_a^*$ for the set-point tracking problem $\mathcal{P}_2$ obtained from Theorem 2.1 (•) and Corollary 2.1 (•); particular set-points tracking trajectory (•).

For the considered coupled tanks systems with the whole set-points tracking control scheme depicted in Figure 2.1, the following PI-like and anti-windup gains have been obtained with the parameters $\eta = 1$ and $\tau_1 = 0.94$ from Theorem 2.1 and the optimization procedure $\mathcal{S}_\delta$ given in (2.37), which provides a maximal allowable bound of the reference signal $|y_{r_k}| \leq \beta = 6.64cm$ around the origin defined in (2.49):

$$K_{P1} = \begin{bmatrix} -0.4363 & 3.3327 \end{bmatrix}, K_{I1} = 0.1076, S_1 = 0.8234, E_{c1} = 1.2279,$$

$$K_{P2} = \begin{bmatrix} 1.3274 & 3.4812 \end{bmatrix}, K_{I2} = 0.1941, S_2 = 1.1240, E_{c2} = 0.6694,$$
$$K_{P3} = \begin{bmatrix} -0.3887 & 2.7935 \end{bmatrix}, K_{I3} = 0.0934, S_3 = 0.5286, E_{c3} = 1.2103,$$
$$K_{P4} = \begin{bmatrix} 0.7631 & 3.7546 \end{bmatrix}, K_{I4} = 0.1698, S_4 = 2.2098, E_{c4} = 1.5900,$$
$$K_{P5} = \begin{bmatrix} 0.1552 & 3.0274 \end{bmatrix}, K_{I5} = 0.1074, S_5 = 1.0855, E_{c5} = 0.8385,$$
$$K_{P6} = \begin{bmatrix} 1.6208 & 3.2999 \end{bmatrix}, K_{I6} = 0.2017, S_6 = 1.0203, E_{c6} = 0.7700,$$
$$K_{P7} = \begin{bmatrix} 1.8054 & 3.3107 \end{bmatrix}, K_{I7} = 0.1997, S_7 = 0.8278, E_{c7} = 0.7859,$$
$$K_{P8} = \begin{bmatrix} 1.3545 & 2.6136 \end{bmatrix}, K_{I8} = 0.1772, S_8 = 1.9622, E_{c8} = 1.4185.$$

With these gains, a comparison of the time-response obtained in simulation as well as the experimental data obtained from the real system is shown in Figure 2.8 with a set-points reference signal reaching the obtained bounds $|y_{r_k}| \leq \beta = 6.64cm$. From this figure, we can see the presence of the fuzzy anti-windup action (Figure 2.8(a)) whenever the actuator saturation occurs (Figure 2.8(c)), modifying the closed-loop behavior to preserve stability.

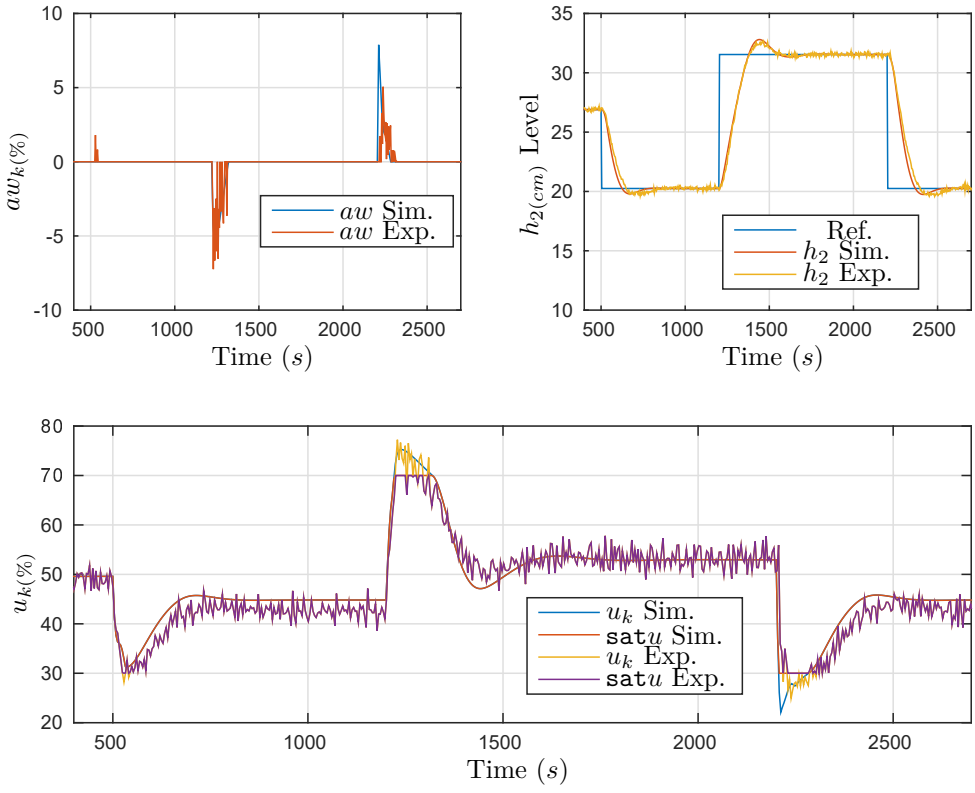

Figure 2.8: Time responses obtained with the PDCaw controller.

For this simulation, the resulting trajectory ξ_k is also shown in Figure 2.7 (see the above mentioned particular trajectory depicted by black dots). It clearly appears that it stays inside the estimated region of attraction $\mathcal{D}_a^*$ for Theorem 2.1 (blue dots), and so remains stable. Moreover, it also clearly shows that this trajectory overpasses the border of the estimated region of attraction for Corollary 2.1, i.e. without anti-windup action. One more time, these observations illustrate the significant improvement of our proposal with the fuzzy anti-windup action.

To conclude this experimental results subsection, let us go back to Corollary 2.1 associated with the optimization procedure $\mathcal{S}_\delta$ given in(2.37), which provides the following gains when the anti-windup scheme is not considered:

$$K_{P1} = \begin{bmatrix} 0.4778 & 6.3142 \end{bmatrix}, K_{I1} = 0.4911, \quad K_{P2} = \begin{bmatrix} 3.7216 & 9.1654 \end{bmatrix}, K_{I2} = 0.9489,$$

$$K_{P3} = \begin{bmatrix} 0.8313 & 6.4683 \end{bmatrix}, K_{I3} = 0.5139, \quad K_{P4} = \begin{bmatrix} 3.9880 & 11.1556 \end{bmatrix}, K_{I4} = 1.0414,$$

$$K_{P5} = \begin{bmatrix} 0.1946 & 4.9830 \end{bmatrix}, K_{I5} = 0.3571, \quad K_{P6} = \begin{bmatrix} 4.2113 & 9.9432 \end{bmatrix}, K_{I6} = 1.0356,$$

$$K_{P7} = \begin{bmatrix} 1.3820 & 6.1739 \end{bmatrix}, K_{I7} = 0.5303, \quad K_{P8} = \begin{bmatrix} 4.1947 & 10.1137 \end{bmatrix}, K_{I8} = 1.0239.$$

In this case, the obtained maximal allowable bound of the reference signal is only $|y_{r_k}| \leq \beta = 1.41cm$ around the origin, i.e. a reduced range in the set-points tracking of the second tank. Whereas, Figure 2.9 presents experimental results with the same set-points reference as for the previous experiment. Obviously, the latter overpasses the allowed reference bounds for the present case, but it allows us to highlight that, when these bounds are not respected, we may have bad transient response due to higher windup effects and, even if the set-points are reached after a longer settling times, there is no guarantee about the overall closed-loop stability.

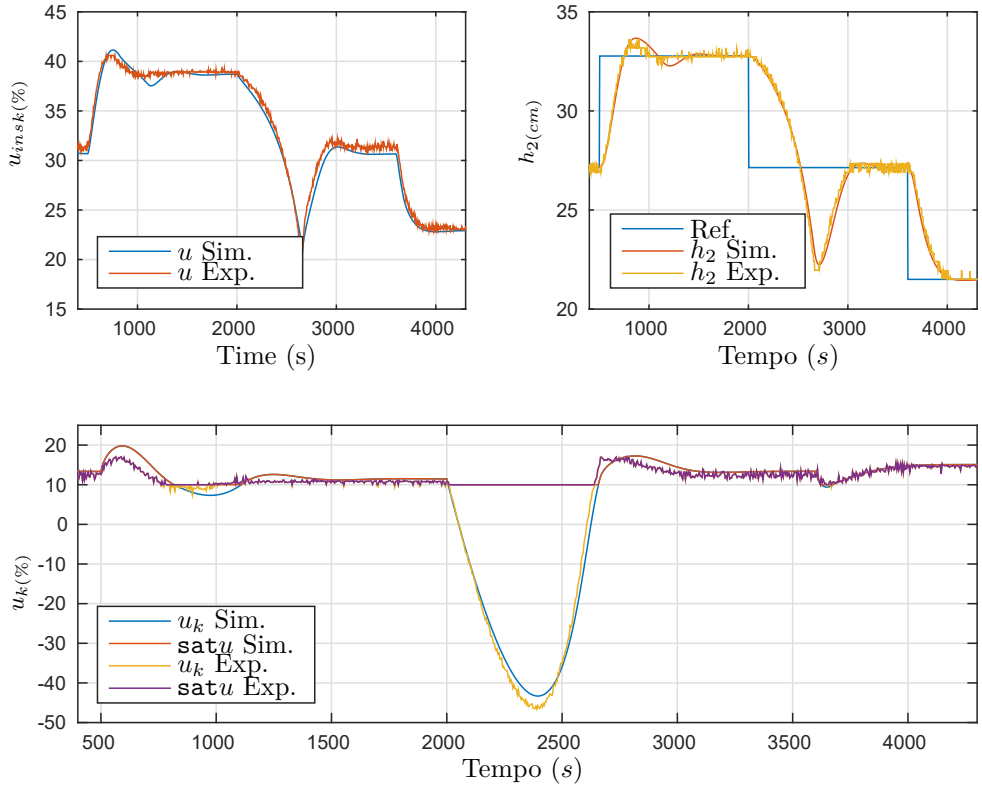

Figure 2.9: Time responses obtained with the PDC controller.

Therefore, the experimental tests show the occurrence of actuators saturation, which indicates that the controller delivers the maximum allowed energy to control the system, leading to better regulation and transient performances, while ensuring local stability.

2.6 Conclusions

In this chapter, we proposed a discrete-time fuzzy PI like controller with fuzzy anti-windup action to stabilize nonlinear discrete-time systems. The saturating actuators are considered in the design method and an estimate of the region of attraction is provided. A fuzzy Lyapunov function is used to certify the discrete-time closed-loop stability and to provide an estimate of the region of attraction. Moreover, the proposed design method can take into account bounded exogenous signals, providing for instance bounds for the set-point variation and ensuring that the closed-loop trajectories do not leave the region of attraction during set-point changes. Our approach has been shown less conservative than recent relevant result from the literature through a numerical example, then applied experimentally to a nonlinear level control system where the measures and control signals are performed with an industrial programmable logic controller (PLC).

The experimental results show the efficiency of the proposal and clearly indicates how the fuzzy anti-windup action can improve the time behavior of the closed-loop system. Additionally, the experimental tests show the occurrence of actuators saturation, which indicates that the controller delivers the maximum allowed energy to control the system, leading to a better regulation and transient performances, while ensuring local stability. The proposed PI-like control methodology with anti-windup action is given as general design conditions, which is not restricted to the test-bench of the coupled tank system described in this chapter. Indeed, it is clear that our approach can found a rich field of applications in the industrial processes where saturation may occur, such like furnaces with oil or gas fuel, chemical and petroleum processes, etc.

However, let us recall that some limitations arise when considering discrete-time control approaches for continuous-time plants. Indeed, if the results presented in this chapter are attractive for the design of point-to-point controllers, they require a constant sampling period, which is challenging to be guaranteed, especially when considering networked controllers, event-triggering schemes or sometimes when using low-cost embedded digital devices. Moreover, this technique frequently implies the choice of a hidebound small sampling period to ensure that the discrete-time model will catch all the plant dynamics. The aforementioned points certainly reduce the appeal of employing the direct discrete-time approach, especially when continuous-time systems involves fast dynamics driven by low cost digital devices. Moreover, these approaches cannot be employed in the context of Networked Controlled Systems (NCS) or when event-triggering control techniques are considered, since these often involves aperiodic sampled control signals. In order to cope with such aperiodicity in sampled-data control of continuous-time plant, an appealing approach is to rewrite the closed-loop dynamics as a continuous-time system with time-varying input delays, see e.g. (Fridman et al., 2004; Hetel et al., 2017). This will be the focus of our investigations in the next chapters, with the design of sampled-data controllers for continuous-time nonlinear systems represented by T-S fuzzy models.

Chapter 3

Aperiodic Sampled-data Controllers Design for Continous-time T-S Models

Résumé en Français : Synthèse de contrôleurs avec échantillonage apériodique pour les modèles T-S décrits en temps continu.

Dans le chapitre précédent, une approche permettant la synthèse de contrôleurs pour les modèles T-S à temps discret a été proposée dans le but de la commande de systèmes non linéaires, possiblement décrits en temps continu. Si cette approche est intéressante en raison de sa simplicité conceptuelle pour une mise en œuvre facilitée pour de nombreuses applications industrielles, il est important de rappeler que cette approche n'est valable que lorsqu'une période d'échantillonnage fixe, et suffisamment petite par rapport à la dynamique du système, est définie. Cependant, il est fréquent qu'une telle contrainte ne puisse être vérifiée. Par exemple, même dans le cadre d'un contrôleur numérique basé sur un protocole point à point, une période d'échantillonnage apériodique peut survenir en raison de l'incertitude sur la fréquence de l'horloge ou, plus généralement, l'architecture d'un système numérique temps réel, peut entraîner des retards de calcul ou une synchronisation imparfaite (Wittenmark et al., 1995; Hetel et al., 2017). De plus, avec le développement des applications utilisant l'Internet des Objets (IoT), les données échantillonnées transitent sur des réseaux de communication où des intervalles d'échantillonnage apériodiques sont généralement inévitables (Fridman, 2014a; de Souza et al., 2021).

*De plus, notons que lorsque de grandes périodes d'échantillonnage sont considérées, l'approche basée sur un modèle à temps discret ne garantit plus la stabilité du système complet en boucle fermée (Hetel et al., 2017). Brièvement présentée dans le **Chapitre 1**, une approche exploitant un retard sur l'entrée pour les contrôleurs basés sur des données échantillonnées est apparue comme un sujet de recherche prometteur en théorie du contrôle. Cette approche consiste en une réécriture de la dynamique en boucle fermée sous la forme d'un système à temps continu avec un retard variable sur l'entrée (Fridman et al., 2004; Hetel et al., 2017). Si de nombreux efforts ont été réalisés pour la stabilisation des systèmes dynamiques linéaires à partir de données échantillonnées, la plupart des applications réelles possède des dynamiques non linéaires, qui motive l'extension de ces approches dans le cadre non linéaire, notamment pour les modèles T-S.*

Pour la synthèse de contrôleurs basée sur des données échantillonnées, une façon classique d'évaluer le conservatisme est de chercher le plus grand intervalle d'échantillonnage admissible $[0, \bar{\eta}]$ qui garantit la stabilisation du système en boucle fermée. Dans le cadre de la synthèse de contrôleurs basée sur des données échantillonnées pour les modèles de type T-S, des réductions successives du conservatisme ont été obtenues. Par exemple, le

choix d'une fonctionnelle de Lyapunov-Krasovskii avec l'utilisation de techniques de relaxation basées sur la formule de Leibniz-Newton et de l'introduction de matrices de décision libres a été considéré dans (Yoneyama, 2010). Ensuite, étant donné que les fonctions d'appartenance possédant un retard impliquées dans le contrôleur ne correspondent pas précisément à celles impliquées dans le système à temps continu à contrôler, les bornes supérieures des erreurs asynchrones des fonctions d'appartenance ont été introduites dans l'obtention des conditions à vérifier (Zhang and Han, 2011; Koo et al., 2017). Dans (Zhu et al., 2012), une amélioration de cette approche a été introduite pour les critères de stabilisation. De plus, les plages de variation des fonctions d'appartenance avec des intervalles d'échantillonnage variables ont été considérées dans (Zhu et al., 2013). Plus récemment, un séparateur de sommets structuré a été utilisé afin de réduire le nombre de contraintes LMIs (Cheng et al., 2017). Cependant, comme expliqué dans la Section 1.4.2, il est important de noter que, dans le cadre des modèles de type T-S, la dynamique du système en boucle fermée implique une structure asynchrone possédant une double somme empêchant l'application des schémas de relaxation usuels (e.g. Lemme 1.2). Pour surmonter cet obstacle, la plupart des auteurs des études mentionnées précédemment ont borné les incertitudes associées, mais sans prêter beaucoup d'attention à leur caractérisation, et en particulier le lien avec les dérivées temporelles des fonctions d'appartenance. Il est donc raisonnable de penser que des améliorations significatives de réduction du conservatisme sont envisageables.

Par conséquent, dans ce chapitre, nous suivons le même objectif que les études mentionnées précédemment, afin de réduire le conservatisme, en proposant de nouvelles conditions à base de LMIs pour la synthèse de contrôleurs échantillonnés pour les modèles T-S décrits en temps continu. Pour cela, inspirée des travaux de (Briat and Seuret, 2012), une fonctionnelle de Lyapunov-Krasovskii « bouclée » est définie et les conditions de stabilité en boucle fermée sont obtenues en appliquant le lemme de Finsler (Lemme 1.4) et les inégalités étendues de Jensen (Lemme 1.8).

Par ailleurs, dans ce chapitre, un schéma de relaxation générique, étendant le lemme de Tuan (Lemme 1.2), est proposé pour tenir compte de la structure à double somme asynchrone apparaissant dans la dynamique en boucle fermée du modèle de type T-S continu commandé par un contrôleur PDC échantillonné. L'avantage de l'approche proposée dans ce chapitre par rapport à une approche basée directement sur un modèle T-S à temps discret est illustré au travers de l'exemple d'un pendule inversé en simulation (Exemple 1.2). Puis une comparaison, montrant des améliorations significatives pour la réduction du conservatisme, est effectuée par rapport aux résultats en lien de la littérature (Yoneyama, 2010; Zhu and Wang, 2011; Zhang and Han, 2011; Zhu et al., 2012; Gunasekaran and Joo, 2019; Zhu et al., 2013; Cheng et al., 2017), à partir d'un modèle simplifié d'un pendule inversé sur un chariot (Wang et al., 1996). Enfin, une validation expérimentale de l'approche de synthèse d'un correcteur basé sur des données échantillonnées est réalisée sur la plateforme Quanser® AERO (Quanser, 2016), illustrant l'efficacité de cette approche sur un système réel.

3.1 Introduction

In the previous chapter, a discrete-time T-S model-based controller design approach has been considered for the control of continuous-time nonlinear systems. If this approach is appealing for its conceptual simplicity with regard to many industrial applications, it is important to recall that it is only suitable when a small enough fixed sampling period can be set in regard to the plant dynamics. However, it often occurs that such requirements cannot be fulfilled. For instance,

even in a point-to-point digital control topology, aperiodic sampling may arise because of clock inaccuracy and system architecture characteristics such as real-time scheduling, which can induce jitters, imperfect synchronization or computation delays (Wittenmark et al., 1995; Hetel et al., 2017). Furthermore, with the growing of Internet of Things (IoT) applications, sampled-data systems are controlled through communication networks where aperiodic sampling intervals are almost inevitable (Fridman, 2014a; de Souza et al., 2021). Nonetheless, it is also well-known that when large sampling periods have to be considered, the direct discrete-time model-based approach may fail to guarantee the closed-loop inter-sampling stability (Hetel et al., 2017).

As introduced in Chapter 1, Section 1.4.2, the input delay approach for sampled-data control emerged as a promising research topic in control theory. It consists of rewriting the closed-loop dynamics as a continuous-time system with input time-varying delay (Fridman et al., 2004; Hetel et al., 2017). If many efforts have been done for the stabilization of linear dynamical systems from sampled-data measurements, most of real applications exhibit nonlinear dynamics, which motivate our interest in extending these approaches to the T-S model-based framework.

When dealing with sampled-data control, a convenient way to check the conservatism of the design conditions is to search for the maximal allowable sampling interval $[0, \bar{\eta}]$, which ensures the closed-loop dynamics stabilization. In the context of the sampled-data control of T-S models, successive conservatism improvements have been obtained. For instance, a Lyapunov-Krasovskii functional (LKF) and relaxation techniques based on the Leibniz-Newton formula and free-weighting matrix has been considered in (Yoneyama, 2010). Then, since the delayed membership functions involved in the controller part do not match the ones involved in the continuous-time plant to be controlled, the upper bounds of the asynchronous errors of the membership functions have been introduced in the design conditions (Zhang and Han, 2011; Koo et al., 2017). In (Zhu et al., 2012), an enlargement scheme has been introduced in the stabilization criteria. Furthermore, the variation ranges of membership functions within variable sampling intervals have been considered in (Zhu et al., 2013). More recently, a structured vertex separator has been used to reduce the number of LMIs constraints (Cheng et al., 2017).

However, as explained in Section 1.4.2, it is important to highlight that, in the T-S model-based framework, the closed-loop dynamics involve an asynchronous double summation structure, which prevents from applying classical relaxation schemes (e.g. Lemma 1.2). To cope with such issue, most of the authors of the above-mentioned studies assumed bounds of these mismatches, without paying much attention to their characterization, especially their relationship to the time-derivatives of the membership function. In this regard, we believe that there is still space for significant conservatism improvements.

Therefore, in this chapter, we follow the same goal as the above-mentioned studies to reduce the conservatism, i.e. the main objective is to propose new relaxed LMI-based conditions for the design of stabilizing aperiodic sampled-data controllers for continuous-time T-S systems. To achieve this goal, a convenient augmented looped LKF candidate is selected, together with the application of bounding lemmas, such as extended Jensen's inequalities (Lemma 1.8 and the Finsler's Lemma (Lemma 1.4). Moreover, in this chapter, a generic relaxation scheme, extending

Tuan's Lemma (Lemma 1.2), is proposed to handle the mismatched double summation structure of parameter dependent closed-loop stability conditions, which occurs in the considered T-S model-based sampled-data control context. The benefit of the proposed sampled-data approach vs conventional discrete-time T-S model-based design is illustrated through the 1-DOF inverted pendulum benchmark, previously introduced as Example 1.2. Then a comparison is proposed showing significant conservatism improvements regarding several previous related results from the literature (Yoneyama, 2010; Zhu and Wang, 2011; Zhang and Han, 2011; Zhu et al., 2012; Gunasekaran and Joo, 2019; Zhu et al., 2013; Cheng et al., 2017), from the benchmark of a simplified model (approximated 2 rules T-S fuzzy model drawn from (Wang et al., 1996)) of an inverted pendulum on a cart. Finally, an experimental validation of the proposed sampled-data design methodology is performed on the Quanser® AERO platform (Quanser, 2016), illustrating its effectiveness on a practical system.

3.2 Considered problem statement for T-S model-based sampled-data control design

Let us consider a continuous-time T-S system given by:

$$\dot{x}(t) = \sum_{i=1}^{r} \alpha_i(z(t)) \left(A_i x(t) + B_i u(t)\right) \tag{3.1}$$

where $z(t) = \begin{bmatrix} z_1(t) & \dots & z_p(t) \end{bmatrix} \in \mathbb{R}^p$ is a known vector of premise variables which only depends (for control purpose) on the entries of the state vector $x(t) \in \mathbb{R}^n$, $u(t) \in \mathbb{R}^m$ is the control input vector, $A_i \in \mathbb{R}^{n\times n}$, $B_i \in \mathbb{R}^{n\times m}$ are known constant matrices describing the dynamics of each polytope and $\alpha_i(z(t)) \geq 0$ are the membership functions satisfying the convex properties $\sum_{i=1}^{r} \alpha_i(z(t)) = 1$.

In this chapter, we consider the stabilization of T-S systems (3.1) from the following sampled-data PDC control law:

$$u(t) = \sum_{i=1}^{r} \alpha_i(z(t_k)) K_i X^{-1} x(t_k) \tag{3.2}$$

where $K_i \in \mathbb{R}^{m\times n}$ and $X^{-1} \in \mathbb{R}^{n\times n}$, for $i \in \mathcal{I}_r$, are the controller gain matrices to be designed.

With such sampled-data controllers, a Zero Order Hold (ZOH) is employed, $\forall t \in [t_k, t_{k+1})$, to maintain $x(t_k)$ from the aperiodic sampling instants $t_k \geq 0$ such that:

$$t_{k+1} - t_k = \eta_k \leq \bar{\eta} \tag{3.3}$$

where the inner sampling intervals bounds $\eta_k > 0$ can be non-uniform over samples with a maximal allowable sampling period $\bar{\eta}$ to be estimated.

For actual $t \in [t_k, t_{k+1})$, let:

$$\tau(t) = t - t_k \in [0, \eta_k) \tag{3.4}$$

where $\dot{\tau}(t) = 1$.

The control law (3.2) can be rewritten as:

$$u(t) = \sum_{i=1}^{r} \alpha_i(z(t-\tau(t)))K_i X^{-1} x(t-\tau(t)) \tag{3.5}$$

Substituting (3.5) in (3.1) gives the following closed-loop dynamics expressed as a T-S system, involving input time-varying delays and mismatching membership functions:

$$\dot{x}(t) = \sum_{i=1}^{r}\sum_{j=1}^{r} \alpha_i(z(t))\alpha_j(z(t-\tau(t)))(A_i x(t) + B_i K_j X^{-1} x(t-\tau(t))) \tag{3.6}$$

In the sequel, to lighten mathematical expressions, we will use the following notations for fuzzy summations of matrices:

$$M_\alpha = \sum_{i=1}^{r} \alpha_i(z(t))M_i,\ M_{\bar{\alpha}} = \sum_{i=1}^{r} \alpha_i(z(t-\tau(t)))M_i$$

and:

$$M_{\alpha\bar{\alpha}} = \sum_{i=1}^{r}\sum_{j=1}^{r} \alpha_i(z(t))\alpha_j(z(t-\tau(t)))M_{ij}$$

Hence, (3.6) yields:

$$\dot{x}(t) = A_\alpha x(t) + B_\alpha K_{\bar{\alpha}} X^{-1} x(t-\tau(t)) \tag{3.7}$$

Note that the sampled-data closed-loop dynamics involves an asynchronous (mismatching) double fuzzy summation structure ($\sum_{i=1}^{r}\sum_{j=1}^{r} \alpha_i(z(t))\alpha_j(z(t-\tau(t)))\dots$), which makes the design of sampled-data controllers (3.5) harder (more conservative) than in the standard continuous or discrete-time cases. This chapter aims at providing less pessimistic conditions to address this issue according to the following problem statement (divided in two points $\mathcal{P}_1$ and $\mathcal{P}_2$).

Problem statement:

$\mathcal{P}_1$: Provide relaxed parameterized LMI-based conditions for the design of the gain matrices K_i and X such that the sampled-data closed-loop dynamics (3.7) is asymptotically stable.

$\mathcal{P}_2$: Propose a generic relaxation scheme to solve inequalities parameterized as $\Lambda_{\alpha\bar{\alpha}} < 0$, which constitutes a double fuzzy summation structure with asynchronous (mismatching) membership functions.

The next section is devoted to address $\mathcal{P}_1$, while improvements for $\mathcal{P}_2$ will be proposed in section 3.4.

3.3 LMI-based sampled-data controller design

In the sequence, the goal is to provide parameterized LMI-based conditions satisfying $\mathcal{P}_1$ (of the above problem statement). The closed-loop dynamics (3.7) resulting in a T-S system with input time-varying delay, we propose to derive these conditions from the following LKF:

$$V(t) = V_1(t) + V_2(t) + V_3(t) + V_4(t) \tag{3.8}$$

where:

$$V_1(t) = x(t)^T L x(t) \tag{3.9}$$

$$V_2(t) = (\eta_k \tau(t) - \tau^2(t))\zeta^T(t) M_{\bar{\alpha}} \zeta(t) \tag{3.10}$$

$$V_3(t) = (\eta_k - \tau(t))\rho^T(t) N_{\bar{\alpha}} \rho(t) \tag{3.11}$$

$$V_4(t) = (\eta_k - \tau(t)) \int_{t-\tau(t)}^{t} \chi^T(s) P_{\alpha\bar{\alpha}} \chi(s) ds \tag{3.12}$$

with $\chi(t) = col\{x(t), \dot{x}(t)\}$ and:

$$\zeta(t) = col\left\{x(t), x(t-\tau(t)), \int_{t-\tau(t)}^{t} x(s)ds, \int_{t-\tau(t)}^{t} \dot{x}(s)ds\right\},$$

$$\rho(t) = col\left\{\int_{t-\tau(t)}^{t} x(s)ds, \int_{t-\tau(t)}^{t} \dot{x}(s)ds\right\}.$$

We motivate the choice of this LKF candidate by the fact that it belongs to the class of looped-functionals, which is a feature that have been shown appealing in the context of sampled-data control for linear systems (Briat and Seuret, 2012, 2015; Seuret and Briat, 2015). Indeed, it is worth to mention that, assuming $L = L^T > 0$, the whole LKF (3.8) is continuous and positive at each sample time t_k since we have $V_1(t_k) > 0$ and $V_\ell(t_k^-) = V_\ell(t_k) = 0$, for $\ell = 2, ..., 4$. Furthermore, the only requirement is that the LKF (3.8) must be monotonously decreasing during the inner sampling intervals, i.e. $\forall t \in [t_k, t_{k+1})$. This implies that, $\forall t \in [0, +\infty)$, it is positive and monotonously decreasing, and so the closed-loop dynamics (3.7) is guaranteed to be stable. In addition, the extended vectors and structures of the decision matrices in (3.10)-(3.12) have been chosen to conveniently avoid sparsity, according to the development of the relaxed LMI-based conditions summarized in the following Theorem, with the help of an extended version of Jensen's inequality (Fridman, 2010) and the Finsler lemma (Skelton et al., 1998) (see Lemma 1.8 and Lemma 1.4 given in Chapter 1).

Theorem 3.1. *: Let $(i,j) \in \mathcal{I}_r^2$ and assume that there exists the scalars $\phi_i > 0$ such that $\forall t, |\dot{\alpha}_i(t)| \leq \phi_i$. For aperiodic sampling periods $\eta_k \leq \bar{\eta}$ ($\bar{\eta}$ to be maximized), the T-S fuzzy model (3.1) is stabilized by the sampled-data PDC controller (3.2) if there exists the matrices $0 < \bar{L} = \bar{L}^T \in \mathbb{R}^{n\times n}$, $\bar{M}_j = \bar{M}_j^T \in \mathbb{R}^{4n\times 4n}$, $\bar{N}_j = \bar{N}_j^T \in \mathbb{R}^{2n\times 2n}$, $\bar{P}_{11ij} = \bar{P}_{11ij}^T \in \mathbb{R}^{n\times n}$, $\bar{P}_{22j} = \bar{P}_{22j}^T \in \mathbb{R}^{n\times n}$, $\bar{P}_{12j} = \bar{P}_{12j}^T \in \mathbb{R}^{n\times n}$, $X \in \mathbb{R}^{n\times n}$, $K_j \in \mathbb{R}^{m\times n}$, $\bar{Y}_{ij} \in \mathbb{R}^{4n\times n}$ and the scalars ε_1, ε_2 and ε_3, such that the following parameterized LMI-based condition is satisfied:*

$$\bar{\Lambda}_{\alpha\bar{\alpha}} = \begin{bmatrix} \bar{\Lambda}_{\alpha\bar{\alpha}}^{11} & * & * & * & * \\ 0 & \bar{\Lambda}_{\alpha\bar{\alpha}}^{22} & * & * & * \\ 0 & \bar{\eta}\bar{Y}_{\alpha\bar{\alpha}} & -\bar{\eta}\bar{P}_{22\bar{\alpha}} & * & * \\ 0 & 0 & 0 & \bar{\Lambda}_{\alpha\bar{\alpha}}^{44} & * \\ 0 & 0 & 0 & 0 & -\bar{P}_{11\alpha\bar{\alpha}} \end{bmatrix} < 0 \tag{3.13}$$

with:

$$\bar{\Lambda}_{\alpha\bar{\alpha}}^{11} = \bar{\Phi}_{\Sigma\alpha\bar{\alpha}}^0 + \mathbb{I}_\varepsilon \bar{G}_{\alpha\bar{\alpha}} + \bar{G}_{\alpha\bar{\alpha}}^T \mathbb{I}_\varepsilon^T, \; \bar{\Lambda}_{\alpha\bar{\alpha}}^{44} = \bar{\Lambda}_{\alpha\bar{\alpha}}^{11} - \bar{\tau}^2 \bar{\Phi}_{2\bar{\alpha}}^2$$

$$\bar{\Lambda}_{\alpha\bar{\alpha}}^{22} = \bar{\eta}^2 \Phi_{2\bar{\alpha}}^2 + \bar{\eta}(\bar{\Phi}_{\Sigma\bar{\alpha}}^1 - \tilde{P}_{\alpha\bar{\alpha}}) + \bar{\Phi}_{\Sigma\alpha\bar{\alpha}}^0 + \mathbb{I}_\varepsilon \bar{G}_{\alpha\bar{\alpha}} + \bar{G}_{\alpha\bar{\alpha}}^T \mathbb{I}_\varepsilon^T,$$

$$\mathbb{I}_\varepsilon = \begin{bmatrix} I & \varepsilon_1 I & \varepsilon_2 I & \varepsilon_3 I \end{bmatrix}^T, \bar{G}_{\alpha\bar{\alpha}} = \begin{bmatrix} A_i X & B_i K_{\bar{\alpha}} & 0 & -X \end{bmatrix},$$

$$\bar{\Phi}^1_{\Sigma\bar{\alpha}} = \mathcal{H}\left(\bar{\eta}\mathbb{E}_1^T \bar{M}_{\bar{\alpha}} \mathbb{E}_2 - \mathbb{E}_1^T \bar{M}_{\bar{\alpha}} \mathbb{E}_1\right) - \mathcal{H}\left(\mathbb{E}_4^T \bar{N}_{\bar{\alpha}} \mathbb{E}_5\right),$$

$$\bar{\Phi}^0_{\Sigma\alpha\bar{\alpha}} = \bar{\eta}\mathbb{E}_1^T \bar{M}_{\bar{\alpha}} \mathbb{E}_1 + \mathcal{H}\left(\bar{\eta}\mathbb{E}_4^T \bar{N}_{\bar{\alpha}} \mathbb{E}_5\right) - \mathcal{H}\left(E^T \bar{Y}_{\alpha\bar{\alpha}}\right) + \begin{bmatrix} \bar{\eta}\bar{P}_{11\alpha\bar{\alpha}} - \bar{P}_{12\bar{\alpha}} & 0 & 0 & \bar{L} + \bar{\eta}\bar{P}_{12\bar{\alpha}} \\ 0 & \bar{P}_{12\bar{\alpha}} & 0 & 0 \\ 0 & 0 & -\eta_k^{-1}\bar{P}_{11\alpha\bar{\alpha}} & 0 \\ * & 0 & 0 & \bar{\eta}\bar{P}_{22\alpha\bar{\alpha}} \end{bmatrix},$$

$$\bar{M}_{\bar{\alpha}} = \begin{bmatrix} \bar{M}_{11\bar{\alpha}} & \bar{M}_{12\bar{\alpha}} & \bar{M}_{13\bar{\alpha}} & \bar{M}_{14\bar{\alpha}} \\ * & \bar{M}_{22\bar{\alpha}} & \bar{M}_{23\bar{\alpha}} & \bar{M}_{24\bar{\alpha}} \\ * & * & \bar{M}_{33\bar{\alpha}} & \bar{M}_{34\bar{\alpha}} \\ * & * & * & \bar{M}_{44\bar{\alpha}} \end{bmatrix}, \tilde{P}_{\alpha\bar{\alpha}} = \begin{bmatrix} \bar{P}_{11\alpha\bar{\alpha}} & 0 & 0 & \bar{P}_{12\bar{\alpha}} \\ 0 & 0 & 0 & 0 \\ 0 & 0 & 0 & 0 \\ * & 0 & 0 & \bar{P}_{22\bar{\alpha}} \end{bmatrix},$$

$$\mathbb{E}_1 = \begin{bmatrix} e_1 \\ e_2 \\ e_3 \\ e_1 - e_2 \end{bmatrix}, \mathbb{E}_2 = \begin{bmatrix} e_4 \\ e_0 \\ e_1 \\ e_4 \end{bmatrix}, \mathbb{E}_4 = \begin{bmatrix} e_3 \\ e_1 - e_2 \end{bmatrix}, \mathbb{E}_5 = \begin{bmatrix} e_1 \\ e_4 \end{bmatrix}.$$

Proof 3.1. *Let us consider the looped LKF candidate (3.8) with $L = L^T > 0$, the closed-loop dynamics (3.7) is stable if, $\forall t \in [t_k, t_{k+1})$:*

$$\dot{V}(t) = \dot{V}_1(t)) + \dot{V}_2(t)) + \dot{V}_3(t)) + \dot{V}_4(t)) < 0 \tag{3.14}$$

To provide less conservative stability conditions, let us consider the following extended state vector:

$$\xi(t) = col\left\{x(t), x(t-\tau(t)), \int_{t-\tau(t)}^{t} x(s)ds, \dot{x}(t)\right\} \tag{3.15}$$

The time-derivative of $V_1(t)$ is straightforwardly obtained as:

$$\dot{V}_1(t) = 2x^T(t)L\dot{x}(t) = \xi^T(t)\Phi_1^0\xi(t), \Phi_1^0 = \begin{bmatrix} 0 & 0 & 0 & L \\ 0 & 0 & 0 & 0 \\ 0 & 0 & 0 & 0 \\ L & 0 & 0 & 0 \end{bmatrix} \tag{3.16}$$

Then, for $V_2(t)$, the time-derivative is computed as:

$$\dot{V}_2(t) = (\eta_k - 2\tau(t))\zeta^T(t)M_{\bar{\alpha}}\zeta(t) + 2(\eta_k\tau(t) - \tau^2(t))\zeta^T(t)M_{\bar{\alpha}}\dot{\zeta}(t) \tag{3.17}$$

Assuming $\zeta(t) = \mathbb{E}_1\xi(t)$ and $\dot{\zeta}(t) = \mathbb{E}_2\xi(t)$, with E_1 and E_2 given above,(3.17) can be rewritten as:

$$\dot{V}_2(t) = \tau^2(t)\xi^T(t)\Phi^2_{2\bar{\alpha}}\xi(t) + \tau(t)\xi^T(t)\Phi^1_{2\bar{\alpha}}\xi(t) + \xi^T(t)\Phi^0_{2\bar{\alpha}}\xi(t) \tag{3.18}$$

with $\Phi^2_{2\bar{\alpha}} = -\mathcal{H}\left(\mathbb{E}_1^T M_{\bar{\alpha}}\mathbb{E}_2\right)$, $\Phi^1_{2\bar{\alpha}} = \mathcal{H}\left(\eta_k\mathbb{E}_1^T M_{\bar{\alpha}}\mathbb{E}_2 - \mathbb{E}_1^T M_{\bar{\alpha}}\mathbb{E}_1\right)$ and $\Phi^0_{2\bar{\alpha}} = \eta_k\mathbb{E}_1^T M_{\bar{\alpha}}\mathbb{E}_1$.
In a similar way, the time-derivative of $V_3(t)$ is given by:

$$\dot{V}_3(t) = -\rho^T(t)N_{\bar{\alpha}}\rho(t) + 2(\eta_k - \tau(t))\rho^T(t)N_{\bar{\alpha}}\dot{\rho}(t), \tag{3.19}$$

and since $\rho(t) = \mathbb{E}_4\xi(t)$ and $\dot{\rho}(t) = \mathbb{E}_5\xi(t)$ we can write:

$$\dot{V}_3(t) = \tau(t)\xi^T(t)\Phi^1_{3\bar{\alpha}}\xi(t) + \xi^T(t)\Phi^0_{3\bar{\alpha}}\xi(t) \tag{3.20}$$

with $\Phi^0_{3\bar{\alpha}} = \mathcal{H}\left(\eta_k \mathbb{E}_4^T N_{\bar{\alpha}} \mathbb{E}_5\right) - \mathbb{E}_4^T N_{\bar{\alpha}} \mathbb{E}_4$ *and* $\Phi^1_{3\bar{\alpha}} = -\mathcal{H}\left(\mathbb{E}_4^T N_{\bar{\alpha}} \mathbb{E}_5\right)$.
Taking the time-derivative of $V_4(t)$*, we get:*

$$\dot{V}_4(t) = (\eta_k - \tau(t))\chi^T(t) P_{\alpha\bar{\alpha}} \chi(t) - \int_{t-\tau(t)}^{t} \chi^T(s) P_{\alpha\bar{\alpha}} \chi(s) ds \tag{3.21}$$

Assuming $P_{\alpha\bar{\alpha}} = \begin{bmatrix} P_{11\alpha\bar{\alpha}} & P_{12\bar{\alpha}} \\ * & P_{22\bar{\alpha}} \end{bmatrix}$ *leads to:*

$$\begin{aligned} \dot{V}_4(t) =& (\eta_k - \tau(t))\chi^T(t) P_{\alpha\bar{\alpha}} \chi(t) - \int_{t-\tau(t)}^{t} x^T(s) P_{11\alpha\bar{\alpha}} x(s) ds \\ & - \int_{t-\tau(t)}^{t} \dot{x}^T(s) P_{22\bar{\alpha}} \dot{x}(s) ds - 2\int_{t-\tau(t)}^{t} x^T(s) P_{12\bar{\alpha}} \dot{x}(s) ds \end{aligned} \tag{3.22}$$

That is to say:

$$\begin{aligned} \dot{V}_4(t) =& (\eta_k - \tau(t))\chi^T(t) P_{\alpha\bar{\alpha}} \chi(t) - \int_{t-\tau(t)}^{t} x^T(s) P_{11\alpha\bar{\alpha}} x(s) ds \\ & - \int_{t-\tau(t)}^{t} \dot{x}^T(s) P_{22\bar{\alpha}} \dot{x}(s) ds - x^T(t) P_{12\bar{\alpha}} x(t) + x^T(t-\tau(t)) P_{12\bar{\alpha}} x(t-\tau(t)) \end{aligned} \tag{3.23}$$

Assuming $P_{11\alpha\bar{\alpha}} > 0$ *and applying Lemma 1.7 on the first integral term, we have:*

$$\begin{aligned} \dot{V}_4(t) \leq& (\eta_k - \tau(t))\chi^T(t) P_{\alpha\bar{\alpha}} \chi(t) - \eta_k^{-1} \int_{t-\tau(t)}^{t} x^T(s) ds P_{11\alpha\bar{\alpha}} \int_{t-\tau(t)}^{t} x(s) ds \\ & - \int_{t-\tau(t)}^{t} \dot{x}^T(s) P_{22\bar{\alpha}} \dot{x}(s) ds - x^T(t) P_{12\bar{\alpha}} x(t) + x^T(t-\tau(t)) P_{12\bar{\alpha}} x(t-\tau(t)) \end{aligned} \tag{3.24}$$

Note that:

$$\int_{t-\tau(t)}^{t} \dot{x}^T(s) ds = \underbrace{\begin{bmatrix} I & -I & 0 & 0 \end{bmatrix}}_{E} \xi(t) \tag{3.25}$$

Hence, assuming $P_{22\bar{\alpha}} > 0$*, which is constant* $\forall t \in [t_k, t_{k+1})$*, and applying Lemma 1.8 on (3.24), for any matrix* $Y_{\alpha\bar{\alpha}}$ *we have:*

$$\begin{aligned} \dot{V}_4(t) \leq & (\eta_k - \tau(t))\chi^T(t) P_{\alpha\bar{\alpha}} \chi(t) + \xi^T(t) \left(-E^T Y_{\alpha\bar{\alpha}} - Y_{\alpha\bar{\alpha}}^T E + \tau(t) Y_{\alpha\bar{\alpha}}^T P_{22\bar{\alpha}}^{-1} Y_{\alpha\bar{\alpha}}\right) \xi(t) \\ & - \eta_k^{-1} \int_{t-\tau(t)}^{t} x^T(s) ds P_{11\alpha\bar{\alpha}} \int_{t-\tau(t)}^{t} x(s) ds - x^T(t) P_{12\bar{\alpha}} x(t) + x^T(t-\tau(t)) P_{12\bar{\alpha}} x(t-\tau(t)), \end{aligned} \tag{3.26}$$

or, equivalently:

$$\dot{V}_4(t) \leq \tau(t) \xi^T(t) \Phi^1_{4\alpha\bar{\alpha}} \xi(t) + \xi^T(t) \Phi^0_{4\alpha\bar{\alpha}} \xi(t) \tag{3.27}$$

with:

$$\Phi^1_{4\alpha\bar{\alpha}} = Y_{\alpha\bar{\alpha}}^T P_{22\bar{\alpha}}^{-1} Y_{\alpha\bar{\alpha}} - \tilde{P}_{\alpha\bar{\alpha}}, \quad \tilde{P}_{\alpha\bar{\alpha}} = \begin{bmatrix} P_{11\alpha\bar{\alpha}} & 0 & 0 & P_{12\bar{\alpha}} \\ 0 & 0 & 0 & 0 \\ 0 & 0 & 0 & 0 \\ * & 0 & 0 & P_{22\bar{\alpha}} \end{bmatrix}$$

and:

$$\Phi^0_{4\alpha\bar{\alpha}} = -\mathcal{H}\left(E^T Y_{\alpha\bar{\alpha}}\right) + \begin{bmatrix} \eta_k P_{11\alpha\bar{\alpha}} - P_{12\bar{\alpha}} & 0 & 0 & \eta_k P_{12\bar{\alpha}} \\ 0 & P_{12\bar{\alpha}} & 0 & 0 \\ 0 & 0 & -\eta_k^{-1} P_{11\alpha\bar{\alpha}} & 0 \\ * & 0 & 0 & \eta_k P_{22\bar{\alpha}} \end{bmatrix},$$

requiring $P_{12\bar{\alpha}} = P_{12\bar{\alpha}}^T$.
So, from (3.16), (3.18), (3.20) *and* (3.27), *the inequality* (3.14) *is satisfied if:*

$$\begin{aligned}\mathcal{P}(\tau(t)) =& \tau^2(t)\xi^T(t)\Phi_{2\bar{\alpha}}^2\xi(t) \\ &+ \tau(t)\xi^T(t)(\Phi_{2\bar{\alpha}}^1 + \Phi_{3\bar{\alpha}}^1 + \Phi_{4\alpha\bar{\alpha}}^1)\xi(t) \\ &+ \xi^T(t)(\Phi_1^0 + \Phi_{2\bar{\alpha}}^0 + \Phi_{3\bar{\alpha}}^0 + \Phi_{4\alpha\bar{\alpha}}^0)\xi(t) < 0\end{aligned} \tag{3.28}$$

Let us recall that acoording Lemma 1.9, (3.28) can be checked if:

$$\mathcal{P}(0) < 0, \tag{3.29}$$

$$\mathcal{P}(\bar{\eta}) < 0, \tag{3.30}$$

$$\mathcal{P}(0) - \tau^2(t)\xi^T(t)\Phi_{2\bar{\alpha}}^2\xi(t) < 0, \tag{3.31}$$

Then, the inequalities (3.29) *and* (3.30) *are verified if,* $\forall \xi^T(t) \neq 0$ *:*

$$\xi^T(t)\left(\Phi_1^0 + \Phi_{2\bar{\alpha}}^0 + \Phi_{3\bar{\alpha}}^0 + \Phi_{4\alpha\bar{\alpha}}^0\right)\xi(t) < 0 \tag{3.32}$$

and

$$\xi^T(t)\left(\bar{\eta}^2\Phi_{2\bar{\alpha}}^2 + \bar{\eta}(\Phi_{2\bar{\alpha}}^1 + \Phi_{3\bar{\alpha}}^1 + \Phi_{4\alpha\bar{\alpha}}^1) + \Phi_1^0 + \Phi_{2\bar{\alpha}}^0 + \Phi_{3\bar{\alpha}}^0 + \Phi_{4\alpha\bar{\alpha}}^0\right)\xi(t) < 0 \tag{3.33}$$

Now, before dealing with (3.32) *and* (3.33), *we will introduce the closed-loop dynamics into the stability conditions. To do so, note that* (3.7) *is equivalent to* $G_{\alpha\bar{\alpha}}\xi(t) = 0$, *with* $G_{\alpha\bar{\alpha}} = \begin{bmatrix} A_\alpha & B_\alpha K_{\bar{\alpha}} X^{-1} & 0 & -I \end{bmatrix}$. *Moreover,* (3.28) *can be rewritten as:*

$$\xi^T(t)\left(\tau^2(t)\Phi_{2\alpha\bar{\alpha}}^2 + \tau(t)(\Phi_{\Sigma\bar{\alpha}}^1 + \Phi_{4\alpha\bar{\alpha}}^1) + \Phi_{\Sigma\alpha\bar{\alpha}}^0\right)\xi(t) < 0 \tag{3.34}$$

with $\Phi_{\Sigma\bar{\alpha}}^1 = \Phi_{2\bar{\alpha}}^1 + \Phi_{3\bar{\alpha}}^1$ *and* $\Phi_{\Sigma\alpha\bar{\alpha}}^0 = \sum_{q=1}^3 \Phi_{q\bar{\alpha}}^0 + \Phi_{4\alpha\bar{\alpha}}^0$.
So, we can apply the Finsler's Lemma (Lemma 1.4) and the inequality (3.34) *is satisfied if there exists* $R \in \mathbb{R}^{4n\times n}$ *such that:*

$$\tau^2(t)\Phi_{2\alpha\bar{\alpha}}^2 + \tau(t)(\Phi_{\Sigma\bar{\alpha}}^1 + \Phi_{4\alpha\bar{\alpha}}^1) + \Phi_{\Sigma\alpha\bar{\alpha}}^0 + RG_{\alpha\bar{\alpha}} + G_{\alpha\bar{\alpha}}^T R^T < 0 \tag{3.35}$$

Hence, (3.32) *and* (3.33) *are satisfied if the following inequalities hold:*

$$\Phi_{\Sigma\alpha\bar{\alpha}}^0 + RG_{\alpha\bar{\alpha}} + G_{\alpha\bar{\alpha}}^T R^T < 0 \tag{3.36}$$

$$\bar{\eta}^2\Phi_{2\alpha\bar{\alpha}}^2 + \bar{\eta}(\Phi_{\Sigma\bar{\alpha}}^1 + \Phi_{4\alpha\bar{\alpha}}^1) + \Phi_{\Sigma\alpha\bar{\alpha}}^0 + RG_{\alpha\bar{\alpha}} + G_{\alpha\bar{\alpha}}^T R^T < 0 \tag{3.37}$$

Let X *regular and* $R = \begin{bmatrix} X^{-1} & \varepsilon_1 X^{-1} & \varepsilon_2 X^{-1} & \varepsilon_3 X^{-1} \end{bmatrix}^T$. *To deal with* (3.36), *pre- and post-multiplying it respectively by* $\mathtt{diag}\{\ X \quad X \quad X \quad X\ \}^T$ *and its transpose, we obtain:*

$$\bar{\Lambda}_{\alpha\bar{\alpha}}^{11} = \bar{\Phi}_{\Sigma\alpha\bar{\alpha}}^0 + \mathbb{I}_\varepsilon \bar{G}_{\alpha\bar{\alpha}} + \bar{G}_{\alpha\bar{\alpha}}^T \mathbb{I}_\varepsilon^T < 0 \tag{3.38}$$

Then, to deal with (3.37), *apply first the Schur complement on* $\Phi_{4\alpha\bar{\alpha}}^1$, *then pre- and post-multiplying it respectively by* $\mathtt{diag}\{\ X \quad X \quad X \quad X \quad X\ \}^T$ *and its transpose, we obtain:*

$$\begin{bmatrix} \bar{\Lambda}_{\alpha\bar{\alpha}}^{22} & * \\ \bar{\eta}\bar{Y}_{\alpha\bar{\alpha}} & -\bar{\eta}\bar{P}_{22\bar{\alpha}} \end{bmatrix} < 0 \tag{3.39}$$

with:

$$\bar{\Lambda}^{22}_{\alpha\bar{\alpha}} = \bar{\eta}^2\bar{\Phi}^2_{2\alpha\bar{\alpha}} + \bar{\eta}(\bar{\Phi}^1_{\Sigma\bar{\alpha}} - \tilde{P}_{\alpha\bar{\alpha}}) + \bar{\Phi}^0_{\Sigma\alpha\bar{\alpha}} + \mathbb{I}_\varepsilon\bar{G}_{\alpha\bar{\alpha}} + \bar{G}^T_{\alpha\bar{\alpha}}\mathbb{I}^T_\varepsilon,$$

and where, in (3.38) *and* (3.39), $\mathbb{I}_\varepsilon = \begin{bmatrix} I & \varepsilon_1 I & \varepsilon_2 I & \varepsilon_3 I \end{bmatrix}^T$, $\bar{G}_{\alpha\bar{\alpha}} = \begin{bmatrix} A_\alpha X & B_\alpha K_{\bar{\alpha}} & 0 & -X \end{bmatrix}$. *Then, to deal with* (3.31), *pre- and post-multiplying it respectively by* $\mathtt{diag}\{\ X \quad X \quad X \quad X\ \}^T$ *and its transpose, we obtain:*

$$\bar{\Lambda}^{44}_{\alpha\bar{\alpha}} = \bar{\Lambda}^{11}_{\alpha\bar{\alpha}} - \tau^2\bar{\Phi}^2_{2\bar{\alpha}} < 0 \tag{3.40}$$

and all decision matrices inside $\bar{\Phi}^2_{2\alpha\bar{\alpha}}$, $\bar{\Phi}^1_{\Sigma\bar{\alpha}}$, $\bar{\Phi}^1_{4\alpha\bar{\alpha}}$ *and* $\bar{\Phi}^0_{\Sigma\alpha\bar{\alpha}}$ *belong to the bijective change of variables:*

$$\bar{D} = X^T D X, \quad D = \{L, M_{11\bar{\alpha}}, \ldots, M_{44\bar{\alpha}}, N_{11\bar{\alpha}}, \ldots, N_{22\bar{\alpha}}, P_{11\alpha\bar{\alpha}}, P_{12\bar{\alpha}}, P_{22\alpha\bar{\alpha}}\}.$$

Finally, concatenating (3.38), (3.39), (3.40), $P_{11\alpha\bar{\alpha}} > 0$ *and* $P_{22\bar{\alpha}} > 0$ *into the same parameterized LMI* ($\Lambda_{\alpha\bar{\alpha}} < 0$), *we obtain the conditions expressed in Theorem 3.1.* □

Before proceeding with the analysis of the results from implementing sampled-data controllers to drive T-S models, it is important to highlight that the inequality (3.13) involves mismatching parameters (membership functions) associated with the sampled-data PDC control law (3.2) and with the continuous-time T-S model (3.1). Indeed, it is known that the input signal is computed only at the discrete-time instants while the system continuously evolves, and this phenomenon produces a mismatch between their membership functions during inter-samplings. Obviously, solving the conditions of Theorem 3.1 for all vertices i and j would be extremely conservative and, due to the membership functions mismatches, we cannot apply directly double fuzzy sums relaxation schemes such like Tuan's Lemma (see Lemma 1.2). To circumvent the mismatch problem, many authors assume $|\alpha_i - \bar{\alpha}_i| \leq \rho_i$ (see e.g. (Cheng et al., 2017)). Moreover, Lemma 1.10 has been proposed as a dedicated relaxation scheme in (Koo et al., 2017). However, the latter doesn't take into consideration some particular characteristics of the membership functions mismatches, especially the fact that their upper bounds ρ_i can be expressed with regards to the upper bounds of the membership functions' derivatives ($|\dot{\alpha}_i| < \phi_i, \forall i \in \mathcal{I}_r$,) and the maximal allowed sampling period ($\bar{\eta}$). Such considerations may help to reduce the conservatism, as proposed in the next section, where an extension of Tuan's Lemma is proposed in the T-S model-based sampled-data controller design framework.

Remark 3.1. *The conditions expressed in Theorem 3.1 are not strictly LMI because of the parameters* ε_1, ε_2 *and* ε_3. *However, as stated in many previous works applying the Finsler's Lemma, see e.g. (Oliveira et al., 2011; Bourahala et al., 2017; Cherifi et al., 2018, 2019), these parameters are usually tuned offline by grid search.*

Remark 3.2. *The proposed sampled-data controller design methodology for T-S systems includes linear systems as a special case by removing parameter dependency for all decision variables in the LMI-based conditions expressed in Theorem 3.1. This particular case will be further investigated in this Chapter, providing an experimental validation of the proposed sampled-data controller design procedure on the Quanser® AERO 2-DOF Helicopter test-bed.*

3.4 Relaxation scheme for T-S model-based sampled-data controller design

Let us recall that standard double fuzzy sums relaxation scheme, such Lemma 1.2 (Tuan et al., 2001), cannot be directly employed in the context of sampled-data control since the closed-loop dynamics (3.7) involves a double fuzzy sum structure with mismatched membership functions ($\alpha\bar{\alpha}$). To circumvent this drawback, one may apply Lemma 1.10 (Koo et al., 2017). However, as previously mentioned, the latter does not take into consideration some particular characteristics of the membership functions mismatches, especially the fact that their upper bounds σ_i can be expressed with regard to the upper bounds of the membership functions' derivatives ($|\dot{\alpha}_i| < \phi_i, \forall i \in \mathcal{I}_r,$) and the maximal allowed sampling period ($\bar{\eta}$). Therefore, with the aim of providing less conservative conditions, we propose the following Theorem as an extension of Tuan's Lemma in the context T-S model-based sampled-data controller design. In this context, the following Lemma will be useful to address the above stated problem.

Lemma 3.1. *(Xie, 1996): Let X and Y be matrices of appropriate dimensions. For any matrix $T > 0$, the following inequality is true:*

$$X^TY + Y^TX \leq X^TTX + Y^TT^{-1}Y \tag{3.41}$$

Theorem 3.2. *(Lopes et al., 2020a): For $(i,j) \in \mathcal{I}_r^2$, let Λ_{ij} be matrices of appropriate dimensions and assume, $\forall t$, $|\dot{\alpha}_i(t)| \leq \phi_i$. The inequality $\Lambda_{\alpha\bar{\alpha}} < 0$ is satisfied if there exists diagonal matrices $T_{ij} > 0$ such that conditions (3.42) and (3.43) hold with:*

$$\Gamma_{ii} < 0, \forall i \in \mathcal{I}_r, \tag{3.42}$$

$$\frac{2}{r-1}\Gamma_{ii} + \Gamma_{ij} + \Gamma_{ji} < 0, \forall\, (i,j) \in \mathcal{I}_r^2, i \neq j, \tag{3.43}$$

with:

$$\Gamma_{ij} = \begin{bmatrix} \Lambda_{ij} + \frac{r-1}{16}T_{ij} & (*) & \dots & (*) \\ \sigma_1\bar{\Lambda}_{ij1} & -T_{ij} & 0 & 0 \\ \vdots & 0 & \ddots & 0 \\ \sigma_{r-1}\bar{\Lambda}_{ijr-1} & 0 & 0 & -T_{ij} \end{bmatrix}$$

where, $\forall \rho \in \mathcal{I}_{r-1}$, $\bar{\Lambda}_{ij\rho} = \Lambda_{i\rho} + \Lambda_{j\rho} - \Lambda_{ir} - \Lambda_{jr}$ and $\sigma_\rho = \min\{1, \phi_\rho\bar{\eta}\}$.

Proof 3.2. *Using the short hand notation for memberships functions $\alpha_i = \alpha_i(z(t))$ and $\bar{\alpha}_i = \alpha_i(z(t-\tau(t)))$ we have:*

$$\begin{aligned} \Lambda_{\alpha\bar{\alpha}} &= \sum_{i=1}^{r}\sum_{j=1}^{r}\alpha_i\bar{\alpha}_j\Lambda_{ij} = \sum_{i=1}^{r}\sum_{j=1}^{r}\alpha_i\alpha_j\left(\Lambda_{ij} + \sum_{\rho=1}^{r}(\bar{\alpha}_\rho - \alpha_\rho)\Lambda_{i\rho}\right) \\ &= \sum_{i=1}^{r}\sum_{j=1}^{r}\alpha_i\alpha_j\left(\Lambda_{ij} + \sum_{\rho=1}^{r}\frac{\bar{\alpha}_\rho - \alpha_\rho}{2}(\Lambda_{i\rho} + \Lambda_{j\rho})\right) \end{aligned} \tag{3.44}$$

Since $\sum_{\rho=1}^{r}(\bar{\alpha}_\rho - \alpha_\rho) = 0 \Leftrightarrow (\bar{\alpha}_r - \alpha_r) = -\sum_{\rho=1}^{r-1}(\bar{\alpha}_\rho - \alpha_\rho)$, $\forall (i,j)$ we can write:

$$\sum_{\rho=1}^{r}\frac{\bar{\alpha}_\rho - \alpha_\rho}{2}(\Lambda_{i\rho} + \Lambda_{j\rho}) = \sum_{\rho=1}^{r-1}\frac{\bar{\alpha}_\rho - \alpha_\rho}{2}\bar{\Lambda}_{ij\rho} \tag{3.45}$$

with $\bar{\Lambda}_{ij\rho} = \Lambda_{i\rho} + \Lambda_{j\rho} - \Lambda_{ir} - \Lambda_{jr}$. *Note that* $\forall \rho \in \mathcal{I}_r$ *we have:*

$$-1 \leq \alpha_\rho - \bar{\alpha}_\rho \leq 1 \tag{3.46}$$

Moreover, by assuming $\forall t$, $|\dot{\alpha}_\rho(t)| \leq \phi_\rho$ *and since* $\tau(t) \in [0, \eta_k)$ *with* $\eta_k \leq \bar{\eta}$, *we also have:*

$$-\phi_\rho \bar{\eta} \leq \alpha_\rho - \bar{\alpha}_\rho = \int_{t-\tau(t)}^{t} \dot{\alpha}_\rho(s) ds \leq \phi_\rho \bar{\eta} \tag{3.47}$$

Thus, from (3.46) *and* (3.47), *we can assert that:*

$$-1 \leq \frac{\bar{\alpha}_\rho - \alpha_\rho}{\sigma_\rho} \leq 1 \text{ with } \sigma_\rho = \min\{1, \phi_\rho \bar{\eta}\} \tag{3.48}$$

Let us now rewrite (3.45) *as:*

$$\sum_{\rho=1}^{r-1} \frac{\bar{\alpha}_\rho - \alpha_\rho}{2} \bar{\Lambda}_{ij\rho} = \mathcal{H}_e \left(\frac{1}{4} \underbrace{\begin{bmatrix} I & \dots & I \end{bmatrix}}_{r-1 \text{ times } I} \Delta_{\alpha\bar{\alpha}} \nabla_{ij} \right) \tag{3.49}$$

where:

$$\Delta_{\alpha\bar{\alpha}} = \begin{bmatrix} \frac{\bar{\alpha}_1 - \alpha_1}{\sigma_1} & 0 & 0 \\ 0 & \ddots & 0 \\ 0 & 0 & \frac{\bar{\alpha}_{r-1} - \alpha_{r-1}}{\sigma_{r-1}} \end{bmatrix} \text{ and } \nabla_{ij} = \begin{bmatrix} \sigma_1 \bar{\Lambda}_{ij1} \\ \vdots \\ \sigma_{r-1} \bar{\Lambda}_{ijr-1} \end{bmatrix}$$

From Lemma 3.1, for any matrices $T_{ij} > 0$, *it yields:*

$$\sum_{\rho=1}^{r-1} \frac{\bar{\alpha}_\rho - \alpha_\rho}{2} \bar{\Lambda}_{ij\rho} \leq \frac{r-1}{16} T_{ij} + \nabla_{ij}^T \Delta_{\alpha\bar{\alpha}} T_{ij}^{-1} \Delta_{\alpha\bar{\alpha}} \nabla_{ij} \tag{3.50}$$

Now, let $T_{ij} > 0$ *be diagonal matrices, since* $\Delta_{\alpha\bar{\alpha}}$ *is also diagonal and* $\Delta_{\alpha\bar{\alpha}} \Delta_{\alpha\bar{\alpha}} \leq I$, $\Delta_{\alpha\bar{\alpha}} T_{ij}^{-1} \Delta_{\alpha\bar{\alpha}} = \Delta_{\alpha\bar{\alpha}} \Delta_{\alpha\bar{\alpha}} T_{ij}^{-1} \leq T_{ij}^{-1}$. *Thus, considering* (3.44), (3.45) *and* (3.50) *and applying Lemma 1.2, then applying the Schur complement, we obtain the conditions expressed in Theorem 3.2.* □

From now, two main points are to be verified: The effectiveness of the sampled-data control design conditions proposed in Theorem 3.1 and the conservatism reduction induced by the asynchronous double fuzzy sums relaxation scheme proposed in Theorem 3.2. This will be done in the next section.

3.5 Illustrative Examples

To illustrate the effectiveness of the proposed sampled-data controller design methodology for continuous-time T-S fuzzy models, three examples are considered. The first one, consisting on a 1-DOF inverted pendulum, is considered to highlight the benefit of sampled-data controller design over conventional discrete-time controller approach when the plant to be driven evolves in continuous-time. The second example is based on an approximated two rules fuzzy model of an inverted pendulum on a cart, drawn from the literature, e.g., (Wang et al., 1996). It is considered for comparison purpose since it has been largely considered in previous sampled-data related

studies, especially to evaluate their successive conservatism improvements. Finally, because the proposed design conditions also holds for linear systems, an experimental validation of the sampled-data controller design procedure, with comparison to conventional continuous-time linear control approaches, is proposed on the Quanser® AERO device in its 2-DOF helicopter configuration.

3.5.1 T-S model-based sampled-data controller design vs conventional discrete-time approach

For this first example, we consider the dynamic equations of a 1-DOF inverted pendulum and its fuzzy T-S representations (with $r = 2$) presented in Examples 1.2 in the continuous-time framework, and 1.3 in the discrete-time framework. Let us first consider the design of a PDC sampled-data controller (3.5) in order to stabilize the continuous-time model of the 1-DOF inverted pendulum, exactly represented by the 2 rules T-S model (1.16) for all $x_1(t)$ with $\rho = -0.217234$. To do so, we apply Theorem 3.1 together with Theorem 3.2, which require to estimate the bounds of the time-derivative of the membership functions, ϕ_1 and ϕ_2. To determine these parameters, let us assume that $x_2(t) \in [-\pi, \pi]$, from the definition of the membership functions (1.15), we have:

$$\forall i \in \mathcal{I}_2,\ |\dot{\alpha}_i(t)| \leq \phi_i = \sup_{\{x_1 \in \mathbb{R}, x_2 \in [-\pi,\pi]\}} \left(\left| \frac{x_1 \cos(x_1) - \sin(x_1)}{(1-\rho)x_1^2} x_2 \right| \right) = 1.1258\, Rad.s^{-1}$$

Then, solving the conditions of Theorem 3.1 with Theorem 3.2 using YALMIP and SeDuMi (Löfberg, 2004) on the MATLAB® environment, with $\varepsilon_1 = 0.35$, $\varepsilon_2 = 3.3$, $\varepsilon_3 = 0.23$, we found a maximal allowed sampling interval $\bar{\eta} = \tau_s = 228ms$ and the following gain matrices for the sampled-data PDC controller (3.2):

$$K_1 = \begin{bmatrix} -0.0265 & -0.0538 \end{bmatrix} \quad X = \begin{bmatrix} 0.0079 & -0.0162 \\ -0.0146 & 0.0987 \end{bmatrix} \tag{3.51}$$
$$K_2 = \begin{bmatrix} -0.0100 & -0.0791 \end{bmatrix}$$

To compare this result, consider now the discrete-time T-S model of the 1-DOF inverted pendulum given in Example 1.3. Applying Theorem 1.5 with the same sampling period $\tau_s = 228\, ms$, we obtain the following gain matrices of a PDC discrete-time controller (1.39):

$$\mathcal{K}_1 = \begin{bmatrix} -10.0379 & -2.6384 \end{bmatrix} \text{ and } \mathcal{K}_2 = \begin{bmatrix} -8.6133 & -2.6384 \end{bmatrix}$$

and a discrete-time Lyapunov function $V(x_k) = x_k^T \mathcal{P} x_k$ with:

$$\mathcal{P} = \begin{bmatrix} 1.9497 & 0.4450 \\ 0.4450 & 0.1020 \end{bmatrix} \times 10^3.$$

To provide a fair comparison, both designed Sampled-Data (SD) controller and Discrete-Time (DT) one are applied to the continuous-time model of the inverted-pendulum. The simulation was performed with an *ODE45* solver to implement the continuous-time evolution of the 1-DOF inverted pendulum represented by (1.2), and the controller was executed with a zero-order hold

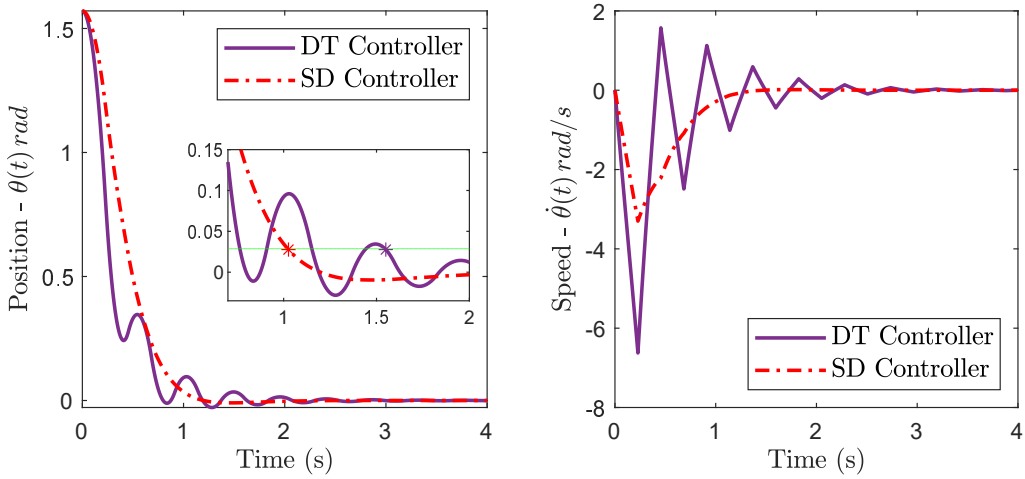

Figure 3.1: Time evolution of the continuous-time model (1.2), driven by the fuzzy discrete-time (DT) PDC controller proposed in Chapter 2 and with the Sampled-Data (SD) PDC controller projected from Theorem 3.1, with $\bar{\eta} = \tau_s = 228ms$.

to keep constants the input signals updated only on the sampling instants $\eta_k = 228ms$. The resulting responses are plotted in Figure 3.1.

From Figure 3.1 it is possible to observe that the trajectories of the states variables for the stabilization problem with the designed SD controller happen to be smoother than the response obtained with the DT controller (applied to the original continuous-time system), especially for the speed variable ($x_2 = \dot{\theta}(t)$). Moreover, it is verified that the equilibrium point (98% of the final value, *i.e.,* 0.0288) is reached about 34% faster with the SD controller, which takes $1.03s$, than with the DT controller, which takes $1.55s$.

Furthermore, we investigate the behavior of the Lyapunov functions obtained with the design of both controllers. In this context, it is important to recall that, from Theorem 3.1, it is ensured that the whole LKF (3.8) is continuous and positive at each sampling time t_k and monotonously decreasing for all t. So, taking benefit of the fact that, at each sampling instant $t = t_k$, we have $V(t_k) = V_1(t_k) = x(t_k)^T L x(t_k)$, with:

$$L = X^{-T}\bar{L}X^{-1} = \begin{bmatrix} 266.2122 & 34.1228 \\ 26.4973 & 13.1448 \end{bmatrix},$$

it is possible to verify that the LFK is indeed monotonously decreasing.

Therefore, Figure 3.2 shows the SD control signal, computed at each instant t_k and maintain by the ZOH for $t \in [t_k, t_{k+1})$, and the evolution of the LKF (3.8). Also, in Figure 3.2, the SD simulation results are compared with the DT controller and the above given DT Lyapunov functions, applied to the continuous-time model for a fair comparison. From this Figure, it is noticed that the Lyapunov function obtained from the Theorem 3.1 (SD controller design) is less energetic (at the sampling instants) than the one obtained from conventional DT approaches. To assert this fact, we also propose to evaluate the euclidean norm of the control input signals

over the interval $t \in [0, 4]$, which is given by:

$$||u(t)||_2 = \sqrt{\int_0^4 |u(s)|^2 \, ds}$$

This results in $||u(t)||_2 = 9.17$ for the DT controller and $||u(t)||_2 = 4.38$ for the SD controller, showing that the implementation of the latter for the 1-DOF inverted pendulum is 2.09 times more efficient in terms of control input energy consumption than the discrete-time controller. Finally, let us recall that the proposed SD controller design methodology summarized by Theorem 3.1 guarantees the closed-loop stability of the continuous-time system, while the conventional DT approach cannot guarantee the inter-sampling stability of continuous-time plants, especially for large sampling periods (Hetel et al., 2017). Indeed, in Figure 3.2, we can observe that the DT Lyapunov function applied to the continuous-time model is not monotonously decreasing during two successive sampling instants. This concludes this first example, showing the effectiveness of this chapter's proposal with regards to conventional discrete-time control approaches.

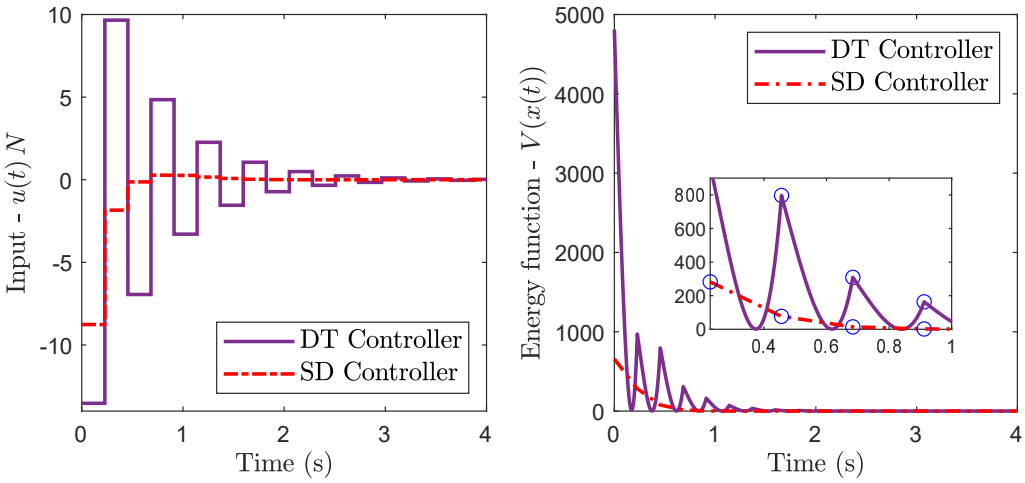

Figure 3.2: Discrete-time state-feedback control input signal $u(t_k)$ and Lyapunov function $x^T(t)Lx(t)$ computed for the CT system and DT model.

3.5.2 Conservatism comparison: Inverted pendulum on a cart benchmark

To illustrate the effectiveness of the proposed sampled-data control approach for T-S models, let us consider the benchmark of an inverted pendulum mounted on a cart depicted in Figure 3.3.

For brevity, the time t will be omitted in the mathematical expression of this section. The nonlinear dynamics of this well-known mechatronic system is given by (Cannon, 1967; Wang et al., 1996):

$$\begin{cases} \dot{x}_1(t) = x_2(t), \\ \dot{x}_2(t) = \frac{g \sin x_1(t) - aml x_2^2(t) \sin(2x_1(t))/2 - a \cos x_1(t) u(t)}{4l/3 - aml \cos^2 x_1(t)}, \end{cases} \tag{3.52}$$

where $x_1(t)$ and $x_2(t)$ are respectively the angle position (rad) and the velocity (rad/s) of the pendulum from the erect position, $g = 9.8\, m/s^2$ is the acceleration of the gravity, $m = 2\, kg$ is

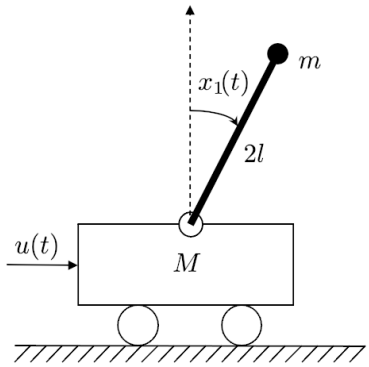

Figure 3.3: Inverted Pendulum mounted on a cart.

the mass of the pendulum, $M = 8\,kg$ is the mass of the cart, $l = 0.5\,m$ is the half length of the pendulum, $u(t)$ is the input actuator force (N) applied to the cart and $a = 1/(m + M)$. The goal here is to stabilize the inverted pendulum for the approximate range $x_1(t) \in (-\pi/2, \pi/2)$. Note that when $x_1(t) = \pm\pi/2$ the system is uncontrollable.

In this subsection, an approximated T-S fuzzy model (3.1) with two fuzzy rules ($r = 2$) of (3.52), drawn from (Wang et al., 1996), is considered for comparison purpose since it has been used in several related previous sampled-data controller design studies in the the literature (see the references given in Table 3.2). This approximated T-S fuzzy model with two rules, valid for $|x_1(t)| < \pi/2$ and $|x_2(t)| \leq \pi$, is specified by the matrices:

$$\begin{aligned} A_1 &= \begin{bmatrix} 0 & 1 \\ \frac{g}{4l/3-aml} & 0 \end{bmatrix}, A_2 = \begin{bmatrix} 0 & 1 \\ \frac{2g}{\pi(4l/3-aml\beta^2)} & 0 \end{bmatrix}, \\ B_1 &= \begin{bmatrix} 0 \\ \frac{-a}{4l/3-aml} \end{bmatrix}, B_2 = \begin{bmatrix} 0 \\ \frac{-a\beta}{4l/3-aml\beta^2} \end{bmatrix}, \beta = cos(88^\circ), \end{aligned} \tag{3.53}$$

and the triangular membership functions:

$$\alpha_1(x_1(t)) = \begin{cases} 1 - \frac{2}{\pi}x_1(t), \text{ if } 0 \leq x_1(t) < \frac{\pi}{2} \\ 1 + \frac{2}{\pi}x_1(t), \text{ if } -\frac{\pi}{2} < x_1(t) < 0 \end{cases} \text{ and } \alpha_2(x_1(t)) = 1 - \alpha_1(x_1(t)) \tag{3.54}$$

In this context, note that, from the triangular membership function we have $|\dot{\alpha}_1| = |\dot{\alpha}_2| = \frac{2}{\pi}|\dot{x}_1|$ and, since $|\dot{x}_1| = |x_2| \leq \pi$, we always have $|\dot{\alpha}_i| \leq 2 = \phi_i$ $(i \in \mathcal{I}_2)$.

Let us remember that, because of the asynchronous double fuzzy summation structure of the parameterized LMIs proposed in Theorem 3.1, conventional relaxation schemes such like Tuan's Lemma (Tuan et al., 2001) cannot be directly applied. In this regard, we have proposed a specific relaxation scheme given by Theorem 3.2. Note also that, to the best of our knowledge, except Lemma 1.10 proposed in (Koo et al., 2017), there was no generic relaxation scheme to cope with this issue in previous related works. This makes Lemma 1.10 proposed in (Koo et al., 2017) suitable to be compared with Theorem 3.2, in order to solve the parameterized LMIs proposed in Theorem 3.1. The result is shown in Table 3.1, where the biggest value of the maximal allowable sampling interval was found with Theorem 3.1 ($\bar{\eta} = 50ms$), outperforming the results obtained with Lemma 1.10 ($\bar{\eta} = 35ms$) by 45.57% (the parameters ε_1, ε_2 and ε_3 were

tuned by a grid search for both results). This confirms the superiority of Theorem 3.2 regarding to Lemma 1.10 (Koo et al., 2017) in terms of conservatism reduction.

Table 3.1: Comparison of maximal $\bar{\eta}$ obtained from Theorem 3.1 with the selected asynchronous double sums relaxation scheme.

Method	ε_1	ε_2	ε_3	$\begin{bmatrix} K_1 \\ K_2 \end{bmatrix}$	X	$\bar{\eta}$
Lemma 1.10 (Koo et al., 2017)	8.25	5	0.28	$\begin{bmatrix} 32.8209 & -43.5959 \\ 46.7316 & -25.2741 \end{bmatrix}$	$\begin{bmatrix} 0.6989 & -2.1227 \\ -2.0760 & 6.4966 \end{bmatrix}$	$35ms$
Theorem 3.2	5.5	3	0.31	$\begin{bmatrix} 0.2054 & 0.0214 \\ 1.2536 & 11.5638 \end{bmatrix}$	$\begin{bmatrix} 0.0062 & -0.0176 \\ -0.0172 & 0.0702 \end{bmatrix}$	$50ms$

In order to illustrate these first results, with the initial condition $x(0) = \begin{bmatrix} \pi/3 & 0 \end{bmatrix}^T$ and a fixed sampling period $\eta_k = \bar{\eta} = 35ms$, Figure 3.4 compares the closed-loop trajectories obtained with both the sampled-data controllers designed from Theorem 3.1 with Theorem 3.2 and Lemma 1.10 (Koo et al., 2017). In this particular case, both are stabilizing the T-S fuzzy model and we can observe than the conservatism improvement raised by Theorem 3.2 makes the control signal slightly less energetic.

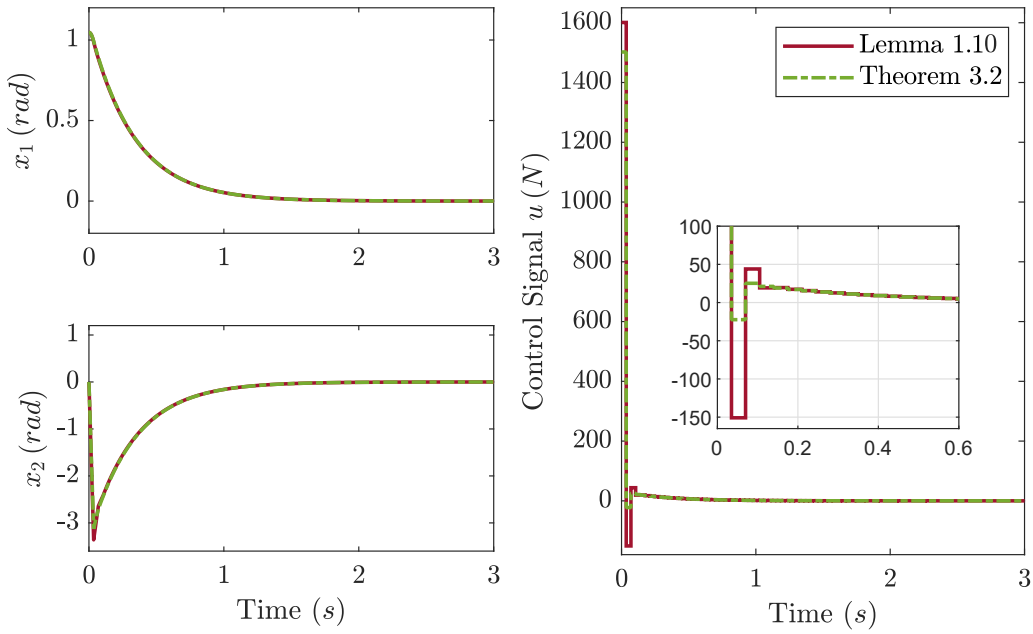

Figure 3.4: Comparison between the trajectories of the inverted-pendulum on a cart, under sampled-data controllers with gains obtained from different methods for the relaxation of the asynchronous double sums of the design conditions.

In addition, Table 3.2 lists the maximal allowable upper bound $\bar{\eta}$ obtained from several previous related results from the literature. Once again, we observe that the present approach outperform these previous results by at least 19.05%, which highlights the significant improvement raised by Theorem 3.1, together with Theorem 3.2, in terms of conservatism.

Table 3.2: Comparison of maximal $\bar{\eta}$ obtained with related previous studies.

Method	$\bar{\eta}$ (ms)
(Yoneyama, 2010)	9
(Zhu and Wang, 2011)	13
(Zhang and Han, 2011)	16
(Zhu et al., 2012)	19
(Gunasekaran and Joo, 2019)	22
(Zhu et al., 2013)	24
(Cheng et al., 2017)	42
Theorem 3.1	**50**

Now, let us consider the maximal allowed sampling interval with $\bar{\eta} = 50ms$, for which only Theorem 3.1 (with Theorem 3.2) provides a solution with guaranteed sampled-data closed-loop stability. Figure 3.5 shows the closed-loop state trajectories of the approximated T-S fuzzy model inverted pendulum from the initial condition $x(0) = \begin{bmatrix}\pi/4 & 0\end{bmatrix}^T$ with a fixed sampling period $\eta_k = \bar{\eta} = 50ms$. In addition, because our proposal also guarantees the closed-loop stability for aperiodic sampling intervals, Figure 3.6 shows the same simulation but with random sampling intervals such that $\eta_k \in [0, 50ms]$. These simulations illustrate the effectiveness of the proposed sampled-data controller design methodology for T-S fuzzy models.

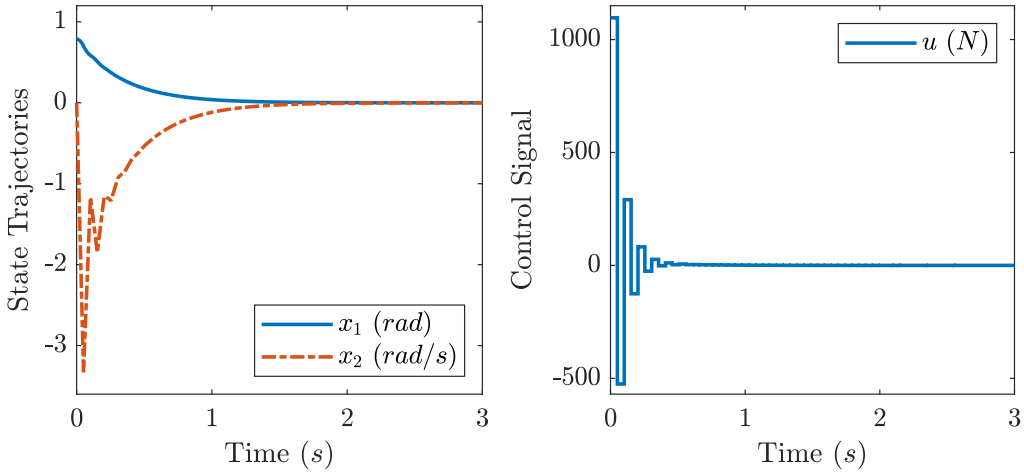

Figure 3.5: Simulation of the states trajectories of the inverted pendulum on a cart with the respectively sampled input control signal for a fixed sampling period $\eta_k = \bar{\eta} = 50ms$.

To conclude this second example, let us discuss some straightforward limitations of the presented results. First of all, it is to be noticed that the conditions proposed to cope with the asynchronous mismatching membership functions in parameterized LMIs leads to assume the bounds of the time-derivatives of the membership functions, i.e. $|\dot{\alpha}_i| < \phi_i, \forall i \in \mathcal{I}_r$. In that purpose, with Theorem 3.2, if $\bar{\eta}\phi_i \geq 1$, then we have $\sigma_i = 1$ and the result can be global when T-S fuzzy models are derived from global sector nonlinearity approaches. Nevertheless, as σ_i gets closer to 1, the results become more conservative. Otherwise, when considering $\sigma_i \leq 1$, the result becomes only local and further investigations on the resulting sampled-data

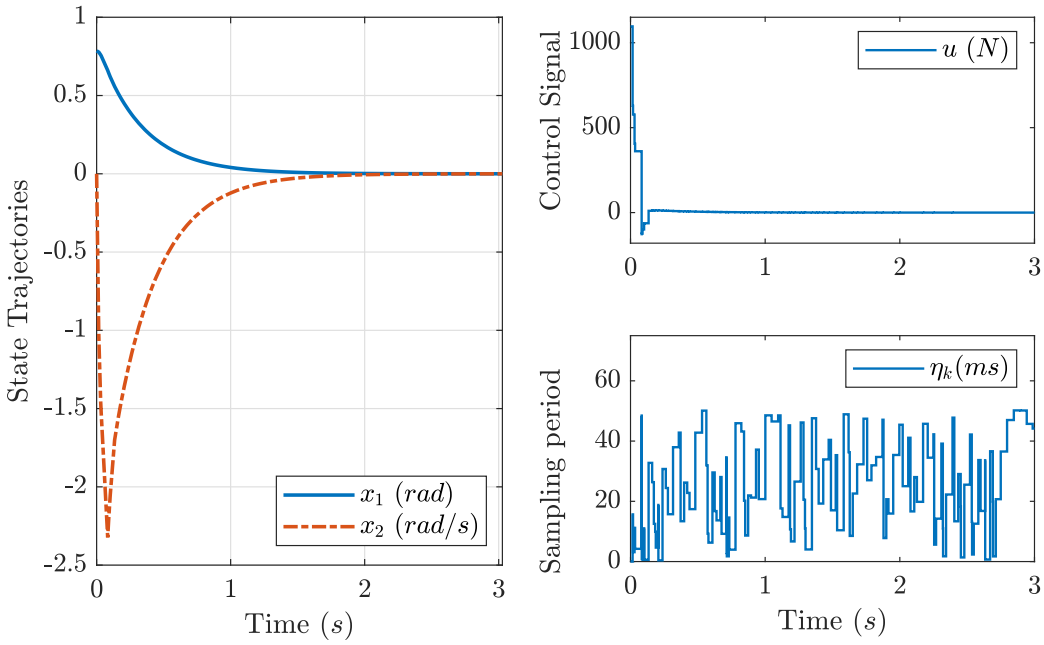

Figure 3.6: Simulation of the states trajectories of the inverted pendulum on a cart with the respectively sampled input control signal computed for variable sampling intervals $\eta_k \in [0, \bar{\eta}]$.

closed-loop domain of attraction would be necessary. This issue will be the focus of the next chapter. Furthermore, it is worth pointing out that the sampled-data controller obtained in this subsection only applies for the approximated two rules fuzzy model provided by (Wang et al., 1996) from which it is designed. As a matter of fact, nothing guarantees that it stabilizes the original nonlinear system (3.52). To assert this fact, applying this two rules sampled-data T-S fuzzy controller to the original nonlinear model (3.52) of the inverted pendulum, with the same initial conditions $x = \begin{bmatrix} \pi/3 & 0 \end{bmatrix}^T$, provides an unstable closed-loop behavior, as shown in Figure 3.7. This highlights the limitation of using such approximated standard T-S fuzzy models, which should be circumvented by considering an exact T-S modeling approach. This will be investigated in the next Chapter, for instance by using sector nonlinearity approach and, when relevant (e.g. for mechanical plants), by extending the proposed results to the class of T-S descriptors.

3.5.3 Linear case study with experimental validation

In this section, we are focused on the real-time implementation of a sampled-data controller employing the gains obtained from the design conditions provided in Theorem 3.1 to drive an unmanned aerial vehicle (UAV) benchmark, which presents some interesting characteristics such as its versatility, maneuverability, and ease of use. Namely, we choose for these experiments the Quanser® AERO benchmark configured as a dual-rotor helicopter (Quanser, 2016). For this real system, some works can be found in the literature dealing with reinforcement learning strategies (Fandel et al., 2018), model reference adaptive controllers (Arabi and Yucelen, 2019b,a) and robust controllers (Subramanian and Elumalai, 2016; Al Hamouch et al., 2019; Steinbusch and

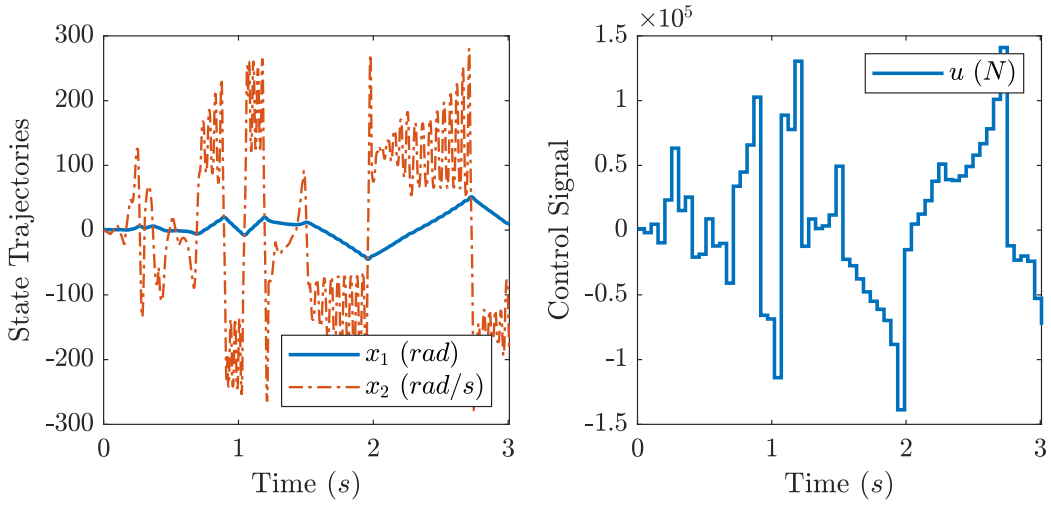

Figure 3.7: Closed-loop state responses and control signal of the nonlinear model (3.52) under the sampled-data controller design from the approximated T-S fuzzy model taken from (Wang et al., 1996).

Reyhanoglu, 2019). Nevertheless, all the above mentioned works consider that the controller evolves in a continuous-time framework and, to the best of the authors knowledge, no previous studies can be found dealing with the design of a sampled-data controller for this system.

In this context, this section presents a real-time experimental validation of the sampled-data controller design procedure proposed in Theorem 3.1. The effectiveness of this proposal is illustrated in simulation, then validated experimentally, and compared to conventional continuous-time PID and Linear-Quadratic Regulators (LQR), which design procedure can be found in the Quanser® AERO laboratory guide (Quanser, 2016; Lopes et al., 2020b).

2-DOF helicopter dynamical model:

The Quanser® AERO, in its essence, is a dual-motor experiment, a reconfigurable platform created for serving advanced control research, simplifying the experimentation of various aerospace systems, from 1-DOF and 2-DOF helicopter to half-quadrotor. Although, it can also be used for teaching control concepts at the undergraduate level. In Figure 3.8 the free-body diagram of the considered benchmark is presented in its 2-DOF Helicopter configuration is presented:

This system is configured as a conventional dual-rotor helicopter with two identical high-efficiency rotors that produce the thrust forces $F_p(t)$ and $F_y(t)$ acting at points with distances r_p and r_y from the *z-axis* along the *x-axis*, respectively. Hence, one propeller generates a torque around the *y-axis* leading to a pitch ($\theta(t)$) motion, while the other one deals with a yaw ($\psi(t)$) motion (around the *z-axis*).

The dynamical model of this benchmark was taken from (Quanser, 2016), and was developed as a simple linear model that takes into account the coupling between the pitch and yaw axis.

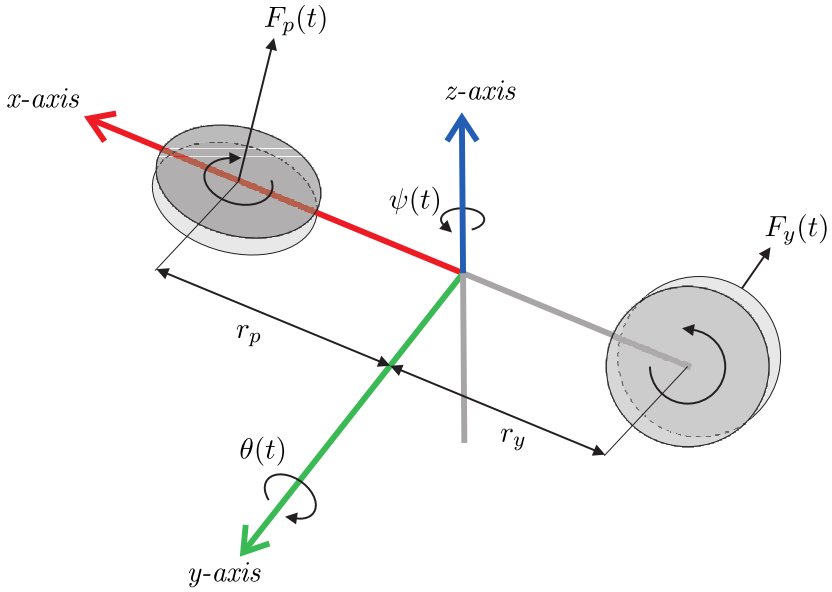

Figure 3.8: Simple free-body diagram of a 2-DOF helicopter system.

The equations of motion of the system are given by:

$$\begin{cases} J_p\ddot{\theta}(t) + D_p\dot{\theta}(t) + K_{sp}\theta = \tau_p(t) \\ J_u\ddot{\psi}(t) + D_y\dot{\psi}(t) = \tau_y(t) \end{cases} \tag{3.55}$$

where the torques acting on the pitch ($\tau_p(t)$) and yaw ($\tau_y(t)$) axes are assumed proportional to the inputs voltages $V_p(t)$ and $V_y(t)$ of the DC-motors such that:

$$\tau_p(t) = K_{pp}V_p(t) + K_{py}V_y(t) \text{ and } \tau_y(t) = K_{yp}V_p(t) + K_{yy}V_y(t), \tag{3.56}$$

with the parameters listed in Table 3.3.

Table 3.3: Quanser®AERO 2-DOF Helicopter Parameters.

	Parameter	Value	Unit
J_p	Moment of Inertia about the pitch axis	0.0215	$kg.m^2$
J_y	Moment of Inertia about the yaw axis	0.0215	$kg.m^2$
K_{sp}	Stiffness about the pitch axis	0.0374	$N.m/rad$
D_p	Pitch viscous friction constant	0.0071	$N.m.s/rad$
D_y	Yaw viscous friction constant	0.0220	$N.m.s/rad$
K_{pp}	Thrust-torque gain acting on pitch axis from pitch propeller	0.0011	$N.m/V$
K_{yy}	Thrust-torque gain acting on yaw axis from yaw propeller	0.0022	$N.m/V$
K_{py}	Thrust-torque gain acting on pitch axis from yaw propeller	0.0021	$N.m/V$
K_{yp}	Thrust-torque gain acting on yaw axis from pitch propeller	-0.0027	$N.m/V$

Then, from (3.55) and (3.56), the following linear state-space model of the 2-DOF Helicopter can be obtained, considering the state vector $x^T(t) = \begin{bmatrix}\theta(t) & \psi(t) & \dot{\theta}(t) & \dot{\psi}(t)\end{bmatrix}$ and the input vector $u^T(t) = \begin{bmatrix}V_p(t) & V_y(t)\end{bmatrix}$:

$$\dot{x}(t) = Ax(t) + Bu(t) \tag{3.57}$$

with:

$$A = \begin{bmatrix} 0 & 0 & 1 & 0 \\ 0 & 0 & 0 & 1 \\ -\frac{K_{sp}}{J_p} & 0 & -\frac{D_p}{J_p} & 0 \\ 0 & 0 & 0 & -\frac{D_y}{J_y} \end{bmatrix} \text{ and } B = \begin{bmatrix} 0 & 0 \\ 0 & 0 \\ \frac{K_{pp}}{J_p} & \frac{K_{py}}{J_p} \\ \frac{K_{yp}}{J_y} & \frac{K_{yy}}{J_y} \end{bmatrix}.$$

Recall that linear systems such like (3.57) constitute a special case of T-S fuzzy models (3.1) with $r = 1$. Hence, Theorem 3.1 can be directly applied (removing the parameter dependency of the decision variables in α and $\bar{\alpha}$) for the design of the following sampled-data controller:

$$u(t) = Fx(t_k) = Fx(t - \tau(t)) \tag{3.58}$$

where $F = KX^{-1} \in \mathbb{R}^{m \times n}$ is the controller gain matrix to be designed and $\tau(t)$ defined in (3.4).

Before going to the simulation and experimental results, the goal of this example is also to provide some comparisons with conventional linear continuous-time control design procedures proposed in the Quanser® AERO laboratory guide (Quanser, 2016), namely a Proportional-Derivative (PD) controller and an LQR-based design state space linear controller, given as follows.

First, decoupled continuous-time PD control laws are proposed for each pitch and yaw axis as (Quanser, 2016):

$$\begin{aligned} u_\theta(t) &= -K_{P_p}\theta(t) - K_{D_p}\dot{\theta}(t) \\ u_\psi(t) &= -K_{P_y}\psi(t) - K_{D_y}\dot{\psi}(t) \end{aligned} \tag{3.59}$$

with the gains :

$$\begin{aligned} K_{P_p} &= 107.7148, & K_{D_p} &= 52.4365, \\ K_{P_y} &= 54.1163, & K_{D_y} &= 19.5924, \end{aligned}$$

designed from standard decoupled second-order transfer functions models and some performances index based on the natural frequency w_n, damping ratio ζ, peak time t_p and overshoot specification P_O.

Then, because the above mentioned PD controllers does not cope with coupling effects, the following linear continuous-time state feedback controller is also proposed (Quanser, 2016):

$$u(t) = -K_{LQR}x(t), \tag{3.60}$$

The design of the gain K_{LQR} is based on the LQR approach where the minimization of the following cost function is considered:

$$J(u(t)) = \int_0^\infty \left(x(t)^T Q x(t) + u(t)^T R u(t) \right) dt \tag{3.61}$$

with:

$$Q = \begin{bmatrix} 200 & 0 & 0 & 0 \\ 0 & 75 & 0 & 0 \\ 0 & 0 & 0 & 0 \\ 0 & 0 & 0 & 0 \end{bmatrix}$$

and:

$$R = \begin{bmatrix} 0.005 & 0 \\ 0 & 0.005 \end{bmatrix},$$

which provides the following gain matrix:

$$K_{LQR} = \begin{bmatrix} 98.2088 & -103.0645 & 32.2643 & -29.0750 \\ 156.3469 & 66.1643 & 45.5122 & 17.1068 \end{bmatrix}.$$

Let us highlight that these controllers are designed in continuous-time and are implemented in the Quanser® lab assuming a very small fixed sampling period (usually $\eta_k = 2ms$), which is satisfactory for a pedagogical tool to teach basics on this topics. Nevertheless, since the embedded electronics of the Quanser®AERO provides only digital computations, from the theoretical point of view, this is not accurate since the inter-sampling stability is not guaranteed in these two cases, especially for large sampling periods.

For the following developments, the direct discrete-time controller design approach is not investigated. This decision relies on the employment of sampling periods greater than those found through the search of a reasonable rate based on the Nyquist and Shanon Criterion for the Quanser® AERO. In a preliminary study, a time constant of $\tau_c = 0.7643s$ was obtained for the linear system, and according to the literature, a proper choice for the sampling period value should be $\tau_s \in [0.0764, 0.19]$. Consequently, the results obtained with a larger sampling period could bring hidden issues like the growth of the Lyapunov function, as discussed in Chapter 1.

Simulation results with a large sampling period:

In this section, we provide some simulation results considering a large sampling period of $\bar{\eta} = 4.5s$. As mentioned in Remark 3.2, a particular case of Theorem 3.1 can be considered for the design of the sampled-data controller (3.58). The result, obtained via YALMIP (Löfberg, 2004) and SEDUMI (Sturm, 1999) solver in MATLAB® with the scalar parameters $\epsilon_1 = 3$, $\epsilon_2 = 1$ and $\epsilon_3 = 300$, is given by the following sampled-data control gain matrix:

$$F = \begin{bmatrix} 0.0432 & 1.1617 & -0.1687 & -0.1789 \\ 0.0530 & -0.6085 & -0.2070 & 0.0937 \end{bmatrix}$$

In this context, Figure 3.9 shows the closed-loop continuous-time responses of the pitch and yaw axis under the design sampled-data control law (3.58) with the initial conditions $x(0) = \begin{bmatrix} 10 & 45 & 0 & 0 \end{bmatrix}^T$. We can verify that the closed-loop sampled-data control systems is successfully stabilized in simulation.

Now, let us consider that the continuous-time controllers (3.59) and (3.60) are implemented on a digital device with the same huge sampling period of $4.5s$. As mentioned above, since this controller does not cope with inter-sampling behavior, the closed-loop systems should be unstable as shown in the simulations depicted in Figure 3.10.

These simulations confirm the significance of considering the proposed sampled-data control methodology for large sampling periods. The next subsection provides an experimental validation.

Experimental validation of the proposed sampled-data controller design:

In the previous subsection, simulation results of the proposed sampled-data control strategy have been proposed with a large sampling period of $4.5s$. Nevertheless, in practice, some

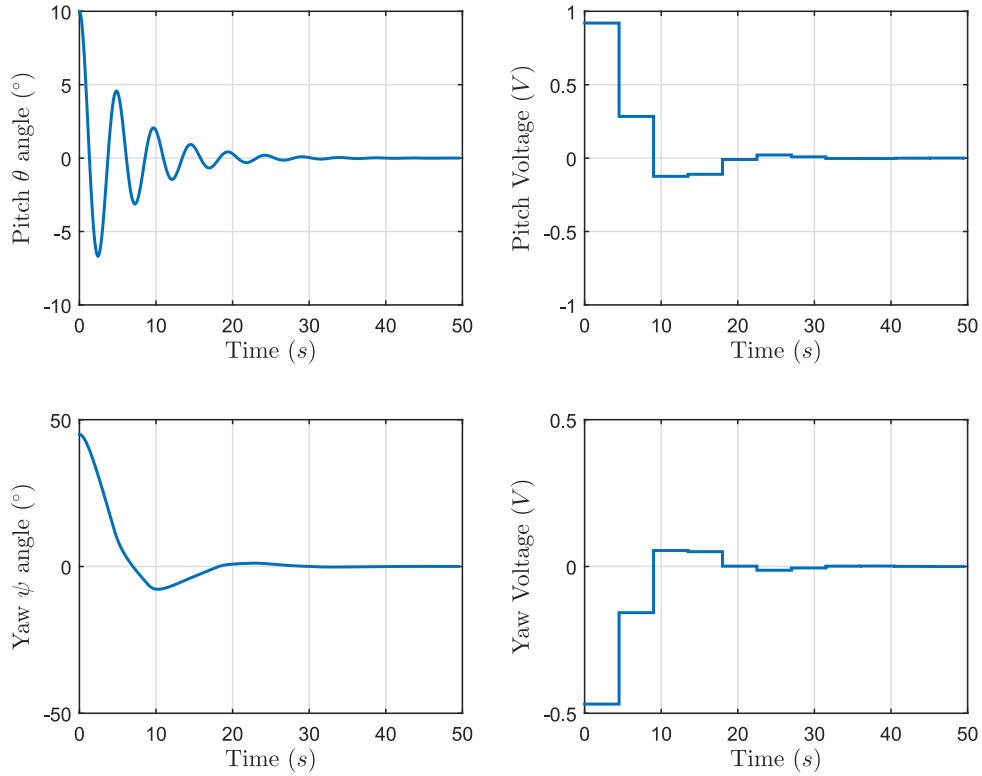

Figure 3.9: Time response of Quanser®AERO model under the Sampled Data Controller.

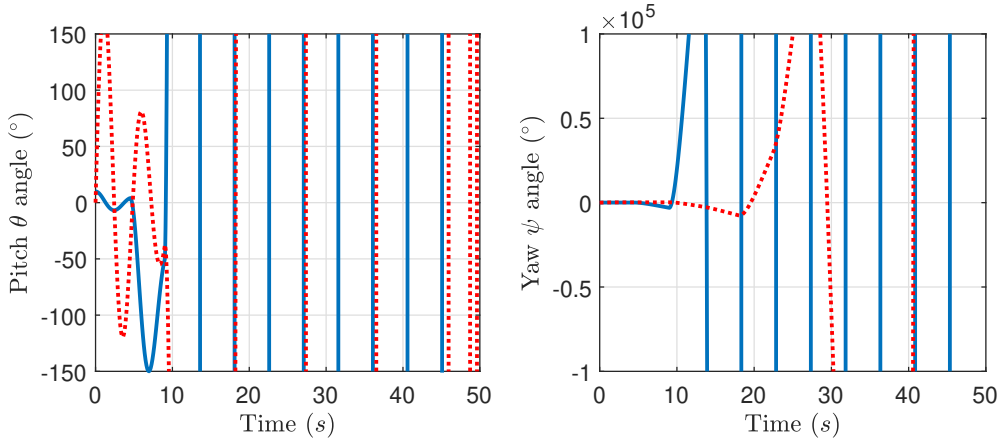

Figure 3.10: Time response of Quanser®AERO model, subjected to the LQR Controller (3.60) (–) and the PD Controllers (3.59) (· · ·) under a sampling period of $4.5s$.

unmodeled phenomena (frictions, motors dead zone which make then static under a tension smaller than 0.4V,...) does not allow a direct implementation with the same values. Hence, to provide a fair comparison with a realistic sampling period, we chose for experimental validation $\eta_k = 150ms$. In this case, Theorem 3.1 has a solution with $\epsilon_1 = 0.25$, $\epsilon_2 = 10$ and $\epsilon_3 = 0.37$, which provide the following sampled-data controller (3.58) gain matrix:

$$F = \begin{bmatrix} -28.4589 & 34.6979 & -27.5479 & 21.9293 \\ -34.9268 & -18.1751 & -33.8088 & -11.4868 \end{bmatrix}.$$

The experimental results are shown in Figure 3.11 where the time response and the input signals (Motors' voltage) are depicted for the PD, the LQR and the sampled-data controller.

We can notice that, while the PD and LQR control plants that are unstable with a sampling period $\eta_k = 150ms$, the sampled-data controller successfully stabilizes the Quanser®AERO.

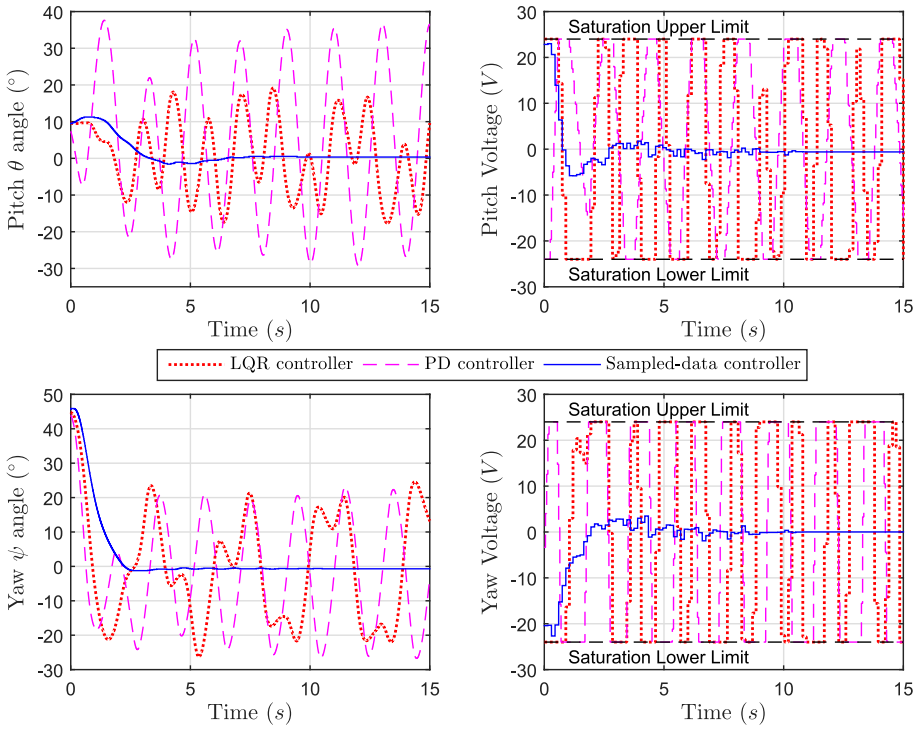

Figure 3.11: Comparison of the time responses of the Quanser®AERO under a sampling period of $150ms$.

Finally, to take benefit of the fact that our conditions hold for aperiodic sampling periods, we proposed the following simple strategy to trigger it. Note that $V_1(t_k) \leq V_1(0)$. The purpose is to update the sampling period η_k at each sampling instant t_k so that, when $V_1(t_k)$ is close to $V_1(0)$, then the updated sampling period η_k is small ($2ms$), and when it is close to 0, then η_k is large ($0.15s$). This strategy can be implemented with an event-triggering mechanism to determine the next sampling instant η_{k+1} for which a new measurement of the states is required to compute the control law (3.58). In this context, to implement the sampled-data control approach based on events, the following simple rule can be proposed:

$$\eta_{k+1} = \frac{0.002 - 0.15}{V_1(0)} V_1(t_k) + 0.15 \tag{3.62}$$

The results from implementing the event-triggering mechanism with the triggering rule defined on (3.62) are depicted in Figure 3.12, in which the simulation results are compared with the experimental ones under the proposed aperiodic sampled-data control scheme.

As expected, the closed-loop system is properly stabilized. However, we can also see some differences during the transients from the simulation and the experimentation. Indeed, in addition to experimental artifacts and unmodeled effects, these can also be due to the actuators saturation, which often occur in practice (here during the first few sampling intervals where the inputs saturate at the motors' voltage limit of $24V$) and which are not taken into account in

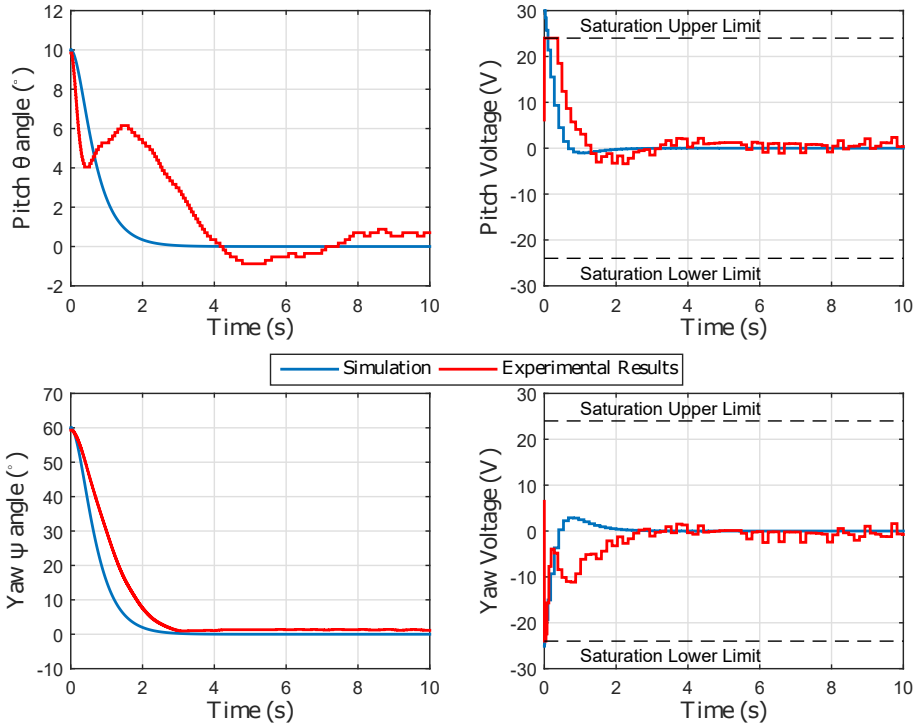

Figure 3.12: Time responses of the Quanser®AERO under triggered sampling period.

the present controller design methodology. This will be another subject considered in the next chapter.

3.6 Conclusion

In this chapter, new LMI-based conditions have been proposed to design sampled-data PDC controllers for continuous-time T-S fuzzy models. Conservatism improvement regarding previous works has been achieved from choosing an appropriated LKF, then by employing useful bounding lemmas together with a second order quadratic polynomial constraints. In addition, generic conditions have been proposed to relax double fuzzy sums with asynchronous MFs involved in T-S model-based sampled-data control plants.

The effectiveness of the proposed sampled-data design conditions and their superiority regarding conventional discrete-time controller design approaches, like those considered in Chapter 2, were illustrated with the 1-DOF inverted pendulum example. Also, the conservatism reduction brought by the design conditions has been compared with previous results and illustrated through the well-known benchmark of an inverted pendulum on a cart. However, the simulation results pointed out that the designed controller guarantees the stability of the approximated T-S model, but fails to stabilize the original nonlinear model. To cope with the previous issue, a new design condition is proposed in the next chapter, extending the results for descriptor systems suitable for describing an exact representation of the nonlinear system through fuzzy T-S modeling for mechanical systems with the sector nonlinearity approach.

Then, the design and the implementation of the proposed sampled-data controller for the

Quanser® AERO 2-DOF helicopter system has been proposed. The results have been validated in simulation as well as experimentally, and the designed sampled-data controller has shown its superiority regarding previous designed continuous-time controllers, especially for large sampling periods. However, these experimental results also highlight the importance of taking into account practical constraints such like input saturation, which will also constitutes one of the improvements proposed in the next chapter.

Finally, let us also point-out that one of the main limitations of the sampled-data controller design proposed in this chapter are generally only local for T-S systems, excepted in the special case where $\mathcal{D}_x = \mathbb{R}^n$ and $\sigma_i = 1$ in Theorem 3.2, which is conservative. Hence, further investigations of the sampled-data closed-loop domain of attraction appears to be necessary and will be one of the main focus of the next chapter.

Chapter 4

Local Aperiodic Sampled-data Control of T-S Descriptors with Input Constraints

Résumé en Français : Contrôle local à base de données apériodiquement échantillonnées des modèles T-S descripteurs avec saturation sur l'entrée.

Ce chapitre vise à fournir quelques extensions permettant de surmonter les obstacles mentionnés dans le chapitre précédent. En effet, à partir des conditions données dans les Théorèmes 3.1 et 3.2 pour la synthèse de correcteurs échantillonnées pour les modèles T-S, on peut conclure que les résultats ne sont valables que localement (voir la fin du Chapitre 1). De plus, à partir de l'exemple proposé dans la Section 3.5.2, il a été montré que lorsque les limites du conservatisme sont atteintes, l'utilisation d'un modèle T-S approximé pour effectuer la synthèse du correcteur peut échouer à stabiliser le système non linéaires initialement considéré. Enfin, à partir des résultats expérimentaux présentés dans la Section 3.5.3, il est important de rappeler que la saturation des actionneurs est à prendre en compte.

Sur la base de ces considérations, dans ce chapitre, la méthodologie présentée précédemment est étendue à la classe des modèles descripteurs de type T-S (Taniguchi et al., 1999; Taniguchi et al., 2000), qui ont montré tout leur intérêt pour représenter avec précision les systèmes mécaniques (Guelton, 2003; Guelton et al., 2008; Bouarar et al., 2010; Arceo et al., 2016; Quintana et al., 2017; Dang et al., 2017; Nguyen et al., 2020), et par conséquent les systèmes mécatroniques commandés de fait par des contrôleurs basés sur des données échantillonnées. De plus, puisque les modèles descripteurs T-S incluent les modèles T-S standards à titre de cas particuliers, ils sont souvent utilisés pour représenter plus précisément une plus grande classe de systèmes, tout en réduisant le conservatisme (Estrada-Manzo et al., 2013, 2019). Par ailleurs, rappelons que les saturations sur l'entrée ont été considérées dans le ***Chapitre 2****, dans le cadre des modèles T-S décrits en temps discret.*

Mis à part les travaux de (Lamrabet et al., 2019), qui visent à proposer des conditions quadratiques relâchées mais sans aucune considération du domaine d'attraction en boucle fermée, il n'existe pas d'autres travaux pré-existants, traitant du problème de la stabilisation locale des modèles T-S continus avec saturations sur l'entrée à base données échantillonnées. Par la suite, inspirées des travaux présentés dans (Tarbouriech et al., 2011; Lopes et al., 2018), de nouvelles conditions prenant en compte la saturation des actionneurs sont proposées, garantissant ainsi la stabilité locale du système en boucle fermée. Afin de tenir compte de la nature locale de ces conditions, due aux contraintes induites par la saturation et/ou au domaine de validité restreint du modèle T-S, nous proposons une analyse

minutieuse du domaine d'attraction du système en boucle fermée, qui peut-être réalisée grâce au choix effectué d'une fonctionnelle non quadratique de Lyapunov-Krasovskii « bouclée » (NQLKF) appropriée. Dans cette optique, deux méthodologies sont proposées. Premièrement, une procédure hors ligne est présentée pour la stabilisation des modèles descripteurs de type T-S commandés par un contrôleur basé sur des données échantillonnées, en exploitant la NQLKF pour l'estimation du domaine d'attraction. Ensuite, pour des cas particuliers de modèles T-S standards, une procédure d'optimisation et d'obtention systématique est proposée afin d'élargir le domaine d'attraction en boucle fermée.

Enfin, notons que, pour des intervalles d'échantillonnage proches de la limite maximum autorisée, on obtient une estimation du domaine d'attraction significativement réduite. Afin de pallier ce problème, une nouvelle méthodologie d'ajustement des paramètres de la loi de commande est proposée. Celle-ci exploite les principes du déclenchement par événements (event-triggering), selon les équipotentielles des fonctions de Lyapunov obtenues pour plusieurs intervalles d'échantillonnage. Cette méthode, illustrée au travers de l'exemple de simulation du pendule inversé sur un chariot, permet d'élargir plus encore l'estimation obtenue du domaine d'attraction en boucle fermée.

4.1 Introduction

This chapter aims at providing some extensions to cope with the limitations pointed-out in the previous chapter. Indeed, from the proposed sampled-data controller design approach for T-S models given in Theorems 3.1 and 3.2, it can be concluded that these results only hold locally (see also Chapter 1, end of Section 1.4.2). Also, from the example provided in Section 3.5.2, it has been shown that, when reaching the limits of conservatism, the proposed approach may fail to stabilize the original nonlinear system, if its T-S model representation is not sufficiently accurate (e.g. when using fuzzy approximations). Finally, from the experimental results provided in Section 3.5.3, the importance of handling the actuators' saturation have been highlighted.

Based on these considerations, in this chapter, the proposed methodology is extended to the class of regular Takagi-Sugeno descriptors (Taniguchi et al., 1999; Taniguchi et al., 2000), which have been shown particularly efficient to accurately represent mechanical plants (Guelton, 2003; Guelton et al., 2008; Bouarar et al., 2010; Arceo et al., 2016; Quintana et al., 2017; Dang et al., 2017; Nguyen et al., 2020), and so mechatronic systems where sampled-data control is inherent. Moreover, because T-S descriptors include as a special case standard T-S models, these are often used to more accurately represent a larger class of systems while reducing the conservatism of their design conditions (Estrada-Manzo et al., 2013, 2019).

Recall that input saturation has been considered in Chapter 2, but in the discrete-time model-based control framework. Despite the work in (Lamrabet et al., 2019), which intended to provide relaxed quadratic conditions but missing the characterization of the domain of attraction, no previous works were found dealing with the sampled-data stabilization for T-S models subject to actuators' saturation. In the following, similarly to (Tarbouriech et al., 2011; Lopes et al., 2018), a generalized sector condition is employed to cope with the actuators' saturation problem, while keeping the local closed-loop sampled-data stability guaranteed.

Therefore, acknowledging the local nature of the proposed sampled-data synthesis, either associated with constraints induced by the saturation, or also due to the restrictions brought by the region of validity of the T-S model, we propose, along this chapter, a careful analysis of the estimation of the sampled-data closed-loop domain of attraction, from the convenient choice of a looped non-quadratic LKF (NQLKF). In that purpose, two methodologies are proposed. First, an offline procedure is presented for T-S descriptors-based sampled-data stabilization, taking full advantage of the NQLKF to enlarge the ensured limits of operation of the controlled system. Then, in the special case of standard T-S models, an optimization procedure is provided to give a systematic enlargement of the estimation of the closed-loop domain of attraction.

Finally, because, for a given maximal allowed upper bound of the sampling intervals, the obtained estimation of the domain of attraction can be quite small, a new gain scheduled event-triggering mechanism, based on the characterization of several Lyapunov level sets, is proposed to further enlarge the resulting closed-loop sampled-data domain of attraction.

4.2 Considered class of systems and problem statement

In this chapter, by extension of the class of nonlinear systems considered in the previous chapters, we will consider nonlinear descriptors with input (actuators) saturation given by:

$$E\big(x(t)\big)\dot{x}(t) = A\big(x(t)\big)x(t) + B\big(x(t)\big)\mathtt{sat}\big(u(t)\big) \tag{4.1}$$

where:

- $x(t) \in \mathbb{R}^n$ is the state vector, $E(x(t)) \in \mathbb{R}^{n\times n}$, $A(x(t)) \in \mathbb{R}^{n\times n}$ and $B(x(t)) \in \mathbb{R}^{n\times m}$ are matrices with nonlinear entries (only depending on the state variables for control purpose), bounded on a compact subset $\mathcal{D}_x$ of the state space defined by:

$$\mathcal{D}_x = \Big\{x(t) \in \mathbb{R}^n \mid \mathfrak{L}_{(j)}x(t) \leq z_{(j)}\Big\} \subseteq \mathbb{R}^n \tag{4.2}$$

  with $\mathfrak{L} \in \mathbb{R}^{\kappa\times n}$, $z \in \mathbb{R}^\kappa$, and $j \in \mathcal{I}_\kappa$,

- $u(t) \in \mathbb{R}^m$ is the control input vector, which may saturate according to actuators limitations, i.e., $\mathtt{sat}(u(t))$ is a decentralized vector valued function with components defined by:

$$\mathrm{sat}(u_{(\ell)}(t)) = \mathrm{sign}(u_{(\ell)}(t))\min(|u_{(\ell)}(t)|, \bar{u}_{(\ell)}), \forall \ell \in \mathcal{I}_m, \tag{4.3}$$

  which also allows us to define the set:

$$\mathcal{D}_u = \{u(t) \in \mathbb{R}^m \mid -\bar{u} \leq \mathtt{sat}(u(t)) \leq \bar{u}\} \tag{4.4}$$

  where $\bar{u}$ is a vector of $\mathbb{R}^m$ with positive components, i.e. $\bar{u}_{(\ell)} \geq 0$, $\forall \ell \in \mathcal{I}_m$.

From the well-known sector nonlinearity approach (Tanaka and Wang, 2001), nonlinear descriptors (4.1) with input saturation can be exactly rewritten, $\forall x(t) \in \mathcal{D}_x$, as T-S descriptors given by:

$$\sum_{i=1}^{r} \alpha_i\big(x(t)\big)E_i\dot{x}(t) = \sum_{i=1}^{r} \alpha_i\big(x(t)\big)\left(A_i x(t) + B_i\mathtt{sat}\big(u(t)\big)\right) \tag{4.5}$$

where, for $i \in \mathcal{I}_r$, $E_i \in \mathbb{R}^{n\times n}$, $A_i \in \mathbb{R}^{n\times n}$, $B_i \in \mathbb{R}^{n\times m}$ are constant matrices, $\alpha_i(x(t)) \geq 0$ are convex membership functions satisfying $\sum_{i=1}^{r} \alpha_i(x(t)) = 1$.

Remark 4.1. *T-S descriptors (4.5) include as special case the class of standard T-S models (3.1) (without input saturation) by considering $E_i = I$, $\forall i \in \mathcal{I}_m$. Moreover, note that descriptor systems are often used in the literature to model singular systems, i.e. when $E(x(t))$ is not invertible (see e.g. (Marx and Ragot, 2008; Li et al., 2016b; Chang et al., 2021)). However, in the sequel of this chapter, we will only focus on the case where $E(x(t))$ is assumed to be regular (invertible) since it has been shown useful to reduce the conservatism in T-S model-based design (Taniguchi et al., 1999; Taniguchi et al., 2000; Tanaka et al., 2007; Bouarar et al., 2007a,b, 2008, 2010; Estrada-Manzo et al., 2013). Furthermore, it is well-known that (regular) descriptors are particularly adequate to represent the dynamics of mechanical plants, by avoiding ill-conditioned matrix inversion, while reducing the number of vertices of resulting T-S models (see e.g (Guelton, 2003; Schulte and Guelton, 2006, 2009; Guelton et al., 2008; Bouarar et al., 2010; Seddiki et al., 2010; Vermeiren et al., 2012; Arceo et al., 2016; Quintana et al., 2017; Dang et al., 2017; Nguyen et al., 2019b, 2020)). Indeed, let us consider a class of d-link mechanical system, which dynamics can be described by:*

$$\mathcal{M}(q(t))\ddot{q}(t) + \mathcal{C}(q(t), \dot{q}(t))\dot{q}(t) + \mathcal{G}(q(t)) = \Gamma(t) \tag{4.6}$$

where $q(t) \in \mathbb{R}^d$ is the vector of generalized coordinates, $\mathcal{M}(q(t)) \in \mathbb{R}^{d\times d}$ is the inertia matrix, $\mathcal{C}(q(t), \dot{q}(t)) \in \mathbb{R}^{d\times d}$ is the Coriolis/centripetal matrix, $\mathcal{G}(q(t))$ is the vector of gravitation and $\Gamma(t) \in \mathbb{R}^d$ is the vector of generalized forces. The vector of gravitation being smooth, we can get $\bar{\mathcal{G}}(q(t)) \in \mathbb{R}^{d\times d}$ such that $\mathcal{G}(q(t)) = \bar{\mathcal{G}}(q(t))q(t)$. Thus, denoting $x(t) = \begin{bmatrix} q^T(t) & \dot{q}^T(t) \end{bmatrix}^T \in \mathbb{R}^n$, $n = 2d$, the dynamical model (4.6) can be rewritten in the affine-in-control continuous-time nonlinear state space descriptor form (4.1) with:

$$E(x(t)) = \begin{bmatrix} I & 0 \\ 0 & \mathcal{M}(x(t)) \end{bmatrix}, A(x(t)) = \begin{bmatrix} 0 & I \\ -\bar{\mathcal{G}}(x(t)) & -\mathcal{C}(x(t)) \end{bmatrix} \text{ and } B(x(t)) = \begin{bmatrix} 0 \\ \mathcal{B}(x(t)) \end{bmatrix}.$$

Finally, note that, since the inertia matrix $M(x(t))$ of a mechanical plant is always positive definite, the descriptor matrix $E(x(t))$ is always invertible.

Now, due to the discrete nature of the controllers, let $t_k \geq 0$ be the sampling instants such that $t_{k+1} - t_k \leq \eta_k \leq \bar{\eta}$, where the inner sampling interval $\eta_k > 0$ can be non-uniform (aperiodic) with a maximal allowable sampling interval $\bar{\eta}$. A Zero-Order Hold (ZOH) is employed to maintain the control signal $\forall t \in [t_k, t_{k+1})$. Hence, for actual $t \in [t_k, t_{k+1})$, let $\tau(t) = t - t_k \in [0, \eta_k)$, where $\dot{\tau}(t) = 1$, and consider the following sampled-data PDC control law for the stabilization of T-S descriptors (4.5):

$$u(t) = \sum_{i=1}^{r} \alpha_i(x(t - \tau(t)))K_i X^{-1} x(t - \tau(t)) \tag{4.7}$$

where $K_i \in \mathbb{R}^{m\times n}$ and $X^{-1} \in \mathbb{R}^{n\times n}$ are the sampled-data controller gain matrices to be designed.

From (4.5) and (4.7), and using the following notations:

$$M_\alpha = \sum_{i=1}^{r} \alpha_i(z(t))M_i,\ M_{\bar{\alpha}} = \sum_{i=1}^{r} \alpha_i(z(t-\tau(t)))M_i$$

and:

$$M_{\alpha\bar{\alpha}} = \sum_{i=1}^{r}\sum_{j=1}^{r} \alpha_i(z(t))\alpha_j(z(t-\tau(t)))M_{ij}$$

to lighten mathematical expressions, the closed-loop sampled-data dynamics can be expressed by the following T-S descriptor model with saturated inputs and time-varying input delays:

$$E_\alpha \dot{x}(t) = A_\alpha x(t) + B_\alpha \mathtt{sat}(K_{\bar{\alpha}} X^{-1} x(t-\tau(t))) \tag{4.8}$$

In this work, to cope with the saturation, let us consider the dead-zone nonlinearity defined by (see Definition 1.2 for more details):

$$\psi(u(t)) = \mathrm{sat}(u(t)) - u(t) \tag{4.9}$$

From this definition, the closed-loop sampled-data dynamics with input saturation (4.8) can be rewritten as the following T-S descriptor with input time-varying delays and with an additional dead-zone nonlinearity:

$$E_\alpha \dot{x}(t) = A_\alpha x(t) + B_\alpha K_{\bar{\alpha}} X^{-1} x(t-\tau(t)) + B_\alpha \psi(K_{\bar{\alpha}} X^{-1} x(t-\tau(t))) \tag{4.10}$$

From now, our goal is to design the gain matrices $K_{\bar{\alpha}}$ and X that guarantee the closed-loop dynamics (4.8) to be stable. This will be done in the next section by extending the results provided in Chapter 3, considering the application of Theorem 3.2. Recall that the latter assume that the time-derivatives of the membership functions are bounded such that the results are valid inside the following set:

$$\mathcal{D}_\phi = \bigcap_{k=1}^{r} \{x(t) \in \mathbb{R}^n : |\dot{\alpha}_k(z)| \leqslant \phi_k\} \tag{4.11}$$

Hence, considering the validity domain $\mathcal{D}_x$ of the T-S descriptor defined by (4.2), the input constraints resulting to the set $\mathcal{D}_u$ defined in (4.4), and the restrictions implied by the set $\mathcal{D}_\phi$ defined in (4.11), the sampled-data closed-loop dynamics (4.10) can only be locally guaranteed, which makes necessary the estimation of the domain of attraction.

Remark 4.2. *In previous literature dealing with continuous-time T-S model-based non-quadratic control, estimating the bounds ϕ_k ($\forall k \in \mathcal{I}_r$) of the time-derivatives of the membership functions $h_k(x(t))$ is, in general, commonly considered as a hard or even impossible task, since this has to be made priory to the design of the closed-loop dynamics, see e.g. (Guerra et al., 2012; Guelton et al., 2014; Cherifi et al., 2019). However, in the local context of our study, assuming $E(x(t))$ regular $\forall x(t) \in \mathcal{D}_x$, when considering known input constraints, i.e. when $u(t)$ belongs to a known closed compact subset $\mathcal{D}_u \subset \mathbb{R}^m$, and $x(t)$ belongs to a known closed compact subset $\mathcal{D}_x \subset \mathbb{R}^n$,*

such bounds can be easily estimated from numerical computation by:

$$\begin{aligned}\phi_k &= \sup_{\{x\in\mathcal{D}_x, u\in\mathcal{D}_u\}} \Big(\big|\nabla_k^T(x)E^{-1}(x)\big(A(x)x+B(x)u\big|\Big)\\ &\geq \big|\nabla_k^T(x(t))E^{-1}(x(t))\big(A(x(t))x(t)+B(x(t))\mathtt{sat}(u(t))\big)\big|\\ &= \big|\nabla_k^T(x(t))\dot{x}(t)\big|\\ &= \big|\dot{\alpha}_k(x(t))\big|\end{aligned} \tag{4.12}$$

This being said, the main objectives of this chapter are summarized in the following problem statement.

Problem statement:

$\mathcal{P}_1$**:** Provide relaxed LMI-based conditions for the design of the gain matrices K_i and X such that the sampled-data closed-loop dynamics (4.10) with input saturation is locally asymptotically stable for the largest as possible admissible upper bound $\bar{\eta}$ of the non-uniform sampling intervals η_k.

$\mathcal{P}_2$**:** Provide a methodology to estimate the domain of attraction $\mathcal{D}_a^*$ of the closed-loop system (4.10).

$\mathcal{P}_3$**:** Based on the satisfaction of $\mathcal{P}_1$ and $\mathcal{P}_2$, provide a gain scheduled event-triggering mechanism to further enlarge the closed-loop domain of attraction.

4.3 Main results

In the sequence, the goal is to provide parameterized LMI-based conditions and methodologies to satisfy $\mathcal{P}_1$, $\mathcal{P}_2$ and $\mathcal{P}_3$ of the above given problem statement. First, the main result is proposed for the class of descriptor systems (4.1), then the special case of standard T-S systems (3.1) is considered to provide a systematic approach for the estimation of the closed-loop domain of attraction. Finally, a gain-scheduled event-triggering mechanism will be proposed to further enlarge the closed-loop domain of attraction.

4.3.1 LMI-based local non-quadratic sampled-data controller design for T-S descriptors

Consider the class of T-S descriptor (4.1) and the closed-loop dynamics presented in (4.10). To provide parameterized LMI-based conditions satisfying $\mathcal{P}_1$ and $\mathcal{P}_2$, we proposed the following Non-Quadratic Lyapunov-Krasovskii Function (NQLKF) candidate:

$$V(t) = \sum_{\ell=1}^{4} V_\ell(t) \tag{4.13}$$

where:

$$V_1(t) = x^T(t)P_\alpha x(t), \tag{4.14}$$

$$V_2(t) = (\eta_k - \tau(t))\rho^T(t)Q_{\alpha\bar{\alpha}}\rho(t), \tag{4.15}$$

$$V_3(t) = (\eta_k - \tau(t))\int_{t-\tau(t)}^{t} \dot{\rho}^T(s)R_{\alpha\bar{\alpha}}\dot{\rho}(s)ds, \tag{4.16}$$

$$V_4(t) = (\eta_k\tau(t) - \tau^2(t))\zeta^T(t)S_{\bar{\alpha}}\zeta(t), \tag{4.17}$$

with:

$$\zeta(t) = \texttt{col}\left\{x(t), x(t-\tau(t)), \int_{t-\tau(t)}^{t} x(s)ds, \int_{t-\tau(t)}^{t} \dot{x}(s)ds\right\}$$

and

$$\rho(t) = \texttt{col}\left\{\int_{t-\tau(t)}^{t} x(s)ds, \int_{t-\tau(t)}^{t} \dot{x}(s)ds\right\}.$$

The following theorem summarizes the proposed LMI-based conditions to address the above-defined problem statements $\mathcal{P}_1$ and $\mathcal{P}_2$ for the sampled-data stabilization of T-S descriptors (4.5) with input saturation.

Theorem 4.1. *Let $(i,j) \in \mathcal{I}_r^2$ and let assume that $\forall t$, $|\dot{\alpha}_i(t)| \leq \phi_i$. For given symmetric bounds $\bar{u} \in \mathbb{R}^m$ of the input vector and for non-uniform sampling intervals $\eta_k \leq \bar{\eta}$ ($\bar{\eta}$ to be maximized), the T-S descriptor (4.5) is locally asymptotically stabilized by the sampled-data PDC controller (4.7) with saturation (see (4.3)), if there exists a diagonal positive matrix $D_j \in \mathbb{R}^{m\times m}$, the matrices $0 < \bar{P}_i = \bar{P}_i^T \in \mathbb{R}^{n\times n}$, $\bar{S}_j = \bar{S}_j^T \in \mathbb{R}^{4n\times 4n}$, $\bar{Q}_{ij} = \bar{Q}_{ij}^T \in \mathbb{R}^{2n\times 2n}$, $\bar{R}_{11ij} = \bar{R}_{11ij}^T \in \mathbb{R}^{n\times n}$, $\bar{R}_{22j} = \bar{R}_{22j}^T \in \mathbb{R}^{n\times n}$, $\bar{R}_{12j} \in \mathbb{R}^{n\times n}$, $X \in \mathbb{R}^{n\times n}$, $K_j \in \mathbb{R}^{m\times n}$, $F_j \in \mathbb{R}^{m\times n}$, $\bar{Y}_{ij} \in \mathbb{R}^{n\times 4n}$, $\bar{M}_{ij}^1 = \bar{M}_{ij}^{1T} \in \mathbb{R}^{n\times n}$, $\bar{M}_{ij}^2 = \bar{M}_{ij}^{2T} \in \mathbb{R}^{2n\times 2n}$, and the scalars ε_1, ε_2, and ε_3, such that the following parameterized inequalities are satisfied:*

$$\begin{bmatrix} \bar{\Lambda}_{\alpha\bar{\alpha}}^{11} & \bar{\eta}\bar{Y}_{\alpha\bar{\alpha}}^T & 0 & 0 & 0 \\ \star & -\bar{\eta}\bar{R}_{22\alpha\bar{\alpha}} & 0 & 0 & 0 \\ \star & \star & \bar{\Lambda}_{\alpha\bar{\alpha}}^{33} & 0 & 0 \\ \star & \star & \star & -\bar{R}_{11\alpha\bar{\alpha}} & 0 \\ \star & \star & \star & \star & \bar{\Lambda}_{\alpha\bar{\alpha}}^{55} \end{bmatrix} < 0, \tag{4.18}$$

$$-\begin{bmatrix} \bar{P}_\rho + \bar{M}_{\alpha\bar{\alpha}}^1 & 0 \\ \star & \bar{Q}_{\rho\bar{\alpha}} + \bar{M}_{\alpha\bar{\alpha}}^2 \end{bmatrix} < 0,\ \forall \rho \in \mathcal{I}_r, \tag{4.19}$$

$$\begin{bmatrix} \bar{P}_\alpha & \star \\ (K_{\bar{\alpha}} - F_{\bar{\alpha}})_{(\ell)} & \bar{u}_{(\ell)}^2 \end{bmatrix} \geq 0,\ \forall \ell \in \mathcal{I}_m, \tag{4.20}$$

with:

$$\bar{\Lambda}_{\alpha\bar{\alpha}}^{11} = -\bar{\eta}^2\mathcal{H}\left(E_4^T\bar{S}_{\bar{\alpha}}E_5\right) + \bar{\eta}\bar{\Phi}_{1\alpha\bar{\alpha}} + \bar{\Phi}_{0\alpha\bar{\alpha}} + \sum_{\rho=1}^{r}\phi_\rho E_0^T(\bar{P}_\rho + \bar{M}_{\alpha\bar{\alpha}}^1) + \bar{\Psi}_{\bar{\alpha}},$$

$$\bar{\Lambda}_{\alpha\bar{\alpha}}^{33} = \bar{\Phi}_{0\alpha\bar{\alpha}} + \sum_{\rho=1}^{r}\phi_\rho(E_0^T(\bar{P}_\rho + \bar{M}_{\alpha\bar{\alpha}}^1)) + \bar{\Psi}_{\bar{\alpha}},\ \bar{\Lambda}_{\alpha\bar{\alpha}}^{55} = \bar{\Lambda}_{\alpha\bar{\alpha}}^{33} + \bar{\eta}^2\mathcal{H}\left(E_4^T\bar{S}_{\bar{\alpha}}E_5\right),$$

$$\bar{\Phi}_{0\alpha\bar{\alpha}} = \mathcal{H}\left(\bar{P}_\alpha^T\bar{A}_{\alpha\bar{\alpha}} + \bar{\eta}E_1^T\bar{Q}_{\alpha\bar{\alpha}}E_2 - E_3^T\bar{Y}_{\alpha\bar{\alpha}}\right) - E_1^T\bar{Q}_{\alpha\bar{\alpha}}E_1 + \bar{\eta}E_2^T\bar{R}_{\alpha\bar{\alpha}}E_2 + \bar{W}_{\alpha\bar{\alpha}} + \bar{\eta}E_4^T\bar{S}_{\bar{\alpha}}E_4,$$

$$\bar{\Phi}_{1\alpha\bar{\alpha}} = -\mathcal{H}\left(E_1^T\bar{Q}_{\alpha\bar{\alpha}}E_2 - \bar{\eta}E_4^T\bar{S}_{\bar{\alpha}}E_5 + E_4^T\bar{S}_{\bar{\alpha}}E_4\right) - E_2^T\bar{R}_{\alpha\bar{\alpha}}E_2,$$

$$\bar{W}_{\alpha\bar{\alpha}} = -e_1^T \bar{R}_{12\bar{\alpha}} e_1 + e_2^T \bar{R}_{12\bar{\alpha}} e_2 - \eta_k^{-1} e_3^T \bar{R}_{11\alpha\bar{\alpha}} e_3,$$

$$\tilde{\bar{P}}_\alpha = \begin{bmatrix} \bar{P}_\alpha & 0 & 0 & 0 & 0 \\ I & \varepsilon_1 I & \varepsilon_2 I & \varepsilon_3 I & I \end{bmatrix}, \bar{A}_{\alpha\bar{\alpha}} = \begin{bmatrix} 0 & 0 & 0 & I & 0 \\ A_\alpha X & B_\alpha K_{\bar{\alpha}} & 0 & -E_\alpha X & B_\alpha D_\alpha \end{bmatrix},$$

$$\bar{\Psi}_{\bar{\alpha}} = -E_6^T \begin{bmatrix} 0 & F_{\bar{\alpha}}^T D_{\bar{\alpha}} \\ \star & 2D_{\bar{\alpha}} \end{bmatrix} E_6, E_0 = \begin{bmatrix} e_1 \\ e_0 \end{bmatrix}, E_1 = \begin{bmatrix} e_3 \\ e_1 - e_2 \end{bmatrix}, E_2 = \begin{bmatrix} e_1 \\ e_4 \end{bmatrix},$$

$$E_3 = \begin{bmatrix} e_1 - e_2 \end{bmatrix}, E_4 = \begin{bmatrix} e_1 \\ e_2 \\ e_3 \\ e_1 - e_2 \end{bmatrix}, E_5 = \begin{bmatrix} e_4 \\ e_0 \\ e_1 \\ e_4 \end{bmatrix}, E_6 = \begin{bmatrix} e_2 \\ e_5 \end{bmatrix}.$$

Furthermore, an estimate of the domain of attraction $\mathcal{D}_a^*$ of the designed closed-loop sampled-data descriptor is obtained by maximizing c such that:

$$\mathcal{D}_a^* = \{x(0) \in \mathbb{R}^n \mid \exists \bar{c} = \max c,\ \mathcal{L}(\bar{c}) \subseteq \mathcal{D}_u \cap \mathcal{D}_x \cap \mathcal{D}_\phi\} \tag{4.21}$$

with $\mathcal{L}(\bar{c}) = \{x \in \mathbb{R}^n \mid x^T P_{\bar{\alpha}} x \leq \bar{c}\}$. Furthermore, an estimate of the domain of attraction taken at $t = t_0$ is obtained by optimizing $V_1(x) = \bar{c} \leq 1$, i.e. by finding the largest equipotential included in $\mathcal{D}_u \cap \mathcal{D}_x \cap \mathcal{D}_\phi$ with $\mathcal{D}_u$, $\mathcal{D}_x$ and $\mathcal{D}_\phi$, respectively defined by (4.4), (4.2) and (4.11).

Proof. Let $P_\alpha = P_\alpha^T > 0$. At the sampling instant t_k we have $V(t_k) > 0$ because $V_1(t_k) > 0$ and $V_\ell(t_k^-) = V_\ell(t_k) = 0$, for $\ell = 2, ..., 4$. In this context, to ensure the asymptotic stability of the closed-loop dynamics (4.10), because the LKF is continuous $\forall t \in [0, +\infty)$, we only need to provide that it is monotonously decreasing $\forall t \in [t_k, t_{k+1})$, i.e.:

$$\dot{V}(t) = \sum_{\ell=1}^{4} \dot{V}_\ell(t) < 0 \tag{4.22}$$

Nevertheless, at this point, the constraints introduced due to the actuators' saturation must be consider on the design. So, from Lemma 2.1, the sector conditions is introduced with (4.22), providing that $x(t-\tau(t)) \in \mathcal{S}((K_{\bar{\alpha}} - F_{\bar{\alpha}})X^{-1}, \bar{u})$, for any diagonal matrix $D_{\bar{\alpha}} > 0$, such that:

$$\dot{V}(t) - 2\psi(K_{\bar{\alpha}} X^{-1} x(t-\tau(t)))^T D_{\bar{\alpha}}^{-1} (\psi(K_{\bar{\alpha}} X^{-1} x(t-\tau(t)) + F_{\bar{\alpha}} X^{-1} x(t-\tau(t))) < 0 \tag{4.23}$$

In the remaining of this proof, let us consider the extended vector:

$$\xi(t) = \texttt{col}\left\{ \ x(t), \quad x(t-\tau(t)), \quad \int_{t-\tau(t)}^{t} x(s)ds, \quad \dot{x}(t), \quad \psi(K_{\bar{\alpha}} X^{-1} x(t-\tau(t))) \ \right\}.$$

Thus, the inequality (4.23) can be rewritten as:

$$\dot{V}(t) + \xi^T(t) \Psi_{\bar{\alpha}} \xi(t) < 0 \tag{4.24}$$

with:

$$\Psi_{\bar{\alpha}} = -E_6^T \begin{bmatrix} 0 & X^{-T} F_{\bar{\alpha}}^T D_{\bar{\alpha}}^{-1} \\ \star & 2D_{\bar{\alpha}}^{-1} \end{bmatrix} E_6 \tag{4.25}$$

Then, considering the arbitrary scalars ε_1, ε_2, and ε_3, and a regular matrix X, let:

$$\tilde{P}_\alpha = \begin{bmatrix} P_\alpha & 0 & 0 & 0 & 0 \\ X^{-1} & \varepsilon_1 X^{-1} & \varepsilon_2 X^{-1} & \varepsilon_3 X^{-1} & D_\alpha^{-1} \end{bmatrix},$$

which, combined with E_0 defined in Theorem 4.1, allow us to rewrite (4.14) as:

$$V_1(t) = \xi^T(t) E_0^T \tilde{P}_\alpha \xi(t) \tag{4.26}$$

where the symmetric condition $E_0^T \tilde{P}_\alpha = \tilde{P}_\alpha^T E_0$ is satisfied.
Hence, the time-derivative of $V_1(t)$ can be written as:

$$\dot{V}_1(t) = 2\xi^T(t) \tilde{P}_\alpha^T E_0 \dot{\xi}(t) + \xi^T(t) E_0^T \dot{\tilde{P}}_\alpha \xi(t) \tag{4.27}$$

Note that the closed-loop dynamics (4.10) can be rewritten as:

$$E_0 \dot{\xi}(t) = \tilde{A}_{\alpha\bar{\alpha}} \xi(t), \text{ with } \tilde{A}_{\alpha\bar{\alpha}} = \begin{bmatrix} 0 & 0 & 0 & I & 0 \\ A_\alpha & B_\alpha K_{\bar{\alpha}} X^{-1} & 0 & -E_\alpha & B_\alpha \end{bmatrix}. \tag{4.28}$$

Then, equation (4.27) can be rewritten as:

$$\dot{V}_1(t) = \xi^T(t) \left(\mathcal{H}(\tilde{P}_\alpha^T \tilde{A}_{\alpha\bar{\alpha}}) + E_0^T \dot{\tilde{P}}_\alpha \right) \xi(t) \tag{4.29}$$

Now, taking the time-derivative of $V_2(t)$ leads to:

$$\dot{V}_2(t) = -\rho^T(t) Q_{\alpha\bar{\alpha}} \rho(t) + (\eta_k - \tau(t))(2\rho^T(t) Q_{\alpha\bar{\alpha}} \dot{\rho}(t) + \rho^T(t) \dot{Q}_{\alpha\bar{\alpha}} \rho(t)) \tag{4.30}$$

With $\rho(t) = E_1 \xi(t)$ and $\dot{\rho}(t) = \texttt{col}\{x(t), \dot{x}(t)\} = E_2 \xi(t)$, equation (4.30) can be rewritten as:

$$\begin{aligned} \dot{V}_2(t) = &- \tau(t) \xi^T(t) \left(\mathcal{H}\left(E_1^T Q_{\alpha\bar{\alpha}} E_2 \right) + E_1^T \dot{Q}_{\alpha\bar{\alpha}} E_1 \right) \xi(t) \\ &+ \xi^T(t) \left(\mathcal{H}\left(\eta_k E_1^T Q_{\alpha\bar{\alpha}} E_2 \right) - E_1^T Q_{\alpha\bar{\alpha}} E_1 + \eta_k E_1^T \dot{Q}_{\alpha\bar{\alpha}} E_1 \right) \xi(t) \end{aligned} \tag{4.31}$$

Next, the time-derivative of $V_3(t)$ is given by:

$$\dot{V}_3(t) = (\eta_k - \tau(t)) \dot{\rho}^T(t) R_{\alpha\bar{\alpha}} \dot{\rho}(t) - \int_{t-\tau(t)}^{t} \dot{\rho}^T(s) R_{\alpha\bar{\alpha}} \dot{\rho}(s) ds \tag{4.32}$$

Let:

$$R_{\alpha\bar{\alpha}} = \begin{bmatrix} R_{11\alpha\bar{\alpha}} & R_{12\bar{\alpha}} \\ \star & R_{22\alpha\bar{\alpha}} \end{bmatrix},$$

and assume:

$$R_{11\alpha\bar{\alpha}} = R_{11\alpha\bar{\alpha}}^T > 0,\ R_{22\alpha\bar{\alpha}} = R_{22\alpha\bar{\alpha}}^T > 0 \tag{4.33}$$

Equation (4.32) is equivalent to:

$$\begin{aligned} \dot{V}_3(t) = &(\eta_k - \tau(t)) \dot{\rho}^T(t) R_{\alpha\bar{\alpha}} \dot{\rho}(t) - \int_{t-\tau(t)}^{t} x^T(s) R_{11\alpha\bar{\alpha}} x(s) ds \\ &- \int_{t-\tau(t)}^{t} \dot{x}^T(s) R_{22\alpha\bar{\alpha}} \dot{x}(s) ds - 2 \int_{t-\tau(t)}^{t} x^T(s) R_{12\bar{\alpha}} \dot{x}(s) ds \end{aligned} \tag{4.34}$$

Note that $\int_{t-\tau(t)}^{t} \dot{x}^T(s) ds = E_3 \xi(t)$ and, $\forall t \in [t_k, t_{k+1})$, $R_{12\bar{\alpha}}$ is constant. Applying Lemma 1.7 and Lemma 1.8 we get:

$$\begin{aligned} \dot{V}_3(t) \leq &(\eta_k - \tau(t)) \dot{\rho}^T(t) R_{\alpha\bar{\alpha}} \dot{\rho}(t) - \eta_k^{-1} \int_{t-\tau(t)}^{t} x^T(s) R_{11\alpha\bar{\alpha}} \int_{t-\tau(t)}^{t} x(s) ds \\ &- x^T(t) R_{12\bar{\alpha}} x(t) + x^T(t - \tau(t)) R_{12\bar{\alpha}} x(t - \tau(t)) \\ &+ \xi^T(t) \left(\tau(t) Y_{\alpha\bar{\alpha}}^T R_{22\alpha\bar{\alpha}}^{-1} Y_{\alpha\bar{\alpha}} - E_3^T Y_{\alpha\bar{\alpha}} - Y_{\alpha\bar{\alpha}}^T E_3 \right) \xi(t) \\ = &\tau(t) \xi^T(t) \left(Y_{\alpha\bar{\alpha}}^T R_{22\alpha\bar{\alpha}}^{-1} Y_{\alpha\bar{\alpha}} - E_2^T R_{\alpha\bar{\alpha}} E_2 \right) \xi(t) \\ &+ \xi^T(t) \left(\eta_k E_2^T R_{\alpha\bar{\alpha}} E_2 - \mathcal{H}\left(E_3^T Y_{\alpha\bar{\alpha}} \right) + W_{\alpha\bar{\alpha}} \right) \xi(t) \end{aligned} \tag{4.35}$$

with $W_{\alpha\bar{\alpha}} = -e_1^T R_{12\bar{\alpha}} e_1 + e_2^T R_{12\bar{\alpha}} e_2 - \eta_k^{-1} e_3^T R_{11\alpha\bar{\alpha}} e_3$.
Now, taking the time-derivative of $V_4(t)$, we obtain:

$$\dot{V}_4(t) = (\eta_k - 2\tau(t))\zeta^T(t) S_{\bar{\alpha}} \zeta(t) + 2(\eta_k \tau(t) - \tau^2(t))\zeta^T(t) S_{\bar{\alpha}} \dot{\zeta}(t) \tag{4.36}$$

With $\zeta(t) = E_4\xi(t)$ and $\dot{\zeta}(t) = E_5\xi(t)$, it yields:

$$\begin{aligned} \dot{V}_4(t) = &- \tau^2(t)\xi^T(t)\mathcal{H}\left(E_4^T S_{\bar{\alpha}} E_5\right)\xi(t) + \xi^T(t)\left(\eta_k E_4^T S_{\bar{\alpha}} E_4\right)\xi(t) \\ &+ \tau(t)\xi^T(t)\mathcal{H}\left(\eta_k E_4^T S_{\bar{\alpha}} E_5 - E_4^T S_{\bar{\alpha}} E_4\right)\xi(t) \end{aligned} \tag{4.37}$$

Thus, from (4.23), (4.29), (4.31), (4.35), and (4.37), the inequality (4.22) is satisfied if:

$$\begin{aligned} \mathcal{P}(\tau(t)) = &- \tau^2(t)\xi^T(t)\mathcal{H}\left(E_4^T S_{\bar{\alpha}} E_5\right)\xi(t) \\ &+ \tau(t)\xi^T(t)\left(\Phi_{1\alpha\bar{\alpha}} + Y_{\alpha\bar{\alpha}}^T R_{22\alpha\bar{\alpha}}^{-1} Y_{\alpha\bar{\alpha}} - E_1^T \dot{Q}_{\alpha\bar{\alpha}} E_1\right)\xi(t) \\ &+ \xi^T(t)\left(\Phi_{0\alpha\bar{\alpha}} + E_0^T \dot{\tilde{P}}_\alpha + \eta_k E_1^T \dot{Q}_{\alpha\bar{\alpha}} E_1\right)\xi(t) < 0 \end{aligned} \tag{4.38}$$

with:

$$\Phi_{1\alpha\bar{\alpha}} = \mathcal{H}\left(\eta_k E_4^T S_{\bar{\alpha}} E_5 - E_1^T Q_{\alpha\bar{\alpha}} E_2 - E_4^T S_{\bar{\alpha}} E_4\right) - E_2^T R_{\alpha\bar{\alpha}} E_2,$$

$$\begin{aligned} \Phi_{0\alpha\bar{\alpha}} = &\mathcal{H}\left(\tilde{P}_\alpha^T \tilde{A}_{\alpha\bar{\alpha}} + \eta_k E_1^T Q_{\alpha\bar{\alpha}} E_2 - E_3^T Y_{\alpha\bar{\alpha}}\right) - E_1^T Q_{\alpha\bar{\alpha}} E_1 \\ &+ \eta_k E_2^T R_{\alpha\bar{\alpha}} E_2 + W_{\alpha\bar{\alpha}} + \eta_k E_4^T S_{\bar{\alpha}} E_4 - E_9^T \Psi_{\bar{\alpha}} E_9. \end{aligned}$$

Let us recall that acoording Lemma 1.9, (4.38) can be checked if:

$$\mathcal{P}(0) < 0, \tag{4.39}$$

$$\mathcal{P}(\bar{\eta}) < 0, \tag{4.40}$$

$$\mathcal{P}(0) - \tau^2(t)\xi^T(t)\mathcal{H}\left(E_4^T S_{\bar{\alpha}} E_5\right)\xi(t) < 0, \tag{4.41}$$

Then, the inequalities (4.39), (4.40) and (4.41) are verified if, $\forall \xi^T(t) \neq 0$:

$$\Phi_{0\alpha\bar{\alpha}} + E_0^T \dot{\tilde{P}}_\alpha < 0, \tag{4.42}$$

$$\begin{aligned} -\bar{\eta}^2\mathcal{H}\left(E_4^T S_{\bar{\alpha}} E_5\right) + \bar{\eta}\left(\Phi_{1\alpha\bar{\alpha}} + Y_{\alpha\bar{\alpha}}^T R_{22\alpha\bar{\alpha}}^{-1} Y_{\alpha\bar{\alpha}} - E_1^T \dot{Q}_{\alpha\bar{\alpha}} E_1\right) \\ + \left(\Phi_{0\alpha\bar{\alpha}} + E_0^T \dot{\tilde{P}}_\alpha + \bar{\eta} E_1^T \dot{Q}_{\alpha\bar{\alpha}} E_1\right) < 0 \end{aligned} \tag{4.43}$$

and

$$\Phi_{0\alpha\bar{\alpha}} + E_0^T \dot{\tilde{P}}_\alpha + \bar{\eta}^2\mathcal{H}\left(E_4^T S_{\bar{\alpha}} E_5\right) < 0, \tag{4.44}$$

Recall that $\sum_{\rho=1}^{r} \dot{\alpha}_\rho(x(t)) = 0$, and for any slack matrix $M_{\alpha\bar{\alpha}}^q$ $(q = 1, 2)$, $\sum_{\rho=1}^{r} \dot{\alpha}_\rho(x(t)) M_{\alpha\bar{\alpha}}^q = 0$.
With $|\dot{\alpha}_\rho(x(t))| \leq \phi_\rho$, if:

$$P_\rho + M_{\alpha\bar{\alpha}}^1 > 0 \text{ and } Q_{\rho\bar{\alpha}} + M_{\alpha\bar{\alpha}}^2 > 0, \forall \rho \in \mathcal{I}_r, \tag{4.45}$$

we get:

$$E_0^T \dot{P}_\alpha \leq \sum_{\rho=1}^{r} \phi_\rho E_0^T (P_\rho + M_{\alpha\bar{\alpha}}^1) \tag{4.46}$$

and:

$$\eta_k E_1^T \dot{Q}_{\alpha\bar{\alpha}} E_1 \leq \eta_k \sum_{\rho=1}^{r} \phi_\rho E_1^T (Q_{\rho\bar{\alpha}} + M^2_{\alpha\bar{\alpha}}) E_1. \tag{4.47}$$

Thus, from (4.46) and (4.47), applying the Schur complement, the inequalities (4.42) and (4.43) are respectively satisfied if:

$$\Phi_{0\alpha\bar{\alpha}} + \sum_{\rho=1}^{r} \phi_\rho (E_0^T (P_\rho + M^1_{\alpha\bar{\alpha}})) < 0, \tag{4.48}$$

$$\begin{bmatrix} \Lambda^{11}_{\alpha\bar{\alpha}} & \eta_k Y^T_{\alpha\bar{\alpha}} \\ \star & -\eta_k R_{22\alpha\bar{\alpha}} \end{bmatrix} < 0, \tag{4.49}$$

with $\Lambda^{11}_{\alpha\bar{\alpha}} = -\bar{\eta}^2 \mathcal{H}\left(E_4^T S_{\bar{\alpha}} E_5\right) + \bar{\eta}\Phi_{1\alpha\bar{\alpha}} + \Phi_{0\alpha\bar{\alpha}} + \sum_{\rho=1}^{r} \phi_\rho E_0^T (P_\rho + M^1_{\alpha\bar{\alpha}})$.
Taking the congruence of (4.33) and (4.45) by $\mathcal{X}_p(X)$ (with appropriate p), where $\mathcal{X}_p(X)$ denotes a diagonal block matrix filled p times in diagonal with $X \in \mathbb{R}^{n\times n}$. Then pre- and post-multiplying (4.44) and (4.48) respectively by $\texttt{diag}\{X, X, X, X, D_{\bar{\alpha}}\}^T$ and its transpose followed by pre- and post-multiplying (4.49) respectively $\texttt{diag}\{X, X, X, X, D_{\bar{\alpha}}, X\}^T$ and its transpose, we obtain the conditions (4.18) (which embed (4.33), (4.44), (4.48) and (4.49)) and (4.19) (which embeds (4.45)) where the decision matrices inside $\bar{\Phi}_{1\alpha\bar{\alpha}}$ and $\bar{\Phi}_{0\alpha\bar{\alpha}}$ belong to the bijective change of variables $\bar{Z} = X^T Z X$, $Z = \{P_\alpha, Q_{\alpha\bar{\alpha}}, R_{11\alpha\bar{\alpha}}, R_{12\bar{\alpha}}, R_{22\alpha\bar{\alpha}} \dots\}$.
In the sequel of the proof, let us focus on the restriction brought by the saturated actuators. Recall that the NQLKF (4.22) is continuous and monotonously decreasing if the previous inequalities hold. Therefore, for every $x(t_k)$ reaching $\mathcal{D}_a$ the systems will be stable and, without loss of generality, the NQLKF taken at t_k allows to define the following level sets:

$$\mathcal{L}(1) = \{x(t-\tau(t)) \in \mathbb{R}^n \,|\, x(t-\tau(t))^T P_\alpha x(t-\tau(t)) \leq 1\} \tag{4.50}$$

Moreover, from the application of Lemma 1.6, we must provide that $x(t-\tau(t))$ is such that $(K_{\bar{\alpha}} - F_{\bar{\alpha}})X^{-1}x(t-\tau(t))$ belongs to $\mathcal{S}(\bar{u})$ (see eq. (1.64)). This holds if both the following conditions hold:

$$\text{If } x(t-\tau(t))^T P_\alpha x(t-\tau(t)) \leq 1, \text{ then } x(t) \in \mathcal{L}(1) \tag{4.51}$$

and, with $Z_{\bar{\alpha}} = ((K_{\bar{\alpha}} - F_{\bar{\alpha}})X^{-1})^T_{(\ell)}((K_{\bar{\alpha}} - F_{\bar{\alpha}})X^{-1})_{(\ell)}/\bar{u}^2_{(\ell)}$:

$$\text{If } x(t-\tau(t))^T Z_{\bar{\alpha}(\ell)} x(t-\tau(t)) \leq 1, \text{ then } (K_{\bar{\alpha}} - F_{\bar{\alpha}})X^{-1}x(t-\tau(t)) \in \mathcal{S}(\cdot) \tag{4.52}$$

Then $\mathcal{L}(1) \subset \mathcal{S}(K_{\bar{\alpha}}X^{-1} - F_{\bar{\alpha}}, \bar{u})$ if:

$$1 \geq x(t-\tau(t))^T P_\alpha x(t-\tau(t)) \geq x(t-\tau(t))^T Z_{\bar{\alpha}(\ell)} x(t-\tau(t)) \tag{4.53}$$

which is granted from the Schur complement if:

$$\begin{bmatrix} P_\alpha & \star \\ ((K_{\bar{\alpha}} - F_{\bar{\alpha}})X^{-1})_{(\ell)} & \bar{u}^2_{(\ell)} \end{bmatrix} \geq 0 \tag{4.54}$$

That is to say, pre- and post-multiplying (4.54) by $diag\{X, 1\}^T$ and its transpose, respectively, we get the conditions (4.20). Finally, note that the conditions of Theorem 4.1 only guarantee

the local asymptotic stability of the designed closed-loop descriptor because the T-S descriptor (4.5) matches (4.1), $\forall x(t) \in \mathcal{D}_x$, and the conditions (4.18), and (4.19) are valid assuming that $\forall t$, $|\dot{\alpha}_i(t)| \leq \phi_i$. Hence, the domain of attraction $\mathcal{D}_a$ of the designed closed-loop system must verify $\mathcal{D}_a \subseteq D_x \cap \mathcal{D}_\phi$ (recall that $\mathcal{D}_a \subseteq D_u$ is granted by (4.20)). Since $V_\ell(0) = 0$, for $\ell = 2, ..., 4$, an estimate $\mathcal{D}_a^*$ of the domain of attraction $\mathcal{D}_a$ is given by (4.21). □

Remark 4.3. *The conditions* (4.18) *and* (4.19) *of Theorem 4.1 are parameterized inequalities, which can be solved via LMI tools from the application of Theorem 3.2. Furthermore, the obtained conditions are not strictly LMI because of the parameters* $\bar{\eta}$, ε_1, ε_2 *and* ε_3. *However, similarly to what has been proposed in Chapter 3 (see Remark 3.1), these parameters can be usually tuned offline by grid search.*

Remark 4.4. *Note that the LKF* (3.8) *considered in Chapter 3 is a special case of the NQLKF* (4.13) *(proposed to prove Theorem 4.1) with* $P_\alpha = L$, $Q_{\alpha\bar{\alpha}} = N_{\bar{\alpha}}$, $R_{\alpha\bar{\alpha}} = P_{\bar{\alpha}}$ *and* $S_{\bar{\alpha}} = \bar{M}_\alpha$. *Moreover, standard T-S models* (3.1) *being a special case of T-S descriptors* (4.1) *with* $E_\alpha = I$, *Theorem 1 in (Lopes et al., 2021) or Theorem 3.1 (when input saturations are not considered) constitute special cases of Theorem 4.1 (assuming* $\bar{M}_{ij}^1 = -\bar{P}$, *and* $\bar{M}_{ij}^2 = -\bar{Q}_j$ *to alleviate conditions* (4.19)*). Consequently, applying Theorem 4.1 instead of these special cases, for descriptors or standard T-S models, with or without input saturation, will provide the less conservative results.*

To conclude this subsection, let us point out that the design conditions given in Theorem 4.1 do not guarantee the global asymptotic stability for the closed-loop system driven by the designed sampled-data controller (4.7). Indeed, from the above-presented design conditions, three main points lead to a local solution: the region of linearity ($\mathcal{D}_u$) of the control inputs inside their bounds due to the actuators' saturation, the domain of validity of the fuzzy T-S model ($\mathcal{D}_x$), and the constraints due to the bounds ϕ of the time-derivative of the membership functions ($\mathcal{D}_\phi$) introduced by the NQLKF (4.13) and Theorem 3.2. Therefore, the characterization of the region of attraction ($\mathcal{D}_a$) must be provided to guarantee a safe operation of the controlled system. Nevertheless, finding the ultimate edge of the full region of attraction ($\mathcal{D}_a$) is a hard or even impossible task. Hence, in Theorem 4.1 we propose a procedure to provide an estimate $\mathcal{D}_a^*$ of such a region. It consists on finding the largest Lyapunov level set $\mathcal{L}(\bar{c}) = \{x \in \mathbb{R}^n \,|x^T P_{\bar{\alpha}} x \leq \bar{c}\}$ with $\bar{c} < 1$ such that:

$$\mathcal{D}_a^* = \{x(0) \in \mathbb{R}^n \mid \exists \bar{c} = \max c,\, \mathcal{L}(\bar{c}) \subseteq \mathcal{D}_u \cap \mathcal{D}_x \cap \mathcal{D}_\phi\}$$

Hence, the computation of $\mathcal{D}_a^*$ can be done through a manual adjusting procedure after solving the LMI conditions of Theorem 4.1. It is important to highlight that it requires the graphical representation of $\mathcal{D}_x$ and $\mathcal{D}_\phi$, which makes tricky and time-consuming the optimization of all involved parameters by trial and errors. In order to reduce the complexity brought by such a manual procedure, in the next subsection, we propose a systematic LMI-based methodology to get the estimate $\mathcal{D}_a^*$ of the region of attraction from an unitary invariant level set approach, but for standard T-S fuzzy models instead of descriptor ones.

4.3.2 Systematic estimation of the domain of attraction for standard T-S models-based sampled-data controller design

In this section, let us consider the class of standard T-S models (3.1) instead of T-S descriptors (4.1). Our goal is to provide complementary conditions to obtain a systematic estimation $\mathcal{D}_a^*$ of the sampled-data closed-loop region of attraction, i.e. to prevent from using the manual optimization procedure described above. To do so, let us recall that such a region is constrained by the regions $\mathcal{D}_u$, $\mathcal{D}_x$ and $\mathcal{D}_\phi$, respectively defined in (4.4), (4.2) and (4.11).

Before going to the main result of this subsection, let us recall that the gradient of $\alpha_k(x(t))$ for $x(t)$ is given by:

$$\nabla_k(x(t)) = \left[\frac{\partial \alpha_k(x(t))}{\partial x_1}, \ldots, \frac{\partial \alpha_k(x(t))}{\partial x_n}\right]^T \tag{4.55}$$

Assuming that, $\forall k \in \mathcal{I}_r$, $\alpha_k(x)$ are continuous with regard to $x \in \mathcal{D}_x$, then we have, $\forall \ell \in \mathcal{I}_n$, $\frac{\partial \alpha_\ell(x(t))}{\partial x_n} \in [\delta_\ell, \bar{\delta}_\ell]$. Therefore, from a sector nonlinearity decomposition, we can write:

$$\nabla_k(x(t)) = \sum_{s=1}^{2^n} \hbar_s(z(t)) \bar{\nabla}_s \tag{4.56}$$

with, $\forall s \in \mathcal{I}_{2^n}$, $\hbar_s(z(t)) \geq 0$, $\sum_{s=1}^{2^n} \hbar_s(z(t)) = 1$, and $\bar{\nabla}_s \in \mathbb{R}^n$ constant vectors of vertices.

The following theorem summarizes the proposed sampled-data controller design conditions for the stabilization of standard T-S models (3.1), including an optimization procedure for the systematic computation of $\mathcal{D}_a^*$.

Theorem 4.2. *Let $(i,j) \in \mathcal{I}_r^2$ and let assume that $\forall t$, $|\dot{\alpha}_i(t)| \leq \phi_i$. With $\bar{\nabla}_s$ ($s \in \mathcal{I}_{2^n}$) defined in (4.56), for given symmetric bounds $\bar{u} \in \mathbb{R}^m$ of the input vector and for non-uniform sampling intervals $\eta_k \leq \bar{\eta}$ ($\bar{\eta}$ to be maximized), the standard T-S model (3.1) (i.e. assuming $E_\alpha = I$) is locally asymptotically stabilized by the sampled-data PDC controller (4.7) with saturation (see (4.3)), if there exists a diagonal positive matrix $D_j \in \mathbb{R}^{m \times m}$, the matrices $0 < \bar{P}_i = \bar{P}_i^T \in \mathbb{R}^{n \times n}$, $\bar{S}_j = \bar{S}_j^T \in \mathbb{R}^{4n \times 4n}$, $\bar{Q}_{ij} = \bar{Q}_{ij}^T \in \mathbb{R}^{2n \times 2n}$, $\bar{R}_{11ij} = \bar{R}_{11ij}^T \in \mathbb{R}^{n \times n}$, $\bar{R}_{22ij} = \bar{R}_{22ij}^T \in \mathbb{R}^{n \times n}$, $\bar{R}_{12ij} \in \mathbb{R}^{n \times n}$, $X \in \mathbb{R}^{n \times n}$, $K_j \in \mathbb{R}^{m \times n}$, $F_j \in \mathbb{R}^{m \times n}$, $\bar{Y}_{ij} \in \mathbb{R}^{n \times 4n}$, $\bar{U}_{ij} = \bar{U}_{ij}^T \in \mathbb{R}^{3n \times 3n}$, $\bar{M}_{ij}^1 = \bar{M}_{ij}^{1T} \in \mathbb{R}^{n \times n}$, $\bar{M}_{ij}^2 = \bar{M}_{ij}^{2T} \in \mathbb{R}^{2n \times 2n}$, and the scalars ε_1, ε_2, and ε_3, such that the following optimization problem is satisfied:*

$$\begin{cases} \max\limits_{\substack{\bar{P}_\alpha > 0, \bar{Q}_\alpha > \bar{R}_{\alpha\bar{\alpha}}, S_{\bar{\alpha}}, \\ K_{\bar{\alpha}}, \bar{Y}_{\alpha\bar{\alpha}}, \bar{M}_{\alpha\bar{\alpha}}^1, \bar{M}_{\alpha\bar{\alpha}}^2, \mathcal{Z}_\alpha > 0}} Trace(X) \\ \text{subject to the PLMIs (4.18), (4.19), (4.20), (4.58) and (4.59),} \end{cases} \tag{4.57}$$

$$\begin{bmatrix} \bar{P}_\alpha & X^T \mathfrak{L}_{(j)}^T \\ \mathfrak{L}_{(j)} X & b_{(j)}^2 \end{bmatrix} \geq 0, \forall j \in \mathcal{I}_\kappa, \tag{4.58}$$

$$\begin{bmatrix} \bar{P}_\alpha & \star \\ \bar{\nabla}_s G_{\alpha\bar{\alpha}} & \phi^2 \end{bmatrix} \geq 0, \forall s \in \mathcal{I}_r. \tag{4.59}$$

In this case, the estimation of the domain of attraction $\mathcal{D}_a^*$ is systematically obtained as:

$$\mathcal{D}_a^* = \mathcal{L}(1) = \{x(0) \in \mathbb{R}^n | x^T P_\alpha x \leq 1\} \subseteq \mathcal{D}_u \cap \mathcal{D}_x \cap \mathcal{D}_\phi \tag{4.60}$$

which edge is readily given by the unit equipotential $x^T P_\alpha x = 1$.

Proof. Starting from the conditions of Theorem 4.1 for the special case of standard T-S models (4.5) (i.e. assuming $E_\alpha = I$), we want to provide an optimization procedure to enlarge $\mathcal{D}_a^* = \mathcal{L}(1)$ expressed in (4.60). Note that $\mathcal{L}(1) \subseteq \mathcal{D}_u$ is already granted by (4.20). Then, without loss of generality, assuming that the initial instant is also the first sampling instant (i.e. $t = t_0 = 0$), $\mathcal{L}(1)$ is defined by:

$$x^T(0)X^{-T}\bar{P}_\alpha X^{-1}x(0) \leq 1 \tag{4.61}$$

From the definition (4.2), the edge of $\mathcal{D}_x$ is given by:

$$\frac{x^T(0)\mathfrak{L}_{(j)}^T\mathfrak{L}_{(j)}x(0)}{b_{(j)}^2} \leq 1,\ \forall j \in \mathcal{I}_\kappa \tag{4.62}$$

Hence, from (4.61) and (4.62), $\mathcal{L}(1) \subseteq \mathcal{D}_x$ is granted by:

$$X^{-T}\bar{P}_\alpha X^{-1} - \frac{\mathfrak{L}_{(j)}^T\mathfrak{L}_{(j)}}{b_{(j)}^2} \geq 0,\ \forall j \in \mathcal{I}_\kappa \tag{4.63}$$

which gives, after congruence by X^T and X:

$$\bar{P}_\alpha - \frac{X^T\mathfrak{L}_{(j)}^T\mathfrak{L}_{(j)}X}{b_{(j)}^2} \geq 0,\ \forall j \in \mathcal{I}_\kappa \tag{4.64}$$

Then, applying the Shur complement, we get (4.58).
Now, let us focus on $\mathcal{D}_\phi$ constrained by:

$$|\dot{\alpha}_k(x(t)))| = |\nabla_k^T(x(t))\dot{x}(t)| \leq \phi_k,\ \forall k \in \mathcal{I}_r \tag{4.65}$$

which edge, for the initial instant $t=t_0=0$, is characterized by:

$$\frac{x^T(0)X^{-T}G_{\alpha\bar{\alpha}}^T\nabla_k^T(x(0))\nabla_k(x(0))G_{\alpha\bar{\alpha}}X^{-1}x(0)}{\phi_k^2} \leq 1 \tag{4.66}$$

with $G_{\alpha\bar{\alpha}} = (A_\alpha X + B_\alpha K_{\bar{\alpha}})$.
From (4.61) and (4.66), the following inequality guarantees $\mathcal{L}(1) \subseteq \mathcal{D}_\phi$:

$$X^{-T}\bar{P}_\alpha X^{-1} - \frac{X^{-T}G_{\alpha\bar{\alpha}}^T\nabla_k^T(x(0))\nabla_k(x(0))G_{\alpha\bar{\alpha}}X^{-1}}{\phi_k^2} \geq 0 \tag{4.67}$$

After congruence by X^T and X, it yields:

$$\bar{P}_\alpha - \frac{G_{\alpha\bar{\alpha}}^T\nabla_k^T(x(0))\nabla_k(x(0))G_{\alpha\bar{\alpha}}}{\phi_k^2} \geq 0 \tag{4.68}$$

Applying the Shur complement, we get:

$$\begin{bmatrix} \bar{P}_\alpha & \star \\ \nabla_k(x(0))G_{\alpha\bar{\alpha}} & \phi^2 \end{bmatrix} \geq 0 \tag{4.69}$$

Note that the condition (4.69) depends on the initial conditions. Nevertheless, knowing that $x(0) \in \mathcal{D}_x$, and considering (4.56), (4.69) is satisfied if:

$$\sum_{s=1}^{2^n} \hbar_s(z(t)) \begin{bmatrix} \bar{P}_\alpha & \star \\ \bar{\nabla}_s G_{\alpha\bar{\alpha}} & \phi^2 \end{bmatrix} \geq 0 \tag{4.70}$$

which is verified if the conditions (4.59) are satisfied.
Note that the completion of (4.20), (4.58) and (4.59) together ensures (4.60). Furthermore, to enlarge the area of $\mathcal{L}(1)$ and consequently the estimation of the region of attraction $\mathcal{D}_a^*$, minimizing the `trace` of P_α leads to maximize the `trace` of X under the constraint (4.61), since $\bar{P}_\alpha = X^{-T} P_\alpha X^{-1}$. This defines the optimization problem (4.57). □

Remark 4.5. *Unfortunately, because of the dependency of the closed-loop dynamics for computing the estimate of the region of attraction from $\mathcal{D}_\phi$ (see. (4.70)), Theorem 4.2 cannot be directly employed for descriptors systems. At this moment, the literature to cope with descriptors is not extensive. However, in (Lendek et al., 2018), the authors brought some interesting ideas in the discrete-time framework, which will be investigated for extension in our further works.*

Remark 4.6. *Note that to obtain a systematic characterization of $\mathcal{L}(1) \subseteq \mathcal{D}_\phi$, we employed a convexification procedure of the gradient (4.56). This may lead to conservatism since it increases the number of LMI vertices to be solved simultaneously. An interesting special case occurs when the ∇_s ($s \in \mathcal{I}_{2^n}$) are symmetric. Indeed, in this special case, $\forall s \in \mathcal{I}_{2^n}$, conditions (4.59) are equivalent by Schur complement, alleviating the pessimism introduced by such convexification. In all the other cases, such convexification procedure should be employed with discretion, i.e. when the T-S fuzzy model involves few rules or when the membership function involves few premises variables. Otherwise, the manual procedure given in Theorem 4.1 should be preferred.*

4.3.3 Gain scheduled event-triggering mechanism to enlarge the closed-loop domain of attraction

From the application of Theorem 4.1 or Theorem 4.2, let us point-out that $\mathcal{D}_a^*$, obtained for a given $\bar{\eta}$, is a contractive Lyapunov level set for the designed closed-loop dynamics. Taking benefit of such a feature, it is possible to propose a simple gain scheduled event-triggering control mechanism to maximize the guaranteed domain of attraction in sampled-data control design. To do so, let $\eta_k \in \{\bar{\eta}_1, \bar{\eta}_2, \ldots, \bar{\eta}_q\}$ be an ordered sequence ($0 < \bar{\eta}_1 < \bar{\eta}_2 < \cdots < \bar{\eta}_q$) of chosen values for triggering the sampling intervals $\eta_k \leq \bar{\eta}$. Then, for each of these values, solve (offline) the conditions of Theorem 4.1 or Theorem 4.2 and store their solutions, $\forall \nu \in \mathcal{I}_q$ and $\forall i \in \mathcal{I}_r$, as P_i^ν, K_i^ν and X_ν. Therefore, for each P_i^ν, we can get $\mathcal{L}^\nu(\bar{c}_\nu)$, with $\bar{c}_\nu \leq 1$ (manually optimized when employing Theorem 4.1) or $\bar{c}_\nu = 1$ (with Theorem 4.2), and we define:

$$\tilde{\mathcal{D}}_a^* = \bigcup_{\nu=1}^{q} \mathcal{L}^q(\bar{c}_q) \tag{4.71}$$

For initial conditions starting in $\tilde{\mathcal{D}}_a^*$ and then at each sampling instant t_k, let:

$$\bar{q}(t_k) = \sup_{\nu \in \mathcal{I}_q} \{x^T(t_k) P_\alpha^\nu x(t_k) \leq \bar{c} \leq 1\} \tag{4.72}$$

We define the following activation function, $\forall \nu \in \mathcal{I}_q$:

$$\mu_\nu(x(t_k)) = \begin{cases} 1, & \text{if } \nu = \bar{q}(t_k) \\ 0, & \text{otherwise} \end{cases} \tag{4.73}$$

Then, we propose the gain scheduled event-triggering sampled-data controller given by:

$$u(t) = \sum_{\nu=1}^{q} \mu_\nu(x(t_k)) K_{\bar{\alpha}}^{\nu} X_\nu^{-1} x(t_k) \tag{4.74}$$

where the actual sampling interval $\eta_k = t_{k+1} - t_k = \bar{\eta}_{\bar{q}(t_k)}$ is updated at each sampling instants t_k.

Therefore, with the considered continuous-time T-S descriptor (4.5), closing the loop with the control law (4.74) ensures the asymptotic stabilization for all initial conditions taken in $\tilde{\mathcal{D}}_a^*$ given in (4.71).

The benefit of using such a simple gain scheduled event-triggering mechanism will be illustrated through simulation examples in the next section.

4.4 Illustrative Examples

In this section, to evaluate the effectiveness of the LMI-based sampled-data controller design conditions proposed in Theorems 4.1 and 4.2, we will consider benchmark models of the inverted pendulum on a cart described in Chapter 3 (see section 3.5.2), which nonlinear dynamics are given by (3.52). First, for comparison purpose and to highlight the improvements raised by the conditions proposed in this chapter, we will consider the approximated two rules T-S fuzzy model investigated in Section 3.5.2. Then, because it has been shown that this approximated models is not suitable to guarantee the stabilization of the full nonlinear model of the inverted pendulum (3.52) (especially when large sampling intervals are considered), a matching T-S descriptor model is then studied. For both these cases, the estimations of the domain of attraction will be provided with discussion for their enlargement.

4.4.1 Benchmark of the approximated fuzzy model of the inverted pendulum

To illustrate the effectiveness of the proposed sampled-data control approach with saturated actuators, let us first consider as benchmark the same approximated two rules T-S fuzzy model of an inverted pendulum on a cart, drawn from (Wang et al., 1996) and presented in Section 3.5.2. For the sake of our study let us assume the actuator saturation as $u(t) \leq \bar{u}$. This model, valid in $\mathcal{D}_x$ defined by $|x_1(t)| < \pi/2$ and $|x_2(t)| \leq \pi$, is given by:

$$\dot{x}(t) = \sum_{i=1}^{2} h_i(x(t)) \left(A_i x(t) + B_i \mathtt{sat}(u(t))\right), \tag{4.75}$$

with the matrices A_1, A_2, B_1 and B_2 given in (3.53), and the membership functions α_1 and α_2 given in (3.54).

Recall that, $|\dot{h}_1(x_1(t))| = |\dot{h}_2(x_1(t))| = \frac{2}{\pi}|\dot{x}_1(t)|$ and, since $|\dot{x}_1(t)| = |x_2(t)| \leq \pi$ defining $\mathcal{D}_\phi$ in (4.11), we always have $|\dot{h}_i(x_1(t))| \leq 2 = \phi_i$. Therefore, solving the conditions of Theorem 4.1, using YALMIP (Löfberg, 2004) and MOSEK (ApS, 2019), with $\varepsilon_1 = 5.6$, $\varepsilon_2 = 1.2$, $\varepsilon_3 = 0.33$ and $\bar{u} = 150N$ provides the following sampled-data PDC controller gains and Lyapunov matrices

with the obtained maximal sampling interval $\bar{\eta} = 50ms$:

$$K_1 = \begin{bmatrix} 8.1111 & -11.9923 \end{bmatrix}, P_1 = \begin{bmatrix} 260.2908 & 73.6741 \\ 73.6741 & 24.1746 \end{bmatrix},$$
$$K_2 = \begin{bmatrix} 33.0175 & 67.2186 \end{bmatrix}, P_2 = \begin{bmatrix} 252.0369 & 74.0583 \\ 74.0583 & 25.4756 \end{bmatrix},$$
$$X = \begin{bmatrix} 0.1560 & -0.4455 \\ -0.4350 & 1.4826 \end{bmatrix}.$$

As shown in Table 4.1, the maximal sampling interval obtained from Theorem 4.1 or Theorem 4.2 outperforms all the previous considered related results, excepted Theorem 3.1 which gives the same value. Moreover, from the definition of the membership functions (3.54), we have $\nabla_1 = -\nabla_2 = \begin{bmatrix} \frac{2}{\pi} & 0 \end{bmatrix}^T$ symmetric, making relevant the use of the optimization procedure proposed in Theorem 4.2 (see Remark 4.6). This explains why the same $\bar{\eta} = 50ms$ is obtained from both Theorem 4.1 and Theorem 4.2.

Table 4.1: Comparison of maximal $\bar{\eta}$ obtained with previous studies.

Method	$\bar{\eta}$ (ms)
(Yoneyama, 2010)	9
(Zhu and Wang, 2011)	13
(Zhang and Han, 2011)	16
(Zhu et al., 2012)	19
(Gunasekaran and Joo, 2019)	22
(Zhu et al., 2013)	24
(Cheng et al., 2017)	42
Theorem 3.1	50
Theorem 4.1	**50**
Theorem 4.2	**50**

To verify the effectiveness of the above designed sampled-data controller law (4.7), a simulation is performed in MATLAB® with the two rules T-S model with actuators saturation. For this simulation, with the initial condition $x_0 = \begin{bmatrix} 0.5 & 0 \end{bmatrix}^T$, the state trajectories and control signals are depicted in Figure 4.1. We can observe that the sampled-data controller successfully stabilizes the T-S model although, during the first few sampling intervals, it saturates.

However, recall that the conditions of Theorem 4.1 and Theorem 4.2 only guarantee the local stabilization. Therefore, the domain of attraction of the closed-loop sampled-data system must be characterized. In this regard, it is important to highlight that, with exception to our preliminary works (Lopes et al., 2021b) and (Lopes et al., 2021a), no other related works on sampled-data controller design provide such analysis.

Figure 4.2(b) provides an estimate of the region of attraction $\mathcal{D}_a^*$ for the previously designed sampled-data controller. This one is found really small regarding to $\mathcal{D}_x$ and $\mathcal{D}_\phi$, because of the small value of $\bar{u} = 150N$ (regarding to the model parameters) considered for the input constraints. Hence, to enlarge the domain of attraction, one may enlarge $\bar{u}$. Figure 4.2(a) shows the results obtained with $\bar{u} = 1500N$. In this case, the following Lyapunov and gain matrices

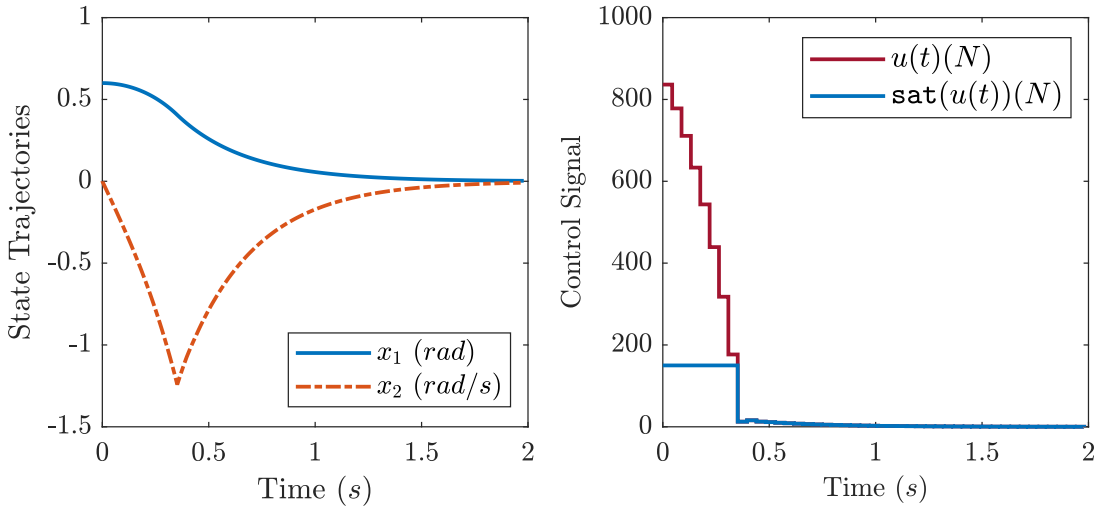

Figure 4.1: Simulation of the state trajectories of the inverted pendulum on a cart with the designed sampled controller, together with the respective saturated input control signal, updated at fixed sampling instants $\eta_k = \bar{\eta} = 50ms$.

are obtained from solving the conditions of Theorem 4.2:

$$K_1 = \begin{bmatrix} 0.2522 & -0.1898 \end{bmatrix}, P_1 = \begin{bmatrix} 32.2726 & -82.6056 \\ -82.6056 & 305.3161 \end{bmatrix},$$
$$K_2 = \begin{bmatrix} 1.1704 & 8.6647 \end{bmatrix}, P_2 = \begin{bmatrix} 28.5697 & -75.6862 \\ -75.6862 & 301.3742 \end{bmatrix},$$
$$X = \begin{bmatrix} 0.0049 & -0.0136 \\ -0.0135 & 0.0543 \end{bmatrix}.$$

This shows that the choice of $\bar{u}$ influences a lot the enlargement of the domain of attraction. Reciprocally, such analysis may be useful for designers to scale the actuators. To illustrate this feature, Figure 4.3 shows the domains of attraction obtained for several values of $\bar{u}$ (i.e., $\bar{u} \in [150, 200, 300, 400, 500, 750, 1000, 1250, 1500, 2000]$), with the largest admissible value of $\bar{\eta} = 50ms$. This figure shows that, for $\bar{u} \geq 1500N$, there is no major improvement as, for $\bar{\eta} = 50ms$, the successive estimations $\mathcal{D}_a^* \subseteq \mathcal{D}_u$ keep closely the same shape and reach the edge of $\mathcal{D}_x \cap \mathcal{D}_\phi$.

It is to be noticed that the above described tests have been obtained for the maximal value $\bar{\eta} = 50ms$, which constitutes the limit of conservatism achieved, i.e. the most constraining case for solving the LMI-based conditions of Theorem 4.1 and Theorem 4.2. This critical case explains why we get P_1 close to P_2, making the shape of $\mathcal{D}_a^*$ constrained to be almost an ellipsoid. In the opposite, it is also possible to set a smaller value of $\bar{\eta} < 50ms$ to relax the LMI-based conditions of Theorem 4.1 and Theorem 4.2. To illustrate this possibility, Figure 4.4 shows the estimation $\mathcal{D}_a^*$ of the domain of attraction obtained for $\bar{\eta} = 1ms$ and for several values of $\bar{u}$ (i.e., $\bar{u} \in [150, 200, 500, 1000, 1500, 2000, 5000, 6000, 7500, 10000]$). It is observed that, for small values of $\bar{\eta}$ and large values of $\bar{u}$, the shape of $\mathcal{D}_a^*$ is now non-quadratic.

At this step, the above tests clearly show the influence of the input saturation on the estimation $\mathcal{D}_a^*$ of the domain of attraction. Let us now focus on the influence of assuming maximal allowable sampling intervals. Figure 4.5 shows the estimates $\mathcal{D}_a^*$ obtained with $\bar{u} = 10000N$ for several values of $\bar{\eta}$ (i.e., $\bar{\eta} \in [1, 5, 10, 15, 20, 25, 35, 45, 40, 50]$). This also clearly shows that the choice of $\bar{\eta}$ influences the shape of $\mathcal{D}_a^*$.

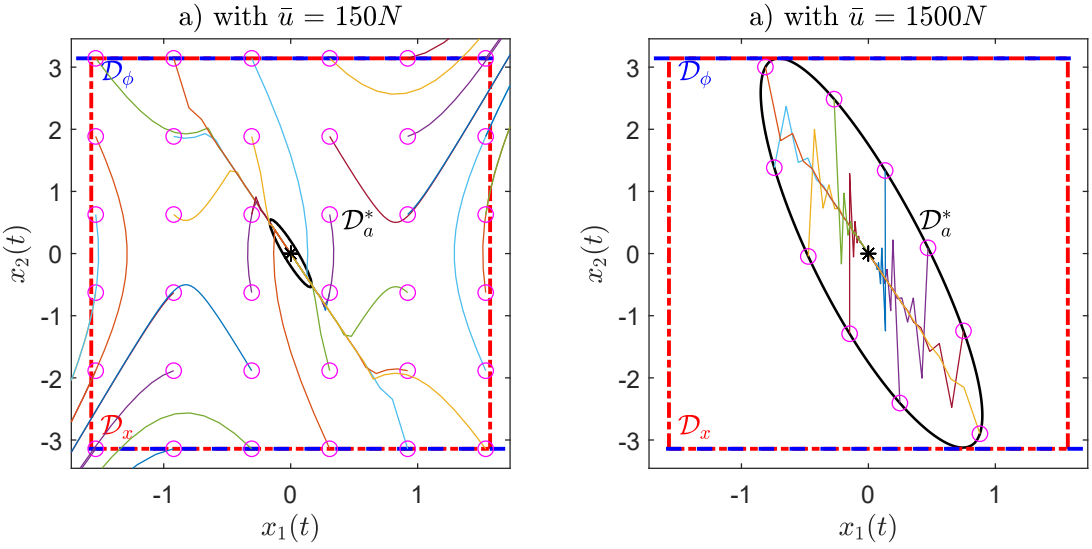

Figure 4.2: Estimates of the region of attraction for two sampled-data controllers designed from Theorem 4.2 to stabilize the T-S model (4.75), assuming different actuators' saturation limits ($\bar{u}$), with its resulting closed-loop trajectories for several initial conditions.

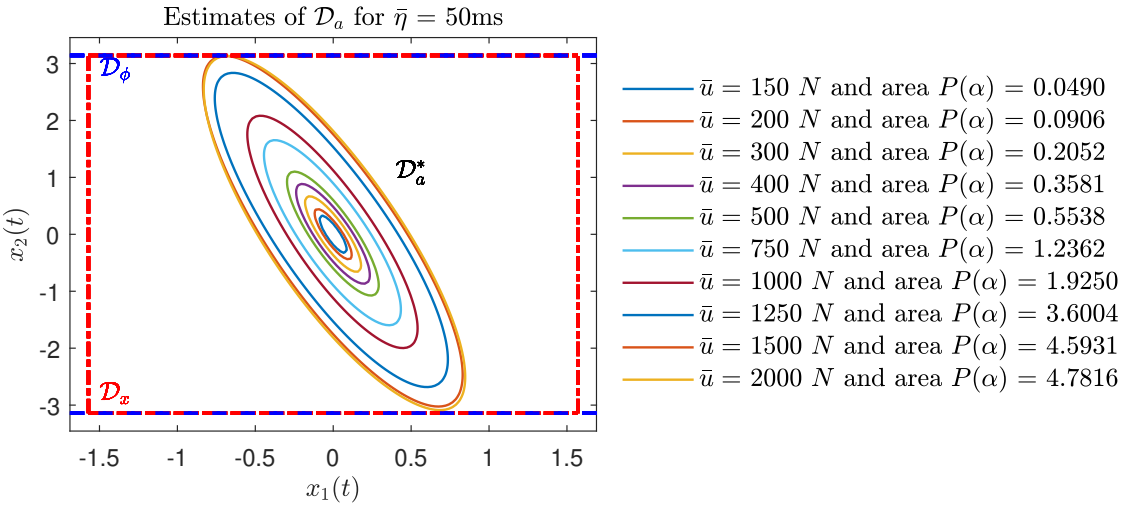

Figure 4.3: Estimates of the Region of Attraction for the maximal allowed sampling interval found from Theorem 4.1, ($\bar{\eta} = 50ms$) assuming various actuators' saturation limits, (i. e. considering different values for $\bar{u}$).

Now, from this last test, let us recall that each $\mathcal{D}_a^*$, obtained for each $\bar{\eta}$, is contractive for its respective closed-loop dynamics since it represents the Lyapunov level set $\mathcal{L}(1)$. Taking benefit of such a feature, we consider the gain scheduled event-triggering mechanism proposed in Subsection 4.3.3 to further extend the guaranteed domain of attraction in sampled-data control design. To do so, solving Theorem 4.2 for each $\eta_k \in [1, 5, 10, 15, 20, 25, 35, 45, 50]$, then storing the results as P_i^ν, K_i^ν and X_ν ($\nu \in \mathcal{I}_{12}$ and $\forall i \in \mathcal{I}_2$). We can apply the gain scheduled event-triggering controller (4.74) to the approximated T-S fuzzy model (4.75) with guaranteed closed-loop stabilization for initial conditions taken in $\tilde{\mathcal{D}}_a^*$ given in (4.71). Figure 4.6 depicts the trajectories of the closed-loop system, the input signals and the evolution of the scheduled sampling intervals with the proposed gain scheduled event-triggering strategy, with two initial

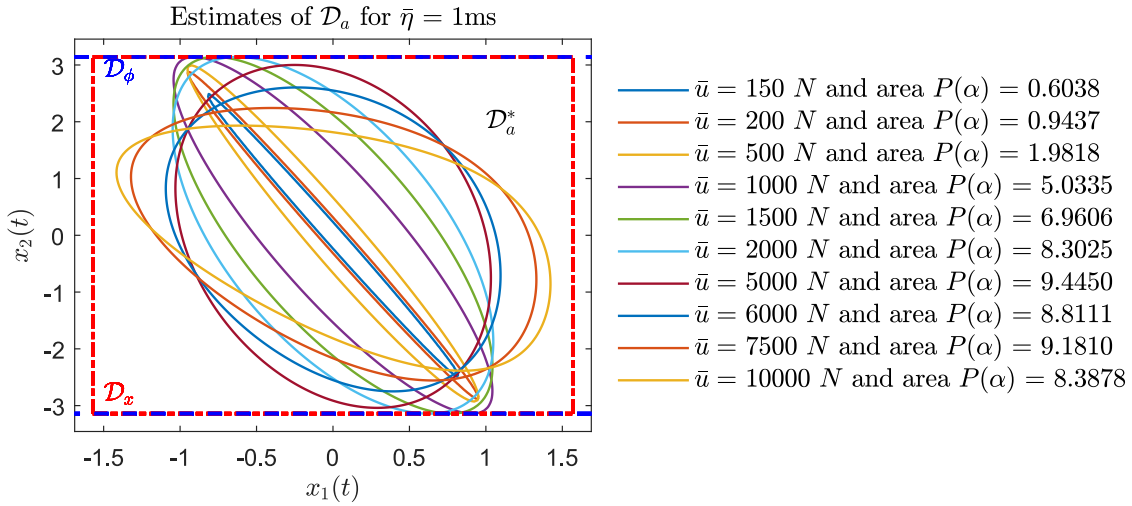

Figure 4.4: Estimates of the Region of Attraction for a sampling interval $\bar{\eta} = 1ms$ found from Theorem 4.2, assuming various actuators' saturation limits, (i. e. considering different values for $\bar{u}$).

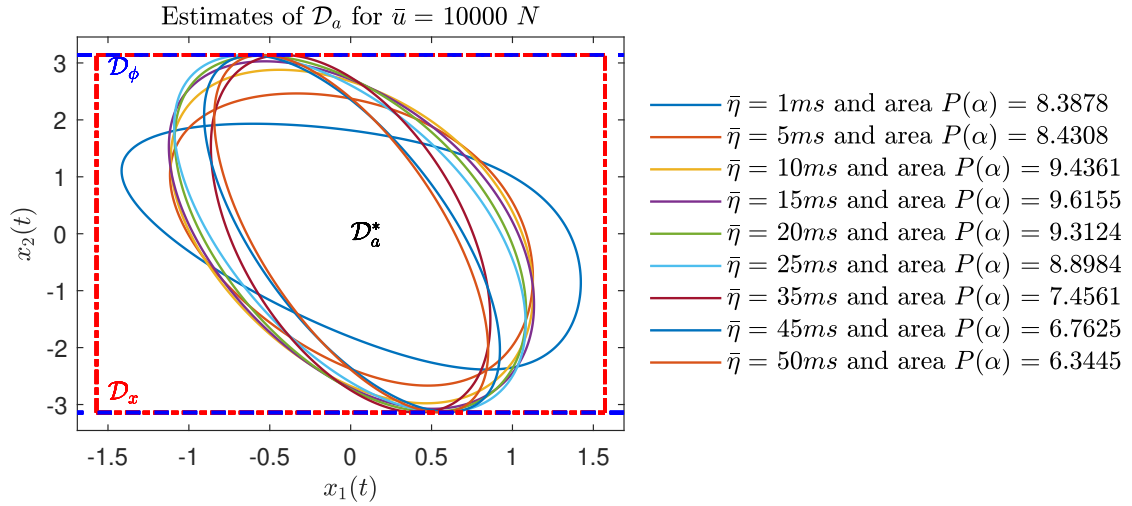

Figure 4.5: Estimates of the Region of Attraction for several maximum allowable sampling interval $\bar{\eta}$ found from Theorem 4.2, assuming $\bar{u} = 10000N$.

conditions taken at the border of $\tilde{\mathcal{D}}_a^*$. We clearly see that, the closed-loop system is stable and, from the first few samples, the selected η_k is small, then increases until the maximal allowed value $\bar{\eta} = 50ms$ (obtained from Theorem 4.2). These shows that this control strategy is high demanding in terms of computation only for the first few samples (during transients), while it quickly becomes undemanding with large sampling intervals. However, we can also notice an important chattering when the maximal allowed sampling period $\eta_k = 50ms$ is selected. This mainly due to the fact that this value is critical in terms of conservatism of the proposed LMI-based conditions, making the designed closed-loop closer to the limit of stability. To mitigate this effect, an easy way is to avoid going to such critical values. Figure 4.7 shows the trajectories of the closed-loop system, the input signals and the evolution of the scheduled sampling intervals, with transient improvements from the proposed gain scheduled event-triggering strategy with

$\eta_k \in [1, 5, 10, 15, 20, 25, 35]$.

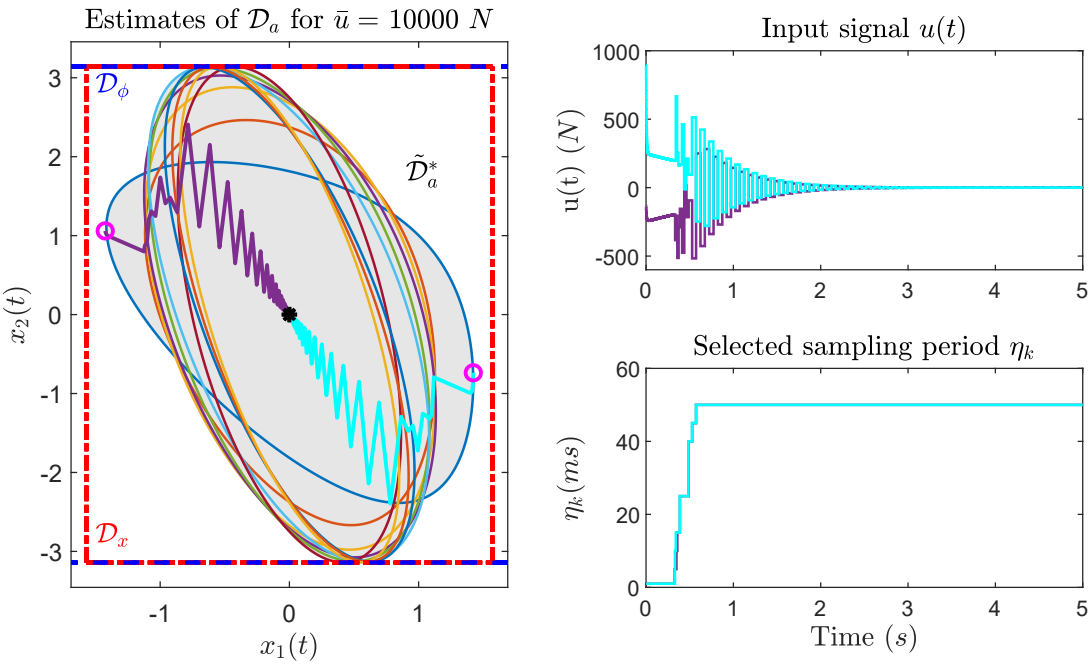

Figure 4.6: Estimates of the Region of Attraction $\tilde{D}_a^*$ (highlighted in gray), control signal and selected sampling period η_k for the gain scheduled event-triggering sampled-data controller proposed in (4.74) and designed from Theorem 4.2 for the 2 rules T-S model with a maximal allowed sampling interval $\bar{\eta} = 50ms$.

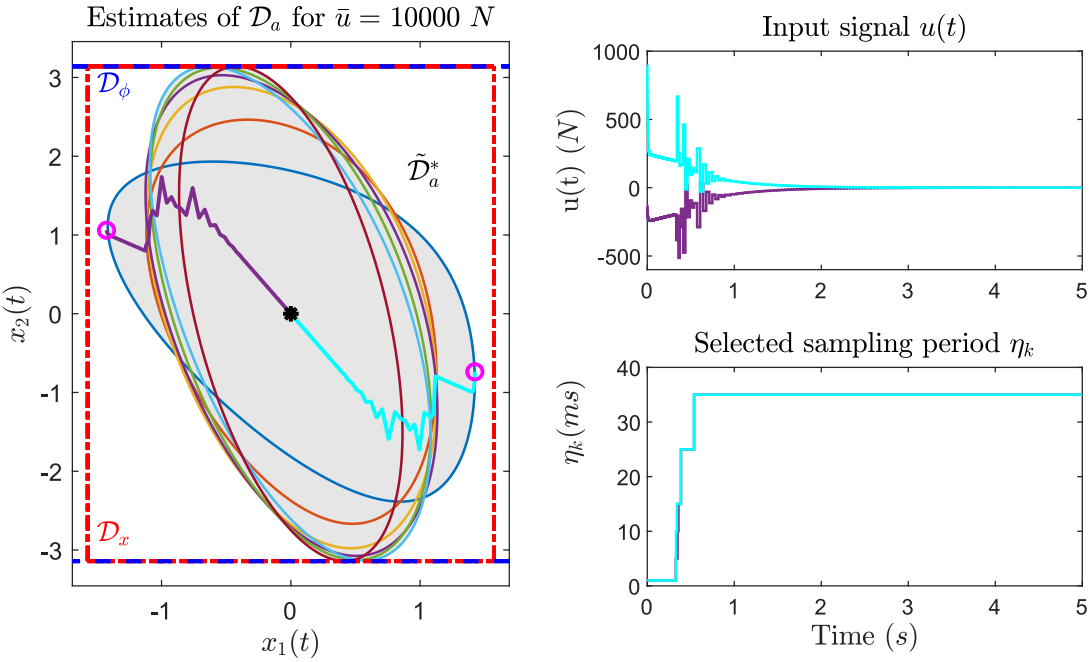

Figure 4.7: Estimates of the Region of Attraction $\tilde{D}_a^*$ (highlighted in gray), control signal and selected sampling period η_k for the gain scheduled event-triggering sampled-data controller proposed in (4.74) and designed from Theorem 4.2 for the 2 rules T-S model with a maximal allowed sampling interval $\bar{\eta} = 35ms$.

All of these tests and simulation illustrate the potential of the proposed sampled-data con-

troller design for T-S fuzzy systems with significant improvements regarding to the previous results presented in Chapter 3 and from the literature. However, as mentioned in Chapter 3 (see the end of Subsection 3.5.2), the sampled-data controller obtained in this subsection only apply for the approximated model (4.75) from which it is designed. As a matter of fact, there is no guarantee that it stabilizes the original nonlinear system. (3.52). Even if it is useful for comparison purpose, this highlights the limitation of using such approximated standard T-S fuzzy models, which should be circumvent by considering an exact T-S model in the descriptor form, as it will be shown in the next subsection.

Remark 4.7. *From the conditions proposed in (Lamrabet et al., 2019), which is the unique previous study found aiming at proposing sampled-data controller design for T-S systems under saturating actuators, we surprisingly obtained a maximal* $\bar{\eta} = 164ms$. *Unfortunately, when performing the simulation with the gains obtained from (Lamrabet et al., 2019), we observed an unstable closed-loop behavior with a strongly saturating input. Moreover, in this paper, no characterization of the closed-loop domain of attraction is provided and, because the authors did not select a looped LKF, this task is pretty much harder or even impossible. Hence, failing to reproduce the claimed results in (Lamrabet et al., 2019), we assume irrelevant a fair comparison with this work.*

4.4.2 Matching T-S descriptor model-based sampled-data controller design

In this subsection, we will consider the full nonlinear model of the inverted pendulum on a cart drawn from (Cannon, 1967; Wang et al., 1996), given by the dynamic equation (3.52). Let us consider the state vector $x(t) = \begin{bmatrix} x_1(t) & x_2(t) \end{bmatrix}^T$, where $x_1(t)$ is the angular position of the inverted pendulum with regard to the erect position, $x_2(t) = \dot{x}_1(t)$ is the angular velocity (rad/s). The nonlinear dynamics (3.52) can be rewritten as a nonlinear descriptor (4.1) with:

$$\begin{aligned} E(x(t)) &= \begin{bmatrix} 1 & 0 \\ 0 & \frac{4l}{3} - aml\cos^2 x_1(t) \end{bmatrix}, \\ A(x(t)) &= \begin{bmatrix} 0 & 1 \\ g\frac{\sin x_1(t)}{x_1(t)} & -\frac{aml}{2}x_2(t)\sin(2x_1(t)) \end{bmatrix}, B(x(t)) = \begin{bmatrix} 0 \\ -a\cos x_1(t) \end{bmatrix}. \end{aligned} \tag{4.76}$$

where $g = 9.8\, m/s^2$ is the acceleration of the gravity, $m = 2\, kg$ is the mass of the pendulum, $M = 8\, kg$ is the mass of the cart, $l = 0.5\, m$ is the half length of the pendulum, $u(t)$ is the input actuator force (N) applied to the cart and $a = 1/(m + M)$.

Recall that the inverted pendulum is not controllable for $x_1 = \frac{\pi}{2}$. Hence, to fairly cope with the previous example, in order to derive a T-S descriptor model (4.5) matching (4.76) we chose to restrict the validity domain $\mathcal{D}_x$ to $|x_1| \leq \theta_0 = 22\pi/45\, rad$ and $|x_2| \leq \pi\, rad/s$. Moreover, note that the nonlinear matrices (4.76) involve four nonlinear entries, bounded on $\mathcal{D}_x$, given by:

$$\begin{aligned} &f_1(x_1(t)) = \cos^2 x_1(t) \in [\underline{f}_1,\ \bar{f}_1],\ \underline{f}_1 = \cos^2\theta_0,\ \bar{f}_1 = 1, \\ &f_2(x(t)) = x_2(t)\sin(2x_1(t)) \in [\underline{f}_2,\ \bar{f}_2],\ \underline{f}_2 = -\pi,\ \bar{f}_2 = \pi, \\ &f_3(x_1(t)) = \frac{\sin x_1(t)}{x_1(t)} \in [\underline{f}_3, \bar{f}_3], \underline{f}_3 = \frac{\sin\theta_0}{\theta_0},\ \bar{f}_3 = 1, \\ &f_4(x_1(t)) = \cos x_1(t) \in [\underline{f}_4,\ \bar{f}_4],\ \underline{f}_4 = \cos\theta_0,\ \bar{f}_4 = 1. \end{aligned} \tag{4.77}$$

Hence, $\forall x(t) \in \mathcal{D}_x$, applying the sector nonlinearity approach on each $f_\ell(x(t))$, we have:

$$f_\ell(x(t)) = w_\ell^1(x(t))\bar{f}_\ell + w_\ell^2(x(t))\underline{f}_\ell, \forall \ell \in \mathcal{I}_4 \tag{4.78}$$

with $w_\ell^1(x(t)) = \frac{f_\ell(x(t))-\underline{f}_\ell}{\bar{f}_\ell-\underline{f}_\ell} \geq 0$, $w_\ell^2(x(t)) = \frac{\bar{f}_\ell-f_\ell(x(t))}{\bar{f}_\ell-\underline{f}_\ell} \geq 0$, and where $w_\ell^1(x(t)) + w_\ell^2(x(t)) = 1$.

Let us notice that, $\forall x(t) \in \mathcal{D}_x$, $w_3^1(x(t))$ closely matches $w_4^1(x(t))$ (and so $w_3^2(x(t))$ and $w_4^2(x(t))$), as shown in Figure 4.8. This fact allows to fairly reduce the number of vertices from $r = 2^4$ to $r = 2^3$, to obtain a tighter closely matching T-S descriptor (4.5) to represent the nonlinear dynamics (3.52) (than the approximated two rules T-S fuzzy models considered in Subsections 3.5.2 and 4.4.1), with the membership functions:

$$\begin{aligned}
h_1(x(t)) &= w_3^1(x(t))w_2^1(x(t))w_1^1(x(t)),\ h_2(x(t)) = w_3^1(x(t))w_2^1(x(t))w_1^2(x(t)),\\
h_3(x(t)) &= w_3^1(x(t))w_2^2(x(t))w_1^1(x(t)),\ h_4(x(t)) = w_3^1(x(t))w_2^2(x(t))w_1^2(x(t)),\\
h_5(x(t)) &= w_3^2(x(t))w_2^1(x(t))w_1^1(x(t)),\ h_6(x(t)) = w_3^2(x(t))w_2^1(x(t))w_1^2(x(t)),\\
h_7(x(t)) &= w_3^2(x(t))w_2^2(x(t))w_1^1(x(t)),\ h_8(x(t)) = w_3^2(x(t))w_2^2(x(t))w_1^2(x(t)).
\end{aligned}$$

and the vertices given by:

$$\begin{aligned}
E_1 = E_3 = E_5 = E_7 &= \begin{bmatrix} 1 & 0 \\ 0 & \frac{4l}{3} - aml\bar{f}_1 \end{bmatrix},\\
E_2 = E_4 = E_6 = E_8 &= \begin{bmatrix} 1 & 0 \\ 0 & \frac{4l}{3} - aml\underline{f}_1 \end{bmatrix},\\
A_1 = A_2 = \begin{bmatrix} 0 & 1 \\ g\bar{f}_3 & -\frac{aml}{2}\bar{f}_2 \end{bmatrix}&, A_3 = A_4 = \begin{bmatrix} 0 & 1 \\ g\bar{f}_3 & -\frac{aml}{2}\underline{f}_2 \end{bmatrix},\\
A_5 = A_6 = \begin{bmatrix} 0 & 1 \\ g\underline{f}_3 & -\frac{aml}{2}\bar{f}_2 \end{bmatrix}&, A_7 = A_8 = \begin{bmatrix} 0 & 1 \\ g\underline{f}_3 & -\frac{aml}{2}\underline{f}_2 \end{bmatrix},\\
B_1 = B_2 = B_3 = B_4 = \begin{bmatrix} 0 \\ -a\bar{f}_4 \end{bmatrix}&, B_5 = B_6 = B_7 = B_8 = \begin{bmatrix} 0 \\ -a\underline{f}_4 \end{bmatrix}.
\end{aligned}$$

Based on the obtained descriptor model, our goal is now to design a sampled-data controller (4.7) for the stabilization of the nonlinear model of the inverted pendulum (3.52). To do so, we will apply Theorem 4.1 together with Theorem 3.2, but remind that they need, as parameter, an estimation of the bounds of the time-derivatives of the membership functions. As quoted in Remark 4.2, these bounds can be approximated as:

$$\phi_k = \sup_{\{x\in\mathcal{D}_x, u\in\mathcal{D}_u\}} \left(\left| x_2 \frac{\partial \alpha_k(x)}{\partial x_1} + \frac{\partial \alpha_k(x)}{\partial x_2} \frac{g\sin x_1 - aml x_2^2 \sin(2x_1)/2 - a\cos x_1 u}{4l/3 - aml\cos^2 x_1} \right| \right), \forall k \in \mathcal{I}_r \tag{4.79}$$

It is worth to highlight that, to estimate the bounds ϕ_k, only an assumption on the input saturation $\bar{u}$ of the inverted pendulum is needed. Hence, to illustrate this fact and to evaluate its effect on the conservatism of the conditions, two cases are considered in the sequel with $\bar{u} = 150N$ and $\bar{u} = 600N$.

Case 1: Assuming an input saturation $\bar{u} = 150N$, we obtain $\phi_1 = \phi_3 = 5.1271$, $\phi_2 = \phi_4 = 3.1851$, $\phi_5 = \phi_7 = 1.3859$, and $\phi_6 = \phi_8 = 4.5953$, which provide $\mathcal{D}_\phi$ (see (4.11)). Then,

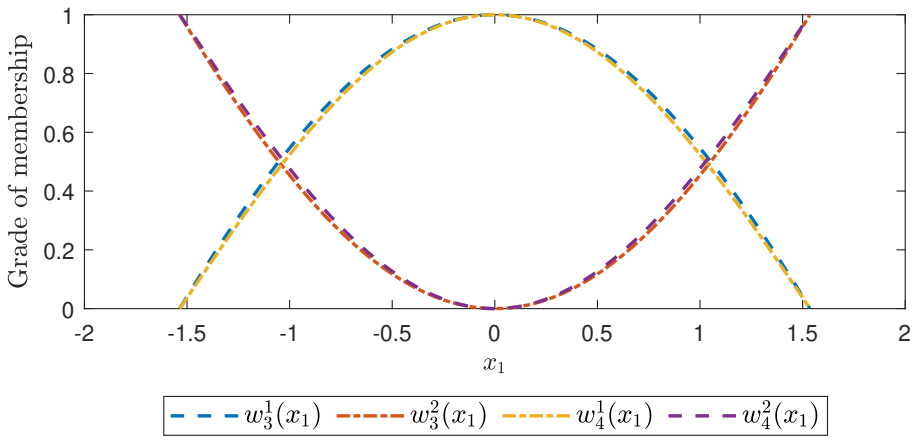

Figure 4.8: Plots of $w_3^1(x)$, $w_4^1(x)$, $w_4^2(x)$ and $w_4^2(x)$ for $x_1 \in \mathcal{D}_x$ illustrating that $w_3^1(x)$ closely matches $w_4^1(x)$ (and so $w_3^2(x)$ and $w_4^2(x)$).

solving Theorem 4.1 with the T-S descriptor model of the inverted pendulum, we get a maximal admissible sampling interval $\bar{\eta} = 13\,ms$ with $\varepsilon_1 = 25$, $\varepsilon_2 = 0.1$, $\varepsilon_3 = 0.50$ (see Remark 4.3) and the following Lyapunov and sampled-data controller gain matrices:

$$P_1 = \begin{bmatrix} 941.0376 & 167.4962 \\ 167.4962 & 61.0837 \end{bmatrix}, P_2 = \begin{bmatrix} 942.8992 & 167.4593 \\ 167.4593 & 61.3492 \end{bmatrix}, P_3 = \begin{bmatrix} 940.9121 & 167.5113 \\ 167.5113 & 61.1039 \end{bmatrix},$$
$$P_4 = \begin{bmatrix} 942.9184 & 167.4391 \\ 167.4391 & 61.2905 \end{bmatrix}, P_5 = \begin{bmatrix} 953.8476 & 166.9646 \\ 166.9646 & 61.3769 \end{bmatrix}, P_6 = \begin{bmatrix} 940.9296 & 169.4752 \\ 169.4752 & 63.2167 \end{bmatrix},$$
$$P_7 = \begin{bmatrix} 953.3323 & 167.0351 \\ 167.0351 & 61.1785 \end{bmatrix}, P_8 = \begin{bmatrix} 940.2385 & 168.6209 \\ 168.6209 & 62.4421 \end{bmatrix}, X = \begin{bmatrix} 0.0517 & -0.0812 \\ -0.1398 & 0.4859 \end{bmatrix},$$
$$K_1 = \begin{bmatrix} 4.4574 & 129.4442 \end{bmatrix}, K_2 = \begin{bmatrix} 5.5659 & 137.8826 \end{bmatrix}, K_3 = \begin{bmatrix} 4.6157 & 138.0546 \end{bmatrix},$$
$$K_4 = \begin{bmatrix} 5.1418 & 138.1374 \end{bmatrix}, K_5 = \begin{bmatrix} 15.7862 & 229.1195 \end{bmatrix}, K_6 = \begin{bmatrix} 13.0720 & 236.1088 \end{bmatrix},$$
$$K_7 = \begin{bmatrix} 16.5081 & 229.0332 \end{bmatrix}, K_8 = \begin{bmatrix} 15.4187 & 231.6737 \end{bmatrix}.$$

Also, for comparison purpose, with the same parameters but with $\bar{\eta} = 1\,ms$, we obtained the following Lyapunov and sampled-data controller gain matrices:

$$P_1 = \begin{bmatrix} 301.8295 & 91.8532 \\ 91.8532 & 30.0210 \end{bmatrix}, P_2 = \begin{bmatrix} 303.5764 & 92.2972 \\ 92.2972 & 30.1343 \end{bmatrix}, P_3 = \begin{bmatrix} 301.6727 & 91.8517 \\ 91.8517 & 30.0380 \end{bmatrix},$$
$$P_4 = \begin{bmatrix} 303.6271 & 92.3014 \\ 92.3014 & 30.1318 \end{bmatrix}, P_5 = \begin{bmatrix} 319.1702 & 94.5980 \\ 94.5980 & 30.4300 \end{bmatrix}, P_6 = \begin{bmatrix} 302.7476 & 92.7151 \\ 92.7151 & 30.4858 \end{bmatrix},$$
$$P_7 = \begin{bmatrix} 328.8480 & 97.2506 \\ 97.2506 & 31.0358 \end{bmatrix}, P_8 = \begin{bmatrix} 303.9880 & 93.4076 \\ 93.4076 & 30.8629 \end{bmatrix}, X = \begin{bmatrix} 1.2460 & -2.3637 \\ -3.7791 & 7.7287 \end{bmatrix},$$
$$K_1 = \begin{bmatrix} 75.7623 & 134.7206 \end{bmatrix}, K_2 = \begin{bmatrix} 73.8606 & 138.9397 \end{bmatrix}, K_3 = \begin{bmatrix} 61.4847 & 186.6479 \end{bmatrix},$$
$$K_4 = \begin{bmatrix} 72.7603 & 139.7980 \end{bmatrix}, K_5 = \begin{bmatrix} 137.9217 & 209.7378 \end{bmatrix}, K_6 = \begin{bmatrix} 120.1067 & 230.4720 \end{bmatrix},$$
$$K_7 = \begin{bmatrix} 113.4025 & 260.9241 \end{bmatrix}, K_8 = \begin{bmatrix} 79.3999 & 309.5599 \end{bmatrix}.$$

From these results, Figure 4.9 shows the closed-loop domains of attraction obtained re-

spectively for $\bar{\eta} = 1ms$ and $\bar{\eta} = 13ms$. We can notice that these are pretty small, but of course, recall that $\bar{u} = 150N$, which is a really small value of the input saturation regarding to the overall mass of the considered benchmark ($9kg$, including the inverted pendulum and the cart). Hence, we may expect better results enlarging $\bar{u}$ as proposed in the next case.

(a) for $\bar{u} = 150N$ and $\bar{\eta} = 1ms$ (b) for $\bar{u} = 150N$ and $\bar{\eta} = 13ms$

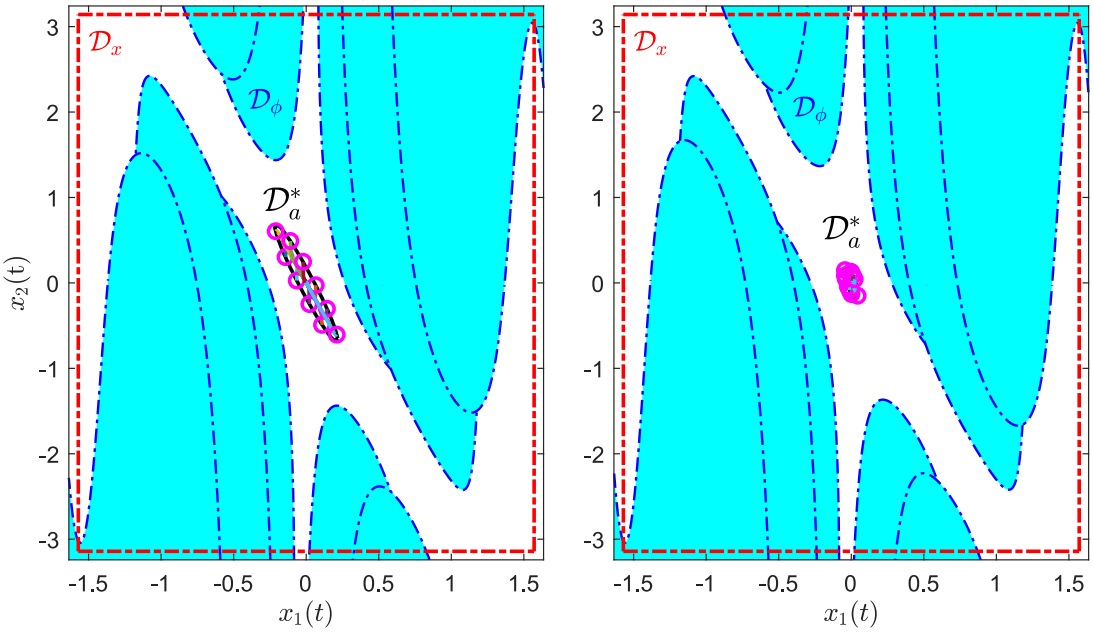

Figure 4.9: (a) Estimated domain of Attraction $\mathcal{D}_A^*$ for the full closed-loop nonlinear model (3.52) under the designed sampled-data controller designed from the T-S descriptor (4.1) (with (4.76)).

Case 2: Assuming an input saturation $\bar{u} = 600N$, we obtain $\phi_1 = \phi_3 = 11.2155$, $\phi_2 = \phi_4 = 5.8319$, $\phi_5 = \phi_7 = 2.5238$, and $\phi_6 = \phi_8 = 5.8610$, which provide $\mathcal{D}_\phi$ (see (4.11)). Then, solving Theorem 4.1 with the T-S descriptor model of the inverted pendulum, we get a maximal admissible sampling interval $\bar{\eta} = 8\,ms$ with the same $\varepsilon_1 = 25$, $\varepsilon_2 = 0.1$, $\varepsilon_3 = 0.50$ (not optimized here just to compare the results with the previous case) and the following Lyapunov and sampled-data controller gain matrices:

$$P_1 = \begin{bmatrix} 79.5568 & 13.2010 \\ 13.2010 & 4.8335 \end{bmatrix}, P_2 = \begin{bmatrix} 79.7112 & 13.1907 \\ 13.1907 & 4.8456 \end{bmatrix}, P_3 = \begin{bmatrix} 79.5535 & 13.2016 \\ 13.2016 & 4.8338 \end{bmatrix},$$
$$P_4 = \begin{bmatrix} 79.7095 & 13.1904 \\ 13.1904 & 4.8448 \end{bmatrix}, P_5 = \begin{bmatrix} 80.6059 & 13.1395 \\ 13.1395 & 4.9034 \end{bmatrix}, P_6 = \begin{bmatrix} 79.8209 & 13.3155 \\ 13.3155 & 4.9913 \end{bmatrix},$$
$$P_7 = \begin{bmatrix} 80.5144 & 13.1363 \\ 13.1363 & 4.8789 \end{bmatrix}, P_8 = \begin{bmatrix} 80.0276 & 13.3622 \\ 13.3622 & 5.0690 \end{bmatrix}, X = \begin{bmatrix} 0.0054 & -0.0078 \\ -0.0143 & 0.0544 \end{bmatrix},$$
$$K_1 = \begin{bmatrix} 0.5531 & 20.1809 \end{bmatrix}, K_2 = \begin{bmatrix} 0.5663 & 20.2454 \end{bmatrix}, K_3 = \begin{bmatrix} 0.5459 & 21.0656 \end{bmatrix},$$
$$K_4 = \begin{bmatrix} 0.5445 & 20.2541 \end{bmatrix}, K_5 = \begin{bmatrix} 2.0693 & 32.3770 \end{bmatrix}, K_6 = \begin{bmatrix} 1.8999 & 32.8605 \end{bmatrix},$$
$$K_7 = \begin{bmatrix} 2.1131 & 32.5504 \end{bmatrix}, K_8 = \begin{bmatrix} 2.2340 & 32.3729 \end{bmatrix}.$$

Again, with the same parameters but now with $\bar{\eta} = 1\,ms$, we obtained the following Lyapunov and sampled-data controller gain matrices:

$$P_1 = \begin{bmatrix} 30.9983 & 9.6668 \\ 9.6668 & 3.1159 \end{bmatrix}, P_2 = \begin{bmatrix} 30.9987 & 9.6669 \\ 9.6669 & 3.1160 \end{bmatrix}, P_3 = \begin{bmatrix} 30.9983 & 9.6668 \\ 9.6668 & 3.1159 \end{bmatrix},$$
$$P_4 = \begin{bmatrix} 30.9987 & 9.6669 \\ 9.6669 & 3.1160 \end{bmatrix}, P_5 = \begin{bmatrix} 33.4916 & 10.2084 \\ 10.2084 & 3.2401 \end{bmatrix}, P_6 = \begin{bmatrix} 31.9907 & 10.0517 \\ 10.0517 & 3.2597 \end{bmatrix},$$
$$P_7 = \begin{bmatrix} 35.7916 & 10.9124 \\ 10.9124 & 3.4349 \end{bmatrix}, P_8 = \begin{bmatrix} 31.6491 & 9.9454 \\ 9.9454 & 3.2406 \end{bmatrix}, X = \begin{bmatrix} 0.2529 & -0.4866 \\ -0.7847 & 1.5620 \end{bmatrix},$$
$$K_1 = \begin{bmatrix} 17.1280 & 17.0347 \end{bmatrix}, K_2 = \begin{bmatrix} 13.2061 & 18.1543 \end{bmatrix}, K_3 = \begin{bmatrix} 16.1393 & 18.5002 \end{bmatrix},$$
$$K_4 = \begin{bmatrix} 14.1980 & 16.8230 \end{bmatrix}, K_5 = \begin{bmatrix} 17.6417 & 21.2581 \end{bmatrix}, K_6 = \begin{bmatrix} 18.1244 & 18.5184 \end{bmatrix},$$
$$K_7 = \begin{bmatrix} 18.4048 & 21.8755 \end{bmatrix}, K_8 = \begin{bmatrix} 17.1452 & 19.8886 \end{bmatrix}.$$

From Figure 4.10, we clearly observe enlargements of the guaranteed closed-loop region of attraction (with $\bar{u} = 600N$) regarding to the previous case (where $\bar{u} = 150N$). Moreover, it is straightforward that the region of attraction obtained with $\bar{\eta} = 1ms$ is significantly larger that the one obtained with the maximal admissible value $\bar{\eta} = 8ms$ found for this case. This motivates the use of the gain scheduled event-triggering mechanism, proposed in Subsection 4.3.3, in order to take benefit of large domain of attraction for initial conditions taken as far as possible from the origin, then gradually reducing the computational demand by increasing the sampling intervals while getting closer to the equilibrium.

(a) for $\bar{u} = 600N$ and $\bar{\eta} = 1ms$ (b) for $\bar{u} = 600N$ and $\bar{\eta} = 8ms$

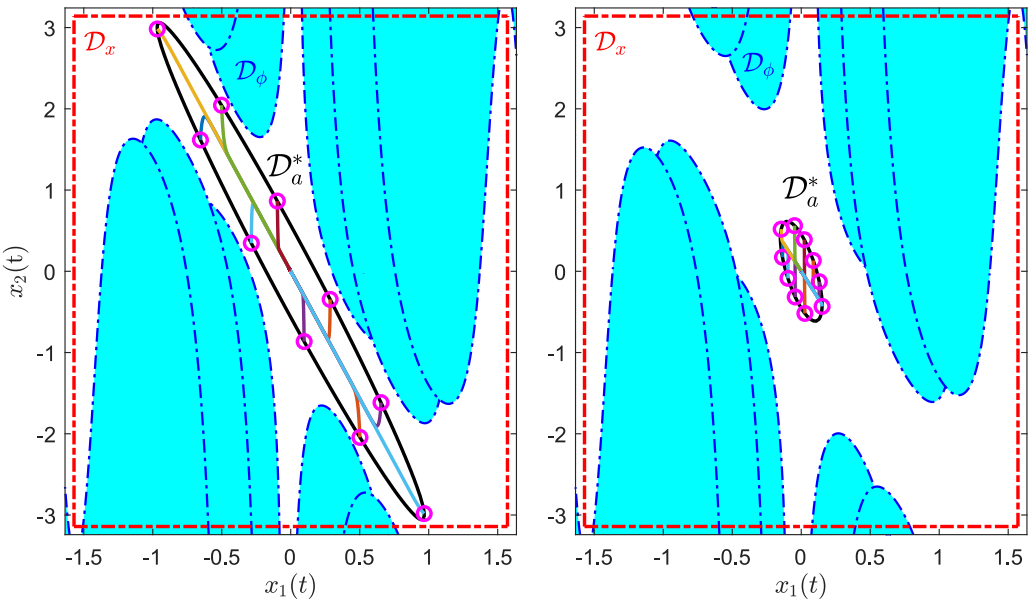

Figure 4.10: (a) Estimated domain of Attraction $\mathcal{D}_A^*$ for the full closed-loop nonlinear model (3.52) under the sampled-data controller designed from the T-S descriptor (4.1) (with (4.76)).

Figure 4.11 shows the simulation results obtained from the application of the proposed gain scheduled event-triggering mechanism. Additionally, Figure 4.12 depicts the state

time response and the overall behavior of the successive Lyapunov-Krasovskii functions (evaluated at each sampling instant $t = t_k$ and selected according to the gain scheduled event-triggering mechanism) of the designed sampled-data closed-loop system with the initial conditions $x^T(0) = \begin{bmatrix} -0.9610 & 3.0550 \end{bmatrix}$, taken at the edge of $\tilde{\mathcal{D}}_a^*$. Recall that each level sets $\mathcal{L}^q(1)$ $(q \in \mathcal{I}_8)$ composing $\tilde{\mathcal{D}}_a^*$ are contractives. This is why the behavior of the successive Lyapunov-Krasovskii functions, selected from the event-triggering laws (4.72) and (4.74), shows jumps when the state trajectories cross these successive level sets, while otherwise monotonously decreasing. All these simulations confirm the effectiveness of the proposed sampled-data controller design procedure and event-triggering mechanism for T-S descriptors.

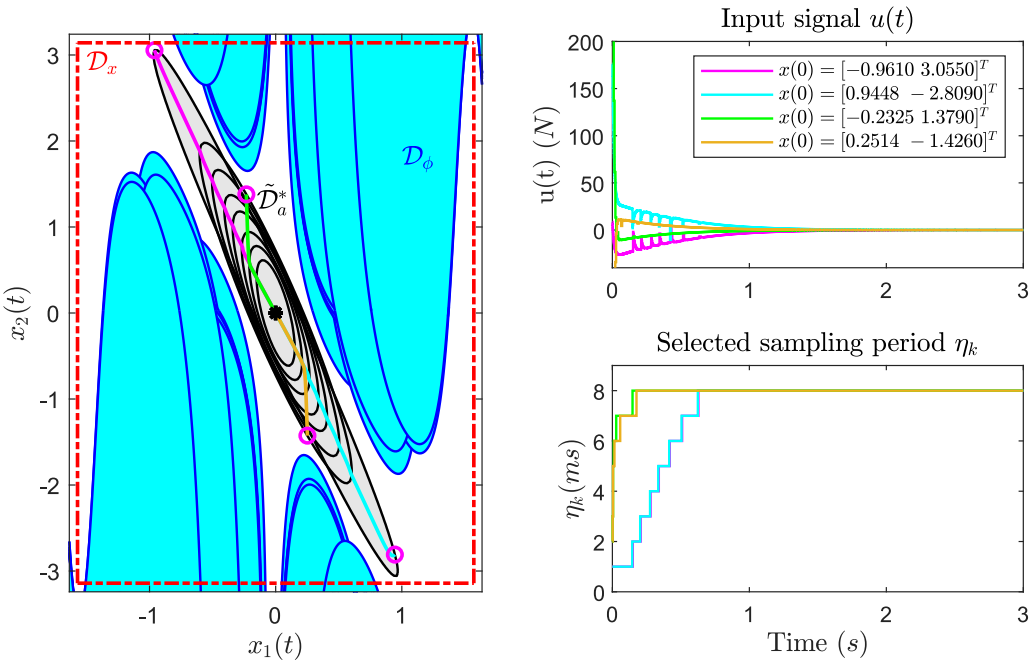

Figure 4.11: Estimates of the Region of Attraction $\tilde{D}_a^*$ (highlighted in gray) for the gain scheduled event-triggering sampled-data controller proposed in (4.74) and designed from Theorem 4.2 for the descriptor (4.1) system with (4.76) and the maximal allowed sampling interval $\bar{\eta} = 8ms$.

Remark 4.8. *From the full T-S descriptor model of the inverted pendulum, we obtain the maximal admissible sampling intervals $\bar{\eta} = 13ms$ for $\bar{u} = 150N$ and $\bar{\eta} = 8ms$ for $\bar{u} = 650N$, which are significantly less than the one obtained from the approximated T-S model (4.75) ($\bar{\eta} = 50ms$). Nevertheless, as shown in the case study of Chapter 3 (see the end of the Subsection 3.5.2), only the descriptor-based sampled-data system is accurately stabilizing the original nonlinear system (3.52). Moreover, from the proposed methodology, a conservatism trade-off between the maximal admissible sampling interval $\bar{\eta}$ and the bounds of the time-derivatives of the membership functions ϕ_k (set here from the choice of $\bar{u}$) can be done so that decreasing $\bar{u}$ allows to increase $\bar{\eta}$, but the price to pay is a contraction of the estimate of the domain of attraction $\tilde{\mathcal{D}}_a^*$ (or vice versa). To the best of the author's knowledge, since the local sampled-data controller design for T-S*

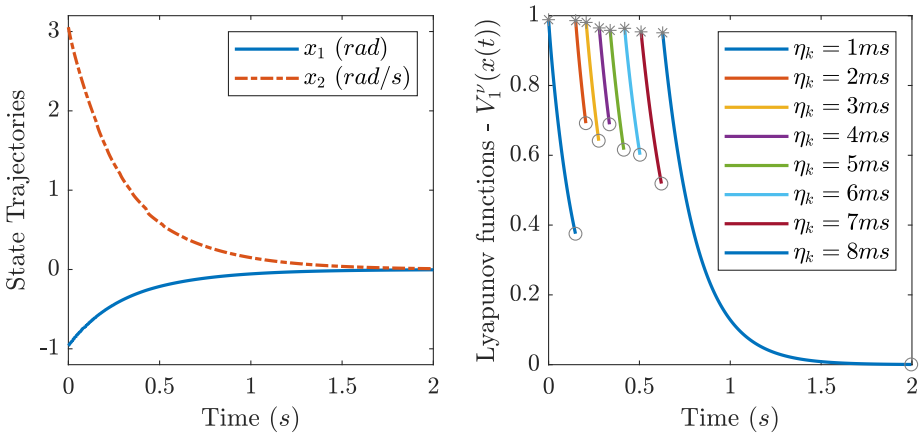

Figure 4.12: Closed-loop state responses and overall behaviour of the successively selected Lyapunov functions of the nonlinear model (3.52) under the sampled-data controller design from the T-S descriptor (4.1) (with (4.76)).

descriptors has not been previously addressed in the literature, excepted in our preliminary result (Lopes et al., 2021b), this simulation study confirms the benefits of the proposed T-S descriptor model-based sampled-data controller design methodology (with or without input saturation).

4.5 Conclusion

In this chapter, from a convenient NQLKF candidate, relaxed sampled-data controller design conditions for a class of regular nonlinear descriptors subject to actuators' saturation have been proposed. It is noticed that such class of systems is interesting to accurately represent mechatronic systems, where sampled-data control is an inherent characteristic. Based on the generalized sector condition, such nonlinear closed-loop sampled data dynamics can be rewritten as regular T-S descriptors with time-varying delays and constrained inputs. The challenge being to provide relaxed LMI-based conditions for this class of systems, extending the conditions proposed in Chapter 3, useful bounding lemmas have been employed together with a second order polynomial constraints. Also, it has been highlighted that such a sampled-data controller design methodology is only valid locally in the T-S model based-framework. Therefore, a careful analysis of the closed-loop domain of attraction has been provided along this chapter. First, for the class of T-S descriptors subject to input saturation, an offline procedure has been proposed to estimate the resulting closed-loop domain of attraction. Then, for the particular case of standard T-S models, a systematic LMI-based optimization procedure has been proposed to realize such an estimate. However, it has been pointed-out that such systematic estimation may bring conservatism (see Remark 4.6), so it must be used with care, only for some particular appropriate cases (small number of T-S vertices, triangular membership functions...). Furthermore, because, for a given maximal allowed upper bound of the sampling intervals, the obtained estimation of the domain of attraction can be quite small, a new gain scheduled event-triggering mechanism, based on the characterization of several Lyapunov invariant level sets, has been proposed to

further enlarge the resulting closed-loop sampled-data domain of attraction.

The effectiveness of these theoretical results has been illustrated through the example of an inverted pendulum on a cart. First, to show the conservatism improvements with regard to the results obtained in Chapter 3 and previous related studies from the literature, the local sampled-data controller design for an approximated 2 rules fuzzy model of this benchmark has been proposed, together with extensive estimations of the closed-loop domain of attraction, for several cases (different upper-bounds of the sampling intervals and/or input saturation). The obtained results shown a significant conservative reduction in regard to the previous ones. However, recalling that the sampled-data controller designed from the approximated standard T-S model may fail to stabilize the full nonlinear model of the inverted pendulum, a tighter closely matching T-S descriptor model has been proposed, which succeeded to guarantee the closed-loop stability, establishing the merit of the proposed methodology. However, for the obtained maximal allowed upper bound of the sampling intervals, the resulting estimation of the closed-loop domain of attraction has been found to be quite small, an illustration of the proposed gain scheduled event-triggering mechanism has been provided, showing its efficiency to enlarge the guaranteed sampled-data closed-loop domain of attraction.

General Conclusion and Perspectives

Along this thesis, we are concerned with providing relaxed LMI-based design conditions to stabilize a class of continuous-time nonlinear systems, represented by Takagi-Sugeno models, and driven by digital devices. In this context, **Chapter 1** has presented the preliminaries on T-S model-based controller design, detailing important steps, such as the usual ways to get a T-S representation. Also, aligned to the main goal of this thesis, basic notions on the discretization of continuous-time T-S models have been presented, together with the basics on stability and LMI-based controller design conditions, in both the continuous and discrete-time frameworks. Then, some limitations of the standard discrete-time approach have been pointed-out and the input-delay approach for sampled-data controllers has been introduced as an elegant alternative to cope with such issues. Once again, the main limitations of this approach in the T-S model framework, such like the locality of the results or the overall conservatism of the design conditions, have been highlighted. Summarizing, the critical analysis presented in this chapter allowed the maturation of the problem statement considered in this thesis, which can be classified into two balanced research lines presented as follows.

First, acknowledging that discrete-time model-based approaches are mainly considered in industrial applications because of their versatility and easy implementation in industrial controllers, some improvements for discrete-time T-S model-based controller design were proposed in **Chapter 2**, with the goal of providing relaxed sampled-data set-points tracking controller design conditions for discrete-time nonlinear models under saturating actuators. In this chapter, a convex optimization methodology to design discrete-time PI-like controllers is presented. The main contribution of **Chapter 2** extends our preliminary results in (Lopes et al., 2018), by including an anti-windup control action to dismiss the slow state variation requirement and, as a consequence, achieving less conservative estimates for both the region of attraction and the allowable amplitude changes in the set-point. In this context, the proposed approach can access an amplitude bound for exogenous signals such that the trajectories of the closed-loop system remain in the region of attraction, ensuring local asymptotic stability through a non-quadratic Lyapunov function. Also, the proposed fuzzy PI-like control law holds a PDC structure while the considered anti-windup fuzzy gain has a non-PDC one, which can be efficiently implemented in embedded industrial applications (Sousa et al., 2018). The proposed approach has been validated in simulation as well as experimentally on the level control of a two coupled nonlin-

ear tanks system available at the CEFET-MG, with significant improvements regarding (Lopes et al., 2018).

If the discrete-time T-S model-based controller design approach was considered because of its appealing conceptual simplicity, especially when the implementation of the controller for industrial applications is required, it was also highlighted that this approach is only suitable when a small enough fixed sampling period can be set regarding the plant dynamics. However, recall that assuming fixed sampling periods is sometimes practically unrealistic. Indeed, even in a point-to-point digital control topology, aperiodic sampling may arise because of clock inaccuracy and/or system architecture characteristics such as real-time scheduling, which can induce jitters, imperfect synchronization or computation delays (Wittenmark et al., 1995; Hetel et al., 2017). Also, when dealing with Networked Controlled Systems (NCS), in which sampled-data systems are controlled through communication networks (Hetel et al., 2017; Fridman, 2014a), aperiodic sampling intervals are almost inevitable. Nonetheless, one may also argue that, when large sampling periods have to be considered, the direct discrete-time model-based approach may fail to guarantee the closed-loop inter-sampling stability (Hetel et al., 2017). To circumvent these drawbacks, the alternative of the input-delay approach for sampled-data control has been investigated in **Chapter 3** and **Chapter 4** in the continuous-time T-S model-based framework. From this approach, the nonlinear sampled-data closed-loop dynamics is rewritten as a continuous-time T-S system with time-varying input delay, as proposed in the linear case, see e.g. (Fridman et al., 2004; Seuret, 2009).

Associated with the fact that most of real applications exhibits nonlinear dynamics, in the aforementioned chapters an extension of this approach for T-S model based framework is presented, and the conservatism reduction is verified by searching the maximal allowable sampling interval $[0, \bar{\eta}]$, for which the closed-loop dynamics stability is guaranteed.

In **Chapter 3**, our first contribution to the synthesis of sampled-data controllers for continuous-time T-S models, based on the input-delay approach, has been presented. Following the previous related works, in this chapter, relaxed LMI-based conditions for the design of stabilizing aperiodic sampled-data controllers for continuous-time T-S systems has been proposed. To achieve this goal, a convenient augmented looped LKF candidate has been selected, together with the application of bounding lemmas, such as extended Jensen's inequalities, the Finsler's Lemma and some convex quadratic polynomial constraints. Additionally, a generic relaxation scheme, extending the well-known Tuan's Lemma, has been proposed to handle the asynchronous double summation structure for parameter dependent closed-loop stability conditions, which occurs in the considered continuous-time T-S model-based sampled-data control context. As usual in related sampled-data control studies, the conservatism reduction is investigated in this chapter by searching the maximal allowable sampling interval $[0, \bar{\eta}]$, for which the LMI-based conditions remain feasible. The benefit of the proposed sampled-data controller design methodology with regard to conventional discrete-time T-S model-based design has been illustrated through the simulation of a 1-DOF inverted pendulum benchmark. Then a comparison has been provided, showing a significant enlargement of the maximal allowed sampling interval regarding to several

previous related results (Yoneyama, 2010; Zhu and Wang, 2011; Zhang and Han, 2011; Zhu et al., 2012; Gunasekaran and Joo, 2019; Zhu et al., 2013; Cheng et al., 2017), using the benchmark of a simplified T-S fuzzy model of an inverted pendulum on a cart. Also, an experimental validation of the proposed sampled-data design methodology is performed on the Quanser® AERO platform (Quanser, 2016), illustrating its effectiveness on a practical system. If the results of this chapter have been shown effective to reduce the conservatism of the design conditions by enlarging the maximal admissible sampling interval, it is also pointed-out that such approach suffers from locality, which require further investigations of the closed-loop domain of attraction, as proposed in the next chapter.

In **Chapter 4**, from a convenient NQLKF candidate, further relaxed sampled-data controller design conditions for a class of regular T-S descriptors subject to actuators' saturation have been proposed. Indeed, despite standard T-S models, such a class of systems is often considered to more accurately represent a larger class of nonlinear systems, especially for mechatronic systems, where constrained sampled-data control is an inherent characteristic. Based on the generalized sector condition, the nonlinear closed-loop sampled data dynamics can be rewritten as regular T-S descriptors with time-varying delays and constrained inputs. The challenge was to provide relaxed LMI-based conditions for this class of systems, extending the conditions proposed in **Chapter 3**, together with a careful analysis of the closed-loop domain of attraction. First, for the class of T-S descriptors subject to input saturation, an offline procedure has been proposed to estimate the resulting closed-loop domain of attraction. Then, for the particular case of standard T-S models, a systematic LMI-based optimization procedure has been proposed to realize such an estimate. However, it has been pointed-out that such systematic estimation may bring conservatism (see Remark 4.6), so it must be used with care, only for some particular appropriate cases (small number of T-S vertices, triangular membership functions...). Furthermore, because, for a given maximal allowed upper bound of the sampling intervals, the obtained estimation of the domain of attraction can be quite small, a new gain scheduled event-triggering mechanism, based on the characterization of several Lyapunov invariant level sets, has been proposed to further enlarge the resulting closed-loop sampled-data domain of attraction. Along this chapter, the results have been validated in simulation through the benchmark of an inverted pendulum, first, with the same approximated T-S fuzzy model considered in **Chapter 3**, to fairly highlight the conservatism improvement and to illustrate the proposed systematic approach to estimate the sampled-data closed-loop domain of attraction. Then, because it has been shown that controllers designed from such an approximated T-S fuzzy model may fail to stabilize the full nonlinear model, a closely matching T-S descriptor model has been proposed. From it, the so designed sampled-data controller has been shown to successfully stabilize the full inverted pendulum nonlinear model, but in a quite small guaranteed estimation of the closed-loop domain of attraction for the obtained maximal allowable sampling interval. Hence, to further enlarge the resulting sampled-data closed-loop of attraction, the benefit of the proposed gain scheduled event triggering mechanism is illustrated.

Summarizing our contribution in the field of sampled-data control for T-S models, let us point-out that, to the best of the author's knowledge, no previous results were found addressing the following points:

- the T-S model-based sampled-data controller design with actuators' saturation; excepted the work of (Lamrabet et al., 2019), which did not provide any estimations of the closed-loop domain of attraction,
- the resulting estimation of the sampled-data closed-loop domain of attraction with enlargement procedures, obtained thanks to the consideration of a convenient looped LKF; except very recent papers (Coutinho et al., 2021; Ma et al., 2021), published in the late stage of this thesis, who provide some interesting results that would merit further investigations and comparison with the present proposal,
- the extension of the T-S model-based sampled-data controller design methodology to the class of nonlinear descriptors, while these have been shown interesting to model mechatronic systems.

Also, along the manuscript, the proposed simulations and experimental results have established the merit of the proposed T-S model-based sampled-data approaches, in both the discrete-time and continuous-time framework. However, there are still some limitations of the proposed approaches, which can be discussed to provide some perspectives of this work.

Regarding the *Direct Design* approach for discrete-time systems, even if an abundant literature already exists, there are still points of interests that catch our attention for further improvements. First of all, like many previous studies in the discrete-time framework, we consider the discrete-time realization of a continuous-time T-S model based on the forward Euler discretization approach (Chen, 1999). However, this discretization leading to approximations, there is space for improvements. In this context, other discretization approaches exist, like Tustin bilinear transforms (Ogata, 1995; Åström and Hägglund, 2011), using Taylor series expansions or the Cayley-Hamilton Theorem (Heemels et al., 2010), or more recently using a descriptor system-based approach in the T-S framework (Braga et al., 2019). Hence, a direct perspective would be to evaluate the improvement raised by these approaches to our discrete-time PI-like tracking controller design conditions, proposed in **Chapter 2**, especially with the expectation of handling nonlinear systems involving faster continuous-time dynamics, or with the aim to further enlarge the resulting estimation of the closed-loop domain of attraction. Then, another perspective that have not been investigated during this PhD work, is event-triggering in the discrete-time framework, see e.g. (de Souza et al., 2021). Such approach could be interesting for some industrial applications where fast sampling periods with regard to the plant dynamics can be set to mitigate computational or network workloads. Furthermore, in **Chapter 2**, we have considered the tracking PI-like controller design problem while investigating the changes in the resulting closed-loop domain of attractions with regard to the changes of set-points (i.e.

piecewise constant desired trajectories). A very interesting perspective would be to propose an extension to the more general case of dynamic trajectory tracking, but in this case the investigation of the closed-loop domain of attraction would be much more complex since its estimate should be dynamically evolving with regard to the desired trajectories at each sampling instant. Of course, many further extensions of the proposed strategies in the discrete-time framework can be done, for instance to cope with output feedback control, NCS with network-induced delays, packet dropouts, cyber-attacks, and so on.

Now, let us focus more on the input-delay approach considered for the stabilization of continuous-time quasi-LPV/T-S models. If the results presented in **Chapter 3** and **Chapter 4** have shown the appeal of the proposed strategy, one must fairly infer its main limitation, which is the extensive computational complexity of the proposed LMI-based conditions. Indeed, like many attempts to reduce the conservatism in the T-S model-based framework, providing relaxed LMI-based conditions often implies an increase of their computational cost. This is particularly true when dealing with sampled-data control since one important way to relax the conditions comes from the strategy employed to cope with their mismatched double-fuzzy sum structure. To this end, we have proposed an extension of the well-known Tuan's Lemma (Tuan et al., 2001) but with an increase of the size of the LMIs. This can be regarded as a drawback but, this also allows to reduce the number of LMIs, i.e. balancing the computational cost. Additionally, to further reduce the conservatism, we proposed looped Lyapunov-Krasovskii functionals for sampled-data controller design, as well as usual bounding lemmas (Extended Jensen's inequality, Finsler lemma...), which introduce several slack decision variables. In the expectation to balance the computational complexity, we may consider, as a first perspective of this work, reducing the number of decision variables (especially free weighting matrices) while considering some more recent and tighter bounding techniques dedicated to time-delayed systems like the use of Wirtinger's or Bessel-Legendre inequalities, see e.g. (Seuret and Gouaisbaut, 2013; Ariba et al., 2018; Seuret and Gouaisbaut, 2018; Bourahala et al., 2019; Nafir et al., 2021). Of course, the high computational costs brought by complex LMI conditions can be regarded as a drawback for this kind of studies. Nevertheless, let us highlight that such computations are done offline. Moreover, let us assume that this concern can be alleviated with the continuous growing of computational capabilities of our daily use computers (i.e. personal computer or, when available, high performance computers). To illustrate this point, note that with the approximated T-S model of an inverted pendulum considered in Subsection 4.4.1, it took 12.97 seconds to solve the conditions of Theorem 4.2 (we use for this test a late 2016 HP laptop having a 2.6GHz Intel Core I7 processor and 16GB of memory). Otherwise, to solve the conditions of Theorem 4.1 with the full T-S matching descriptor model of the inverted pendulum (given in Section 4.4.2), the computational burden was significantly more extensive, i.e. an average of 45 minutes per tests, with the same computer.

Many other points can merit some attention to further reduce the conservatives of the proposed LMI-based conditions for the T-S model-based sampled-data controller design. First, to

handle the asynchronous double summation structure of the parameter-dependent LMI-based design conditions, we have proposed an extension of the Tuan's Lemma, summarized in Theorem 3.2. This one is based on the application of the Peterson Lemma (Xie, 1996), which can be further relaxed thanks to some of its extensions (Briat, 2008). Also, our approach implies an overall extension of the size of the LMI conditions to be checked, and so possibly affects the computational costs or conservatism for large-scale systems. In this context, some mitigation would be welcome, for instance by considering the introduction of more information about the membership functions, like a recently proposed approach to cope with the bounds of their time-derivatives (Gunasekaran and Joo, 2019). Also, from the proposed looped LKF, the closed-loop Lyapunov stability conditions leads to a quadratic inequality (second order polynomial in $\tau(t)$), whose negativeness is handled by some convexity conditions (Zhu et al., 2016), which are somewhat conservative. In a recent work (de Oliveira and Souza, 2020), some necessary and sufficient conditions have been proposed to cope with such quadratic constraints. However, we intended to apply them in our context but, with our sampled-data design approach, we faced sparsity in the obtained LMI-based constraints, and so an unsolvable convex optimization problem. Once again, following this way with more scrutiny can be interesting to further reduce the conservatism. Another point which can merit further refinement is the gain scheduled event-triggering mechanism proposed to enlarge the estimation of the guaranteed closed-loop domain of attraction. Indeed, noticing that the Lyapunov level set is found inside a compact set of the state space defining the validity domain of the T-S model-based design, further improvements can be obtained by optimizing this domain of validity for each scheduling conditions. This point will be the subject of our next investigations. Finally, in the prospect of future practical applications, the proposed sampled-data controller design methodology can be extended to cope with external disturbances, for instance by considering a H_∞ criterion (see e.g. (Kim et al., 2021; Bourahala et al., 2021), by considering static output-feedback controllers (Bouarar et al., 2013), extending recently proposed event-triggering approaches (Rouamel et al., 2021) to the T-S model-based framework, or, similarly to what has been proposed in **Chapter 2**, by extending the input-delay approach to cope with PI-like sampled-data controllers. However, for this last point, from the author's preliminary investigation, some issues are still to be unlocked, especially to deal with the necessary time hybridization of the integral and/or anti-windup actions.

This being said, from these prospects on T-S model-based sampled-data controller design for continuous-time nonlinear systems, the door is now open for a wide range of further deve lopments.

Traduction en Français de la Conclusion Generale et des Perspectives:

Au sein de ce manuscrit de thèse de doctorat, des conditions de synthèse à base de LMIs relâchées ont été proposées pour la stabilisation d'une classe de systèmes non linéaires décrits en temps continu, représentés par des modèles Takagi-Sugeno, et contrôlés par des dispositifs numériques. Dans le **Chapitre 1**, les préliminaires sur la synthèse de lois de commande pour les modèles T-S ont été présentés, ainsi que les différentes façons d'obtenir une représentation T-S. En outre, conformément à l'objectif principal de cette thèse, des notions de base sur la discrétisation des modèles T-S en temps continu ont été présentées, ainsi que les bases sur la stabilité et les conditions LMIs de synthèse des contrôleurs, dans les cadres continu ou discret. Ensuite, certaines limites de l'approche standard à temps discret ont été soulignées et l'approche dite "à retard sur l'entrée" pour la synthèse de contrôleurs échantillonnés pour les systèmes continus a été introduite comme une alternative élégante pour faire face à de tels problèmes. Encore une fois, les principales limites de cette approche dans le cadre des modèles T-S, comme l'obtention de résultats locaux ou le conservatisme des conditions de synthèse, ont été soulignées. En résumé, l'analyse critique présentée dans ce chapitre a permis la maturation de l'énoncé des problèmes considérés dans cette thèse, qui peut être classée en deux lignes de recherche présentées comme suit.

Tout d'abord, reconnaissant que les approches basées sur des modèles à temps discret sont principalement considérées dans les applications industrielles en raison de leur polyvalence et de leur facilité de mise en œuvre, certaines améliorations pour les mo dèles T-S discret ont été proposées dans le **Chapitre 2**. L'objectif était de fournir une méthodologie d'optimisation convexe pour concevoir des contrôleurs discrets de type PI. La principale contribution du **Chapitre 2** est d'etendre nos résultats préliminaires (Lopes et al., 2018), en incluant une action anti-windup pour s'affranchir de l'hypothèse d'une variation lente de l'état et, en conséquence, fournir des estimations moins conservatives de la région d'attraction, ainsi que des changements d'amplitude admissibles des point de consigne. Dans ce contexte, l'approche proposée permet d'estimer l'amplitude maximale de signaux exogènes afin que les trajectoires du système en boucle fermée restent dans la région d'attraction, assurant une stabilité asymptotique locale grâce à une fonction de Lyapunov non quadratique. En outre, la loi de commande floue de type PI proposée adopte une structure PDC alors que le gain de l'action anti-windup adopte une structure non-PDC, qui peuvent être efficacement mis en œuvre dans les applications industrielles embarquées (Sousa et al., 2018). L'approche proposée a été validée en simulation et expérimentalement à partir du contrôle de niveau d'un système de deux réservoirs non linéaires couplés disponible au CEFET-MG, avec des améliorations significatives vis-à-vis de résultats préliminaires présentés dans (Lopes et al., 2018).

Si l'approche de synthèse du contrôleur basé sur un modèle T-S à temps discret a été envisagée en raison de sa simplicité conceptuelle attrayante, en particulier lorsque la mise en œuvre du contrôleur pour des applications industrielles est nécessaire, il a également été souligné que cette approche n'est appropriée que lorsqu'une période d'échantillonnage suffisamment petite et fixe peut être déterminée au regard de la dynamique continue du système à commander. Toutefois, il faut rappeler que l'hypothèse de périodes d'échantillonnage fixes est parfois irréaliste dans la pratique. En effet, même lorsqu'une topologie de contrôle numérique point-à-point est considérée, l'échantillonnage apériodique peut survenir en raison de l'inexactitude de l'horloge et/ou des caractéristiques de l'architecture du système telles que l'ordonnancement en temps réel, ce qui peut induire une synchronisation imparfaite ou des retards de calcul (Wittenmark et al., 1995; Hetel et al., 2017). En outre, lorsqu'il s'agit de systèmes contrôlés au travers d'un réseau

de communication, la considération d'intervalles d'échantillonnage apériodique sont souvent inévitables (Hetel et al., 2017; Fridman, 2014a). Néanmoins, on peut également faire valoir que, lorsque de grandes périodes d'échantillonnage doivent être prises en compte, l'approche directe fondée sur un modèle à temps discret peut ne pas garantir la stabilité en boucle fermée du système continu entre les instants d'échantillonnage (Hetel et al., 2017). Pour contourner ces inconvénients, l'approche alternative de la *Synthèse continue-échantillonnée* a été étudiée dans les **Chapitres 3** et **4** pour la stabilisation des modèles T-S continus. À partir de cette approche, la dynamique non linéaire en boucle fermée est réécrite comme un système T-S à temps continu avec un retard variable sur l'entrée, tel que proposé pour les systèmes linéaires, e.g. (Fridman et al., 2004; Seuret, 2009).

Associé au fait que la plupart des applications réelles présentent une dynamique non linéaire, dans les chapitres susmentionnés, une extension de cette approche pour le cadre des modèle T-S est présentée, et la réduction du conservatisme est vérifiée en recherchant l'intervalle d'échantillonnage maximal autorisé $[0, \bar{\eta}]$, pour lequel la stabilité dynamique en boucle fermée est garantie.

Dans le **Chapitre 3**, notre première contribution à la synthèse des contrôleurs échantillonnés pour les modèles T-S continus, basée sur l'approche de la *Synthèse continue-échantillonnée*, a été présentée. Dans la continuité des travaux existants, des conditions à base de LMIs relâchées ont été proposées pour la synthèse de contrôleurs à échantillonnage apériodique stabilisant les systèmes T-S décrits en temps continu. Pour atteindre cet objectif, une LKF "bouclée" augmentée a été sélectionnées, associée à l'application de lemmes de majoration, tels que des inégalités étendues de Jensen, le Lemme de Finsler et des contraintes polynomiales quadratiques convexes. En outre, un schéma de relaxation générique a été proposé. Celui-ci permet l'extension du célèbre Lemme de Tuan, pour tenir compte de la structure en double somme des conditions de stabilité en boucle fermée, dépendantes de paramètres asynchrones. Similairement aux précédentes études pour la commande échantillonnée des modèles T-S continus, la réduction du conservatisme est étudiée dans ce chapitre en cherchant l'intervalle d'échantillonnage maximal autorisé $[0, \bar{\eta}]$, pour lequel les conditions de synthèse demeurent faisables. L'avantage de la méthode de *Synthèse continue-échantillonnée* vis-à-vis de la méthode de *Synthèse Directe* à base de modèles T-S discrets a été illustré par la simulation d'un modèle de pendule inversé à un degré de liberté. Ensuite, une comparaison a été fournie, montrant un élargissement significatif de l'intervalle d'échantillonnage maximal autorisé par rapport à plusieurs résultats connexes précédents (Yoneyama, 2010; Zhu and Wang, 2011; Zhang and Han, 2011; Zhu et al., 2012; Gunasekaran and Joo, 2019; Zhu et al., 2013; Cheng et al., 2017), en utilisant l'exemple d'un modèle T-S approximé d'un pendule inversé sur un chariot. Enfin, une validation expérimentale de la méthodologie de *Synthèse continue-échantillonnée* proposée est effectuée sur la plate-forme AERO de Quanser® (Quanser, 2016), illustrant son efficacité sur un système réel. Si les résultats de ce chapitre se sont révélés efficaces pour réduire le conservatisme des conditions de synthèse de correcteur en élargissant l'intervalle d'échantillonnage maximal admissible, il est également souligné que cette approche souffre de n'être valide que localement, ce qui justifie des investigations plus approfondies du domaine d'attraction en boucle fermée, comme proposé dans le chapitre suivant.

Dans le **Chapitre 4**, des conditions relâchées de *Synthèse continue-échantillonnée* pour la classe de systèmes T-S descripteurs réguliers, soumis à la saturation des actionneurs, ont été proposées. En effet, en dépit des modèles T-S standard, cette classe de systèmes descripteurs est souvent considérée comme représentant de façon plus précise une plus grande classe de systèmes non linéaires, en particulier pour les systèmes mécatroniques, où le contrôle à base de données échantillonnées est une caractéristique inhérente. Le défi de ce chapitre consiste donc à fournir des conditions

LMIs relâchées pour la *Synthèse continue-échantillonnée* des modèles T-S descripteurs soumis à saturation sur l'entrée, en étendant les conditions proposées dans le **Chapitre 3**, ainsi qu'en proposant une analyse minutieuse du domaine d'attraction en boucle fermée. Tout d'abord, pour la classe de descripteurs T-S soumis à la saturation sur l'entrée, une procédure hors ligne a été proposée pour estimer le domaine d'attraction en boucle fermée qui résulte de la *Synthèse continue-échantillonnée*. Ensuite, pour le cas particulier des modèles T-S standards, une procédure d'optimisation systématique à base de contraintes LMI a été proposée pour réaliser une telle estimation. Cependant, il a été souligné que cette estimation systématique peut apporter du conservatisme (voir Remarque 4.6), et il faut donc l'utiliser avec précaution, pour des classes particulières de modèles T-S comportant un faible nombre de sommets ou des fonctions d'appartenance triangulaires. En outre, parce que, pour une limite supérieure donnée des intervalles d'échantillonnage, l'estimation obtenue du domaine d'attraction peut être relativement restreinte, une nouvelle méthodologie d'ajustement des paramètres de la loi de commande est proposée. Celle-ci exploite les principes du déclenchement par événements (event-triggering), selon les équipotentielles des fonctions de Lyapunov obtenues pour plusieurs intervalles d'échantillonnage, permettant ainsi d'étendre plus encore l'estimation obtenue du domaine d'attraction en boucle fermée. Tout au long de ce chapitre, les résultats ont été validés en simulation au travers de l'exemple d'un pendule inversé, d'abord, avec le même modèle T-S approximé que celui pris en compte dans le **Chapitre 3**, afin de mettre en évidence l'amélioration du conservatisme et d'illustrer l'approche systématique proposée dans le **Chapitre 4**. Ensuite, comme il a été montré que les contrôleurs conçus à partir d'un modèle T-S approché peuvent ne pas stabiliser le modèle non linéaire complet, une modélisation exacte sous la forme d'un modèle T-S descripteur a été proposée. Le contrôleur à temps discret ainsi conçu a permis de stabiliser avec succès le modèle non linéaire continu précis du pendule inversé, mais avec une estimation du domaine d'attraction en boucle fermée relativement petite pour l'intervalle obtenu d'échantillonnage maximal autorisé. Par conséquent, en élargissant davantage l'estimation du domaine d'attraction, l'avantage du mécanisme proposé pour l'ajustement des paramètres de la loi de commande est illustré.

En résumant notre contribution dans le domaine de *Synthèse continue-échantillonnée* pour les modèles T-S, soulignons que, à la connaissance de l'auteur, très peu de résultats antérieurs portant sur les points suivants existent :

- la synthèse de contrôleurs basés sur des données échantillonnés apériodiques pour les modèles T-S avec saturation des actionneurs ; excepté le travail de (Lamrabet et al., 2019), où aucune considération n'est portée sur l'estimation du domaine d'attraction en boucle fermée,
- l'estimation du domaine d'attraction en boucle fermée et ses procédures d'optimisation, obtenue grâce à la prise en compte d'une LKF "bouclée" adéquate ; à l'exception des très récents articles publiés par (Coutinho et al., 2021; Ma et al., 2021) à la fin du déroulement de cette thèse, et qui fournissent des résultats intéressants qui mériteraient d'être approfondis et comparés avec notre proposition,
- l'extension de la méthodologie de *Synthèse continue-échantillonnée* pour la classe des modèles T-S descripteurs, qui s'avère intéressante pour traiter de la commande des systèmes mécatroniques.

Tout au long de ce manuscrit, les simulations proposées et les résultats expérimentaux ont permis d'illustrer le mérite des approches proposées de commande échantillonnée

pour les modèle T-S, tant dans le cadre du temps discret que dans le cadre du temps continu. Cependant, les approches proposées présentent encore certaines limitations, qui peuvent être discutées pour fournir des perspectives de ce travail.

En ce qui concerne l'approche de *Synthèse Directe* pour les systèmes décrits en temps discret, même si une abondante littérature existe déjà, il y a encore des points d'intérêt qui retiennent notre attention pour de futures améliorations. Tout d'abord, comme de nombreuses études précédentes dans le contexte du temps discret, nous considérons la discrétisation d'un modèle T-S en temps continu via la célèbre transformation d'Euler (Chen, 1999). Cependant, la discrétisation conduisant à des approximations, des améliorations sont toujours possibles. Dans ce contexte, il existe d'autres approches de discrétisation, comme la transformation bilinéaire de Tustin (Ogata, 1995; Åström and Hägglund, 2011), en utilisant des décompositions en série de Taylor ou le Théorème de Caley-Hamilton (Heemels et al., 2010). Par conséquent, une perspective directe serait d'évaluer l'amélioration potentielle de ces approches avec les conditions de *Synthèse Directe* proposé dans le **Chapitre 2**, en particulier dans l'optique de leur application à des systèmes non linéaires impliquant des dynamiques continues plus rapides, ou dans le but d'élargir davantage l'estimation résultante du domaine d'attraction en boucle fermée. Ensuite, une autre perspective qui n'a pas été étudiée au cours de ce travail de doctorat est le déclenchement d'événements dans le cadre du temps discret, e.g. (de Souza et al., 2021). Une telle approche pourrait être intéressante pour certaines applications industrielles où des périodes d'échantillonnage rapides peuvent être définies vis-à-vis de la dynamique du système à contrôler et, le cas échéant, d'atténuer la charge dans le cas de la commande en réseau. En outre, dans le **Chapitre 2**, on a considéré la *Synthèse Directe* de contrôleurs discrets de type PI tout en étudiant les effet des changements de points de consigne (i.e. trajectoires désirées constantes par morceaux) sur l'estimation du domaine d'attractions en boucle fermée. Une perspective très intéressante serait de proposer une extension au cas plus général de suivi de trajectoire dynamique, mais dans ce cas l'étude du domaine d'attraction en boucle fermée serait beaucoup plus complexe puisque son estimation devrait évoluer dynamiquement par rapport aux trajectoires souhaitées, et ceci à chaque instant d'échantillonnage. Bien entendu, de nombreuses autres extensions des stratégies proposées dans le cadre de la synthèse en temps discret peuvent être réalisées, par exemple pour le retour de sortie, pour les NCS avec des retards induits par le réseau, des pertes de paquets, des cyber-attaques, etc.

Á présent, portons notre attention sur l'approche de *Synthèse continue-échantillonnée* proposée pour la stabilisation des modèles quasi-LPV/T-S en temps continu. Si les résultats présentés dans le **Chapitre 3** et le **Chapitre 4** ont démontré l'attrait de la stratégie proposée, il faut également admettre sa principale limitation qui consiste en une complexité et un coût de calcul élevé des conditions à base de LMIs. En effet, comme dans de nombreuses tentatives pour réduire le conservatisme des conditions de synthèse pour les modèle T-S, fournir des conditions LMIs relâchées entraîne généralement une augmentation du coût de calcul. Cela est particulièrement vrai dans le cas de la *Synthèse continue-échantillonnée*, car une façon importante de réduire le conservatisme vient de la stratégie employée pour faire face à la structure de double somme asynchrone. À cette fin, nous avons proposé une extension du célèbre Lemme de Tuan (Tuan et al., 2001), mais qui résulte en une augmentation de la taille des LMIs. Cela peut être considéré comme un inconvénient, mais cela permet également de réduire le nombre de contraintes LMIs. De plus, pour réduire encore le conservatisme, nous avons proposé des fonctions Lyapunov-Krasovskii "bouclées" pour la synthèse de contrôleurs échantillonnés, associées

à l'utilisation de lemmes de majoration usuels (inégalité étendue de Jensen, Lemme de Finsler...), qui introduisent plusieurs variables de décision libres. Dans l'espoir de réduire la complexité des calculs, nous pouvons envisager, comme première perspective de ce travail, de réduire le nombre de variables de décision (en particulier les matrices de décision libres) tout en tenant compte de certaines techniques plus récentes proposées pour l'analyse des systèmes avec retards, comme par exemple l'utilisation des inégalités de Wirtinger ou de Bessel-Legendre (Seuret and Gouaisbaut, 2013; Ariba et al., 2018; Seuret and Gouaisbaut, 2018; Bourahala et al., 2019; Nafir et al., 2021). Bien entendu, les coûts de calcul élevés induits par des conditions LMIs complexes peuvent être considérés comme un inconvénient pour ce type d'études. Néanmoins, soulignons que de tels calculs sont effectués hors ligne. De plus, nous pouvons envisager que cette préoccupation peut être atténuée par la croissance continue des capacités de calcul de nos ordinateurs personnels ou, lorsqu'ils sont disponibles, de supercalculateurs tel que le centre de calcul ROMEO de l'Université de Reims Champagne-Ardenne. Pour illustrer ce point, notons qu'avec le modèle T-S approximé du pendule inversé considéré dans la section 4.4.1, il a fallu $12,97$ secondes pour résoudre les conditions du Théorème 4.2 (nous avons utilisé pour ce test un ordinateur portable HP datant de fin 2016 avec un processeur Intel Core I7 de $2,6$ GHz et 16 Go de mémoire RAM). Aussi, pour résoudre les conditions du Théorème 4.1 avec le modèle complet sous la forme T-S descripteur du pendule inversé (donné dans la section 4.4.2), la charge de calcul était beaucoup plus importante, i.e. une moyenne de 45 minutes par test, avec le même ordinateur.

De nombreux autres points mériteraient une certaine attention pour rêlacher davantage les conditions LMIs proposées pour la synthèse du contrôleur échantillonné pour les mo dèles T-S. Tout d'abord, afin de tenir compte de la structure en double somme asynchrone des conditions LMIs dépendantes des paramètres, nous avons proposé une extension du Lemme de Tuan, résumée dans le Théorème 3.2. Celle-ci est basée sur l'application du Lemme de Peterson (Xie, 1996), qui peut être encore relâchée, par exemple en consi dérant ses extensions proposées dans (Briat, 2008). En outre, notre approche implique une augmentation de la taille des conditions LMIs à vérifier, et affecterait donc éventuellement le coût de calcul ou le conservatisme pour les systèmes de grande taille. Dans ce contexte, certaines mesures de relaxation seraient les bienvenues, par exemple en envisageant l'introduction de plus d'informations sur les fonctions d'appartenance, telle que l'approche récemment proposée pour faire face aux limites de leurs dérivés temporelles (Gunasekaran and Joo, 2019). De plus, à partir des LKF "bouclée" proposées, les conditions de stabilité en boucle fermée conduisent à une inégalité quadratique (polynôme de second ordre en $\tau(t)$), dont la négativité est traitée par des conditions de convexité (Zhu et al., 2016), qui peuvent s'avérer quelque peu conservatives. Dans une étude récente (de Oliveira and Souza, 2020), des conditions nécessaires et suffisantes ont été proposées pour faire face à de telles contraintes quadratiques. Cependant, nous avions l'intention de les appliquer dans notre cadre théorique, mais nous nous sommes heurtés à l'obtention de contraintes LMIs "creuses", et qui ont donc conduit à un problème d'optimisation convexe insoluble. Encore une fois, poursuivre nos efforts pour résoudre ce problème pourrait s'avérer très intéressant afin de réduire davantage le conservatisme. Un autre point qui mérite d'être affiné est le mécanisme de déclenchement d'événements programmé proposé pour augmenter l'estimation du domaine d'attraction en boucle fermée. En effet, remarquant que l'ensemble des équipotentielles de Lyapunov se trouve à l'intérieur d'un ensemble compact de l'espace d'état définissant le domaine de validité du modèle T-S, d'autres améliorations peuvent être obtenues en optimisant ce domaine de validité pour chaque condition de synthèse. Ce point fera l'objet de nos prochains travaux. Enfin, dans la perspective de

futures applications pratiques, la méthodologie proposée pour la synthèse de contrôleurs échantillonnés peut être étendue pour faire face aux perturbations externes, par exemple en considérant un critère H_∞ (e.g. (Kim et al., 2021; Bourahala et al., 2021), en considérant le retour de sortie statique (Bouarar et al., 2013), en étendant les approches de déclenchement d'événements que nous avons récemment proposées (Rouamel et al., 2021) au cas des modèle T-S ou, de manière similaire à ce qui a été proposé dans le **Chapitre 2**, en étendant les conditions de *Synthèse continue-échantillonnée* pour des contrôleurs échantillonnées de type PI. Cependant, pour ce dernier point, une première investigation de l'auteur a soulevé certains verrous qui doivent encore être débloquées, en particulier pour traiter l'hybridation du temps nécessaire pour implémenter les actions intégrales et/ou anti-windup sur des dispositifs de commande numérique.

Ceci étant dit, à partir de ces perspectives sur la *Synthèse continue-échantillonnée* de contrôleur échantillonné pour la stabilisation des systèmes non linéaires décrits en temps continu et représentés par des modèles T-S, la porte est maintenant grande ouverte pour un large éventail d'autres développements.

Bibliography

Al Hamouch, A., Tuqan, M., Bardawil, C., and Daher, N. (2019). Investigating Performance of Adaptive and Robust Control Schemes for Quanser AERO. In *2019 Fourth International Conference on Advances in Computational Tools for Engineering Applications (ACTEA)*, 1–6.

ApS, M. (2019). *The MOSEK optimization toolbox for MATLAB manual. Version 9.0.* URL http://docs.mosek.com/9.0/toolbox/index.html.

Arabi, E. and Yucelen, T. (2019a). Experimental results with the set-theoretic model reference adaptive control architecture on an aerospace testbed. In *AIAA Scitech 2019 Forum*, 0930.

Arabi, E. and Yucelen, T. (2019b). A set-theoretic model reference adaptive control architecture with dead-zone effect. *Control Engineering Practice*, 89, 12 – 29.

Arceo, J.C., Vázquez, D., Estrada-Manzo, V., Márquez, R., and Bernal, M. (2016). Nonlinear convex control of the Furuta pendulum based on its descriptor model. In *2016 13th International Conference on Electrical Engineering, Computing Science and Automatic Control (CCE)*, 1–6.

Ariba, Y., Gouaisbaut, F., Seuret, A., and Peaucelle, D. (2018). Stability analysis of time-delay systems via Bessel inequality: A quadratic separation approach. *International Journal of Robust and Nonlinear Control*, 28(5), 1507–1527.

Åström, K.J. and Hägglund, T. (2011). *Computer-Controlled Systems: Theory and Design*. Dover Books on Electrical Engineering. Dover Publications, 3 edition.

Blanco, Y., Perruquetti, W., and Borne, P. (2001). Non quadratic stability of nonlinear systems in the Takagi-Sugeno form. In *2001 European Control Conference (ECC)*, 3917–3922.

Blažič, S., Škrjanc, I., and Matko, D. (2002). Globally stable model reference adaptive control based on fuzzy description of the plant. *International Journal of Systems Science*, 33(12), 995–1012.

Bouallegue, S., Hagg, J., Ayadi, M., and Benrejeb, M. (2012). PID type fuzzy logic controller tuning based on particle swarm optimization. *Engineering Applications of Artificial Intelligence*, 25, 484–493.

Bouarar, T., Guelton, K., and Manamanni, N. (2010). Robust fuzzy Lyapunov stabilization for uncertain and disturbed Takagi–Sugeno descriptors. *ISA Transactions*, 49(4), 447 – 461.

Bouarar, T., Guelton, K., Mansouri, B., and Manamanni, N. (2007a). LMI Stability Conditions for Takagi-Sugeno Uncertain Descriptors. In *2007 IEEE International Fuzzy Systems Conference*, 1–6.

Bouarar, T., Guelton, K., and Manamanni, N. (2007b). LMI based H_∞ controller design for uncertain Takagi-Sugeno descriptors subject to external disturbances. *IFAC Proceedings Volumes*, 40(21), 49–54. 3rd IFAC Workshop on Advanced Fuzzy and Neural Control.

Bouarar, T., Guelton, K., and Manamanni, N. (2013). Robust non-quadratic static output feedback controller design for Takagi-Sugeno systems using descriptor redundancy. *Eng. Appl. Artif. Intell.*, 26, 739–756.

Bouarar, T., Guelton, K., Manamanni, N., and Billaudel, P. (2008). Stabilization of uncertain Takagi-Sugeno descriptors: A fuzzy Lyapunov approach. In *2008 16th Mediterranean Conference on Control and Automation*, 1616–1621.

Bourahala, F., Guelton, K., Manamanni, N., and Khaber, F. (2017). Relaxed Controller Design Conditions for Takagi–Sugeno Systems with State Time-Varying Delays. *International Journal of Fuzzy Systems*, 19(5), 1406–1416.

Bourahala, F. and Guelton, K. (2017). A Finsler-based result for the stability analysis of Takagi-Sugeno fuzzy models with interval time-varying delays. In *2017 11th Asian Control Conference (ASCC)*, 1743–1748.

Bourahala, F., Guelton, K., and Lopes, A.N.D. (2019). Relaxed Non-Quadratic Stability Conditions for Takagi-Sugeno Systems with Time-Varying Delays: A Wirtinger's Inequalities approach. In *2019 IEEE International Conference on Fuzzy Systems (FUZZ-IEEE)*, 1–6.

Bourahala, F., Rouamel, M., and Guelton, K. (2021). Improved robust $\mathcal{H}_\infty$ stability analysis and stabilization of uncertain systems with stochastic input time-varying delays. *Optimal Control Applications and Methods*, 42(5), 1512–1530.

Boyd, S., El Ghaoui, L., Feron, E., and Balakrishnan, V. (1994). *Linear Matrix Inequalities in System and Control Theory*. SIAM - Studies in Applied Mathematics.

Braga, M.F., Campos, V.C.S., and Frezzatto, L. (2019). Improved Discretization Method for Uncertain Linear Systems: A Descriptor System Based Approach. In *2019 IEEE 58th Conference on Decision and Control (CDC)*, 7069–7074.

Brecher, C., Müller, A., Dassen, Y., and Storms, S. (2021). Automation technology as a key component of the Industry 4.0 production development path. *The International Journal of Advanced Manufacturing Technology*.

Briat, C. (2008). *Commande et Observation Robustes des Systèmes LPV Retardées*. Ph.d. thesis, Institut National Polytechnique de Grenoble - INPG.

Briat, C. and Seuret, A. (2012). A looped-functional approach for robust stability analysis of linear impulsive systems. *Systems & Control Letters*, 61(10), 980–988.

Briat, C. and Seuret, A. (2015). On the necessity of looped-functionals arising in the analysis of pseudo-periodic, sampled-data and hybrid systems. *International Journal of Control*, 88(12), 2563–2569.

Cannon, J. (1967). *Dynamics of physical systems*. McGraw-Hill, 1 edition.

Chadli, M. and Guerra, T.M. (2012). LMI Solution for Robust Static Output Feedback Control of Discrete Takagi–Sugeno Fuzzy Models. *IEEE Transactions on Fuzzy Systems*, 20(6), 1160–1165.

Chang, W.J., Su, C.L., and Tsai, M.H. (2021). Derivative-Based Fuzzy Control Synthesis for Singular Takagi-Sugeno Fuzzy Systems with Perturbations. In *2021 International Symposium on Electrical, Electronics and Information Engineering*, 136–140. Association for Computing Machinery, New York, NY, USA.

Chen, C.T. (1999). *Linear System Theory and Design*. Oxford University Press, New York, 3 edition.

Chen, S.Y., Hung, Y.H., and Gong, S.S. (2016). Speed Control of Vane-Type Air Motor Servo System Using Proportional-Integral-Derivative-Based Fuzzy Neural Network. *International Journal of Fuzzy Systems*, 18(6), 1065–1079.

Cheng, W., Wang, D., Zhu, X., and Wang, Y. (2017). H_∞ stabilization for sampling fuzzy systems with asynchronous constraints on membership functions. *IEEE Access*, 5, 1524–1533.

Cherifi, A., Guelton, K., and Arcese, L. (2014). Non-PDC controller design for Takagi-Sugeno models via line-integral Lyapunov functions. In *2014 IEEE International Conference on Fuzzy Systems (FUZZ-IEEE)*, 2444–2450.

Cherifi, A., Guelton, K., and Arcese, L. (2018). Uncertain TS model-based robust controller design with D-stability constraints—A simulation study of quadrotor attitude stabilization. *Engineering Applications of Artificial Intelligence*, 67, 419–429.

Cherifi, A., Guelton, K., Arcese, L., and Leite, V.J. (2019). Global non-quadratic D-stabilization of Takagi–Sugeno systems with piecewise continuous membership functions. *Applied Mathematics and Computation*, 351, 23–36.

Coutinho, P.H., Peixoto, M.L., Bernal, M., Nguyen, A.T., and Palhares, R.M. (2021). Local Sampled-Data Gain-Scheduling Control of quasi-LPV Systems. *IFAC-PapersOnLine*, 54(4), 86–91.

Dang, Q.V., Vermeiren, L., Dequidt, A., and Dambrine, M. (2017). Robust stabilizing controller design for Takagi–Sugeno fuzzy descriptor systems under state constraints and actuator saturation. *Fuzzy Sets and Systems*, 329, 77–90.

de Oliveira, F.S. and Souza, F.O. (2020). Further refinements in stability conditions for time-varying delay systems. *Applied Mathematics and Computation*, 369, 124866.

de Souza, C., Tarbouriech, S., Leite, V.J., and Castelan, E.B. (2021). Co-design of an event-triggered dynamic output feedback controller for discrete-time LPV systems with constraints. *Journal of the Franklin Institute*.

Di Ferdinando, M. and Pepe, P. (2019). Sampled-data emulation of dynamic output feedback controllers for nonlinear time-delay systems. *Automatica*, 99, 120–131.

Dragos, C.A., Preitl, S., Petriu, E.M., Radac, M.B., and Stînean, A.I. (2011). Alternative Control Solutions for Vehicles with Continuously Variable Transmission. A Case Study. In 2011 15^{th} *International Conference on System Theory, Control and Computing*, 1–6.

Du, H. and Zhang, N. (2009). Fuzzy Control for Nonlinear Uncertain Electrohydraulic Active Suspensions With Input Constraint. *IEEE Transactions on Fuzzy Systems*, 17(2), 343–356.

Estrada-Manzo, V., Lendek, Z., and Guerra, T.M. (2019). An alternative LMI static output feedback control design for discrete-time nonlinear systems represented by Takagi-Sugeno models. *ISA transactions*, 84, 104–110.

Estrada-Manzo, V., Guerra, T.M., Lendek, Z., and Bernal, M. (2013). Improvements on non-quadratic stabilization of continuous-time Takagi-Sugeno descriptor models. In *2013 IEEE International Conference on Fuzzy Systems (FUZZ-IEEE)*, 1–6.

Fan, X., Yi, Y., and Ye, Y. (2017). *Mechatronics and Robotics Engineering for Advanced and Intelligent Manufacturing*, volume 3, chapter DOB Tracking Control for Systems with Input Saturation and Exogenous Disturbances via T-S Disturbance Modelling, 445 – 455. Spring.

Fandel, A., Birge, A., and Miah, S. (2018). Development of Reinforcement Learning Algorithm for 2-DOF Helicopter Model. In *2018 IEEE 27th International Symposium on Industrial Electronics (ISIE)*, 553–558.

Fateh, M.M. (2010). Robust Voltage Control of Electrical Manipulators in Task-Space. *International Journal of Innovative Computing, Information and Control*, 6(6), 2691–2700.

Fattah, A.J. and Abdel-Qader, I. (2015). Performance and Comparison Analysis of Speed Control of Induction Motors using Improved Hybrid PID-Fuzzy Controller. In 2015 *IEEE International Conference on Electro/Information Technology*, 575–580.

Fridman, E. (2001). New Lyapunov-Krasovskii functionals for stability of linear retarded and neutral type systems. *Systems & Control Letters*, 43(4), 309 – 319.

Fridman, E. (2014a). *Introduction to Time-Delay Systems: Analysis and Control*. Birkhäuser Basel, 1 edition.

Fridman, E. and Shaked, U. (2002). An improved stabilization method for linear time-delay systems. *IEEE Transactions on Automatic Control*, 47(11), 1931–1937.

Fridman, E. and Shaked, U. (2003). Delay-dependent stability and H_∞ control: Constant and time-varying delays. *International Journal of Control*, 76(1), 48–60.

Fridman, E. (2010). A refined input delay approach to sampled-data control. *Automatica*, 46(2), 421 – 427.

Fridman, E. (2014b). Tutorial on Lyapunov-based methods for time-delay systems. *European Journal of Control*, 20(6), 271 – 283.

Fridman, E., Seuret, A., and Richard, J.P. (2004). Robust sampled-data stabilization of linear systems: an input delay approach. *Automatica*, 40(8), 1441 – 1446.

Gahinet, P., Nemirovski, A., Laub, A.J., and Chilali, M. (1995). *LMI Control Toolbox for Use with MATLAB*. MathWorks partner series. MathWorks.

Gao, H., Liu, F., Wang, T., and Yin, S. (2015). Setpoints Compensation for Nonlinear Industrial Processes with Disturbances Based on Fuzzy Logic Control. In *IECON* 2014 - 40^{th} *Annual Conference of the IEEE Industrial Electronics Society*, 2611–2616.

Gasso, K., Mourot, G., and Ragot, J. (2000). Fuzzy rule based optimisation: a pruning and merging approach. In *2000 IEEE International Conference on Systems, Man and Cybernetics*, volume 1, 67–72.

Goebel, R., Sanfelice, R.G., and Teel, A.R. (2009). Hybrid dynamical systems. *IEEE Control Systems Magazine*, 29(2), 28–93.

Gonzalez, A. and Guerra, T.M. (2014). An improved robust stabilization method for discrete-time fuzzy systems with time-varying delays. *Journal of the Franklin Institute*, 351(2014), 5148–5161.

Guelton, K. (2003). *Estimation des caractéristiques du mouvement humain en station debout. Mise en oeuvre d'observateurs flous sous forme descripteurs*. Ph.d. thesis, L'Université de Valenciennes et du Hainaut-Cambrest.

Guelton, K., Cherifi, A., and Arcese, L. (2014). Some Refinements on Stability Analysis and Stabilization of Second Order T-S Models Using Line-Integral Lyapunov Functions. *IFAC Proceedings Volumes*, 47(3), 7988–7993. 19th IFAC World Congress.

Guelton, K., Bouarar, T., and Manamanni, N. (2009). Robust dynamic output feedback fuzzy Lyapunov stabilization of Takagi-Sugeno systems - A descriptor redundancy approach. *Fuzzy Sets and Systems*, 160, 2796–2811.

Guelton, K., Delprat, S., and Guerra, T.M. (2008). An alternative to inverse dynamics joint torques estimation in human stance based on a Takagi–Sugeno unknown-inputs observer in the descriptor form. *Control Engineering Practice*, 16(12), 1414 – 1426.

Guelton, K., Guerra, T.M., Bernal, M., Bouarar, T., and Manamanni, N. (2010). Comments on Fuzzy Control Systems Design via Fuzzy Lyapunov Functions. *IEEE Transactions on Systems, Man, and Cybernetics, Part B (Cybernetics)*, 40(3), 970–972.

Guerra, T.M., Bernal, M., Guelton, K., and Labiod, S. (2012). Non-quadratic local stabilization for continuous-time Takagi-Sugeno models. *Fuzzy Sets and Systems*, 201, 40–54.

Guerra, T.M., Sala, A., and Tanaka, K. (2015). Fuzzy control turns 50: 10 years later. *Fuzzy Sets and Systems*, 281, 168–182. Special Issue Celebrating the 50th Anniversary of Fuzzy Sets.

Guerra, T.M., Kruszewski, A., and Lauber, J. (2009). Discrete Tagaki Sugeno models for control: Where are we? *Annual Reviews in Control*, 33(1), 37–47.

Guerra, T.M. and Vermeiren, L. (2004). LMI-based relaxed nonquadratic stabilization conditions for nonlinear systems in the Takagi-Sugeno's form. *Automatica*, 40, 823–829.

Gunasekaran, N. and Joo, Y.H. (2019). Robust Sampled-data Fuzzy Control for Nonlinear Systems and Its Applications: Free-Weight Matrix Method. *IEEE Transactions on Fuzzy Systems*, 27(11), 2130–2139.

Hale, J.K. and Lunel, S.M.V. (1993). *Introduction to Functional Differential Equations*. Applied Mathematical Sciences. Springer, New York, NY.

Hamzaa, M.F., Yapa, H.J., and Choudhury, I.A. (2017). Cuckoo search algorithm based design of interval Type-2 Fuzzy PID Controller for Furuta pendulum system. *Engineering Applications of Artificial Intelligence*, 62, 134–151.

Han, X. and Ma, Y. (2019). Sampled-data Robust $\mathcal{H}_\infty$ Control for T-S Fuzzy Time-delay Systems with State Quantization. *International Journal of Control, Automation and Systems*, 17(1), 46–56.

Heemels, W., van de Wouw, N., Gielen, R.H., Donkers, M.C.F., Hetel, L., Olaru, S., Lazar, M., Daafouz, J., and Niculescu, S. (2010). Comparison of overapproximation methods for stability analysis of networked control systems. In *HSCC '10: Proceedings of the* 13^{th} *ACM International Conference on Hybrid Systems: Computation and Control*.

Hetel, L., Daafouz, J., Tarbouriech, S., and Prieur, C. (2013). Stabilization of linear impulsive systems through a nearly-periodic reset. *Nonlinear Analysis: Hybrid Systems*, 7(1), 4–15. IFAC World Congress 2011.

Hetel, L., Fiter, C., Omran, H., Seuret, A., Fridman, E., Richard, J.P., and Niculescu, S.I. (2017). Recent developments on the stability of systems with aperiodic sampling: An overview. *Automatica*, 76, 309 – 335.

Hu, T. and Lin, Z. (2003). Composite quadratic Lyapunov functions for constrained control systems. *IEEE Transactions on Automatic Control*, 48(3), 440–450.

Hua, C., Wu, S., and Guan, X. (2020). Stabilization of T-S Fuzzy System With Time Delay Under Sampled-Data Control Using a New Looped-Functional. *IEEE Transactions on Fuzzy Systems*, 28(2), 400–407.

Ichalal, D., Marx, B., Maquin, D., and Ragot, J. (2016). A method to avoid the unmeasurable premise variables in observer design for discrete time TS systems. In *2016 IEEE International Conference on Fuzzy Systems (FUZZ-IEEE)*, 2343–2348.

Jaadari, A., Guerra, T.M., Sala, A., Bernal, M., and Guelton, K. (2012). New controllers and new designs for continuous-time Takagi-Sugeno models. In *IEEE International Conference on Fuzzy Systems*, 1–7. Brisbane, Australia.

Jadbabaie, A. (1999). A reduction in conservatism in stability and $\mathcal{L}_2$ gain analysis of Takagi-Sugeno fuzzy systems via linear matrix inequalities. *IFAC Proceedings Volumes*, 32(2), 5451–5455. 14th IFAC World Congress 1999, Beijing, Chia, 5-9 July.

Jia, X.C., Chi, X.B., Han, Q.L., and Zheng, N.N. (2014). Event-triggered fuzzy $\mathcal{H}_\infty$ control for a class of nonlinear networked control systems using the deviation bounds of asynchronous normalized membership functions. *Information Sciences*, 259, 100–117.

Johansson, K.H. (2000). The Quadruple-Tank Process: A Multivariable Laboratory Process with an Adjustable Zero. *IEEE Transactions on Control Systems Technology*, 8(3), 456 – 465.

Jungers, M. and Castelan, E.B. (2011). Gain-scheduled output control design for a class of discrete-time nonlinear systems with saturating actuators. *System and Control Letters*, 60(3), 315–325.

Kailath, T. (1980). *Linear Systems*. Prentice Hall, 1 edition.

Kawamoto, S., Tada, K., Ishigame, A., and Taniguchi, T. (1992). An Approach to Stability Analysis of Second Order Fuzzy Systems. In *Proceedings of First IEEE International Conference on Fuzzy Systems*, volume 1, 1427–1434.

Khalil, H.K. (2001). *Nonlinear Systems*. Prentice Hall, 1$^{\text{st}}$ edition.

Kim, E. and Lee, H. (2000). New approaches to relaxed quadratic stability condition of fuzzy control systems. *IEEE Transactions on Fuzzy Systems*, 8(5), 523–534.

Kim, H.S., Lee, K., and Joo, Y.H. (2021). Decentralized sampled-data fuzzy controller design for a VTOL UAV. *Journal of the Franklin Institute*, 358(3), 1888–1914.

Kim, H.S., Park, J.B., and Joo, Y.H. (2018). Sampled-data control of fuzzy systems based on the intelligent digital redesign method via an improved fuzzy Lyapunov functional approach. *IET Control Theory & Applications*, 12(1), 163–173.

Kim, J.H. (2016). Further improvement of jensen inequality and application to stability of time-delayed systems. *Automatica*, 64, 121–125.

Klug, M., Castelan, E.B., Leite, V.J.S., and Silva, L.F.P. (2015). Fuzzy dynamic output feedback control through nonlinear Takagi-Sugeno models. *Fuzzy Sets and Systems*, 263, 92–111.

Kmetóvá, J., Vasickaninová, A., and Dvoran, J. (2013). Neuro-fuzzy control of exothermic chemical reactor. In 2013 - *International Conference on Process Control (PC)*, 168–172.

Kong, L. and Yuan, J. (2019). Disturbance-observer-based fuzzy model predictive control for nonlinear processes with disturbances and input constraints. *ISA Transactions*.

Koo, G.B., Park, J.B., and Joo, Y.H. (2017). An improved digital redesign for sampled-data fuzzy control systems: Fuzzy Lyapunov function approach. *Information Sciences*, 406-407, 71–86.

Lam, H.K. (2012). Stabilization of Nonlinear Systems Using Sampled-Data Output-Feedback Fuzzy Controller Based on Polynomial-Fuzzy-Model-Based Control Approach. *IEEE Transactions on Systems, Man, and Cybernetics, Part B*, 42(1), 258–267.

Lam, H.K. (2018). A review on stability analysis of continuous-time fuzzy-model-based control systems: From membership-function-independent to membership-function-dependent analysis. *Engineering Applications of Artificial Intelligence*, 67, 390–408.

Lamrabet, O., Ech-charqy, A., Tissir, E.H., and Haoussi, F.E. (2019). Sampled data Control for Takagi-Sugeno Fuzzy Systems with Actuator Saturation. *Procedia Computer Science*, 148, 448 – 454.

Laurain, T., Lauber, J., and Palhares, R.M. (2018). Avoiding Matrix Inversion in Takagi-Sugeno-Based Advanced Controllers and Observers. *IEEE Transactions on Fuzzy Systems*, 26(1), 216–225.

Lee, T.H. and Park, J.H. (2018). New Methods of Fuzzy Sampled-Data Control for Stabilization of Chaotic Systems. *IEEE Transactions on Systems, Man, and Cybernetics: Systems*, 48(12), 2026–2034.

Lendek, Z., Nagy, Z., and Lauber, J. (2018). Local stabilization of discrete-time TS descriptor systems. *Engineering Applications of Artificial Intelligence*, 67, 409–418.

Li, H., Wang, J., and Shi, P. (2016a). Output-Feedback Based Sliding Mode Control for Fuzzy Systems With Actuators Saturation. *IEEE Transactions on Fuzzy Systems*, 24(6), 1282–1293.

Li, L. and Liu, X. (2009). New results on delay-dependent robust stability criteria of uncertain fuzzy systems with state and input delays. *Information Sciences*, 179(8), 1134–1148.

Li, W., Feng, Z., Sun, W., and Zhang, J. (2016b). Admissibility analysis for Takagi-Sugeno fuzzy singular systems with time delay. *Neurocomputing*, 205, 336–340.

Lin, A.Y., Huang, H.N., Shiu, C.Y., and Hwang, J.L. (2008). Implementation of fuzzy controller for measuring instantaneous arterial blood pressure via tissue control method. *IET Control Theory & Applications*, 2(1), 40–50.

Liu, K., Fridman, E., and Xia, Y. (2020). *Networked Control Under Communication Constraints*. Springer, Singapore, 1 edition.

Löfberg, J. (2004). YALMIP : a toolbox for modeling and optimization in MATLAB. In *2004 IEEE International Conference on Robotics and Automation (IEEE Cat. No.04CH37508)*, 284–289.

Lopes, A.N.D., Arcese, L., Guelton, K., and Cherifi, A. (2020b). Sampled-data Controller Design with Application to the Quanser AERO 2-DOF Helicopter. In *2020 IEEE International Conference on Automation, Quality and Testing, Robotics (AQTR)*, 1–6.

Lopes, A.N.D., Guelton, K., Arcese, L., and Leite, V.J.S. (2021). Local sampled-data controller design for T-S fuzzy systems with saturated actuators. *IEEE Control Systems Letters*, 5(4), 1169–1174.

Lopes, A.N.D., Guelton, K., Arcese, L., Leite, V.J.S., and Bourahala, F. (2020a). Finsler-based Sampled-data Controller Design for Takagi-Sugeno Systems. *IFAC-PapersOnLine*, 53(2), 7965–7970.

Lopes, A.N.D., Leite, V.J.S., and Silva, L.F.P. (2018). On the integral action of discrete-time fuzzy T-S control under saturated actuator. In *2018 IEEE International Conference on Fuzzy Systems (FUZZ-IEEE)*, 1–8.

Lopes, A.N.D., Arcese, L., and Guelton, K. (2021a). Synthèse non-quadratic de contrôleurs échantillonnés pour les modèles flous de type T-S décrits en temps continu. In *Rencontres Francophones sur la Logique Floue et ses Applications (LFA2021)*, 117–124. Paris, France.

Lopes, A.N.D., Guelton, K., Arcese, L., and Leite, V.J. (2021b). Sampled-data Controller Design for Mechatronic Systems Described by Takagi-Sugeno Descriptors. In *2021 IEEE/ASME International Conference on Advanced Intelligent Mechatronics (AIM)*, 653–660.

Lopes, A.N.D., Leite, V.J.S., Silva, L.F.P., and Guelton, K. (2020b). Anti-windup TS Fuzzy PI-like Control for Discrete-Time Nonlinear Systems with Saturated Actuators. *International Journal of Fuzzy Systems*, 22, 46–61.

Lv, X., Fei, J., and Sun, Y. (2019). Fuzzy PID controller design for uncertain networked control systems based on T-S fuzzy model with random delays. *International Journal of Fuzzy Systems*, 21(2), 571–582.

Lyapunov, A.M. (1992). The general problem of the stability of motion. *International Journal of Control*, 55(3), 531–534.

Ma, W., Jia, X.C., and Chi, X. (2021). Exponential stabilization of sampled-data fuzzy systems via a parameterized fuzzy Lyapunov-Krasovskii functional approach. *Journal of the Franklin Institute*, 358(11), 5750–5770.

Ma, X.J., Sun, Z.Q., and He, Y.Y. (1998). Analysis and design of fuzzy controller and fuzzy observer. *IEEE Transactions on Fuzzy Systems*, 6(1), 41–51.

Marouf, S., Mahboobi Esfanjani, R., Akbari, A., and Barforooshan, M. (2016). T–S fuzzy controller design for stabilization of nonlinear networked control systems. *Engineering Applications of Artificial Intelligence*, 50, 135–141.

Marquéz, R., Guerra, T.M., Bernal, M., and Kruszewski, A. (2017). Asymptotically necessary and sufficient conditions for Takagi-Sugeno models using generalized non-quadratic parameter-dependent controller design. *Fuzzy Sets and Systems*, 306, 48–62.

Marx, B. and Ragot, J. (2008). Stability and L_2-Norm Bound Conditions for Takagi-Sugeno Descriptor Systems. *IFAC Proceedings Volumes*, 41(2), 9976–9981. 17th IFAC World Congress.

Mehdi, N., Rehan, M., Malik, F.M., Bhatti, A.I., and Tufail, M. (2014). A novel anti-windup framework for cascade control systems: An application to underactuated mechanical systems. *ISA Transactions*, 53(3), 802 – 815.

Mishra, P., Kumar, V., and Rana, K.P.S. (2015). Stiction Combating Intelligent Controller Tuning: A Comparative Study. In 2015 - *International Conference on Advances in Computer Engineering and Applications (PC)*, 534–541.

Molchanov, A. and Pyatnitskiy, Y. (1989). Criteria of asymptotic stability of differential and difference inclusions encountered in control theory. *Systems & Control Letters*, 13, 59–64.

Morère, Y. (2001). *Mise en oeuvre de lois de commande pour les modèles flous de type Takagi-Sugeno*. Ph.d. thesis, L'Université de Valenciennes et du Hainaut Cambrésis.

Mozelli, L., Palhares, R., Souza, F., and Mendes, E. (2009). Reducing conservativeness in recent stability conditions of TS fuzzy systems. *Automatica*, 45(6), 1580–1583.

Nafir, N., Ahmida, Z., Guelton, K., Bourahala, F., and Rouamel, M. (2021). Improved robust $\mathcal{H}_\infty$ stability analysis and stabilisation of uncertain and disturbed networked control systems with network-induced delay and packets dropout. *International Journal of Systems Science*, 52(16), 3493–3510.

Naghavi, A. (2007). Asymmetric Labor Markets, Southern Wages and the Location of Firms. *Review of Development Economics*, 11(3), 463–481.

Naghshtabrizi, P., Hespanha, J.P., and Teel, A.R. (2008). Exponential stability of impulsive systems with application to uncertain sampled-data systems. *Systems & Control Letters*, 57(5), 378–385.

Nguyen, A.T., Márquez, R., and Dequidt, A. (2017). An augmented system approach for LMI-based control design of constrained Takagi-Sugeno fuzzy systems. *Engineering Applications of Artificial Intelligence*, 61, 96–102.

Nguyen, A.T., Dequidt, A., Nguyen, V.A., Vermeiren, L., and Dambrine, M. (2020). Fuzzy Descriptor Tracking Control with Guaranteed $\mathcal{L}_\infty$ Error-Bound for Robot Manipulators. *Transactions of the Institute of Measurement and Control*, 43(6), 1404 – 1415.

Nguyen, A.T., Taniguchi, T., Eciolaza, L., Campos, V., Palhares, R., and Sugeno, M. (2019a). Fuzzy control systems: Past, present and future. *IEEE Computational Intelligence Magazine*, 14(1), 56–68. doi: 10.1109/MCI.2018.2881644.

Nguyen, V.A., Nguyen, A.T., Dequidt, A., Vermeiren, L., and Dambrine, M. (2019b). Nonlinear Tracking Control with Reduced Complexity of Serial Robots: A Robust Fuzzy Descriptor Approach. *International Journal of Fuzzy Systems*, 21.

Niculescu, S.I., de Souza, C., Dugard, L., and Dion, J.M. (1998). Robust exponential stability of uncertain systems with time-varying delays. *IEEE Transactions on Automatic Control*, 43(5), 743–748.

Nishikawa, M., Katayama, H., Yoneyama, J., and Ichikawa, A. (2000). Design of output feedback controllers for sampled-data fuzzy systems. *International Journal of Systems Science*, 31(4), 439–448.

Nouri, A., Salhi, I., Elwarraki, E., Beid, S.E., and Essounbouli, N. (2017). DSP-based implementation of self-tunning fuzzy controller for three-level boost converter. *Electric Power Systems Research*, 17, 286–297.

O'Dwyer, A. (2009). *Handbook of PI and PID controller tunning rules*. Imperial College Press, 3^{rd} edition.

Ogata, K. (1995). *Discrete-Time Control Systems*. Pearson, 2 edition.

Ogata, K. (2010). *Engenharia de Controle Moderno*. Pearson Education, 5 edition.

Oliveira, R.C.L.F., de Oliveira, M.C., and Peres, P.L.D. (2011). Robust state feedback LMI methods for continuous-time linear systems: Discussions, extensions and numerical comparisons. In *2011 IEEE International Symposium on Computer-Aided Control System Design (CACSD)*, 1038–1043.

Ounnas, D., Ramdani, M., Chenikher, S., and Bouktir, T. (2016). Optimal Reference Model Based Fuzzy Tracking Control for Wind Energy Conversion System. *International Journal of Renewable Energy research*, 6(3), 1129–1236.

Pan, Y. and Yang, G.H. (2017). Event-triggered fuzzy control for nonlinear networked control systems. *Fuzzy Sets and Systems*, 329, 91–107. Theme: Control.

Peaucelle, D., Arzelier, D., Bachelier, O., and Bernussou, J. (2000). A new robust D-stability condition for real convex polytopic uncertainty. *Systems & Control Letters*, 40(1), 21–30.

Peng, C., Ma, S., and Xie, X. (2017). Observer-Based Non-PDC Control for Networked T–S Fuzzy Systems With an Event-Triggered Communication. *IEEE Transactions on Cybernetics*, 47(8).

Peng, C., Tian, Y.C., and Tian, E. (2008). Improved delay-dependent robust stabilization conditions of uncertain T-S fuzzy systems with time-varying delay. *Fuzzy Sets and Systems*, 159(20), 2713–2729.

Precup, R.E., Preitl, S., Petriu, E.M., Tar, J.K., Tomescu, M.K., and Pozna, C. (2009). Generic two-degree-of-freedom linear and fuzzy controllers for integral process. *Journal of the Franklin Institute*, 346, 980–1003.

Preitl, S. and Precup, R.E. (2006). Sensitivity study of a class of fuzzy control systems. *Periodica Polytechnica Electrical Engineering*, 50(3-4), 255–268.

Preitl, S., Precup, R.E., and Preitl, Z. (2005). Sensitivity Analysis of Low Cost fuzzy controlled servo systems. In 2005 - 16^{th} *IFAC World Congress*, 342–347.

Qiao, W.Z. and Mizumoto, M. (1996). PID type fuzzy controller and parameters adaptive method. *Fuzzy Sets and Systems*, 78, 23–35.

Quanser (2016). Quanser aero user manual. URL https://www.quanser.com/products/quanser-aero/.

Quintana, D., Estrada-Manzo, V., and Bernal, M. (2017). Real-time parallel distributed compensation of an inverted pendulum via exact Takagi-Sugeno models. In *2017 14th International Conference on Electrical Engineering, Computing Science and Automatic Control (CCE)*, 1–5.

Rhee, B.J. and Won, S. (2006). A new fuzzy Lyapunov function approach for a Takagi–Sugeno fuzzy control system design. *Fuzzy Sets and Systems*, 157(9), 1211 – 1228. Fuzzy Concepts Applied to Food Control Quality Control.

Rouamel, M., Bourahala, F., Lopes, A.N.D., Nafir, N., and Guelton, K. (2021). Mixed Actual and Memory Data-based Event-Triggered $\mathcal{H}_\infty$ Control Design for Networked Control Systems. *IFAC-PapersOnLine*, 54(4), 80–85.

Sala, A. (2009). On the conservativeness of fuzzy and fuzzy-polynomial control of nonlinear systems. *Ann. Rev. in Control*, 33(1), 48–58.

Sala, A. and Ariño, C. (2007). Asymptotically necessary and sufficient conditions for stability and performance in fuzzy control: Applications of Polya's theorem. *Fuzzy Sets Syst.*, 158, 2671–2686.

Sari, N.N., Jahanshahi, H., and Fakoor, M. (2019). Adaptive fuzzy PID control strategy for spacecraft attitude control. *International Journal of Fuzzy Systems*, 21(3), 769–781.

Scherer, C., Gahinet, P., and Chilali, M. (1997). Multiobjective output-feedback control via LMI optimization. *IEEE Transactions on Automatic Control*, 42(7), 896–911.

Schulte, H. and Guelton, K. (2006). Modelling and simulation of two-link robot manipulators based on Takagi Sugeno fuzzy descriptor systems. In *2006 IEEE International Conference on Industrial Technology*, 2692–2697.

Schulte, H. and Guelton, K. (2009). Descriptor modelling towards control of a two link pneumatic robot manipulator: A T–S multimodel approach. *Nonlinear Analysis: Hybrid Systems*, 3(2), 124–132.

Seddiki, L., Guelton, K., and Zaytoon, J. (2010). Concept and Takagi–Sugeno descriptor tracking controller design of a closed muscular chain lower-limb rehabilitation device. *IET Control Theory & Applications*, 4(8), 1407–1420.

Seuret, A. and Gouaisbaut, F. (2013). Wirtinger-based integral inequality: Application to time-delay systems. *Automatica*, 49(9), 2860–2866.

Seuret, A. (2009). Stability analysis for sampled-data systems with a time-varying period. In *Proceedings of the 48h IEEE Conference on Decision and Control (CDC) held jointly with 2009 28th Chinese Control Conference*, 8130–8135.

Seuret, A. (2012). A novel stability analysis of linear systems under asynchronous samplings. *Automatica*, 48(1), 177–182.

Seuret, A. and Briat, C. (2015). Stability analysis of uncertain sampled-data systems with incremental delay using looped-functionals. *Automatica*, 55, 274–278.

Seuret, A. and Gouaisbaut, F. (2018). Stability of Linear Systems With Time-Varying Delays Using Bessel–Legendre Inequalities. *IEEE Transactions on Automatic Control*, 63(1), 225–232.

Shamma, J. (1988). *Analysis and design of gain scheduled control systems*. Ph.d. thesis, Massachusetts Institute of Technology, Department of Mechanical Engineering.

Shamma, J.S. and Cloutier, J.R. (1993). Gain-scheduled missile autopilot design using linear parameter varying transformations. *Journal of Guidance Control and Dynamics*, 16, 256–263.

Skelton, R., Iwasaki, T., and Grigoriadis, K. (1998). *A unified algebraic approach to linear control design*. Taylor and Francis, London.

Sousa, A.C., Leite, V.J.S., and Rubio Scola, I. (2018). Affordable control platform with MPC application. *Studies in Informatics and Control*, 27, 265–274.

Steinbusch, A. and Reyhanoglu, M. (2019). Robust Nonlinear Tracking Control of a 2-DOF Helicopter System. In *2019 12th Asian Control Conference (ASCC)*, 1649–1654.

Sturm, J.F. (1999). Using sedumi 1.02, a MATLAB toolbox for optimization over symmetric cones. *Optimization methods and software*, 11(1-4), 625–653.

Subramanian, R.G. and Elumalai, V.K. (2016). Robust MRAC augmented baseline LQR for tracking control of 2-DoF helicopter. *Robotics and Autonomous Systems*, 86, 70 – 77. doi: https://doi.org/10.1016/j.robot.2016.08.004.

Sun, Y., Xu, J., Qiang, H., Wang, W., and Lin, G. (2019). Hopf bifurcation analysis of maglev vehicle-guideway interaction vibration system and stability control based on fuzzy adaptive theory. *Computers in Industry*, 108, 197–209.

Takagi, T. and Sugeno, M. (1985). Fuzzy identification of systems and its applications to modeling and control. *IEEE Transactions on Systems, Man and Cybernetics*, SMC-15(1), 116–132.

Tamilarasi, D. and Sivakumaran, T.S. (2018). Fuzzy PI Control of Symmetrical and Asymmetrical Multilevel Current Source Inverter. *International Journal of Fuzzy Systems*, 20(2), 426–443.

Tanaka, K., Hori, T., and Wang, H.O. (2001). A fuzzy Lyapunov approach to fuzzy control system design. In *Proceedings of the 2001 American Control Conference*, volume 6, 4790–4795 vol.6.

Tanaka, K., Hori, T., and Wang, H.O. (2003). A Multiple Lyapunov Function Approach to Stabilization of Fuzzy Control Systems. *IEEE Transactions on Fuzzy Systems*, 11(4), 582–589.

Tanaka, K., Ikeda, T., and Wang, H.O. (1998). Fuzzy regulators and fuzzy observers: relaxed stability conditions and LMI-based designs. *IEEE Transactions on Fuzzy Systems*, 6(2), 250–265.

Tanaka, K. and Wang, O. (2001). *Fuzzy Control Systems Design and Analysis: A Linear Matrix Inequality Aproach*. John Wiley and Sons.

Tanaka, K., Ohtake, H., and Wang, H.O. (2007). A Descriptor System Approach to Fuzzy Control System Design via Fuzzy Lyapunov Functions. *IEEE Transactions on Fuzzy Systems*, 15(3), 333–341.

Tanaka, K. and Sugeno, M. (1992). Stability analysis and design of fuzzy control systems. *Fuzzy Sets and Systems*, 45, 135–156.

Taniguchi, T., Tanaka, K., Ohtake, H., and Wang, H.O. (2001). Model Construction, Rule reduction and robust compensation for generalized form of Takagi-Sugeno fuzzy systems. In *IEEE Transactions on Fuzzy Systems*, volume 9, 525–538.

Taniguchi, T., Tanaka, K., and Wang, H.O. (2000). Fuzzy descriptor systems and nonlinear model following control. *IEEE Transactions on Fuzzy Systems*, 8, 442–452.

Taniguchi, T., Tanaka, K., Yamafuji, K., and Wang, H. (1999). Fuzzy descriptor systems: stability analysis and design via LMIs. In *Proceedings of the 1999 American Control Conference*, volume 3, 1827–1831.

Tarbouriech, S., Garcia, G., da Silva Jr., J.M.G., and Queinnec, I. (2011). *Stability and Stabilization of Linear Systems with Saturating Actuators*. Springer.

Tuan, H.D., Apkarian, P., Narikiyo, T., and Yamamoto, Y. (2001). Parameterized Linear Matrix Inequality Techniques in Fuzzy Control System Design. *IEEE Transactions on fuzzy systems*, 9(2), 324–332.

Vermeiren, L., Dequidt, A., Afroun, M., and Guerra, T.M. (2012). Motion control of planar parallel robot using the fuzzy descriptor system approach. *ISA Transactions*, 51(5), 596–608.

Wang, H.O., Tanaka, K., and Grinn, M.F. (1996). An approach to fuzzy control of nonlinear systems: stability and design issues. *IEEE Transactions on Fuzzy Systems*, 4(1), 14–23.

Wang, Y., L.Zou, Zhao, Z., and Bai, X. (2019). $\mathcal{H}_\infty$ fuzzy PID control for discrete time-delayed T-S fuzzy systems. *Neurocomputing*, 332, 91–99.

Wang, Y., Karimi, H.R., Lam, H.K., and Shen, H. (2018). An Improved Result on Exponential Stabilization of Sampled-Data Fuzzy Systems. *IEEE Transactions on Fuzzy Systems*, 26(6), 3875–3883.

Wang, Y., Xia, Y., and Zhou, P. (2017). Fuzzy-Model-Based Sampled-Data Control of Chaotic Systems: A Fuzzy Time-Dependent Lyapunov–Krasovskii Functional Approach. *IEEE Transactions on Fuzzy Systems*, 25(6), 1672–1684.

Wittenmark, B., Nilsson, J., and Torngren, M. (1995). Timing problems in real-time control systems. In *Proceedings of 1995 American Control Conference - ACC'95*, volume 3, 2000–2004 vol.3.

Xiaodong, L. and Qing-ling, Z. (2003). New approaches to $\mathcal{H}_\infty$ controller designs based on fuzzy observers for T-S fuzzy systems via LMI. *Automatica*, 39, 1571–1582.

Xie, L. (1996). Output feedback $\mathcal{H}_\infty$ control of systems with parameter uncertainty. *International Journal of Control*, 63(4), 741–750.

Xie, X., Yue, D., Zhang, H., and Peng, C. (2017a). Control synthesis of discrete-time TS fuzzy systems: reducing the conservatism whilst alleviating the computational burden. *IEEE Transactions on Cybernetics*, 47(9), 2480–2491.

Xie, X., Yue, D., Zhang, H., and Peng, C. (2017b). Control synthesis of discrete-time TS fuzzy systems: reducing the conservatism whilst alleviating the computational burden. *IEEE Transactions on Cybernetics*, 47(9), 2480–2491.

Yi, Y. and Guo, L. (2009). Constrained PI Tracking control for the output pdfs based on T-S fuzzy model. *International Journal of Innovative Computing, Information and Control*, 5(2), 349–358.

Yi, Y., Li, T., and Guo, L. (2008). Statistic Tracking Control for Non-Gaussian Systems Using T-S Fuzzy Model. In 2008 - 17^{th} *IFAC World Congress*, 11564–11569.

Yoneyama, J. (2010). Robust H_∞ control of uncertain fuzzy systems under time-varying sampling. *Fuzzy Sets and Systems*, 161(6), 859 – 871.

Yu, G.R. and Huang, Y.J. (2009). T-S Fuzzy Control of Magnetic Levitation Systems Using QEA. In 2009 - 4^{th} *International Conference on Innovative Computing, Information and Control (ICICIC)*, 1110–1113.

Yu, G.R., Huang, Y.J., and Huang, L.W. (2010). T-S Fuzzy Control for Magnetic Levitation Systems Using Quantum Particles Swarm Optimization. In 2010 - *SICE Annual Conference*, 48–53.

Zaccarian, L. and Teel, A.R. (2011). *Modern Anti-windup Synthesis: control augmentation for actuator saturation*. Princeton University Press, Princeton, NJ, 1 edition.

Zeng, H.B., Teo, K.L., He, Y., and Wang, W. (2019). Sampled-data stabilization of chaotic systems based on a T-S fuzzy model. *Information Sciences*, 483, 262–272.

Zerar, M., Guelton, K., and Manamanni, N. (2008). Linear fractional transformation based $\mathcal{H}_\infty$ output stabilization for Takagi-Sugeno fuzzy models. *Mediterranean Journal of Measurement and Control*, 4(3), 111–121.

Zhang, D. and Han, Q. (2011). $\mathcal{H}_\infty$ control design for network-based T-S fuzzy systems with asynchronous constraints on membership functions. In *IECON 2011 - 37th Annual Conference of the IEEE Industrial Electronics Society*, 2584–2589.

Zhang, D., Nguang, K., Srinivassan, D., and Yu, L. (2017). Distributed Filtering for Discrete-time T-S Fuzzy Systems with Incomplete Measurements. *IEEE Transactions on Fuzzy Systems*, 1–10.

Zhang, D., Han, Q.L., and Jia, X. (2015). Network-based output tracking control for T–S fuzzy systems using an event-triggered communication scheme. *Fuzzy Sets and Systems*, 273, 26–48. Theme: Control Engineering.

Zhang, X.M. and Han, Q.L. (2013). Novel delay-derivative-dependent stability criteria using new bounding techniques. *International Journal of Robust and Nonlinear Control*, 23(13), 1419–1432.

Zhu, X., Chen, B., Yue, D., and Wang, Y. (2012). An Improved Input Delay Approach to Stabilization of Fuzzy Systems Under Variable Sampling. *IEEE Transactions on Fuzzy Systems*, 20(2), 330–341.

Zhu, X., Lin, H., and Xie, X. (2016). Sampled-Data Fuzzy Stabilization of Nonlinear Systems Under Nonuniform Sampling. *IEEE Transactions on Fuzzy Systems*, 24(6), 1654–1667.

Zhu, X.L. and Wang, Y. (2011). Stabilization for sampled-data neural network-based control systems. *IEEE Transactions on Systems, Man, and Cybernetics, Part B*, 41(1), 210–221.

Zhu, X.L., Chen, B., Wang, Y., and Yue, D. (2013). $\mathcal{H}_\infty$ stabilization criterion with less complexity for nonuniform sampling fuzzy systems. *Fuzzy Sets and Systems*, 225, 58–73.

Contributions à la Synthèse de Contrôleurs Échantillonnés pour les Modèles Takagi-Sugeno

Ce travail étudie la stabilisation des systèmes non linéaires à temps continu pilotés par des dispositifs numériques, dans le but de relâcher les conditions de synthèse et d'améliorer l'estimation du domaine d'attraction en boucle fermée pour des intervalles d'échantillonnage aussi grands que possible. Tout d'abord, la commande des systèmes non linéaires soumis à la saturation des actionneurs, représentés par des modèles Takagi-Sugeno (T-S) à temps discret avec des contraintes sur l'entrée, est étudiée. L'accent est mis sur la conception de contrôleurs de type PI en temps discret avec une compensation anti-windup pour suivre des points de consigne constants par morceaux. Parallèlement, une procédure d'optimisation est proposée pour l'élargissement du domaine d'attraction garanti en boucle fermée. Ensuite, pour contourner certains inconvénients des approches basées sur un modèle à temps discret, tels que les approximations du modèle et l'exigence d'un intervalle d'échantillonnage fixe, l'approche consistant à réécrire la dynamique en boucle fermée sous la forme d'un système continu à retard variable sur l'entrée est considérée. Par conséquent, à partir d'une fonction de Lyapunov-Krasovskii (LKF) bouclée et l'application de lemmes de majoration, de nouvelles conditions LMI relâchées sont proposées pour la synthèse de contrôleurs échantillonnées stabilisant les modèles T-S à temps continu. Cependant, dans ce contexte, des fonctions d'appartenance asynchrones apparaissent dans la formulation de la boucle fermée et donc dans les conditions de synthèse, qui ne peuvent être traitées avec les schémas de relaxation usuels. Pour faire face à ce problème, une extension du Lemme de Tuan est proposée. Par la suite, l'approche de contrôle échantillonnées proposée est étendue à la classe plus générale des descripteurs T-S décrits en temps continu et soumis à la saturation des entrées. En soulignant que, dans le cadre des modèles T-S à temps continu, les contrôleurs échantillonnées conçus ne garantissent que localement la stabilité en boucle fermée, une analyse minutieuse du domaine d'attraction en boucle fermée est proposée. En outre, après avoir remarqué que, pour de larges intervalles d'échantillonnage admissibles, l'estimation résultante du domaine d'attraction en boucle fermée peut être assez petite, un nouveau mécanisme d'ajustement de la loi de commande par déclenchement d'événement est proposé pour élargir davantage cette estimation. Tout au long du manuscrit, des simulations et des résultats expérimentaux établissent le mérite des approches proposées pour la commande échantillonnée des modèles T-S.

Modèles Takagi-Sugeno, Commande échantillonnée, Synthèse LMI, Saturation des actionneurs, Stabilisation locale.

Contributions to the Design of Sampled-Data Controllers for Takagi-Sugeno Models

This work investigates the stabilization of continuous-time nonlinear systems driven by digital devices, with the goal of relaxing the design conditions and enhancing the estimation of the closed-loop domain of attraction for largest as possible sampling intervals. First, the control of nonlinear systems subject to actuators saturation, represented by discrete-time Takagi-Sugeno (T-S) models with input constraints, is investigated. The focus relied on the design of discrete-time PI-like controllers with an anti-windup compensation to track piece-wise constant set-points. Meanwhile, an optimization procedure is proposed for the enlargement of the guaranteed closed-loop domain of attraction. Then, to circumvent some drawbacks of the discrete-time model-based approaches, such as model approximations and the requirement of a fixed sampling interval, the input-delay approach for sampled-data systems is investigated. Therefore, from a convenient looped Lyapunov-Krasovskii Functional (LKF) and the application of some bounding lemmas, new relaxed LMI-based conditions are proposed for the design of sampled-data controllers to stabilize continuous-time T-S models. However, in this context, asynchronous membership functions arise from the closed-loop formulation and so from the design conditions, which cannot be handle with usual relaxation schemes. Hence, to cope with such issue, an extension of the well known Tuan's Lemma is proposed in this context of sampled-data control for continuous-time T-S models. Furthermore, the proposed sampled-data control approach is extended to the more general class of T-S descriptors subject to input saturation. Highlighting that, in the continuous-time T-S model-based framework, the designed sampled-data controllers only locally guarantee the closed-loop stability, a careful analysis of the closed-loop domain of attraction is proposed. Also, after noticing that, for large admissible sampling intervals, the resulting estimation of the closed-loop domain of attraction may be quite small, a new gain-scheduled event-triggering mechanism is proposed to further enlarge such estimation. Along the manuscript, simulations and experimental results establish the merit of the proposed approaches for the sampled-data control of T-S models.

Takagi-Sugeno models, Sampled-data control, LMI-based design, Saturated Actuators, Local Stabilization.

Discipline : AUTOMATIQUE, SIGNAL, PRODUCTIQUE, ROBOTIQUE

Spécialité : AUTOMATIQUE

Université de Reims Champagne-Ardenne

CRESTIC - EA3804

UFR Sciences Exactes et Naturelles
Moulin de la Housse
BP 1039 - 51687 Reims CEDEX 2